DISS. ETH NO. 24051

Strategies for yield recovery after soil compaction assessed by multi-level phenotyping

A thesis submitted to attain the degree of

DOCTOR OF SCIENCES of ETH ZURICH

(Dr. sc. ETH Zurich)

presented by:

Tino Colombi

MSc. ETH in Agricultural Sciences

born on 31st of May 1988

citizen of Lugano (TI)

accepted on the recommendation of:

Prof. Dr. Achim Walter (examiner)

Prof. Dr. Thomas Keller (co-examiner)

Prof. Dr. Dani Or (co-examiner)

2017

"Our days are as bleak as we permit.

Reach beyond the sun,

where hopelessness has yet to spread.

Reach beyond…"

Reach Beyond the Sun, Shai Hulud, Metal Blade Records

Table of Contents

Summary

It is estimated that today around 68 million hectares of arable land are degraded due to soil compaction. The major cause for soil compaction is the use of heavy agricultural machinery in modern agriculture. The changes in soil structure, which are induced by compaction, result not only in increased soil bulk density but also in a shift of the pore size distribution towards pores of smaller diameter. Furthermore, soil compaction results in an increase of pore tortuosity and the connectivity of pores decreases due to compaction. These soil structural alterations lead to increased soil mechanical impedance and decreased fluid transport rates, which adversely affect root growth. Consequently resource uptake by roots is reduced resulting in decreased crop productivity. In spite of the available information about the influence of compaction on soil structure, soil physical functions and plant responses, little is known about processes driving the recovery of compacted soils. Beside abiotic phenomena such as shrink-swell cycles, bioturbation by plant roots and earthworms is suggested to play a key role for the recovery of soil physical functions and thus agricultural productivity after a compaction event.

The overall aim of the presented thesis was to identify possible strategies that contribute to the recovery of crop productivity after soil was compacted. These strategies were evaluated by an approach, which may be referred as "multi-level" phenotyping. Multi-level phenotyping describes the approach to use different phenotyping methods to simultaneously assess a multitude of plant traits. Furthermore, experiments are conducted at different experimental scales and in different plant species or in different genotypes of a single species. In the framework of the presented thesis, phenotypic properties were determined from the root tissue to the canopy level under field and laboratory conditions. Phenotyping methodologies included X-ray computed tomography, bright field microscopy, digital image processing and the quantification of root system properties from excavated root stocks as well as root and shoot biomass measurements. Experiments were performed with major mono- and dicotyledonous crop species and a set of fourteen phenotypically diverse wheat varieties. Soil physical quantifications including measurements of bulk density, mechanical impedance and fluid transport characteristics complemented the phenotypic assessments.

As a first step it was tested to what extent soil columns may serve as a model system for the field by comparing plant phenotypic responses to soil compaction between the field and soil columns. Soybean and triticale were grown in small soil columns under controlled conditions and in the field in compacted and loose soil. In both species and environments, increased soil bulk density resulted in decreasing numbers of lateral roots and root thickening. These root phenotypic responses to soil compaction coincided with decreased shoot biomass. Furthermore, it could be shown that roots of soybean, wheat and maize were attracted by artificial macropores that were inserted into compacted soil in the field and in soil columns. These results demonstrated that soil columns are suited to simulate the belowground environment plants encounter in the field and can therefore be used as model systems. However, since experiments in soil columns are restricted to young plants, it is challenging to determine influences of soil physical properties, which occur later during plant development, under controlled conditions.

One possibility to overcome the adverse effects of soil compaction on crop productivity is to select for crop varieties, into which root traits are integrated that allow plant growth to be maintained when soil is compacted. Prior to the implementation of such breeding programmes, root traits that are of advantage under increased soil bulk density need to be identified. To do so, fourteen wheat cultivars were grown in soil columns, which were packed to three different soil bulk densities representing loose, moderately and severely compacted soil. The genetic diversity in response to increased soil strength among these varieties was evaluated with respect to root elongation rates and root-shoot relationships. In a first experiment roots were grown for 48 hours in soil before being washed out and scanned with a high-resolution flatbed scanner. From these scans root tip geometry and root elongation rates were evaluated. Under severe compaction in particular but also under moderate compaction it could be shown that root elongation rate correlated significantly with the root tip geometry. Varieties with an acute root tip opening angle penetrated deeper into compacted soil than varieties with a rather blunt tip opening angle. Combining cone penetrometer tests with information about the root tip shape enabled penetration forces and stresses, which occurred during root growth, to be estimated. These calculations showed that lower root tip radius to length ratios are related to decreased penetration stresses enabling the root to elongate faster in compacted soil. In a second

experiment the same varieties were grown for 23 days under the same conditions as described above. Simultaneous quantification of root numbers from X-ray computed tomography scans and the development of plant height showed that the development of the root system is closely related to shoot growth. Under moderate compaction, shoot biomass after 23 days of growth was positively correlated to root numbers. This demonstrated that –at least under moderate compaction– the genotypic capacity to maintain the number of roots in response to increased soil strength, resulted in increased early plant vigour.

Apart from using the genetic diversity to overcome compaction induced limitations to crop growth, soil management approaches may contribute as well to yield recovery after soil compaction. Artificial macropores were inserted into compacted field soil and into soil that was compacted in soil columns. Compared to compacted soil without artificial macropores, the presence of such vertical pores in compacted soil resulted in increased fluid transport rates. Using X-ray computed tomography enabled the interaction of soybean, wheat and maize roots with these artificial macropores to be quantified. In all three species the quantified root-pore interaction was observed to be the result of directed rather than random root growth. The obtained results suggested that depending on the species, the macropores fulfilled different purposes to growing roots. Maize roots were using these pores as pathways of least resistance and grew within the artificial macropores. Wheat roots instead predominantly crossed the pores suggesting that they used the pores as a source of oxygen. In soybean both modes of root-pore interactions occurred to an equal extent. At the field scale, the presence of artificial macropores in compacted soil enabled all species to compensate for poor early vigour at later developmental stages. This compensation resulted in increased shoot biomass of plants, which were grown on perforated compacted soil compared to plants grown on compacted soil without artificial macropores.

The results presented in the current thesis strongly suggested that both genetic diversity within a single species and soil management such as soil perforation may contribute to yield recovery after a compaction event. Since the proposed approaches led to increased root growth, they will most likely also accelerate the recovery of soil physical functions and soil structural properties, which were affected by compaction.

Zusammenfassung

Es wird geschätzt, dass heute rund 68 Millionen Hektar Ackerland durch Bodenverdichtung degradiert sind. Die Hauptursache für Bodenverdichtung ist der Einsatz von schweren Landmaschinen in der modernen Landwirtschaft. Die Veränderungen in der Bodenstruktur, die durch Verdichtung hervorgerufen werden, führen neben einer erhöhten Bodenschüttdichte auch zu einer Verschiebung der Porengrößenverteilung zu Poren mit kleinerem Durchmesser. Zusätzlich führt Bodenverdichtung zu einem Anstieg der Porentortuosität und die Konnektivität der Poren untereinander nimmt ab. Diese bodenstrukturellen Veränderungen führen zu erhöhten Eindringwiderständen und reduzieren Fluidtransportraten, was das Wurzelwachstum und somit die Ressourcenaufnahme und die landwirtschaftliche Produktivität reduziert. Trotz der verfügbaren Informationen über den Einfluss von Verdichtung auf die Bodenstruktur und bodenphysikalische Funktionen sowie die Reaktionen von Pflanzen darauf, ist wenig Wissen vorhanden über Prozesse, die die strukturelle Erholung des Bodens nach einer Verdichtung beeinflussen. Neben abiotischen Phänomenen wie Quell-Schrumpf Zyklen zählt Bioturbation durch Pflanzenwurzeln und Regenwürmern zu den wichtigsten Prozessen für die Wiederherstellung der physikalischen Funktionen des Bodens. Folglich nimmt Bioturbation eine zentrale Rolle ein, bei der Rückgewinnung der Fruchtbarkeit und Produktivität von Ackerböden nach einer Verdichtung.

Das übergeordnete Ziel der vorliegenden Arbeit war es, mögliche Strategien zu identifizieren, die zur Wiederherstellung der landwirtschaftlichen Produktivität auf verdichteten Böden beitragen. Diese Strategien wurden anhand eines Vorgehens evaluiert, das als "mehrstufige" Phänotypisierung bezeichnet werden kann. Mehrstufige Phänotypisierung beschreibt den Ansatz, verschiedene Phänotypisierungsmehtoden zu verwenden, um gleichzeitig eine Vielzahl von Pflanzeneigenschaften zu erfassen. Darüber hinaus werden Experimente in verschiedenen experimentellen Skalen und in verschiedenen Pflanzenarten und Genotypen einer einzelnen Spezies durchgeführt. Im Rahmen der vorliegenden Arbeit wurden phänotypische Eigenschaften von der Gewebe- bis zur Bestandesebene unter Feld- und Laborbedingungen quantifiziert. Die verwendeten Phänotypisierungsmehtoden umfassten Röntgen-Computertomographie, Hellfeldmikroskopie, digitale Bildverarbeitung, die

Quantifizierung von Wurzelsystemeigenschaften anhand von ausgegrabenen Wurzelstöcken sowie Bestimmungen der Wurzel- und Sprossbiomasse. Das verwendete Pflanzenmaterial umfasste global wichtige mono- und dikotyle Nutzpflanzen und vierzehn phänotypisch verschiedene Weizensorten. Bodenphysikalische Quantifizierungen einschließlich Messungen der Bodendichte, mechanischer Impedanz und Fluidtransportraten ergänzten die phänotypischen Erhebungen.

In einem ersten Schritt wurde untersucht inwieweit Bodensäulen als Modellsystem für das Feld dienen können, indem phänotypische Reaktionen auf Bodenverdichtung zwischen Feld und Bodensäulen verglichen wurden. Soja und Triticale wurden in kleinen Bodensäulen unter kontrollierten Bedingungen und auf dem Feld verdichtetem und lockerem Boden ausgesetzt. In beiden Spezies und Umgebungen führte eine erhöhte Bodendichte zu einer Verringerung der Anzahl der Seitenwurzeln und zu einer Verdickung der Wurzeln. Ausserdem nahm die oberirdische Biomasse als Reaktion auf Bodenverdichtung ab. Darüber hinaus konnte im Feld und unter kontrollierten Bedingungen gezeigt werden, dass Soja-, Weizen- und Maiswurzeln aktiv zu künstliche Makroporen hinwuchsen. Diese Ergebnisse legen nahe, dass die unterirdische Umwelt, welcher Pflanzen im Feld ausgesetzt sind, in Bodensäulen simuliert werden kann und solche Säulen daher als Modellsysteme in Frage kommen. Da Experimente in Bodensäulen jedoch auf junge Pflanzen beschränkt sind, können Einflüsse des Bodens, die in späteren Entwicklungsstadien auftreten, nur schwer in solchen Modellsystemen quantifiziert werden.

Eine Möglichkeit die negativen Effekte von Bodenverdichtung zu überwinden besteht darin Pflanzensorten zu züchten, deren Wurzeln an die Bedingungen in verdichtetem Boden angepasst sind. Ob dies möglich ist wurde untersucht, indem vierzehn verschiedene Weizensorten in Bodensäulen drei verschiedenen Bodendichten –locker, moderat und stark verdichtet– ausgesetzt wurden. Anhand von Wurzelwachstumsraten und Wurzel-Spross Beziehungen wurde die genetische Vielfalt zwischen diesen Sorten in Bezug auf die erhöhte Bodendichte untersucht. In einem ersten Experiment wuchsen die Wurzeln für 48 Stunden im Boden, bevor sie ausgewaschen und mit einem hochauflösenden Flachbettscanner gescannt wurden. Dies ermöglichte die Wurzelspitzengeometrie und die Wurzelwachstumsrate zu bestimmen. Insbesondere bei schwerer Verdichtung aber auch bei moderater Verdichtung konnte gezeigt werden, dass das Wurzelwachstum signifikant mit dem

Wurzelspitzenöffnungswinkel korrelierte. Sorten mit einem spitzen Öffnungswinkel drangen tiefer in verdichteten Boden ein als Sorten mit einem eher stumpfen Spitzenöffnungswinkel. Die Kombination von Penetrometermessungen mit den Informationen über die Wurzelspitzenform ermöglichte es Kräfte und Drücke abzuschätzen, die während des Wurzelwachstums auftraten. Diese Berechnungen zeigten, dass spitze Öffnungswinkel der Wurzelspitze mit verringerten Penetrationsdrücken zusammenhängen, die es der Wurzel erlaubten, weiter in den verdichteten Boden einzudringen. In einem zweiten Experiment wuchsen die gleichen Sorten für 23 Tage unter den oben beschriebenen Bedingungen. Die gleichzeitige Quantifizierung der Anzahl von Wurzeln mit Hilfe von Röntgen-Computertomographie und die Entwicklung der Pflanzenhöhe zeigten, dass die Entwicklung des Wurzelsystems eng mit dem Sprosswachstum zusammenhängt. Unter moderater Verdichtung, korrelierte die oberirdische Biomasse nach 23 Tagen Wachstum positiv mit der Wurzelanzahl. Dies zeigte, dass –zumindest unter moderater Verdichtung– das vom Genotyp abhängende Potential die Anzahl der Wurzeln unter erhöhter Bodendichte aufrechtzuerhalten, zu einer erhöhten frühen Wüchsigkeit führt.

Abgesehen von der Nutzung der genetischen Vielfalt zur Überwindung des verminderten Pflanzenwachstums auf verdichtetem Boden, können Bodenbewirtschaftungsansätze zum selben Zweck beitragen. Im Feld und in Bodensäulen wurde verdichteter Boden perforiert und so wurden künstliche Makroporen geschaffen. Im Vergleich zu verdichtetem Boden, der nicht perforiert war, wurden in perforiertem verdichtetem Boden höhere Fluidtransportraten gemessen. Mit Hilfe von Röntgen-Computertomographie konnten die Interaktionen zwischen Soja-, Weizen- und Maiswurzeln mit diesen künstlichen Makroporen quantifiziert werden. Bei allen drei Spezies wurde beobachtet, dass die quantifizierte Wurzel-Poren Interaktion ein Ergebnis von gerichtetem und nicht zufälligem Wurzelwachstum war. Die gemachten Beobachtungen legen nahe, dass die Makroporen je nach Pflanzenart unterschiedliche Zwecke für die Wurzeln erfüllten. Maiswurzeln verwendeten diese Poren als Weg des geringsten Widerstands und wuchsen in den künstlichen Makroporen. Bei Weizen hingegen wurde beobachtet, dass Wurzeln diese Poren zumeist kreuzten und nicht darin wuchsen, was darauf hindeutet, dass Weizen diese künstlichen Poren als Sauerstoffquelle nutzten. Bei Soja traten beide Formen der Interaktion in gleicher Häufigkeit auf. Unter Feldbedingungen führte die Anwesenheit künstlicher Makroporen in verdichtetem Boden dazu, dass alle drei untersuchten

Pflanzenarten die schlechte Frühentwicklung in den späteren Wachstumsstadien kompensieren konnten. Diese Kompensation resultierte in einer erhöhten oberirdischen Biomasse bei Pflanzen, die auf perforiertem verdichtetem Boden wuchsen als bei Pflanzen, die verdichtetem aber nicht perforiertem Boden ausgesetzt waren.

Die in der vorliegenden Arbeit vorgestellten Ergebnisse legen nahe, dass sowohl die genetische Vielfalt innerhalb einer Spezies als auch Bodenbearbeitungsmassnahmen wie das Perforieren von verdichtetem Boden dazu beitragen, die landwirtschaftliche Produktivität nach einem Verdichtungsereignis wiederherzustellen. Da die vorgeschlagenen Ansätze zu einem erhöhten Wurzelwachstum führten, werden sie wahrscheinlich auch die Widerherstellung von bodenphysikalischen Funktionen und bodenstrukturellen Eigenschaften beschleunigen, die durch Verdichtung verändert wurden.

x

1. General introduction

1.1. Soils, their physical fertility and contribution to terrestrial life

Soil has been named the skin of the earth due to its function as the interface between the litho- and the biosphere in most terrestrial ecosystems (Kaiser, 2004). Since most terrestrial plants acquire water and nutrients directly from soil, soils are essential for all forms of terrestrial life including human civilisations (McNeill, 2004; Wall and Six, 2015). Compared to the atmosphere or water bodies, soils are characterized by their inherent heterogeneity of physical, chemical and biological properties at considerably small spatial scales. This spatial heterogeneity shapes the ecosystem, in which roots and soil inhabiting organisms like earthworms and soil microorganisms live. Roots, soil micro-biota and the soil macro-fauna encounter gaseous, liquid and solid phases simultaneously and their environment may change within volumes at the cubic millimetre scale when they grow or move through soil (Walter et al., 2009).

The term "soil fertility" is commonly used to describe the capacity of a certain soil type under a given climate to support plant growth. The fertility of a soil results from the combination of physical, chemical and biological properties, which often interact with each other (Abbott and Murphy, 2007). While chemical and biological soil fertility directly relates to the nutritional requirements of plants, soil physical fertility relates rather indirectly to these requirements. Physical fertility does not refer to the abundance or availability of water or nutrients but to the conditions roots encounter when they have to reach those essential resources. Besides climatic influences, soil physical conditions are largely influenced by soil structure, which can be defined as the spatial arrangement and density of particles and aggregates (Angers and Caron, 1998). This spatial arrangement and the resulting pore network define soil physical functions such as water retention, mechanical impedance and soil oxygen status, which directly affect root growth. Hence, root growth, resource acquisition and crop production can either be promoted or limited by different soil structural and soil physical properties (e.g. Goss and Russell, 1980; Masle and Passioura, 1987; Bengough and Mullins, 1991; Thomson et al., 1992; Beemster et al., 1996; Young et al., 1997; Bengough et al., 2011; Valentine et al., 2012; Dresbøll et al., 2013; Broughton et al., 2015; Nagel et al., 2015).

1.2. Soil compaction

Soil compaction, which is often caused by the use of heavy agricultural machinery (Tracy et al., 2011), is seen today as one of the major forms of land degradation. It is estimated that globally around 68 million hectares of arable land are degraded due to compaction and about half of the this compacted land is found in Europe (Van den Akker and Canarache, 2001; Hamza and Anderson, 2005; Batey, 2009). Compacted soils are characterized by a set of altered soil physical properties and functions, which adversely affect root growth and may result in significant yield decrease (Botta et al., 2010; Arvidsson et al., 2014; Arvidsson and Håkansson, 2014). Since soil compaction leads to decreased soil porosity, measurements of soil bulk density are often used to describe the severity of compactness. However, it has been proposed that measuring only bulk density is not sufficient to assess the physical fertility of soil in general and of compacted soil in particular (Stirzaker et al., 1996).

1.2.1. Effects of compaction on soil physical functions

The decrease of total porosity in compacted soils is mainly concentrated on macropores leading to a shift of pore size distribution towards pores of smaller diameters (Tubeileh et al., 2003; Bottinelli et al., 2014; Chen et al., 2014a). Besides lower (macro-)porosity, compacted soils show decreased pore connectivity and higher pore tortuosity compared to uncompacted soils (Lipiec and Hatano, 2003; Kuncoro et al., 2014a). These changes in soil structure due to compaction affect different soil physical functions, which may impede root growth. Compacted soils exert higher mechanical impedance to growing roots since the void space, which is needed to displace soil particles, is decreased (Valentine et al., 2012; Suzuki et al., 2013; Hernandez-Ramirez et al., 2014). As a consequence of increased mechanical impedance, roots need to apply more force for the penetration of soil and plants need to invest more energy into root growth (Atwell, 1993; Iijima et al., 2003b; Ruiz et al., 2016).

The shift of pore size distribution towards pores of small diameters also leads to lower plant available water content in compacted soils (Lipiec and Hatano, 2003). Therefore, compacted soils are more likely to dry out by evapotranspiration than undisturbed soils, which further increases soil mechanical impedance. Furthermore, the soil structural changes underlying soil compaction, namely low macro porosity and decreased pore connectivity, affect fluid transport characteristics. Hydraulic

conductivity, air permeability and gas diffusion rates are decreased in compacted soils in comparison to uncompacted soils (Stirzaker et al., 1996; Chen et al., 2014a; Kuncoro et al., 2014a; Scholl et al., 2014; Kuncoro et al., 2014b). This increases the risk of waterlogging, particularly after heavy rainfall, and therefore hypoxic conditions in compacted soils (Tracy et al., 2011).

1.2.2. Recovery from compaction

Despite the information about influences of soil compaction on soil structure and related soil physical functions, relatively little is known about the recovery of compacted soils. Soil compaction may happen within a few seconds to minutes, whereas the recovery of compacted soil is supposed to take years to decades (e.g. Hakansson and Reeder, 1994; Besson et al., 2013; Bottinelli et al., 2014). Processes that are involved in the recovery of compacted soils include abiotic phenomena like shrink-swell cycles, which result from fluctuations of soil moisture and freeze-thaw cycles (Dexter, 1991; Besson et al., 2013; Bottinelli et al., 2014; Jabro et al., 2014). Apart from this, bioturbation by plant roots and earthworms is suggested to be the major driver for structural recovery after compaction. Roots contribute to this not only by creating new macropores, which often exceed the depth of macropores created by earthworms, but also by local soil drying and the resulting crack formation (Dexter, 1991; Lesturgez et al., 2004; Bottinelli et al., 2014; Scholl et al., 2014). Therefore, approaches that enhance root growth in compacted soils will accelerate the recovery of soil physical functions and agricultural productivity after a compaction event. This may refer on the one hand to management practices like different tillage operations or crop rotations, which promote root growth into compacted soil layers. On the other hand such approaches may encompass the identification of functional root traits that help to maintain root growth and productivity on compacted soils, which then could be integrated into breeding programmes. To identify such strategies a holistic understanding about the interactions of roots and their physical environment is needed (Batey, 2009).
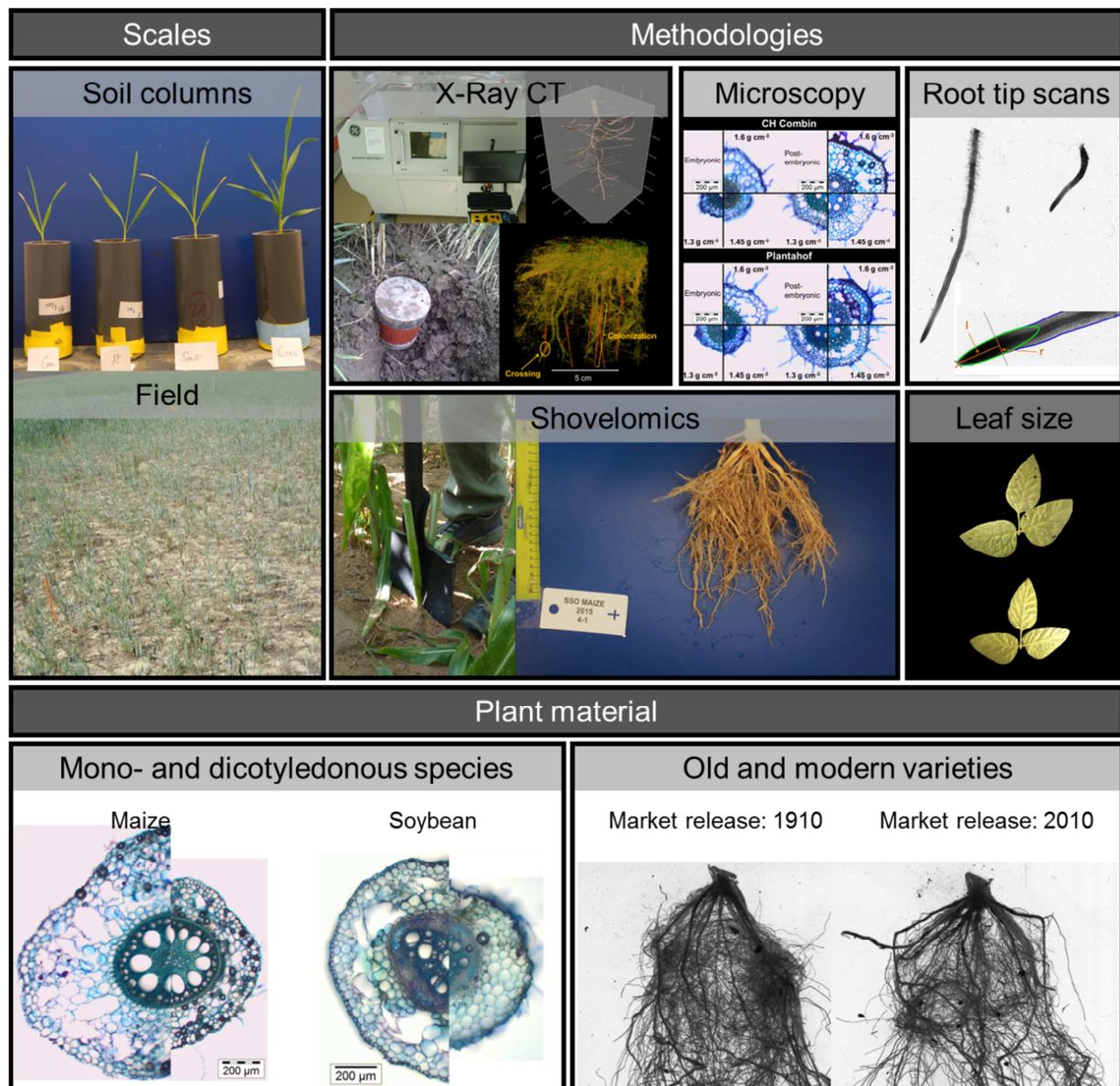
1.3. Plant phenotyping

The term "phenotyping" describes the quantitative assessment of the appearance of an organism resulting from the organism's genetic background and environmental influences (e.g. Walter et al., 2015). In the case of plants this may refer to plant anatomy, biochemical properties, the quantification

of plant growth, plant architecture or physiological properties. Tremendous technical advancement, mostly in the field of digital image processing enabled to increase the precision and throughput of phenotyping in recent years (Zhu et al., 2011; Masuka et al., 2012; Passioura, 2012; Walter et al., 2012; Rahaman et al., 2015; Walter et al., 2015). Such modern but also traditional phenotyping approaches are recognized as a powerful tool to understand the responses of plants to biotic and abiotic stress. Furthermore, phenotyping can be used to identify superior genotypes for certain environmental conditions and to assess the relationships between agricultural management and crop production.

1.3.1. Multi-level phenotyping

The approach to combine different phenotyping methodologies at different experimental and temporal scales can be summarized as multi-level phenotyping (Rahaman et al., 2015). This may refer to the simultaneous assessment of root and shoot growth or the combination of studies under controlled and field conditions. Multi-level phenotyping can also be used to describe approaches that combine quantifications at different organizational levels of a plant. Microscopic investigations at the plant tissue level can be combined with plant morphological and architectural properties and even with quantifications at the canopy level (Walter et al., 2015). Furthermore, multi-level phenotyping may also encompass aspects of plant-environment interactions and the question how certain phenotypic traits relate to plant (eco-)physiological processes (Masuka et al., 2012; Lynch, 2013; White et al., 2013; Lynch, 2015; Walter et al., 2015). In the framework of the presented thesis the term multi-level phenotyping was chosen, since different phenotyping approaches were used at various temporal and experimental scales. Experiments were conducted under controlled and field conditions and phenotypic properties were quantified from the plant tissue to the canopy level in different species and varieties. Thereby below- and aboveground phenotyping was combined with the assessment of soil physical and structural properties (Figure 1.1).

Figure 1.1: Illustration of multi-level phenotyping as used in the current thesis: Whole plant phenotype assessment at the column and the field scale using different methods including: X-ray computed tomography (CT), bright field microscopy, high-resolution flatbed scans, manual quantifications from excavated root stocks (Shovelomics) as well as automated leaf size measurements. Experiments were conducted with different plant species and varieties.

1.3.2. Approaches used for multi-level root phenotyping

Due to the limited accessibility of roots, especially under field conditions, the quantitative assessment of root traits remains difficult and laborious. Nevertheless, the combination of different methodologies is suggested to be a promising approach to better understand how plants interact with their belowground physiochemical environment. Most likely due to the growing awareness about the importance of roots for crop productivity (Lynch, 1995; Bengough et al., 2011; Zhu et al., 2011;

Lynch, 2013; Bishopp and Lynch, 2015), new approaches and technologies were developed, which increased precision and throughput of root phenotyping. As for shoot traits, digital image processing is used extensively nowadays to quantitatively assess a multitude of root traits (Zhu et al., 2011).

Independently of the experimental scale, root phenotyping may address the quantification of various traits including root growth rates, growth directions or the vertical distribution of roots in soil (e.g. Porterfield and Musgrave, 1998; McKenzie et al., 2009; Vollsnes et al., 2010; Trachsel et al., 2013; Grieder et al., 2014; Saengwilai et al., 2014b). The quantification of root system architecture, which describes the spatial configuration of the root system in soil (Lynch, 1995), can be used to relate root phenotypic properties of different species and genotypes to plant performance under various soil physical and chemical conditions (e.g. Tracy et al., 2012b; Miguel et al., 2013; Trachsel et al., 2013; Bao et al., 2014; Wu et al., 2014; Saengwilai et al., 2014b; Colombi et al., 2015; York et al., 2015; Zhan and Lynch, 2015). Furthermore, the description of root morphology and anatomy may also be used to determine effects of the genetic background and environmental conditions on plant growth and appearance (e.g. Thomson et al., 1992; Striker et al., 2007; Chimungu et al., 2014; Chimungu et al., 2015; Bengough et al., 2016). Despite certain approaches for automation (Burton et al., 2012; Chimungu et al., 2015a; York et al., 2015), the quantification of root anatomical traits is still done manually from images acquired from bright field microscopes (Alameda and Villar, 2012; Lipiec et al., 2012; Bao et al., 2014; Passot et al., 2016). In recent years several new technologies were developed and optimized, which can be used for the quantification of root growth, root architecture, root morphology and also root-soil interactions.

1.3.2.1. Methods used under controlled conditions

Different phenotyping platforms were developed to assess root growth, root system properties and their relation to shoot performance under controlled conditions. Systems, in which roots grow on filter paper and the expansion of the root system is imaged in regular intervals, offer the possibility to determine root responses to different nutrient supplies and link this to shoot growth (Le Marié et al., 2014; Richard et al., 2015; in 't Zandt et al., 2015; Le Marié et al., 2016). Other systems, in which roots are grown in a transparent media, can be used to quantify root systems and their growth in three

dimensions (Iyer-Pascuzzi et al., 2010; Downie et al., 2012). Such systems have the advantage that root system properties can be quantified non-destructively –but due to the artificial growth media– upscaling of the results to field conditions may be difficult. Roots can be quantified in soil-filled rhizotrons under conditions that are closer to field situations. In such systems root growth and root system properties can also be quantified continuously since roots are recorded along a transparent plate. In such systems a large number of plants can be screened at the same time or root growth can be assessed in temporal resolutions of less than one hour (e.g. Vollsnes et al., 2010; Nagel et al., 2012; Bengough et al., 2016). Furthermore, root responses to heterogeneously distributed nutrients, partial waterlogging or compartments of different soil bulk densities can be quantified in rhizotrons (Dresbøll et al., 2013; Pfeifer et al., 2014a; Lemming et al., 2016).

The major limitation of a lot of such systems is that quantifications are restricted to two dimensions and hence interactions of roots with soil structure cannot be adequately quantified. Non-destructive three dimensional imaging approaches like X-ray computed tomography or magnetic resonance imaging offer the opportunity to overcome this limitation. Both approaches were successfully used to visualize and quantify root systems and root-soil interactions *in-situ* (Flavel et al., 2012; Mairhofer et al., 2012; Tracy et al., 2012b; Mairhofer et al., 2013; Tracy et al., 2013; Bao et al., 2014; Metzner et al., 2014; Mairhofer et al., 2015; Metzner et al., 2015; Pfeifer et al., 2015). Such non-destructive imaging approaches provide the opportunity to quantify root growth and root system development continuously (Tracy et al., 2012a; Tracy et al., 2012b; Tracy et al., 2013; Metzner et al., 2014). Furthermore, interactions of roots with the surrounding soil and the influence of root growth on soil macroporosity could be quantified using X-ray computed tomography (Tracy et al., 2013; Bao et al., 2014). Despite the availability of software tools that automate certain procedures (Mairhofer et al., 2012; Mairhofer et al., 2013; Mairhofer et al., 2015; Metzner et al., 2015; Pfeifer et al., 2015), the quantification of root system properties from such three dimensional scans is time-consuming. Due to this but also due to scanning times, which often exceed 30 minutes, the throughput than can be achieved using X-ray computed tomography or magnetic resonance imaging is limited.

Most of the so far outlined root phenotyping methodologies are restricted to experiments performed under controlled conditions. For field-grown plants, pioneering work was done in the 20th century, when root systems of various crops were described in the field in high detail (Weaver J.E. et al., 1924; Weaver, 1925; Kutscherea and Lichtenegger, 1960). Since then, new methods were developed and combined to quantify root system properties and root-soil interactions. In recent years, methods enabling a quantitative assessment of root systems received increasing attention. An approach, which was used intensively during the last decade is to quantify a set of root traits from excavated root stocks. This so-called "shovelomics" method enables to assess root system architectural and root morphological traits in large diversity sets at high throughput (Trachsel et al., 2011; Burridge et al., 2016). Shovelomics was successfully combined with investigations under controlled conditions, which allowed relating root numbers in different maize genotypes to the genotypic tolerance to drought and low nitrogen supply. Furthermore, in these studies stable isotope analyses were used to show how root system architectural traits affect the depth from which plants acquire water and nitrogen (Saengwilai et al., 2014b; Zhan et al., 2015; Gao and Lynch, 2016). Similarly, stable isotope analyses were combined with root anatomical measurements in order to relate water uptake to root anatomical properties (Chimungu et al., 2014a; Chimungu et al., 2014b). Pictures of excavated and washed root stocks can be automatically processed resulting in an even higher throughput than manual quantifications (Zhong et al., 2009; Grift et al., 2011; Bucksch et al., 2014; Colombi et al., 2015).

Compared to other approaches used in the field, the major advantage of shovelomics is that it is relatively simple to apply and a multitude of traits can be assessed at the same time. However, shovelomics does not allow quantifying rooting depth or the interaction between roots and the soil matrix. Root length or biomass measurements obtained from soil cores are still used to determine rooting depth, which is often expressed as the depth at which 95% of all roots occur (e.g. Hamza and Anderson, 2005; Trachsel et al., 2013; Chimungu et al., 2014b; Zhan and Lynch, 2015). Such measurements can be combined with shovelomics or similar approaches in order to relate root architectural or anatomical properties to rooting depth and root foraging (e.g. Chimungu et al., 2014a;

Chimungu et al., 2014b; Saengwilai et al., 2014b; Gao and Lynch, 2016). Undisturbed soil cores can also be used to study interactions of roots with soil macropores. To do so, intact soil cores are broken apart and soil-macropore interactions are quantified using dissection microscopes (White and Kirkegaard, 2010). Such interactions were also studied by means of endoscopy or by quantifications along soil profile walls and within soil monoliths (Athmann et al., 2013; Kautz et al., 2013; Perkons et al., 2014). However, these approaches are time- consuming and therefore the throughput is very limited in comparison to shovelomics. Nevertheless, the combination of different root phenotyping methodologies, which may address root architecture, morphology and anatomy as well as root-soil interactions, with the evaluation of different soil properties is a promising approach to enhance the fundamental understanding of soil-plant relationships.

1.4. Phenotypic responses to soil compaction

As outlined above, the structural degradation, which characterizes compacted soils, cause a set of abiotic stresses that affect root and shoot growth. Increased mechanical impedance is correlated to the penetration forces and stresses the soil exerts on growing roots, which is related to the energy plants have to invest into soil exploration (Iijima et al., 2003b; Bengough et al., 2011; Ruiz et al., 2015; Ruiz et al., 2016). Similar to dry or flooded soils, productivity on compacted soils may be limited by low plant available water content or low soil oxygen, respectively. Low concentrations of oxygen in soil air may cause a shift from aerobic to anaerobic root respiration (Blackwell and Wells, 1983; Saglio et al., 1983; Thomson et al., 1992), whereas low plant available water directly decreases photosynthesis (Tubeileh et al., 2003; Galmés et al., 2013; Grzesiak et al., 2013; Lynch, 2013). Hence, the adverse effects of soil compaction on plant growth result from a combination of increased mechanical impedance, soil hypoxia and limited water availability.

1.4.1. Root responses to soil compaction

Depending on the severity of soil compaction, root growth is reduced or may stop completely and the development of the entire root system is delayed (Goss and Russell, 1980; Atwell, 1990; Bengough and Mullins, 1991; Young et al., 1997; Croser et al., 1999a; Croser et al., 1999b; Tracy et al., 2012b). Under field conditions soil compaction results in shallower root growth and decreased

rooting depth (Barraclough and Weir, 1988; Botta et al., 2010; Hernandez-Ramirez et al., 2014; Chen et al., 2014b). Furthermore, soil compaction was observed to increase cell production rates in the root meristem and to accelerate cell detachment from the root cap into the rhizosphere. These detached cells, act as a lubricant and therefore reduce interfacial friction between the root and the soil (Bengough and McKenzie, 1997; Iijima et al., 2003a).

Soil compaction causes a set of alterations in the root phenotype including root architectural, morphological and anatomical responses. Root thickening as an adjustment to compacted soil was observed under field and controlled conditions in a wide range of species (Barraclough and Weir, 1988; Materechera et al., 1992; Iijima and Kato, 2007; Ramos et al., 2010; Tracy et al., 2012b; Grzesiak et al., 2013; Siczek et al., 2013; Hernandez-Ramirez et al., 2014; Chen et al., 2014b). Since increased root diameters decrease root penetration stress and the risk of root buckling, root thickening is seen to be an acclimation to increased mechanical impedance facilitating the penetration of compacted soil (Materechera et al., 1992; Kirby and Bengough, 2002; Chimungu et al., 2015a). This increase of root diameters coincided in several small grain cereals with an enlargement of the root cortex (Iijima and Kato, 2007; Lipiec et al., 2012). Another common response of plants to soil compaction is a decrease in the number of roots. In particular the number of lateral roots is reduced, which can be determined directly or with proxy measures such as specific root length of different diameter classes (Barraclough and Weir, 1988; Tracy et al., 2012b; Grzesiak et al., 2014; Hernandez-Ramirez et al., 2014; Pfeifer et al., 2014a; Chen et al., 2014b). Remarkably, very similar adjustments of the root phenotype were reported in response to flooding or drought. Both stresses not only decrease root growth but also cause increased root diameters and decreasing root numbers (Thomson et al., 1992; Striker et al., 2007; Dresbøll et al., 2013; Yamauchi et al., 2014; Nagel et al., 2015).

Beside root architectural, morphological or anatomical changes, it was observed that plants promote root growth into spots of the soil with soil physical conditions that are more favourable for root growth. Wheat and barley showed increased root growth in loose soil compartments, while root growth in denser parts of the soil was reduced (Bingham and Bengough, 2003; Pfeifer et al., 2014a). Such preferential growth was also reported to happen on much smaller scales. A number of studies showed that roots use natural or artificially created soil macropores as pathways of least resistance to

reach deeper soil layers (Stirzaker et al., 1996; de Freitas et al., 1999; White and Kirkegaard, 2010; Athmann et al., 2013; Han et al., 2015). This behaviour of roots is particularly pronounced when the mechanical impedance of the surrounding bulk soil is high. It was suggested that roots grow actively towards soil macropores to exploit them as a path of least resistance (Stirzaker et al., 1996; White and Kirkegaard, 2010). The behaviour of roots to grow towards macropores and use them as a path of least resistance was described with the term "trematotropism" (Dexter, 1986). As a result of this, root growth of plants grown on compacted soil, which was perforated, increased compared to plants grown on compacted soil that was not perforated (Stirzaker et al., 1996; de Freitas et al., 1999; Pfeifer et al., 2014b).

1.4.2. Shoot responses to soil compaction

Impeded root growth in compacted soils limits the volume of soil that can be reached and hence results in decreased nutrient and water uptake. In seedlings of maize, barley and wheat leaf growth rates decreased within minutes to hours in response to increased soil mechanical impedance (Masle and Passioura, 1987; Beemster et al., 1996; Young et al., 1997). Similar results were observed in young broccoli plants, where leaf area was decreased in response to increased soil bulk density (Montagu et al., 2001). Consequently, decreased dry biomass due to compaction was observed in a wide range of plants including major mono- and dicotyledonous crops already at the seedling stage (Buttery et al., 1998; de Freitas et al., 1999; Montagu et al., 2001; Grzesiak et al., 2013; Tracy et al., 2013; Grzesiak et al., 2014). Decreased crop growth and productivity due to compacted soils was observed not only in young but also in mature plants, which were grown under field conditions (Barraclough and Weir, 1988; Boone et al., 1994; Czyż, 2004; Botta et al., 2006; Botta et al., 2010; Siczek and Lipiec, 2011; Arvidsson et al., 2014; Arvidsson and Håkansson, 2014).

1.4.3. Differences in the susceptibility to soil compaction between species and genotypes

In spite of the similar responses of different crops to soil compaction, it is known that species may significantly differ in their susceptibility to compacted soils. Compaction induced yield decreases of legumes were reported to be larger in comparison to yield penalties in cereals (Arvidsson and Håkansson, 2014). Also root growth may be more or less affected by soil compaction when comparing

different species. Maize roots were reported to be more sensitive to increased mechanical impedance than roots of soybean or small grain cereals (Bushamuka and Zobel, 1998; Busscher et al., 2000b; Grzesiak et al., 2014). Not only between but also within single crop species differences in the tolerance to soil compaction have been demonstrated. Genetic variability with respect to the capability of roots to penetrate compacted soil layers was observed among different wheat genotypes (Kubo et al., 2004; Kubo et al., 2006). Also when comparing root numbers under compaction among different triticale, maize, narrow-leafed lupin or soybean genotypes genetic diversity could be shown (Bushamuka and Zobel, 1998; Grzesiak et al., 2014; Chen et al., 2014b). These genetic differences were also related to differences in shoot biomass under compaction between the genotypes assessed (Kubo et al., 2006; Chen et al., 2014b). Furthermore, it was observed that root morphological and anatomical properties like root or stele diameter and cortical cell size predict bending and tensile strength of different maize genotypes (Chimungu et al., 2015a). There is also theoretical and experimental evidence that the geometry of the root tip relates to the ability of roots to penetrate compacted soil. Theoretical considerations showed that the shape of a root tip affects how cavities are expanded when roots elongate in soil, which then relates to the involved forces and stresses (Greacen et al., 1968). Similar to this, it has been observed that roots lacking of a root cap exert higher penetration stresses and compact the soil at their forefront when growing through soil. Both of these phenomena resulted in decreased root growth of decapped roots compared to roots, which have an intact root cap (Iijima et al., 2003b; Vollsnes et al., 2010).

1.5. Aims and structure of the thesis

Despite the information about plant responses to soil compaction and comparisons between species and genotypes, relatively little is known about how yields can be recovered after compaction. In order to identify possible strategies for this, detailed understanding of root-soil relationships is needed. Multi-level phenotyping is a promising approach to better understand how roots respond to soil compaction, to identify root traits that help to maintain plant productivity under conditions of compaction and to evaluate how different soil management approaches affect whole plant development.

1.5.1. Research aims and hypotheses

The overall aim of the presented thesis was to identify strategies, which contribute to the recovery of crop yields after arable soil was compacted. Possible approaches include on the one hand soil management operations such as tillage and soil perforation that may remediate particular adverse effects of soil compaction on plant growth. On the other hand such approaches refer to the breeding of new crop cultivars, in which specific root traits are integrated that enable the plant to tolerate compaction induced stresses. Both strategies aim to enhance root growth, which does not only increase crop productivity but will also help to restore certain soil physical functions, which were adversely changed due to compaction. In order to evaluate these approaches, the following hypotheses were made:

Hypothesis 1: Phenotypic responses to soil compaction are comparable between plants grown in the field and plants grown under controlled conditions in soil columns. Hence, soil columns may serve as a model system for the field.

Hypothesis 2: There is genetic variability with respect to responses and the tolerance to soil compaction within a single crop species, which potentially can be used in plant breeding programmes. This encompasses traits that facilitate penetration of compacted soils and traits that increase shoot growth under compaction.

Hypothesis 3: Roots grow actively towards artificial macropores that were inserted into compacted soil leading to increased crop productivity in comparison to plants grown on compacted soil without artificial macropores.

1.5.2. Use of multi-level phenotyping

The outlined hypotheses were tested using the approach of multi-level phenotyping in combination with quantifications of soil physical parameters. Experiments were conducted in the field and in soil columns, which were used as a model system under controlled conditions. All field experiments were performed in the soil structure observatory (SSO), which was established as a long-term field experiment at Agroscope Zurich (8°31' E, 47°27' N, 443 m above sea level). The overall aim of the SSO is to quantify natural phenomena involved in the recovery of soil structure and soil physical

functions after compaction. This includes abiotic processes such as shrink-swell and freeze-thaw cycles as well as biotic processes like earthworm and plant root bioturbation. In March 2014 parts of the field were compacted by multiple track-by-track passing with a heavy four wheel agricultural vehicle. The total weight of the vehicle was 34 t and the tyre inflation pressure was 3.2 bar resulting in a wheel load of 80 kN. After compaction different soil management treatments including crop rotations with and without tillage, permanent grass-legume mixture and bare soil were installed in the SSO in three blocks. For experiments in soil columns, homogenized and sieved field soil from the SSO was used. Depending on the aims of the different chapters, different soil physical properties such as bulk density, mechanical impedance or fluid transport characteristics were quantified (Supporting Information Table S1.1).

Irrespective of the scale, plant phenotypic properties were quantified on different organizational levels of plants ranging from the plant tissue to the canopy level (Figure 1.1). Consequently different methodological approaches were used to assess different root phenotypic properties. Root anatomy was evaluated from root cross sections by means of bright field microscopy. High-resolution flatbed scans combined with automatic image processing enabled to quantify root tip geometry. X-ray computed tomography was used to determine root architecture, root system development, root morphology and root-soil interactions. Furthermore, root system architecture and root morphology was quantified from excavated root stocks following the shovelomics approach and rooting depth was assessed from soil cores. These evaluations were complemented by quantifications of shoot traits such as leaf area and leaf area index measurements and the determination of shoot biomass and leaf growth rates (Supporting Information Table S1.1).

1.5.3. Chapter overview

In chapter 2 the main objective was to evaluate, whether phenotypic responses to soil compaction are comparable between the field and controlled conditions. Furthermore, these responses were compared between monocotyledonous (triticale, × *Triticosecale*; winter wheat, *Triticum aestivum* L.) and dicotyledonous (soybean, *Glycine max* L.) species and related to soil physical properties, which characterize compacted soil. Root phenotyping in the field was based on shovelomics, including

architectural and morphological quantifications and measurements of rooting depth from soil cores. Under controlled conditions, root architecture and morphology were determined by means of X-ray computed tomography. Root anatomy was quantified in root cross sections from plants grown in the field and soil columns using bright field microscopy. Furthermore, dry shoot biomass and leaf area index were determined as plant vigour indicators. Soil physical properties were quantified by bulk density measurements and cone penetrometer tests.

In chapter 3 the geometry of root tips was used to predict root elongation rates under different levels of soil mechanical impedance in fourteen winter wheat varieties (*Triticum aestivum* L.). After 48 hours of growth at three levels of soil bulk density, roots were washed from the soil and root tip geometry, root elongation rate and root diameter were assessed from high-resolution flatbed scans. This enabled to evaluate the influence of root tip geometry on soil penetration capability. The information about the shape of the root tips was combined with cone penetrometer measurements what allowed estimating forces and penetration stresses occurring during root growth. Using these physical quantities, the influence of different root tip geometries on cavity expansion was discussed. Furthermore, root anatomy and morphology was quantified in plants of the same varieties, which were grown for 23 days under the same soil bulk densities. These root morphological and anatomical quantities were used to determine mechanical and physiological implications of root adjustments to increased soil mechanical impedance.

In chapter 4 the genetic diversity of root architectural traits and early plant vigour in wheat (*Triticum aestivum* L.) under three different levels of soil compaction was assessed. Fourteen winter wheat varieties were grown for 23 days in soil columns and root system development as well as shoot growth was quantified in weekly intervals. The number of axial and lateral roots was counted manually from reconstructed X-ray computed tomography scans. At the same time plant height, leaf and tiller number were determined what enabled to relate root system to shoot development. These quantifications were complemented by final shoot and root biomass measurements and cone penetrometer tests. Furthermore, heritability estimations were performed to determine how stable root and shoot traits are when plants are exposed to compacted soils.

In chapter 5 the interaction of roots with artificial macropores, which were inserted into compacted soil and their influence on plant growth was quantified. Furthermore, it was tested whether roots grow actively towards these artificial soil macropores. The experiments were performed in the field and under controlled conditions in soil columns with soybean (*Glycine max* L.), winter wheat (*Triticum aestivum* L.) and maize (*Zea mays* L.). Compacted soil was perforated along a 2 by 2 cm grid with stainless steel wires. Soil cores of 10 cm diameter and height were excavated from the field and scanned with an X-ray computed tomography system. Under controlled conditions plants were grown for 20 days until scanning. From these scans, root-macropore interactions could be quantified and it could be determined whether roots grew actively towards these pores. Plant vigour quantifications consisted of shoot and root dry weight measurements and the determination of leaf area with respect to different leaf positions at the shoot. Soil bulk density, mechanical impedance, air permeability and gas diffusivity were quantified to characterize the soil physical properties.

Chapter 2: Root responses of triticale and soybean to soil compaction in the field are reproducible under controlled conditions

Tino Colombi[1,*] and Achim Walter[1]

[1]ETH Zurich, Institute of Agricultural Sciences (IAS), Zurich, Switzerland

[*]Corresponding author. Email: tino.colombi@usys.ethz.ch

Abstract

Soil compaction includes a set of underlying stresses, which limit root growth such as increased impedance and limited oxygen availability. The current study aimed i) to find acclimations of triticale ($\times$ *Triticosecale*) and soybean (*Glycine max* L.) roots to compacted soils in the field, ii) which are reproducible under controlled conditions and iii) to associate these responses with soil physical properties. Plants were grown at two different soil bulk densities in the field and under controlled conditions representing mature root systems and the seedling stage, respectively. Diameters, lateral branching densities, the cortical proportion within the total root cross section and the occurrence of cortical aerenchyma of main roots were quantified. Soil compaction caused decreasing root branching and increasing cortical proportions in both crops and environments. In triticale, root diameters and the occurrence of aerenchyma increased in response to compaction in the field and under controlled conditions. In soybean, these acclimations occurred at an initial developmental stage but due to radial root growth not in mature roots. These results showed that responses of root systems to compacted soils in the field are to a large extent reproducible under controlled conditions, enabling increased throughput, phenotyping-based breeding programmes in the future. Furthermore, the occurrence of aerenchyma clearly indicated the important role of limited oxygen availability in compacted soils on root growth.

2.1. Introduction

Soil compaction is a major threat to arable land especially in regions where mechanized agriculture dominates (Hamza and Anderson, 2005; Batey, 2009). In Europe and on a global level it is estimated that 33 million (Van den Akker and Canarache, 2001) and 68 million hectares (Hamza and Anderson, 2005), respectively, of arable land are degraded by soil compaction, which is mainly caused by heavy agricultural machinery (Tracy et al., 2011). Especially macro- and mesopores disappear during soil compaction resulting in decreased soil porosity and pore connectivity (Chen et al., 2014a) and increased soil bulk density (Hernandez-Ramirez et al., 2014; Kuncoro et al., 2014a). These initial effects of soil compaction on soil physical properties cause a set of subsequently altered properties affecting plant productivity: On the one hand increased levels of soil compaction cause increased mechanical impedance (Valentine et al., 2012; Hernandez-Ramirez et al., 2014). On the other hand soil compaction causes slower water infiltration rates (Lipiec and Hatano, 2003) and reduces hydraulic conductivity (Ozcoban et al., 2013), air permeability (Chen et al., 2014a; Kuncoro et al., 2014b) and gas diffusivity (Kuncoro et al., 2014b) resulting in higher risks of water logging and anaerobic conditions (Tracy et al., 2011). Both increased penetration resistance and the risk of anaerobic conditions decrease root growth and therefore the agricultural productivity in production systems that are affected by soil compaction (Hamza and Anderson, 2005; Batey, 2009; Walter et al., 2009; Tracy et al., 2011; Valentine et al., 2012). The severity of soil compactness is usually quantified by measurements such as soil porosity, bulk density and mechanical impedance (Barraclough and Weir, 1988; Materechera et al., 1992; Arvidsson and Håkansson, 2014; Hernandez-Ramirez et al., 2014). These measurements are often preferred over more laborious methods such as the analysis of gas diffusivity, air permeability or hydraulic conductivity to describe the level of soil compaction. However, various studies showed that increased soil bulk densities and therefore increased penetration resistances are correlated with decreased hydraulic conductivity, air permeability or gas diffusivity (Czyż, 2004; Simojoki et al., 2008; Kuncoro et al., 2014b).

Despite the amount of information about processes happening during compaction, relatively little information is available about processes during the recovery of compacted soils. Besides abiotic

phenomena such as wetting-drying cycles, bioturbation by plant roots was suggested to play a crucial role during the recovery of compacted soils (Dexter, 1991; Lesturgez et al., 2004). In order to accelerate soil recovery by root bioturbation, root traits are needed, which enable the plant to maintain or enhance root growth in compacted soil. A broad understanding of the phenotypic responses of root systems to soil compaction is required (Hamza and Anderson, 2005) to identify such root system traits. Root system architecture, which describes coarse structures and the spatial configuration of root systems in the soil (Lynch, 1995), is altered by soil compaction. In small soil columns lateral root number of different small grain cereals (Grzesiak et al., 2014; Pfeifer et al., 2014a) and tomato (Tracy et al., 2012b) grown under controlled conditions decreased in response to increased soil bulk density and impedance. In similar experiments it has also been observed that axial root numbers of wheat and triticale (Coelho Filho et al., 2013; Grzesiak et al., 2013) were smaller in compacted than uncompacted soil. Furthermore, soil compaction in small soil columns caused increased root diameters in small grain cereals (Grzesiak et al., 2013; Pfeifer et al., 2014a), tomato (Tracy et al., 2012b), soybean (Ramos et al., 2010) and pea (Iijima and Kato, 2007; Siczek et al., 2013). Recent advances in the development of high-resolution X-ray micro computed tomography enabled to study root architectural traits in soil columns over time with a minimum of disturbance to the plant (Hargreaves et al., 2009; Flavel et al., 2012; Mairhofer et al., 2012).

Such studies under controlled conditions have the advantage that they enable far higher throughputs than field studies. Furthermore, soil moisture contents and therefore also mechanical impedance can be controlled and anaerobic conditions are generally avoided (Coelho Filho et al., 2013; Grzesiak et al., 2013; Pfeifer et al., 2014a). In the field instead, soil water contents are fluctuating over the growing season and especially after heavy rainfalls anaerobic conditions occur due to poor water infiltration rates on compacted soils (Batey, 2009). Only a limited number of studies dealing with root architectural traits under soil compaction were conducted in the field so far. Results from soil cores showed that rooting depths of wheat (Barraclough and Weir, 1988) and soybean (Botta et al., 2010) decreased in response to soil compaction. Specific root lengths of small grain cereals (Barraclough and Weir, 1988; Hernandez-Ramirez et al., 2014) and mean root diameters of cereals and pea (Materechera et al., 1992; Hernandez-Ramirez et al., 2014) were larger in compacted soils

20

compared to uncompacted plots. Using soil cores, root system architecture traits such as axial or lateral root number and root diameters cannot be measured directly. Instead, averaged diameters or specific root lengths serve as proxy measurements for actual architectural traits. The recently published "shovelomics" method enables to evaluate a set of root architectural traits from excavated root systems at relatively high throughput (Trachsel et al., 2011). Shovelomics allowed to quantify architectural differences among sets of different maize (Trachsel et al., 2011; Colombi et al., 2015) and cowpea genotypes (Bucksch et al., 2014). Using shovelomics, Chen et al. (2014b) observed increased taproot diameters under soil compaction compared to uncompacted conditions in narrow-leafed lupins.

Beside architectural responses to soil compaction, anatomical traits are also affected by increased soil strength. So far these results are restricted to a few studies, which were all conducted under controlled conditions. In response to soil compaction root cortical areas were increased in roots of cereals (Lipiec et al., 2012), pea (Iijima and Kato, 2007) and saplings of narrow-leaved ash (Alameda and Villar, 2012). Generally, these root architectural and anatomical acclimations were either associated with increased bulk densities and impedances or just with soil compaction without further specifications. Just two studies (Iijima and Kato, 2007; Hernandez-Ramirez et al., 2014) suggested a link between reduced gas and solute transport rates and altered root phenotypes. The ability to reproduce results from the field under controlled conditions and at high throughputs will be crucial for successful incorporation of desired traits into breeding programmes.

This study aimed to find i) responses of root architecture and anatomy in mature roots of triticale and soybean to soil compaction in the field, which ii) can be reproduced under controlled conditions in young roots and to iii) link these phenotypic responses to altered soil physical properties caused by soil compaction. Crops were grown in the field and under controlled conditions with the same soil at two different soil bulk densities. Root architectural responses to soil compaction were evaluated using shovelomics and X-ray computed tomography and root anatomical traits were quantified by bright field microscopy. These evaluations were complemented by measurements of soil bulk density, mechanical impedance and plant vigour traits.

21

2.2. Material and Methods

Both, laboratory and field experiments were conducted with the same loam soil (Pseudogleyed Cambisol) composed of 25% clay, 50% silt and 25% sand. For the experiments under controlled conditions field soil was taken from the top 15 cm.

2.2.1. Root nomenclature and abbreviations

For triticale four different root classes have been looked at: the primary root (PR), seminal roots (SR), nodal roots (NR) and lateral roots (LR) of PR, SR and NR. For nodal roots the whorl from which they emerged was considered in the nomenclature as a subscript (i.e. NR_{No1} and NR_{No3} mean the nodal root from the oldest and third oldest whorl, respectively). In soybean, traits at the taproot (TR) and adventitious roots (AR) were measured. Thereby the roots emerging between the soil level and the location where the seed was placed were named as AR (Figure 2.1).
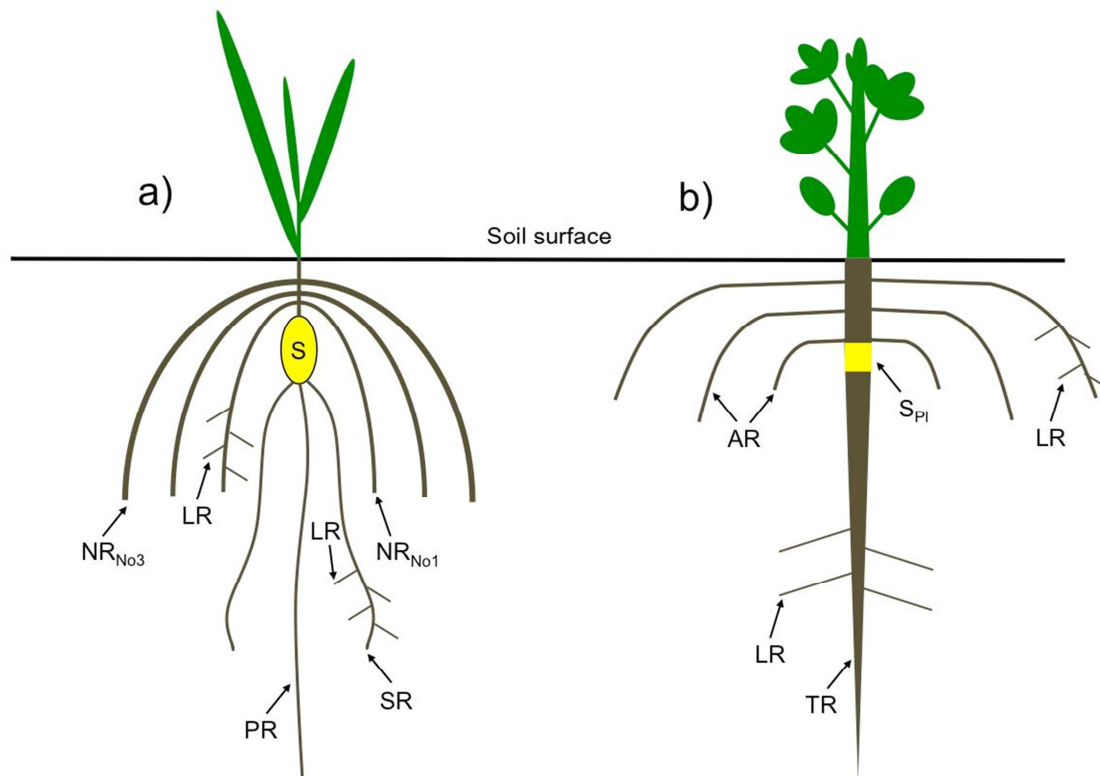
Figure 2.1: Schematic illustration of a) triticale root system with seed (S), primary (PR), seminal (SR) and nodal roots from the first (NR_{No1}) and third whorl (NR_{No3}) and lateral roots (LR). b) Soybean root system with location where the seed was placed (S_{Pl}), taproot (TR), adventitious roots (AR) and lateral roots (LR).

2.2.2. Experiment I: field conditions

The field site is located near Zurich, Switzerland at the agricultural research station of Agroscope Reckenholz (8°31' E, 47°27' N, 443 m above sea level). In spring 2014 the soil structure observatory (SSO) was established as a block experiment with three replications. The aim of the SSO is to study processes that drive the recovery of compacted soils including both abiotic processes such as shrink-swell cycles and biotic processes like bioturbation by plant roots and earthworms. One year before soil compaction a perennial grass-legume mixture was established. For the first year of the SSO experiment, soybean (*Glycine max* L., variety Merlin) and triticale (× *Triticosecale*, variety Trado) stands were established as model dicot and monocot crops of global and regional importance.

2.2.2.1. Soil compaction and tillage

At the end of March 2014 parts of the field were compacted using a fully loaded self-propelled agricultural vehicle with four wheels and a tyre width of 1.05 m. With a total weight of the vehicle of 34 t and a tyre inflation pressure of 3.2 bar, the wheel load was 80 kN. The soil in the soybean field was turned with a mouldboard plough prior to compaction to avoid severe weed pressure. Soil compaction was done by triple track-by-track passing at soil moisture content around field capacity. Remaining plants from the previous grass-legume stand were sprayed with glyphosate solution. The soil in the control plots of both crops (Ctrl), which were not compacted, was tilled conventionally with a mouldboard plough to a depth of approximately 22 cm. One half of the compacted plots intended for triticale were ploughed in the same way to simulate subsoil compaction (SSCom). In a third treatment the topsoil remained compacted (TSCom) and the triticale seeds were sown into the compacted soil using a direct seed drill. To ensure proper germination of the soybean the top 5 cm of the compacted soil (Com) were tilled using a chisel plough.

2.2.2.2. Plant material and growth conditions

Summer triticale was sown on the 3rd of April 2014 at a density of 280 individuals per m^2 and fertilised with 93.2 kg N ha^{-1}, 105 kg K ha^{-1} and 8.5 kg Mg ha^{-1}. Total precipitation from sowing to harvest was 435 mm and mean daily minimum and maximum temperatures were 10.3°C and 20.3°C, respectively. Soybean seeds were inoculated with rhizobia of the species *Bradyrhizobium japonicum*

(*HiStick, Becker Underwood, BASF, Little Hampton, United Kingdom*). Seeds were sown on the 20th of May 2014 at a density of 60 plants per m^2 and fertilised with 50 kg K ha^{-1} and 4.3 kg Mg ha^{-1}. The mean daily minimum and maximum temperatures during the growth period were 11.9°C and 21.3°C, respectively and the cumulative precipitation was 528 mm. Crop protection measures for both crops were applied if needed according to good agricultural practice.

2.2.2.3. Soil physical properties

Soil bulk densities were determined shortly after sowing in two depths at three different points in each plot. Undisturbed soil samples of 100 ml were taken from 10 and 30 cm depth and oven dried at 105°C for at least 4 days to determine dry bulk density. Mechanical impedance was measured using an Eijkelkamp penetrologger (*Eijkelkamp Agrisearch Equipment, Giesbeek, The Netherlands*) with a cone base area of 1 cm^2 and an apex angle of 60°. Five insertions were done in each plot and measured impedance values were averaged over 10 cm segments. The gravimetric water contents at measurement were around 24%.

2.2.2.4. Root system architecture

Root system architectural traits were determined for both crops 42 and 91 days after sowing (DAS). For triticale these time points represented the stage of tillering and full flowering, while for soybean they corresponded to the stage of side-shoot initiation and major grain filling. Per plot the root systems of four individual plants were excavated with a shovel in a cylinder of 25 cm diameter and depth. The excavated samples were put in soap water for about 30 min to facilitate washing.

Using the scoreboard approach (Colombi et al., 2015) several root architectural traits were determined manually. For triticale this included the number of whorls occupied with nodal roots, the number of NR and for soybean the number of AR. Lateral branching density expressed as lateral root number per cm of main root was determined in triticale at one representative NR from the first whorl and in soybean at one representative AR and at the TR. Lateral roots were counted in 2 cm segments starting at 4 and 9 cm from the root base. Furthermore, the outermost angle of the root system to the soil surface was measured along an arc with a radius of 5 cm for both crops at a 5° scale. To determine root diameters high-resolution pictures (pixel edge length: 70 to 80 μm) of single roots were taken

with an 18 megapixel camera (*Canon EOS 600D, Canon, Tokyo Japan*), which was mounted on a

tripod with external illumination sources. Together with a size reference images were taken of one

representative NR_{No1} and NR_{No3}, the TR and of one representative AR per excavated root system.

Diameters were measured in ImageJ version 1.49g (*National Institute of Health, Bethesda MD, United States*) 5 and 10 cm from the root base, respectively.

To gain an idea about rooting depth, three soil samples of 5 cm diameter and 50 cm length per plot

were taken using a petrol-run soil driller (*humax Bohrsonden, Martin Burch AG, Rothenburg Switzerland*) at 91 DAS. These samples were cut into 10 cm segments and roots were washed out over

a fine meshed sieve and cleaned from other organic material. The roots were oven dried at 60°C, their

dry mass was recorded and the depths at which 95% of the roots occurred (D95) were linearly

interpolated.

2.2.2.5. Root anatomy

Root samples for anatomical evaluation were taken from the root systems sampled at 91 DAS. In

triticale one representative NR from the first and third whorl were sampled. In soybean one

representative AR and the TR were evaluated. Roots were fixed and stored at 4°C in FAA (acetic

formaldehyde:alcohol:acetic acid:distilled water; 10:50:5:35) until processing. Even though severely

damaged roots had to be discarded from certain analyses, anatomical traits of two to four roots of all

root classes (NR_{No1}, NR_{No3}, TR, AR) could be evaluated from each single plot. Cross sections of 100

to 200 μm thickness were cut by hand with a razorblade and stained for 1 min with toluidine blue

solution (0.25% in distilled water). In triticale cross sections were taken at 2 and 5 cm from the root

base, whereas cross sections from soybean roots were taken at 5, 10 and 15 cm from the root base. The

cross sections were placed on a glass slide and photographed by a camera with a resolution of one

megapixel (*Olympus XC10, Olympus Corporation, Tokyo, Japan*) connected to a microscope

(*Olympus AX70, Olympus Corporation, Tokyo, Japan*). Root anatomical properties were evaluated

from TIFF images in ImageJ using a pen track-pad. The area of the total cross section and the area of

the vascular cylinder (ArV) were measured in mm^2. By subtracting ArV from the total area the cortical

area (ArC) in mm^2 was obtained. The cortical proportion (ArCP) expressed in percent was calculated

as the share of ArC in the total cross section area. Furthermore, the percentage of root cortex

aerenchyma (RCA) within the root cortex was measured (Table 2.1).

Table 2.1: Abbreviations of focal root anatomical traits of triticale and soybean.

Abbreviation	Trait description	Unit
ArV	Vascular Area	mm^2
ArC	Cortical area	mm^2
ArCP	Cortical proportion in total cross section area	%
RCA	Aerenchyma proportion in root cortex	%

2.2.2.6. Plant vigour measurements

One day before the excavation of the root systems at both time points (42 and 91 DAS) leaf

greenness of the same plants was recorded using a SPAD-meter (*SPAD-502, Konica, Tokyo, Japan*).

Reported values represent average values of three individual measurements performed at the youngest

fully developed leaf. Shoots of the plants used for root system measurements were dried at 60°C for

three days and the shoot dry mass was determined. The number of tillers and side shoots were counted

in triticale and soybean, respectively, at both time points. Furthermore, the leaf area index (LAI) was

measured as an indicator for the vigour of the entire canopy. Five measurements in each plot were

conducted with a LAI meter (*LAI-2200C, LI-COR Inc., Lincoln NE, United States*) under constant

light conditions.

2.2.3. Experiment II: controlled conditions

2.2.3.1. Treatments and growth conditions

Field soil was air dried to approximately 20% gravimetric water content, homogenized and sieved

through a 2 mm sieve. To mimic the conditions of the field, soil was packed to 1.34 g cm^{-3} and 1.6 g

cm^{-3} as the loose (Ctrl) and compacted (Com) treatment, respectively. The soil was packed into small

columns of 3.4 cm diameter and 15 cm height in six segments of 2 cm height. To ensure homogeneous

packing surfaces of each layer were slightly abraded prior to packing another layer. The columns were

open at the bottom in order to avoid standing water. Seeds of triticale and soybean were germinated

for 48 hours at 24°C and seeds with radicles of the same length were selected. On top of the packed soil a 0.5 cm layer of loose soil (1 g cm^{-3}) was added. A hole of 1 mm diameter and 7 mm length was inserted in the centre into which the emerged radicle was placed and seeds were covered with 1.5 cm loose soil (1 g cm^{-3}). The same inoculant used in the field was added to the soybean seeds. Plants were grown throughout 14 days in a growth chamber at a relative humidity of 65%, mean day and night temperatures of 18.7°C and 24.1°C, respectively and 14 h light per day. In order to mimic wet but not waterlogged conditions, soil moisture content was kept at field capacity during the entire growth period by daily weighing. Additionally, winter wheat (*Triticum aestivum* L., variety Arina) as a cereal crop of global importance was grown under the same conditions. Every treatment was replicated four times.

Mechanical impedance was determined in three additional soil columns of the same bulk densities at field capacity using a cone with an apex angle of 60° and a cone base area of 0.2 cm^{2}, which was connected to a force transducer (*LC703, OMEGA Engineering Inc., Stamford CT, United States*). In each sample the cone was inserted three times to a depth of 1.5 cm resulting in approximately 1500 force measurements per insertion. The measured force values were divided by the cone base area and averaged for each column.

2.2.3.2. Root system architecture measured with computed tomography

The top 5 cm of the soil columns were scanned with an X-ray micro computed tomography system (Phoenix v|tome|x s 240; GE Sensing and Inspection Technologies GmbH, Wunstorf, Germany) 2, 5, 8, 11 and 14 days after sowing (DAS). The scanner was set at 100 kV, 370 μA, with 0.4 mm copper filter and binning of 2 by 2 voxel was used to reduce noise in the scans. Per scan 1600 images (no averaging) were acquired resulting in scan times of 12 minutes and a voxel edge length of 50 μm. To check for influences of X-ray radiation on plant dry mass production, two additional columns of each treatment were added, which were not scanned. Root architectural parameters were obtained manually from reconstructed volume files in Visual Studio Max 2.2 (*Volume Graphics GmbH, Heidelberg, Germany*). Initial root penetration into packed soil was determined from the reconstructed volume files of the first scan 2 DAS. At each time point the number of LR was counted for PR and SR of cereals

and TR of soybean in a 2 cm segment starting 2 cm from the root base. The diameter of the primary root and one representative seminal root in triticale and wheat and the taproot in soybean were measured 3 cm from the root base. At the end of the growth period also the number of NR and the number of AR were counted in both cereal species and soybean, respectively from cleaned root systems.

2.2.3.3. Root anatomy

After 14 days of growth, the soil columns were emptied gently and the soil was rinsed from the intact root systems. For root anatomical analysis, segments of 1 cm length were sampled 3 cm from the root base of the PR and SR for triticale and of the TR for soybean. The procedure of tissue fixation, sample preparation and trait quantification was the same as described above. In winter wheat samples for anatomical measurements were taken from the PR only.

2.2.3.4. Plant vigour

To determine leaf greenness three measurements at the youngest fully developed leaf were conducted 14 DAS with a SPAD-meter and averaged. Afterwards shoots were removed, the root systems were washed and roots and shoots were dried at 60°C for at least three days before weighing.

2.2.4. Statistical evaluation

For statistical evaluation analyses of variance (ANOVA) were performed and means were compared using ANOVA least significant difference (LSD) tests. All calculations were performed in R *version 3.1.3* (R Core Team, 2015). The soil physical properties were evaluated per depth for both crop stands together using the compaction level ($i = 5$, TSCom, SSCom and Ctrl for triticale and Com and Ctrl for soybean) as explanatory variable. Root and shoot related traits were evaluated separately for each crop. Plant vigour, root architectural traits and anatomical traits from experiment II were evaluated using one way ANOVAs with the compaction levels as explanatory variables. Root anatomical parameters from field samples were evaluated with the following model:

$$Y_{ij} = \mu + \alpha_i + \beta_j + (\alpha\beta)_{ij} + \varepsilon_{ij} \quad (2.1)$$

where Y is the plot-mean trait value of each root class (NR_{No1}, NR_{No3}, TR, AR) of the ith compaction treatment (for triticale: i = TSCom, SSCom, Ctrl; for soybean: i = Com, Ctrl) and at the jth distance (for triticale: j = 2 cm, 5 cm; for soybean: j = 5 cm, 10 cm, 15 cm); α is the effect of the compaction treatment, β the effect of the distance of the evaluated cross section from the root base, $\alpha\beta$ the effect of the interaction between the compaction treatment and the distance from the root base and ε the residual error. All effects were treated as fixed effects.

2.3. Results

### 2.3.1. Experiment I: field conditions

2.3.1.1. Physical soil properties

Soil bulk density and mechanical impedance were significantly affected by the compaction and tillage operations. Compaction without subsequent ploughing in the triticale field (TSCom) or just shallow chiselling to a depth of 5 cm in the soybean field (Com) resulted in a bulk density of 1.51 g cm^{-3} and 1.46 g cm^{-3}, respectively, at 10 cm depth. The bulk density at 10 cm depth in both control treatments (Ctrl) which were not compacted and in the treatment, which received conventional inversion tillage after compaction (SSCom), was around 1.35 g cm^{-3}. At 30 cm depth the bulk densities did not differ significantly among the different compaction and tillage treatments except for the Ctrl group of triticale (Table 2.2). The highest mechanical impedance in the top 10 cm was measured in TSCom with 1.97 MPa followed by Com in the soybean plots with 1.14 MPa. In both Ctrl treatments and in the SSCom treatment impedance values below 1 MPa were measured in the top 10 cm. In the following two depths from 10 to 20 cm and from 20 to 30 cm the impedance values in TSCom and Com remained significantly higher than in SSCom and both Ctrls. Between 30 and 40 cm the mechanical impedance did not differ significantly between treatments (Table 2.2).

2.3.1.2. Root system architecture

At the first sampling time point 42 DAS triticale grown under topsoil compaction showed a significant reduction in the number of whorls occupied with nodal roots. In TSCom one to two whorls where developed, whereas in the other treatments (SSCom and Ctrl) two to three whorls were counted. 91 DAS the lowest number of whorls was observed again in TSCom with two whorls followed by

29

SSCom with four and Ctrl with five whorls (Table 2.3). Soil compaction significantly decreased the number of nodal roots at both time points. The lowest number was observed in TSCom with 5.1 and 7.7 NR per plant 42 and 91 DAS, respectively. In SSCom 8.4 and 17.0 and in Ctrl 9.9 and 25.3 NR per plant were counted 42 and 91 DAS, respectively (Table 2.3). Furthermore, nodal roots of triticale grew shallower under soil compaction. The smallest angles between the outermost root and the soil surface were observed in TSCom (42 DAS: 35°, 91 DAS: 29°) followed by the SSCom (42 DAS: 45°, 91 DAS: 44°) and the Ctrl group (42 DAS: 59°, 91 DAS: 58°, Table 2.3). Since 42 DAS most root systems showed less than three whorls and root systems in TSCom were poorly developed, architectural traits could just be investigated in NR_{No1} at 5 cm. 91 DAS root systems were much further developed and parameters could be measured 5 and 10 cm from the root base in NR_{No1} and NR_{No3}. Diameters of NR_{No1} measured 5 cm from the root base were significantly increased by soil compaction at both time points (Figure 2.2). At both sampling time points the largest diameters were measured in plants from the TSCom treatment with around 0.9 mm followed by SSCom with around 0.8 mm and Ctrl with around 0.6 mm. 91 DAS the same effects were also observed at 10 cm from the root base of NR_{No1} and 5 cm and 10 cm from the root base of NR_{No3} (Supporting Information Table S2.1). Lateral branching at NR_{No1} decreased in TSCom and SSCom compared to Ctrl at both sampling time points. In the Ctrl treatment 4.9 and 4.4 LR cm^{-1} were counted between 4 and 6 cm from the root base 42 and 91 DAS, respectively. These numbers decreased 42 DAS to 2.4 and 2.8 LR cm^{-1} in SSCom and TSCom, respectively and 91 DAS to 3.4 and 2.5 LR cm^{-1} in SSCom and TSCom, respectively (Figure 2.2). 91 DAS the same responses were also observed between 9 and 11 cm from the root (Supporting Information Table S2.1). Remarkably, even though the topsoil in SSCom was ploughed and showed the same bulk density and impedance values as the Ctrl group (Table 2.2), root diameters and the number of LR of triticale determined in the topsoil were affected in the same way as in TSCom.
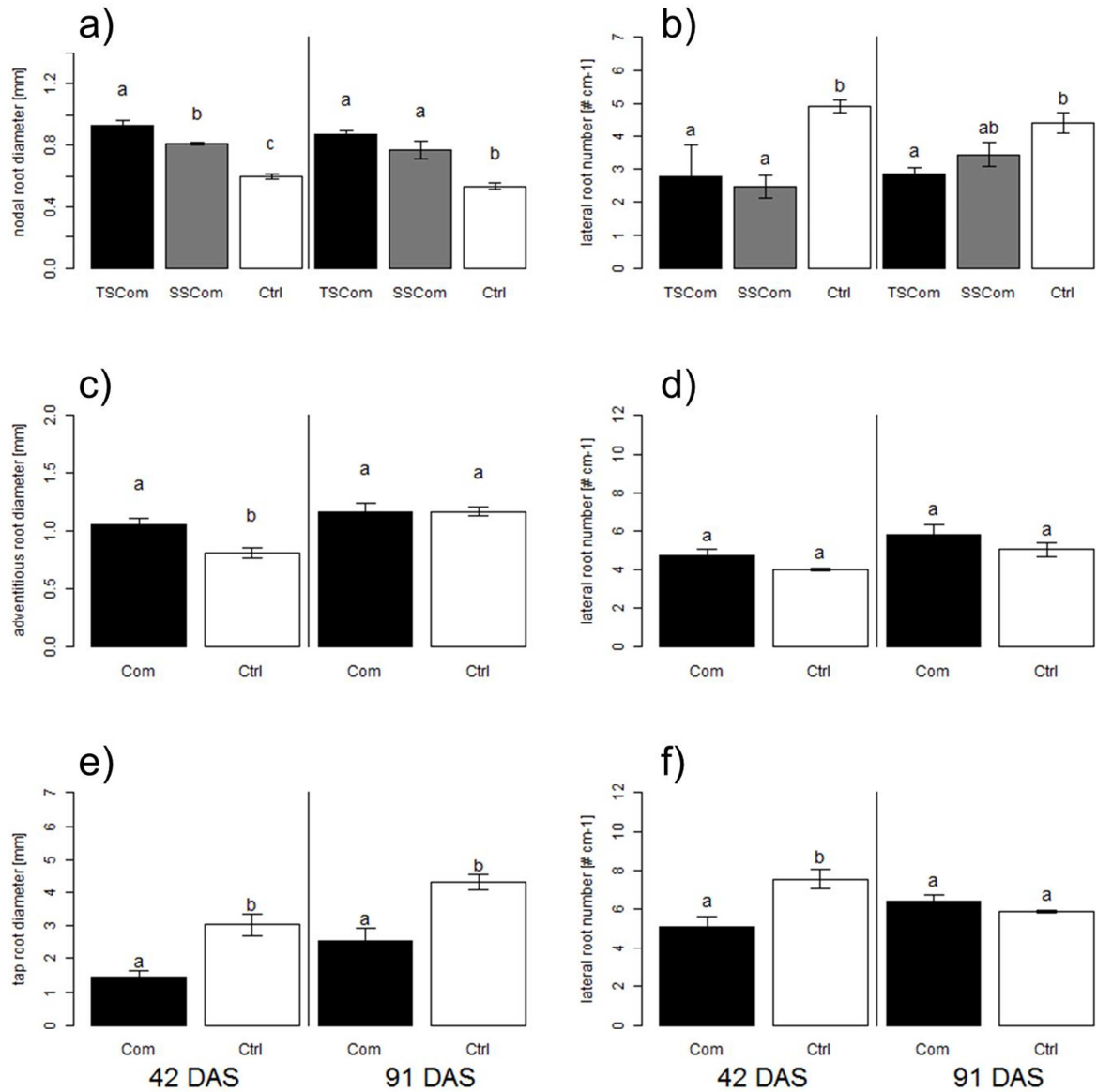
Figure 2.2: Root architectural traits measured 5 cm from the root base of field-grown a) and b) triticale nodal roots from the first whorl under topsoil compaction (TSCom), subsoil compaction (SSCom) and control conditions (Ctrl), c) and d) soybean adventitious roots under soil compaction with shallow tillage (Com) and control conditions (Ctrl) and e) and f) soybean taproots under Com and Ctrl. Different letters indicate significant differences of the means using least significant difference test at $p < 0.05$, error bars represent standard errors ($n = 3$).

Table 2.2: Treatment means of soil physical properties in the field: dry bulk densities and mean penetrometer impedance of 10 cm segments measured in the triticale field under topsoil compaction (TSCom), subsoil compaction (SSCom) and uncompacted conditions (Ctrl) and the soybean field under compaction with shallow tillage (Com) and uncompacted conditions (Ctrl). Different letters indicate significant differences of the means based on ANOVA with least significant difference test at $p < 0.05$ (n = 3).

		Triticale			Soybean		
	Depth	TSCom	SSCom	Ctrl	Com	Ctrl	LSD
Bulk density [g cm^{-3}]	10	1.51^a	1.33^b	1.37^b	1.46^a	1.33^b	0.060
	30	1.58^a	1.56^{ab}	1.49^b	1.55^{ab}	1.50^{ab}	0.085
Mechanical impedance [MPa]	0-10	1.97^a	0.76^{bc}	0.82^{bc}	1.14^b	0.63^c	0.47
	10-20	2.59^a	1.16^c	0.95^c	1.79^b	1.07^c	0.44
	20-30	2.38^a	1.51^b	1.21^b	2.03^a	1.32^b	0.49
	30-40	2.19	1.95	1.81	2.13	2.14	0.48

No significant differences of the number of AR in response to soil compaction were observed for soybean at both sampling time points (Table 2.3). The angle between the root system and the soil surface differed significantly between Com and Ctrl 42 DAS (Com: 32°, Ctrl: 51°) but not 91 DAS (Com and Ctrl: 30°, Table 2.3). Root diameters of soybean roots responded differently to soil compaction than diameters of triticale roots. Roots in an early stage, represented by adventitious roots 42 DAS, showed significantly larger diameters in Com than in Ctrl (Figure 2.2). AR diameters 5 cm from the root base were 1.06 mm under compacted and 0.81 mm under uncompacted conditions. 10 cm from the root base, AR diameters under compacted and uncompacted conditions did not differ significantly (Com: 0.61 mm, Ctrl: 0.53 mm). 91 DAS diameters of adventitious roots were comparable between Com and Ctrl at 5 cm (Figure 2.2) and 10 cm from the root base (Supporting Information Table S2.1). Taproot diameters were decreased in response to soil compaction at both sampling time points (Figure 2.2). Under compaction taproot diameters 5 cm from the root base were 1.5 mm and 2.6 mm 42 and 91 DAS, respectively. These values increased in the uncompacted plots to 3.0 mm and 5.3 mm at the early and late sampling time point, respectively. These results suggested that soybean root diameters in an early stage increased in response to soil compaction. However, subsequent secondary thickening was decreased under compaction leading to smaller root diameters in

Com than Ctrl at later stages. The number of lateral roots emerging from TR was generally reduced under soil compaction but the response to compaction was less pronounced as in triticale. Significantly lower numbers of LR in Com compared to Ctrl were counted 42 DAS at 5 cm from the root base (Figure 2.2). Under compacted conditions the taproot was occupied with 5.1 LR cm^{-1} and 7.5 LR cm^{-1} in the uncompacted treatment. These effects were not observed 91 DAS in the same segment (Figure 2.2) but between 9 and 11 cm from the base (Supporting Information Table S2.1).

In terms of rooting depth 91 DAS, both crops showed the same responses to changed physical soil conditions. Interpolated D95 values in triticale were at 29.2, 36.6 and 38.7 cm depth under TSCom, SSCom and Ctrl, respectively. For soybean under compaction the D95 was at 37.8 cm and under uncompacted conditions at 42.0 cm depth (Table 2.3).

Table 2.3: Treatment means of root architectural traits 42 and 91 DAS from field-grown triticale under topsoil compaction (TSCom), subsoil compaction (SSCom) and without compaction (Ctrl) and field-grown soybean on compacted soil with shallow tillage (Com) and without compaction (Ctrl). Different letters indicate significant differences of the means based on ANOVA with least significant test at $p < 0.05$ (n = 3).

		Triticale			Soybean		
DAS	**Trait**	**TSCom**	**SSCom**	**Ctrl**	**Trait**	**Com**	**Ctrl**
42	Number of whorls	1.4[a]	2.4[b]	2.8[b]			
	Number of NR	5.1[a]	8.4[b]	9.9[b]	Number of AR	16.4	14.3
	Outermost root angle to the soil surface [°]	35.6[a]	45.3[b]	59.2[c]	Outermost root angle to the soil surface [°]	32.1[a]	50.8[b]
91	Number of whorls	2.1[a]	4.1[b]	5.0[c]			
	Number of NR	7.7[a]	17.0[b]	25.3[c]	Number of AR	18.0	18.4
	Outermost root angle to the soil surface [°]	27.1[a]	44.4[b]	58.3[c]	Outermost root angle to the soil surface [°]	30.4	30.4
	D95	29.2[a]	36.6[ab]	38.7[b]	D95	37.8[a]	42.0[b]

Abbreviations: NR = nodal root, AR = adventitious root, D95 = depth at which 95% of the roots occur

2.3.1.3. Root anatomy

As observed for root architectural traits, most anatomical traits responded significantly to soil compaction, again either consistent or contradictory among different species and root classes.

In triticale the area of the vascular cylinder was not affected by the soil compaction treatments whereas both measurements of the cortical area (ArC and ArCP) responded to soil compaction (Table 2.4). In Ctrl the cortex at 2 cm from the root base of NR_{No1} made up 51% of the total cross section area, this proportion increased in SSCom to 77% and in TSCom to 83%. The same responses of ArCP were measured in cross sections of NR_{No1} taken from 5 cm from the root base (Ctrl: 48%, SSCom: 70%, TSCom: 87%). Furthermore, soil compaction had a tremendous influence on the formation of root cortex aerenchyma (Table 2.4). In cross sections taken at 2 cm from the root base of NR_{No1} aerenchyma occupied 35% and 14% of the root cortex in TSCom and SSCom, respectively, whereas in Ctrl the formation of aerenchyma was not observed (Figure 2.3). Due to large variation in SSCom, similar but insignificant differences of RCA in response to the compaction treatments were found at 5 cm from the root base. Since plants in TSCom did not develop a third whorl occupied with nodal roots, traits of NR_{No3} could only be compared between SSCom and Ctrl. At NR_{No3} the compaction treatment had no significant influence on any measured anatomical trait (Table 2.4). Except for ArV and ArC of NR_{No3} the distance from the base of root at which cross sections were taken had no significant effect on anatomical traits. No anatomical trait showed any response to the interaction between the distance from the root base and the compaction treatment (Table 2.4).

As observed for triticale, the interaction between the compaction treatment and the distance from the root base, at which cross sections were taken, had no significant influence on anatomical traits in soybean (Table 2.4). Anatomical traits of the taproot responded significantly to the distance at which the cross sections were cut (Table 2.4). Significant responses of the anatomy of soybean TR to soil compaction were observed for ArV, ArC and ArCP (Table 2.4). Mean values for ArV and ArC of the cross sections taken at three distances from the root base (5, 10 and 15 cm) decreased under compaction by 75% and 65%, respectively, compared to the control treatment. The values for the cortical proportion in the total cross section were increased due to compaction, being most pronounced in samples at 5 and 10 cm from the root base. In sections taken at 5 cm from the root base ArCP was 40% in Com and 34% in Ctrl and at 10 cm 53% in Com and 38% in Ctrl. The occurrence of root cortex aerenchyma in the taproot was not affected by soil compaction (Figure 2.3) while for adventitious roots the occurrence of RCA was affected by soil compaction (Table 2.4). In cross

sections taken at 15 cm from the root base, RCA occupied 24% of the root cortex of AR in Com and 6% in Ctrl. At 5 and 10 cm from the root base these differences occurred (Figure 2.3) but were not significant. Other anatomical traits of AR did not respond significantly to soil compaction and the distance from the root base at which cross sections were taken did not influence any evaluated anatomical trait (Table 2.4).
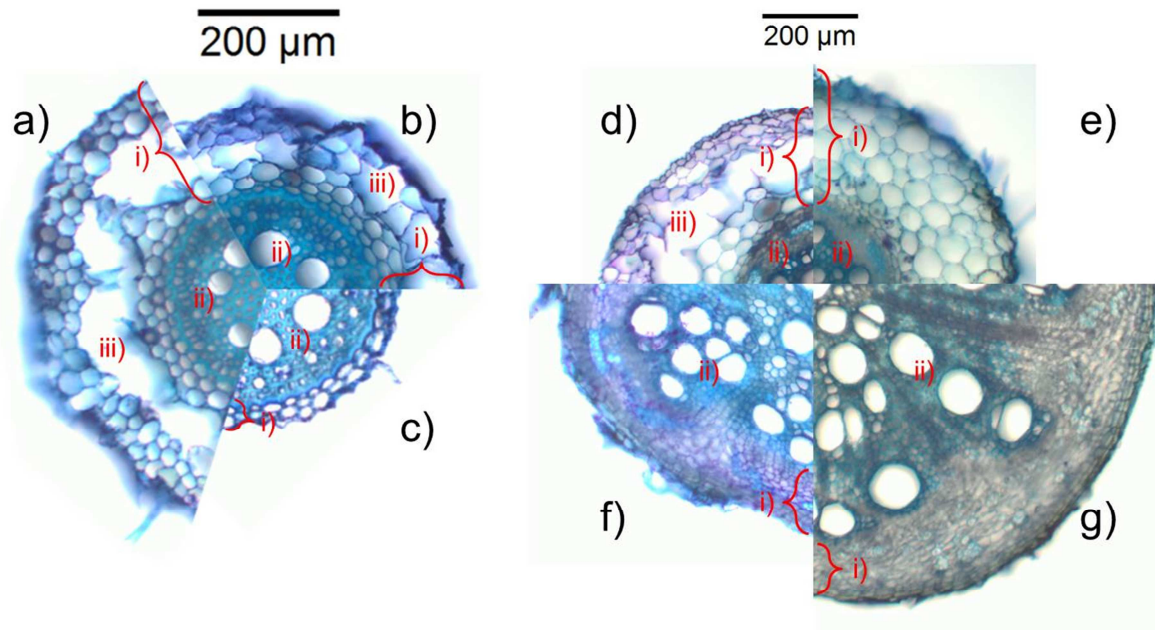
Figure 2.3: Root anatomy of (left) nodal roots of triticale grown under a) topsoil compaction, b) subsoil compaction and c) uncompacted soil at 2 cm from the root base and (right) d) and e) adventitious roots and f) and g) taproots of soybean grown under d) and f) compaction and e) and g) loose soil at 10 cm from the root base. i) Root cortex, ii) vascular cylinder and iii) root cortex aerenchyma.

Linear regressions between different anatomical traits of all treatment-distance combinations, including the results obtained under controlled conditions, showed distinctly different patterns for triticale and soybean. While in triticale an increasing area of cross sections was positively related to an increasing share of the root cortex ($R^2 = 0.44$, $p < 0.01$) the opposite trend was observed for soybean roots ($R^2 = 0.42$, $p < 0.05$). Large ArCP were measured for roots with a relatively small cross section area (Figure 2.4). Furthermore, the cortical area in mm^2 and the occurrence of RCA were not significantly related in soybean but in triticale ($R^2 = 0.54$, $p < 0.01$). Increased root cortical areas of triticale roots were related to increased percentages of aerenchyma in the cortex (Figure 2.4).

Table 2.4: Responses of root anatomical traits of triticale and soybean under field (F) and controlled conditions (CC) to soil compaction (Com), the distance from the root base (Dist) and their interaction. * and ** denote significant responses at $p < 0.05$ and $p < 0.01$ respectively, n.s. denotes non-significant responses (F: n = 3, CC: n = 4). Abbreviations cf. Table 2.1.

	F: triticale NR_{No1}			F: triticale NR_{No3}			CC: triticale PR	CC: triticale SR
Trait	**Com**	**Dist**	**Com:Dist**	**Com**	**Dist**	**Com:Dist**	**Com**	**Com**
ArV [mm^2]	n.s.	n.s.	n.s.	n.s.	**	n.s.	n.s.	n.s.
ArC [mm^2]	**	n.s.	n.s.	n.s.	**	n.s.	n.s.	**
ArCP [%]	**	n.s.	n.s.	n.s.	n.s.	n.s.	*	**
ArC/ArV	**	n.s.	n.s.	n.s.	n.s.	n.s.	*	*
RCA [%]	*	n.s.	n.s.	n.s.	n.s.	n.s.	**	**

	F: soybean TR			F: soybean AR			CC: soybean TR
Trait	**Com**	**Dist**	**Com:Dist**	**Com**	**Dist**	**Com:Dist**	**Com**
ArV [mm^2]	**	**	n.s.	n.s.	n.s.	n.s.	n.s.
ArC [mm^2]	**	**	n.s.	n.s.	n.s.	n.s.	n.s.
ArCP [%]	**	*	n.s.	n.s.	n.s.	n.s.	**
ArC/ArV	**	*	n.s.	n.s.	*	n.s.	**
RCA [%]	n.s.	n.s.	n.s.	**	n.s.	n.s.	*

Abbreviations: NR_{No1} = nodal root from the first whorl, NR_{No3} = nodal root from the third whorl, TR = taproot, AR = adventitious root, PR = primary root, SR = seminal root
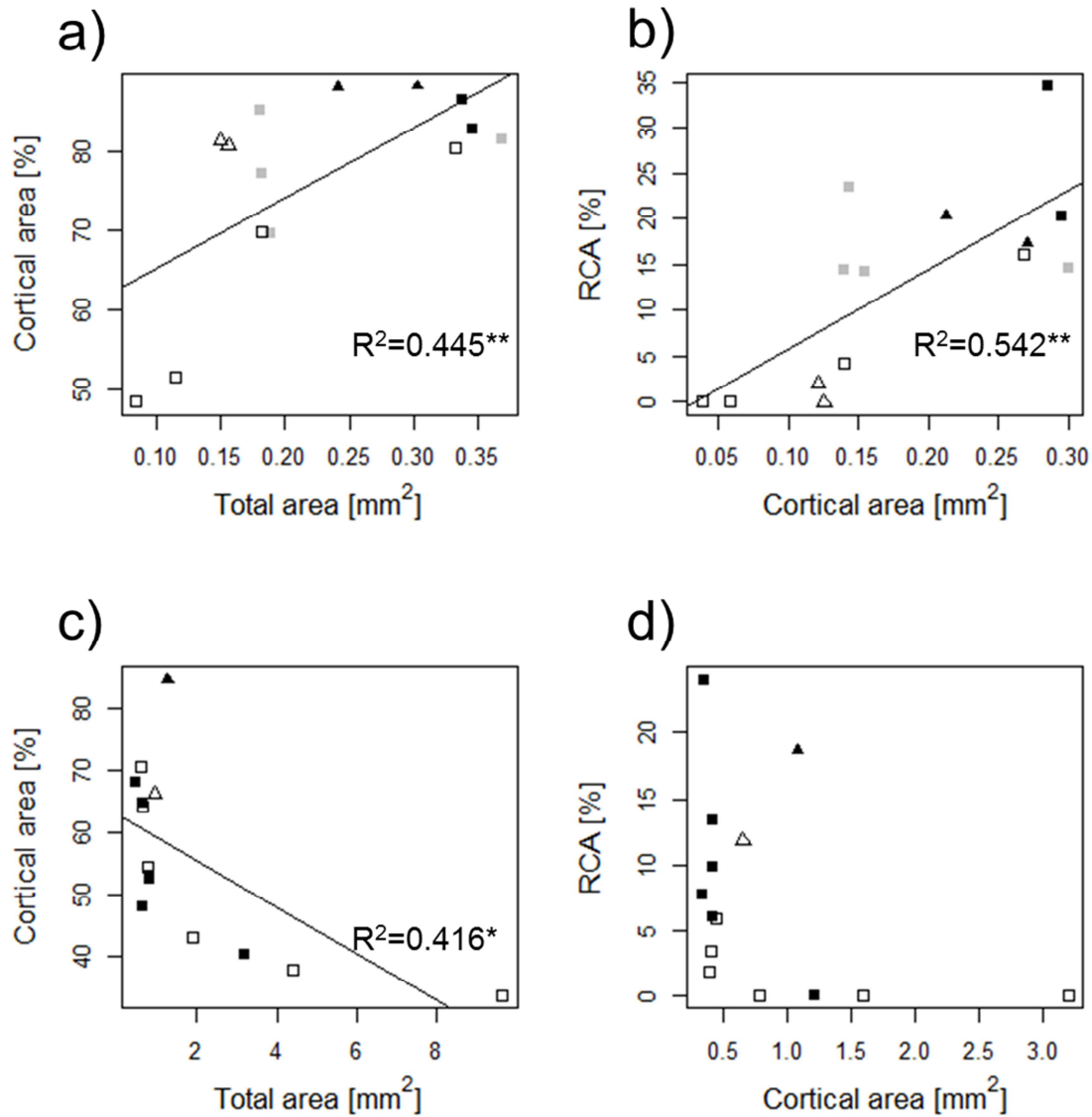
Figure 2.4: Linear regressions and multiple r-squared of a) and c) total cross section area and relative root cortical area as a percentage of the total area and c) and d) absolute cortical area and the percentage of root cortex aerenchyma (RCA) of a) and b) triticale and c) and d) soybean at different distances from the root base. Different symbol shapes indicate the environment (triangle: controlled conditions (CC), squares: field (F)), open symbols represent uncompacted soil, closed grey and black symbols represent sub- and topsoil compaction, respectively. * and ** indicated significant correlations at $p < 0.05$ and $p < 0.01$, respectively (CC: n = 4, F: n = 3).

2.3.1.4. Plant vigour

Shoot dry weights and leaf area indices responded significantly 42 and 91 DAS to the different compaction treatments. Dry shoot biomass of single triticale plants in TSCom was reduced by around 75% and around 85% compared to SSCom and Ctrl, respectively. Responses of LAI to soil

compaction were in a similar range as shoot dry weights (Table 2.5). Soybean single plant dry weights and LAI were also reduced due to soil compaction but to a smaller extent than in triticale. Plant dry weight decreased under compaction by 52% and 32% compared to the uncompacted treatment 42 and 91 DAS, respectively. At the first and second time point LAI decreased by 67% and 17%, respectively due to soil compaction (Table 2.5). SPAD values were significantly reduced for both crops in compacted plots compared to control plots 42 DAS but not 91 DAS (Table 2.5).

2.3.2. Experiment II: controlled conditions

Mechanical impedance increased from 0.43 ($\pm$ 0.06, s.e.m.) MPa in loosely packed columns to 1.01 ($\pm$ 0.09, s.e.m.) MPa in densely packed columns. Initial soil penetration of the radicle, represented by the rooting depth 2 DAS, decreased under compaction by 74% in triticale, 82% in soybean and 56% in wheat compared to respective control groups.

2.3.2.1. Root system architecture

Most of the root architectural responses observed under controlled conditions coincided with results obtained in the field. Lateral root initiation was tremendously slower in compacted compared to loose soil in both crops (Figure 2.5). At the end of the growth period 14 DAS triticale SR were occupied with 1.75 LR cm^{-1} and 0.75 LR cm^{-1} in uncompacted and compacted soil, respectively. Lateral branching at soybean TR was reduced from 7.3 LR cm^{-1} in loose soil to 1.4 LR cm^{-1} in compacted soil. Root diameters of SR and TR of triticale and soybean, respectively increased in response to increased soil bulk density (Figure 2.5). In triticale the measured diameters of seminal roots 14 DAS increased from 0.42 mm in Ctrl to 0.61 mm in Com. Primary root diameters of triticale under compaction were also significantly larger (0.55 mm) than in the control group (0.44 mm). Taproot diameters of soybean seedlings increased under compaction similar to adventitious root diameters in the field. 14 DAS taproot diameters in Com were 1.10 mm and 0.89 mm in Ctrl. Furthermore, in the compacted treatment 9.3 AR were counted while this number was decreased to 6.5 AR in the control group. For triticale no responses of soil compaction on the number of NR could be observed since their initiation just started when plants were harvested. The responses of winter wheat

root architecture to increased soil bulk density were the same as described for triticale (Supporting Information Figure S2.1 and Table S2.2).

2.3.2.2. Root anatomy

As observed in the field, soil compaction caused higher cortical proportions in roots of soybean and triticale seedlings (Table 2.4). In soybean the share of the root cortex within the total cross section area of the taproot was 18% larger in the compacted compared to the uncompacted treatment. In triticale ArCP of primary and seminal roots were increased by around 10% in response to soil compaction. Cortical areas measured in mm^2 were also significantly increased under compaction in triticale PR and SR but not in soybean TR. The area of the vascular cylinder remained unaffected by soil compaction in all evaluated roots of both crops (Table 2.4). Both, triticale and soybean roots showed significantly increased root cortex aerenchyma under soil compaction (Table 2.4). This was most pronounced in SR of triticale where 20% of the root cortex was occupied by RCA under compaction, while no RCA occurred in the uncompacted treatment. Under compaction RCA made up 17% of the cortex of triticale PR whereas just 2% of the cortex were occupied by RCA in the uncompacted treatment. In soybean TR the increase of RCA as a response to soil compaction was smaller but still significant (Com: 18.6%, Ctrl: 11.8%). As for root architecture, anatomical responses of wheat to soil compaction were comparable with the responses of triticale (Supporting Information Table S2.2).

Table 2.5: Upper part: treatment means of plant vigour traits 42 and 91 days after sowing (DAS) from field-grown triticale under topsoil compaction (TSCom), subsoil compaction (SSCom) and without compaction (Ctrl) and field-grown soybean on compacted soil with shallow tillage (Com) and without compaction (Ctrl). Lower part: treatment means of plant vigour traits of triticale and soybean under controlled conditions measured 14 DAS under compacted (Com) and loose soil (Ctrl). Different letters indicate significant differences of the means based on ANOVA with least significant test at $p < 0.05$ (n = 3).

			Triticale			Soybean		
Environment	**DAS**	**Trait**	**TSCom**	**SSCom**	**Ctrl**	**Trait**	**Com**	**Ctrl**
Field	42	Shoot DW [g]	0.0488^a	0.266^b	0.340^b	Shoot DW [g]	1.052^a	2.207^b
		LAI [m² m⁻²]	0.872^a	2.906^b	3.643^b	LAI [m² m⁻²]	1.220^a	3.713^b
		SPAD	30.70^a	41.87^b	44.80^c	SPAD	33.22^a	37.57^b
		Number of tillers	0.2^a	2.4^b	3.7^c	Number of side shoots	0	0
	91	Shoot DW [g]	0.692^a	2.836^b	4.260^c	Shoot DW [g]	15.150^a	22.150^b
		LAI [m² m⁻²]	0.407^a	3.081^b	4.259^c	LAI [m² m⁻²]	5.529^a	6.639^b
		SPAD	43.93	48.40	49.17	SPAD	42.41	43.69
		Number of tillers	0.0^a	0.6^{ab}	1.1^b	Number of side shoots	2.5^a	1.0^b
Environment	**DAS**	**Trait**	**Com**	**Ctrl**		**Trait**	**Com**	**Ctrl**
Controlled condition	14	Shoot DW [g]	0.0259	0.0423		Shoot DW [g]	0.197	0.225
		Root DW [g]	0.0198	0.0195		Root DW [g]	0.0175^a	0.0305^b
		Root-shoot ratio	0.776^a	0.437^b		Root-shoot ratio	0.0890	0.141
		SPAD	32.12	37.60		SPAD	41.62	42.70

DW = dry weight, LAI = leaf area index
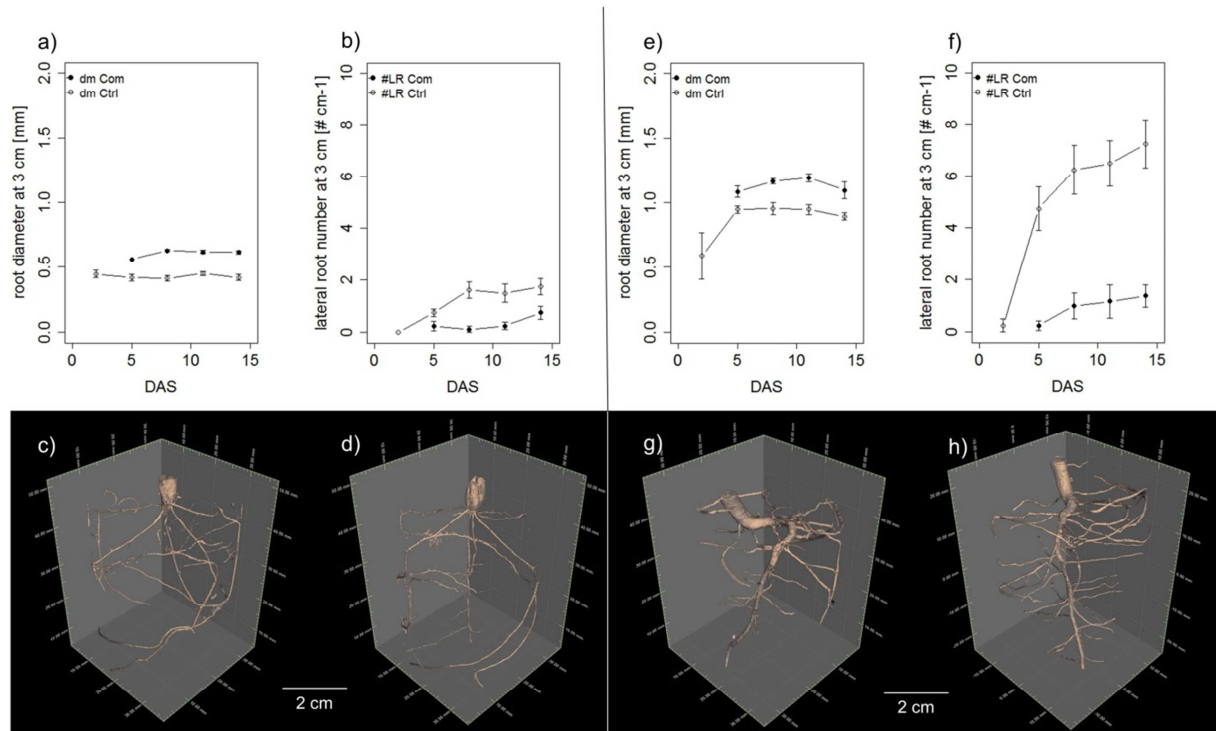
Figure 2.5: Root diameters (dm) of a) triticale seminal roots and e) soybean taproots and lateral root number (#LR) at b) triticale seminal roots and f) soybean taproots grown under compacted (Com) and loosely (Ctrl) packed soil and measured 2, 5, 8, 11 and 14 days after sowing (DAS). Error bars represent standard errors (n = 4). Typical pictures of triticale roots from c) Com and d) Ctrl and soybean roots from e) Com and h) Ctrl.

2.3.2.3. Plant vigour

The exposure to X-ray radiation showed no influence on root or shoot biomass of triticale, soybean and wheat. Shoot biomass was reduced in soybean and triticale crops under compaction but neither in soybean nor in triticale this reduction was significant (Table 2.5). Total root biomass of triticale was not affected by the different compaction treatments, whereas the root-shoot ratio was significantly increased in response to increased soil strength (Table 2.5). In soybean the root dry biomass was reduced significantly from 0.030 g to 0.018 g comparing the control with the compacted treatment (Table 2.5). The different levels of soil compaction did not affect SPAD values of both crops (Table 2.5). In wheat, shoot biomass was reduced in response to soil compaction, but root biomass and SPAD were not affected (Supporting Information Table S2.2).

2.4. Discussion

The primary aim of this study was to determine whether root architectural and anatomical responses of mature roots to compacted soils in the field can be reproduced under controlled conditions in young roots. In the field and under controlled conditions higher bulk densities in the compacted treatments caused increased mechanical impedance compared with the uncompacted treatments. In both crops used –triticale and soybean– soil compaction caused alterations of root architectural and anatomical traits. Generally, these responses to soil compaction were comparable between the two species, different developmental stages and environments. However, differences were observed with respect to anatomical responses of the root systems to soil compaction: secondary thickening caused different responses of young and mature soybean roots, respectively, and pronounced differences between the cereal and the legume were observed as well.

2.4.1. Root architectural responses to soil compaction

2.4.1.1. Shallower root growth under soil compaction

In the current study soil compaction caused soybean and triticale roots to grow shallower and penetrate the soil less deep. Angles between the root crown and the soil surface of triticale were 15° to 30° smaller under compaction than under loose conditions and the D95 at flowering was reduced significantly due to soil compaction. For soybean the D95 was also significantly reduced due to soil compaction, while shallower root angles were observed only at the first sampling time point. These contradictory results may be explained by the fact, that the number of adventitious roots (Table 2.3) and their lateral branching density (Figure 2.2) were higher at the second compared to the first sampling time point. However, these results corresponded to previous field studies, where root angles of narrow-leafed lupins were more shallow (Chen et al., 2014b) and rooting depths of wheat (Barraclough and Weir, 1988; Chen et al., 2014b) and soybean (Botta et al., 2010) decreased due to soil compaction. Increased topsoil rooting due to soil compaction in wheat was shown in a previous study under controlled conditions (Nosalewicz and Lipiec, 2014). Since the diameter of the investigated soil columns was relatively small, horizontal root growth may have been restricted. Therefore, the penetration depth of the radicle into the bulk soil was taken as a measurement for the

direction of root growth instead of root angles. The initial root penetration 2 DAS decreased in triticale, soybean and also wheat by 56 to 82% due to increased soil bulk density as observed for wheat and pea (Iijima and Kato, 2007). In the field the number of nodal roots in triticale decreased between 15% and 70% under top- and subsoil compaction compared to the uncompacted treatment (Table 2.3), which corresponded to results obtained under controlled conditions (Grzesiak et al., 2013). In soybean the number of adventitious roots was increased in response to increased soil bulk density 14 DAS under controlled conditions. Yet, in the field number of AR was not altered due to compaction.

2.4.1.2. Decreased lateral root number under soil compaction

Lateral root growth was suggested to be increased under soil compaction to compensate reduced axial root growth (Bengough et al., 2011), which was not observed in the current study. Instead, lateral root numbers of field-grown triticale and soybean were reduced in response to soil compaction. Remarkably, lateral branching density in the topsoil was lower in SSCom than in Ctrl (Figure 2.2), even though soil bulk density and mechanical impedance in the topsoil was not different between the two treatments (Table 2.2). In soybean the number of LR at the taproot was reduced in response to increased soil strength but not at adventitious roots (Figure 2.2). In other field studies decreasing specific root lengths under soil compaction were reported for field-grown barley (Hernandez-Ramirez et al., 2014), wheat (Barraclough and Weir, 1988) and narrow-leafed lupins (Chen et al., 2014b). Such measurements can be related to lateral branching density but are influenced to a large extent by root diameters and different root classes present in the soil. However, these observations correspond to the results obtained in the current study. Reduced number of lateral roots have been reported under controlled conditions at similar levels of soil compaction for tomato (Tracy et al., 2012b), barley (Pfeifer et al., 2014a) and triticale (Grzesiak et al., 2014). This was also shown in the current study for triticale, soybean and wheat under controlled conditions. Lateral root initiation was delayed in all species (Figure 2.5, Supporting Information Figure S2.1) indicating that the same responses of the lateral root system to soil compaction occurred in both environments at different developmental stages.

2.4.1.3. Root diameters responded differently to soil compaction among crops and developmental stages

While rooting depths, growth directions and root numbers showed mostly consistent responses to soil compaction, acclimations of root diameters to increased soil compaction differed among species. As observed for mature wheat (Materechera et al., 1992) and barley (Hernandez-Ramirez et al., 2014) root diameters of triticale increased in the field in response to soil compaction. Nodal root diameters in TSCom were 38 to 63% larger compared to Ctrl. As seen for lateral root numbers, compacted subsoil affected root diameters in the topsoil leading to a significant increase of root diameters in SSCom compared to Ctrl (Figure 2.2). This was consistent to the results obtained under controlled conditions for primary and seminal roots of triticale (Figure 2.5) and wheat (Supporting Information Figure S2.1). Also under controlled conditions increasing root diameters as a response to compacted soils have been observed in barley (Pfeifer et al., 2014a) and triticale (Grzesiak et al., 2013). In soybean secondary root thickening showed a large effect on the responses of root diameters to soil compaction. Diameters of young roots in the field, represented by adventitious roots 42 DAS, were 15 to 31% larger in Com than Ctrl (Figure 2.2). This response corresponded to seedlings under controlled conditions, in which the taproot diameter also increased in almost the same order of magnitude in response to soil compaction (Figure 2.5). Similar results were reported in previous studies with soybean (Ramos et al., 2010), tomato (Tracy et al., 2012b) and pea (Iijima and Kato, 2007). However, as roots became more mature diameters were indifferent between Com and Ctrl or even larger under Ctrl compared to Com (Figure 2.2), which was not observed in mature narrow-leafed lupins (Chen et al., 2014b). Smaller diameters of soybean roots at later stages showed, that not only root elongation was lower under compaction but also radial root growth was slower in response to increased soil strength.

2.4.2. Root anatomical responses to soil compaction

2.4.2.1. Root cortical proportion explained altered root diameters

In triticale increased root diameters in response to soil compaction were related to increased cortical proportions within the root cross sections. The area of the vascular cylinder remained unaffected by soil compaction, whereas cortical areas and proportions increased significantly due to

soil compaction in both environments (Table 2.4). This corresponded to other studies on seedlings of triticale, wheat, rye, barley (Lipiec et al., 2012) and rice (Iijima and Kato, 2007) and partially to wheat in the current study (Supporting Information Table S2.2). Furthermore, increasing total root cross section areas were positively correlated ($R^2 = 0.44$, $p < 0.01$) with increased cortical proportions (Figure 2.4), suggesting that increased root diameters were caused by larger root cortices. Positive correlations of increasing cortical proportions and root diameters were observed in 30-day-old wild mono- and dicotyledonous plant species exposed to flooding (Striker et al., 2007). Contradictory to the results from Striker et al. (2007), the relationship between total root cross section areas and cortical proportions of soybean roots was negative ($R^2 = 0.42$, $p < 0.05$). Larger cross sections were related to a smaller share of cortical tissue (Figure 2.4), which was mainly caused by slower secondary thickening under compaction. As reported for pea seedlings (Iijima and Kato, 2007) and saplings of narrow-leafed ash (Alameda and Villar, 2012), cortical proportions of the taproot increased as a response to compacted soils in both environments. However, this increase in ArCP was related under controlled conditions to increased (Figure 2.5) and in the field to decreased TR diameters (Figure 2.2). The vascular area of the TR in the field, which was 75% smaller in the compacted compared to the uncompacted treatment, also indicated decreased radial root growth.

2.4.2.2. Soil compaction induced the formation of root cortex aerenchyma

The occurrence of root cortex aerenchyma has primarily been related to flooded and therefore anaerobic conditions (Thomson et al., 1992; Thomas et al., 2005; Yamauchi et al., 2013; Takahashi et al., 2014). If oxygen diffusion rates in soils are reduced or inhibited, RCA provides oxygen to the growing root tip. Recent studies also reported, that the formation of RCA in maize was increased by low nitrogen supply (Saengwilai et al., 2014a) and drought (Chimungu et al., 2015b). In the current study soil compaction caused increasing percentages of RCA in triticale and to a smaller extent also in soybean (Figure 2.3).

The fraction of the root cortex that was occupied with RCA increased under controlled conditions in PR and SR of triticale and to a larger extent in NR of triticale in the field (Table 2.4). In both compaction treatments in the field (TSCom and SSCom) the occurrence of RCA was higher than in

Ctrl. Furthermore, increased root cortical areas were positively correlated ($R^2 = 0.54$, $p < 0.01$) with increased percentages of RCA in the root cortex (Figure 2.4), which was previously observed in the grass species *Paspalidium geminatum* under flooding (Striker et al., 2007). In young soybean roots, represented by TR under controlled conditions and AR from the field, soil compaction also induced the formation of RCA (Table 2.4). In older soybean root tissue the growing vascular cylinder closed RCA during secondary thickening (Figure 2.3). The occurrence of RCA in both crops has been observed before under flooded or anaerobic growth conditions (Thomson et al., 1992; Watkin et al., 1998; Shimamura et al., 2003; Thomas et al., 2005; Xu et al., 2013; Marashi and Mojaddam, 2014; Yamauchi et al., 2014) but not under soil compaction.

2.4.3. Links between plant responses to compaction and altered soil properties

Soil compaction was quantified in this study using the two most common measurements: bulk density and mechanical impedance. In the field and under controlled conditions, soil compaction caused a significant increase of both parameters (Table 2.2), resulting in decreasing plant vigour (Table 2.5). This has been observed in numerous studies under field (Barraclough and Weir, 1988; Czyż, 2004; Botta et al., 2010; Siczek and Lipiec, 2011; Arvidsson et al., 2014) and controlled conditions (Buttery et al., 1998; Bingham and Bengough, 2003; Grzesiak et al., 2013; Grzesiak et al., 2014; Pfeifer et al., 2014a).

2.4.3.1. Root phenotypic acclimations to compaction were not only triggered by increased mechanical impedance

Increased root diameters and larger root cortices were often seen as a direct acclimation of roots to increased mechanical impedance (Materechera et al., 1992; Alameda and Villar, 2012; Lipiec et al., 2012; Jin et al., 2013; Chen et al., 2014b). Materechera et al. (1992) explained this by suggesting that thicker roots facilitated the penetration of compacted soils, while Alameda and Villar (2012) proposed that axial growth is more affected by soil compaction than radial growth. Decreased lateral branching under compaction could also be associated to increased mechanical impedance, since lateral roots are relatively thin compared to axial roots. These effects of increased soil bulk density and impedance under compaction were also observed in the current study for triticale and soybean. Under controlled

and field conditions the number of LR decreased in both crops but root diameters (Figure 2.2 and 2.5) and cortical areas and proportions (Figure 2.3) increased as an acclimation to soil compaction. However, certain root phenotypic responses to soil compaction observed in the current study could not only be explained by increased bulk density and mechanical impedance alone.

Even though the determined soil physical properties in the topsoil of the treatment with subsoil compaction and the uncompacted treatment were not significantly different (Table 2.2), root architectural and anatomical traits of triticale were different. In SSCom lateral root numbers were decreased and root diameters (Figure 2.2) and cortical areas (Figure 2.3) were higher compared to Ctrl. Most likely, these reactions were caused by slower water infiltration and therefore reduced oxygen availability due to the compacted subsoil. This is supported by numerous studies, in which larger root diameters and root cortices were observed as a response to flooding of wheat (Yamauchi et al., 2014), tomatoes (Dresbøll et al., 2013) and wild mono- and dicotyledonous plants (Striker et al., 2007). Furthermore, it is known that soil compaction decreases water infiltration rates and hydraulic conductivities (Lipiec and Hatano, 2003; Ozcoban et al., 2013; Kuncoro et al., 2014b) resulting in higher risks of anaerobic conditions. Grzesiak et al. (2014) observed in a recent laboratory study that maize and triticale genotypes, which were relatively tolerant to water logging were also relatively tolerant to soil compaction. The occurrence of root cortex aerenchyma in both crops of our study was a further strong indication for low oxygen availability under soil compaction (Figure 2.3). The positive correlation of root cortical area and aerenchyma in triticale (Figure 2.4) suggested also, that larger root cortices not only facilitate penetration into compacted layers but also provide more potential space for RCA.

By combining architectural and anatomical responses of roots to soil compaction, responses of root systems to such conditions could be classified into two categories: Initially larger root diameters facilitate the penetration of compacted layers and enable the root to overcome higher mechanical impedance as suggested in other studies (Materechera et al., 1992; Chen et al., 2014b). Subsequently, the formation of RCA allows oxygen to flow towards the root tip to maintain growth. The ability to do so will differ between genotypes, which leaves a lot of room for detailed investigations in future studies. The fact that a lot of aspects were comparable between the field and laboratory experiment

suggests that a rapid screening process of large genotype numbers in breeding programmes might be possible in laboratory studies under controlled conditions.

2.5. Conclusions

Our results showed that acclimation responses of root phenotypes of soybean and triticale, which occur in the field at later developmental stages, are to a large extent reproducible under controlled conditions at the seedling stage. Triticale showed very consistent responses of root architectural and anatomical parameters to soil compaction throughout the entire growth period. In soybean instead, initial responses to compacted soils such as increased root diameters and root cortex aerenchyma did not occur at later growth stages due to secondary thickening. By combining architectural and anatomical measurements we could show how roots respond to different stresses caused by soil compaction. Thicker roots with a higher cortical proportion within the cross section were likely associated to higher mechanical impedance whereas the occurrence of root cortex aerenchyma were a result of reduced oxygen availability. These findings suggest that a holistic view considering a set of abiotic stresses is needed when searching for root phenotypes adapted to compacted soils. The investigations of different genotypes of the same species will bring further insights into the relationship of root phenotypes and plant productivity under soil compaction.

Chapter 3: Root tip shape governs root elongation rate under increased soil strength in wheat

Tino Colombi[1*], Norbert Kirchgessner[1], Achim Walter[1] and Thomas Keller[2,3]

[1]ETH Zurich, Institute of Agricultural Sciences (IAS), Switzerland

[2]Agroscope, Department of Agroecology and Environment, Zurich, Switzerland

[3]Swedish University of Agricultural Sciences, Department of Soil and Environment, Uppsala, Sweden

[*]Corresponding author, tino.colombi@usys.ethz.ch

Abstract

Increased soil strength due to soil compaction or soil drying is a major limitation to root growth and crop productivity. Energy requirement for root growth increases with soil strength due to increased root penetration stress. This study aimed to quantify how genotypic diversity of root tip geometry and root diameter influences root elongation under different levels of soil strength and to determine the extent to which roots adjust to increased soil strength. Fourteen wheat varieties were grown in soil columns packed to three bulk densities representing low, moderate and high soil strength. Under moderate and high soil strength smaller root tip opening angle was correlated with higher root elongation rate, whereas root diameter was not related to root elongation. Based on cavity expansion theory, it was found that an acute tip opening angle reduced penetration stress thus enabling higher root elongation rates in soils with greater strength. Furthermore, it was observed that roots could only partially adjust to increased soil strength. Root thickening was bounded by a maximum diameter and root tips did not become more acute in response to increased soil strength. The obtained results demonstrated that root tip geometry is a pivotal trait governing root penetration stress and therefore the energy required for the penetration of soil with greater strength. As root elongation rate was correlated to root tip opening angle, root tip geometry needs to be taken into account when selecting for crop varieties that may tolerate high soil strength.

3.1. Introduction

Crops, like most other terrestrial plant species, acquire essential resources they need for growth from soil. To do so, roots need to grow through soil to access water and nutrient pools. Increased mechanical impedance, which can be caused by compacted soil layers or soil drying, is the major limitation to root elongation and hence adversely affects soil exploration and resource uptake (Masle and Passioura, 1987; Materechera et al., 1992; Bengough et al., 2006; Bengough et al., 2011; Kautz et al., 2013). Under increased soil strength, roots need to exert higher forces in order penetrate soil successfully. This leads to higher penetration stresses and therefore root growth and soil exploration require more energy when soil strength is increased (Atwell, 1990a; Bengough et al., 2011; Ruiz et al., 2015; Ruiz et al., 2016). When soil mechanical impedance is increased, root elongation rate decreases within hours and may entirely cease, leading to significant yield losses (Bengough and Mullins, 1991; Young et al., 1997; Valentine et al., 2012). The integration of functional root traits, which enable for resource acquisition at minimum energetic costs, into breeding programmes is a promising approach to improve agricultural productivity under limited soil fertility (Bishopp and Lynch, 2015). Soil penetration mechanics needs to be combined with investigations of the root phenotype in order to identify functional root properties enabling for an efficient exploration of high strength soil.

Plants use different strategies to overcome the limitations imposed by increased soil strength on root growth and crop productivity. Barley and wheat have been found to preferentially increase the extension of their root system into loose compartments of the soil when other compartments are compacted (Bingham and Bengough, 2003). Furthermore, roots of different cereals, maize and soybean have been shown to use natural or artificial macropores as pathways of least resistance in compacted soil or dense subsoil (Stirzaker et al., 1996; White and Kirkegaard, 2010; Colombi et al., 2017). Compensatory root growth into loose compartments and use of macropores in soils of high strength were found to be beneficial for shoot growth compared with uniformly compacted soil (Stirzaker et al., 1996; Bingham and Bengough, 2003; Colombi et al., 2017). However, to ensure adequate root-soil contact, which is required for the uptake of plant nutrients (Stirzaker et al., 1996; Tracy et al., 2011), roots need to grow into bulk soil.

Root thickening is one of the most common responses of roots when growing through soil with higher mechanical impedance. This adjustment of roots to increased soil strength reduces the risk of root buckling and decreases the mechanical stress acting on the root during penetration (Materechera et al., 1992; Kirby and Bengough, 2002; Chimungu et al., 2015). Root thickening in response to increased soil strength has been observed in a wide range of species under field and laboratory conditions and often coincides with increased cortical area (Atwell, 1990b; Materechera et al., 1992; Grzesiak et al., 2013; Siczek et al., 2013; Chen et al., 2014; Hernandez-Ramirez et al., 2014; Colombi and Walter, 2016). Since root thickening decreases penetration stress and stabilizes roots, thick roots are likely to be an advantage in soils with increased mechanical impedance (Materechera et al., 1992; Kirby and Bengough, 2002; Chimungu et al., 2015). A recent study showed that the genotypic cortical thickness in maize is related to bending strength and hence to the risk of root buckling (Chimungu et al., 2015). As a consequence of to the increased volume to length ratio in thicker roots, plants need to invest more resources into soil exploration when soil strength increases (Atwell, 1990a). Cell turnover and cell detachment rates at the root cap were reported to increase when soil is compacted (Iijima et al., 2003a), which further increases the metabolic costs of root growth and resource acquisition. These cells, which are released from the root cap into the rhizosphere act together with mucilage as a lubricant reducing the interfacial friction between the growing root tip and the soil (Bengough and McKenzie, 1997; McKenzie et al., 2013).

There is evidence that the penetrability of soil is not only influenced by the diameter of the root but also by the geometry of the root tip. Model predictions have shown that the stress experienced by a growing root is concentrated around the root tip (Kirby and Bengough, 2002). Simulations of stress field distributions around cones inserted into soil show that this distribution changes with changing cone opening angle. For cones with an acute opening angle the stress field is distributed around the cone, whereas for blunt cones the stress field is located at the cone forefront (Ruiz et al., 2016). Similar results were obtained when comparing local soil compaction that is induced by growing roots between maize roots lacking of an intact cap and maize roots with a cap (Vollsnes et al., 2010). These findings can be related to the form of cavity expansion and the soil deformation pattern. Blunting of a root tip or a cone leads to a shift from a rather cylindrical to a more spherical deformation pattern,

52

which causes penetration forces and stresses to increase (Greacen et al., 1968). This increase has been shown to happen when root tips are blunted due to the removal of the root cap (Iijima et al., 2003b). Furthermore, the lack of a root cap results in decreased root elongation rates in comparison to roots with an intact cap (Iijima et al., 2003b; Vollsnes et al., 2010). The forces and stresses that occur at a root tip during soil penetration can be measured directly in soil (Iijima et al., 2003b) or in free air and nutrient solutions (Misra et al., 1986; Bengough and Kirby, 1999; Azam et al., 2013; Bizet et al., 2016). As an alternative, cone penetrometer measurements combined with quantifications of root tip and cone geometry can be used to calculate root tip penetration forces and stresses (McKenzie et al., 2013). Despite the available information, mechanical processes governing root elongation are still poorly understood (Bengough et al., 2011). Thus, conclusive information about root traits that may improve soil penetrability, resource acquisition and crop productivity when soil strength is increased is missing.

The aims of the present study were i) to quantify whether and how the genotypic diversity of root tip geometry and root diameter are related to root elongation rate in soil of different strength and ii) to quantify adjustments in root tip properties, root morphology and root anatomy to increased mechanical impedance. This information was then used to iii) discuss the mechanical and physiological implications of observed genotypic differences and phenotypic adjustments to increased soil strength. Experiments were performed with 14 winter wheat cultivars (Triticum aestivum L.) in soil columns with bulk densities of 1.3 g cm^{-3}, 1.45 g cm^{-3} and 1.6 g cm^{-3}, representing loose, moderately and severely compacted soil, respectively. Root tip geometry, morphology and elongation rate in 2-day-old seedlings were quantified from high-resolution flatbed scans. Combining this information with cone penetrometer tests enabled root penetration forces and stresses occurring during growth to be calculated. Furthermore, root morphology and anatomy were quantified in embryonic and post-embryonic roots of 23-day-old plants.

3.2. Material and Methods

3.2.1. Soil physical conditions, plant material and growth conditions

The soil used was homogenized and sieved field soil (2 mm) that was excavated from the top 15 cm of an agricultural field at Agroscope Zurich (8°31'E, 47°27'N, 443 m above sea level). The soil is classified as a Pseudogleyed Cambisol with a topsoil pH ($CaCl_2$) of 6.9. The textural composition is 25% clay, 50% silt and 25% sand and organic carbon content in the topsoil is 1.7%. After sieving, the soil was stored at 3°C until further use. Different levels of soil mechanical impedance were achieved by different packing densities. The soil was packed in six layers of 2 cm height into PVC columns of 4.9 cm diameter and 15 cm height to low (1.3 g cm^{-3}), moderate (1.45 g cm^{-3}) and high (1.6 g cm^{-3}) soil bulk density. The surface of each layer was slightly abraded to ensure homogeneous packing. In addition, four soil cores of 5.1 cm diameter and 5 cm height per soil bulk density treatment were packed in 1 cm layers and slowly saturated from below. They were equilibrated on a ceramic plate, to determine gravimetric water content at -100 hPa suction potential, which is commonly taken to represent field capacity (Schjonning and Rasmussen, 2000). Soil mechanical impedance was measured by two individual cone penetrometer insertions into the center of the bottom of these soil cores at an insertion speed of 4 mm min^{-1}. The steel cone used (2.5 mm radius, 4.33 mm length, semi-opening angle 30°) had a recessed shaft and was connected to a force transducer (*LC 703, OMEGA Engineering Inc., Stamford CT, USA*). To calculate the mean penetration force, values from the point at which the cone was fully inserted into the soil until 1.5 cm penetration depth were averaged (~ 650 force measurements).

Experiments were conducted with 14 Swiss winter wheat (*Triticum aestivum* L.) cultivars released from public breeding programmes between 1910 and 2010 (Supporting Information Table S3.1). The plants were grown in a growth chamber at 63% relative humidity and an average temperature of 21.4° C with a day-night cycle of 14/10 h. Incident light was 510 (± 33, SD) µmol s^{-1} m^{-2} and soil moisture was kept constant at a gravimetric water content corresponding to -100 hPa by daily weighing and watering during the duration of the experiments.

3.2.2. Experiment 1: Root tip geometry, morphology and root elongation rate

3.2.2.1. Root growth and image acquisition

Seeds were pre-germinated at 25°C for 48 hours. For each soil bulk density-genotype combination, four seeds of similar size in which the tip of the first embryonic roots were just visible, were selected. They were placed with the emerging roots facing downwards into a small pit of around 5 mm height and 3 mm diameter pinched out from the soil and then covered with loose soil (1 g cm^{-3}). To ensure that roots were penetrating the soil and to avoid artifacts of root pull-out effects, the soil columns were covered with cotton tissue and a perforated steel plate. After 48 h of growth under the conditions described, the roots were washed out from the soil. For each treatment level six individual roots, which were not touching the border of the PVC column were selected, fixed in FAA (acetic formaldehyde:alcohol:acetic acid:distilled water; 10:50:5:35) and stored at 3°C. The roots were scanned in a flatbed scanner (*Epson Expression 11000 XL, Seiko Epson Corporation, Japan*) at a resolution of 2400 dpi resulting in a pixel edge length of 10.6 μm.

3.2.2.2. Image processing

Root tip geometry was analyzed using a novel tool called Root Tip Scan Analysis (*ROSTA*), which was programmed in a MatLab 2016a environment (*The Mathworks, Natick MA, USA*). In *ROSTA*, regions of interest containing single root tips are selected manually from the scans obtained, while subsequent steps run completely automatically. Using Otsu's method (Otsu, 1979) root tips were segmented from the background and the perimeter of the root tip is recognized. The root tip perimeter was then refined by applying an active contour on the grey value gradient as a feature map (inspired by Blake and Isard, 1998) and an ellipse was fitted on the refined root tip boundary. To do so, the boundary point closest to the best fit line was taken as the initial point, around which 25 points in both directions along the root tip perimeter were taken into account for a first fit of the ellipse. The second and final fit of the ellipse was based on all boundary points located in the half of the ellipse facing the root tip (Mitchell, 2008). Root tip length and root tip radius were then determined as the semi-major and semi-minor axis of the ellipse, respectively (Figure 3.1). Root length and root diameter were measured manually in ImageJ version 1.50b (*National Institute of Health, Bethesda MD, United*

States). Root shaft diameter was measured at three random positions along the root and averaged. Since the root tip diameter was slightly lower than the diameter along the root shaft, root volume was calculated using the average of the three manual diameter measurements along the root.
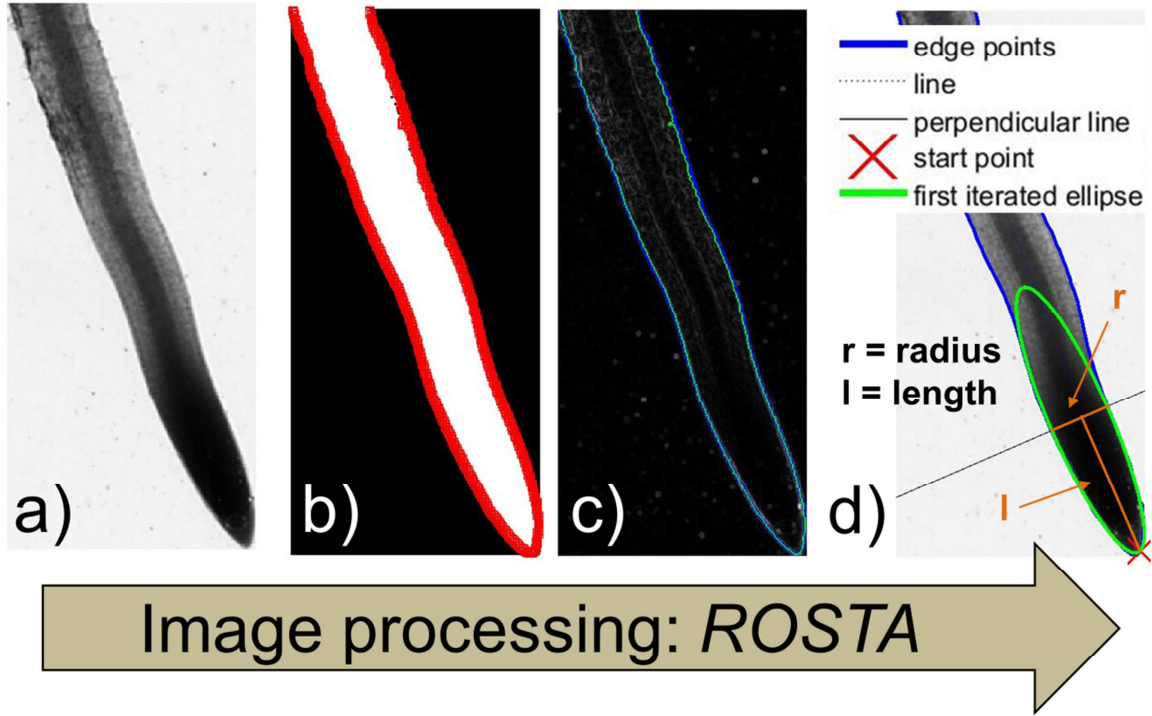
Figure 3.1: Image processing and determination of root tip geometry using Root Scan Tip Analysis (*ROSTA*) software: a) Area of interest containing root tip with pixel edge length of ~ 0.01 mm, b) segmented root tip and perimeter, c) refinement of perimeter using active contour fitting d) and fitting of ellipse on the refined root tip boundary and determination root tip radius and length.

3.2.2.3. Calculation of root penetration force and stress

The force measured with a cone penetrometer ($F_{Z,M\,C}$) consists of a radial and an axial component, which are further influenced by forces resulting from interfacial friction between the cone and the soil (Greacen et al., 1968; Bengough and Mullins, 1990; Bengough and Mullins, 1991). Based on cavity expansion theory, Ruiz et al. (2016) showed that the radial force exerted by the cone ($F_{r\,C}$) can be calculated as:

$$F_{r\,C} = \pi r_C{}^2 \cot(\alpha_C)\sigma_r \quad (3.1)$$

where r_C is the radius at the cone basis, α_C is the semi-apex angle of the cone and σ_r is the radial stress. From Eq 3.1, the frictionless steady-state axial force ($F_{z\,C}$) is obtained as:

$$F_{z\,C} = F_{r\,C} \tan(\alpha_C) = \pi r_C{}^2 \cot(\alpha_C)\sigma_r \tan(\alpha_C) = \pi r_C{}^2\sigma_r \quad (3.2)$$

We considered interfacial friction between the cone and the soil as proposed by Ruiz et al. (2016). The total axial force for the cone ($F_{Z,M\,C}$) is then given by:

$$F_{Z,M\,C} = F_{z\,C}[\mu_C \cot(\alpha_C) + 1] = \pi r_C{}^2\sigma_r[\mu_C \cot(\alpha_C) + 1] = \pi r_C{}^2\sigma_r \left[\mu_C \frac{l_C}{r_C} + 1\right] \quad (3.3)$$

where r_C and l_C represent the base radius and the length of the cone, respectively. The radial stress (σ_r) is then readily calculated as:

$$\sigma_r = \frac{F_{Z,M\,C}}{\pi r_C{}^2 \left[\mu_C \dfrac{l_C}{r_C} + 1\right]} \quad (3.4)$$

Assuming a conical shape of the root tip, the total force acting in the axial direction of the root tip ($F_{Z,M\,Rc}$) is:

$$F_{Z,M\,Rc} = F_{z\,R}[\mu_R \cot(\alpha_R) + 1] = \pi r_R{}^2\sigma_r[\mu_R \cot(\alpha_R) + 1] = \pi r_C{}^2\sigma_r \left[\mu_R \frac{l_R}{r_R} + 1\right] \quad (3.5)$$

where r_R and l_R represent the base radius and the length of the root tip, respectively. Substituting Eq 3.4 into Eq 3.5 allows calculating the total axial penetration force exerted by a root tip during soil penetration under the assumption of a conical shape ($F_{Z,M\,Rc}$) as a function of cone penetrometer force ($F_{Z,M\,C}$):

$$F_{Z,M\,Rc} = \frac{r_R{}^2 \left[\mu_R \dfrac{l_R}{r_R} + 1\right]}{r_C{}^2 \left[\mu_C \dfrac{l_C}{r_C} + 1\right]} F_{Z,M\,C} \quad (3.6)$$

For a spheroid shape of the root tip, Eq 3.5 needs to be slightly modified. The shape factor of an elliptical half-spheroid was used in a previous study to account for the spheroid shape (McKenzie et al., 2013). For the total axial force of a spheroid root tip shape ($F_{Z,M\,Rs}$) the following applies:

$$F_{Z,M\,Rs} = F_{z\,R} \left[\mu_R \frac{\pi l_R}{2 r_R} + 1\right] = \pi r_R{}^2\sigma_r \left[\mu_R \frac{\pi l_R}{2 r_R} + 1\right] \quad (3.7)$$

Substituting Eq 3.4 into Eq 3.7 allows estimation of the total axial penetration force exerted by a root tip during soil penetration under the assumption of a spheroid shape ($F_{Z,M\,Rs}$) as a function of cone penetrometer force ($F_{Z,M\,C}$):

$$F_{Z,M\,Rs} = \frac{r_R{}^2}{r_C{}^2} \frac{\left[\mu_R \frac{\pi l_R}{2 r_R} + 1\right]}{\left[\mu_C \frac{l_C}{r_C} + 1\right]} F_{Z,M\,C} \quad (3.8)$$

For our calculations, we used a coefficient of friction at the root-soil interface (μ_R) of 0.1, which is suggested to be typical for boundary lubricants (Hutchings, 1992) and a metal-soil friction coefficient (μ_C) of 0.5 (Bengough et al., 1997). Root penetration stress for a conical (S_{Rc}) and spheroid (S_{Rs}) root tip shape was then calculated by dividing axial root force by root tip base area ($\pi r_R{}^2$):

$$S_{Rc} = \frac{F_{Z,M\,Rc}}{\pi r_R{}^2} \quad (3.9)$$

$$S_{Rs} = \frac{F_{Z,M\,Rs}}{\pi r_R{}^2} \quad (3.10)$$

Equations 3.6 and 3.8 are likely to overestimate $F_{Z,M\,Rc}$ and $F_{Z,M\,Rs}$, respectively because of the different geometries of the cone and the root tip. The cone used here had a radius to length ratio of 0.58, whereas in roots the average tip radius to length ratio was around 0.23 (Table 3.1). The tip radius to length ratio represents the inverse of a conical shape factor (iSF_{cone}). When root tips were described with a spheroid, the average inverse shape factor ($iSF_{spheroid}$) was around 0.15 (Table 3.1). It has been shown that there is substantial compressive deformation ahead of the tip when iSF is large, resulting in a "spherical" deformation field. In contrast, when iSF is small, there is little deformation in front of the tip and the deformation pattern is rather "cylindrical" (Vollsnes et al., 2010; Ruiz et al., 2016). Greacen et al. (1968) showed that expansion of a cylindrical cavity requires only 25% to 40% of the pressure required to expand a spherical cavity of the same diameter. Eq 3.6 and Eq 3.8 only account for possible differences in root tip shape between treatments with respect to friction but not with respect to differences in cavity forms. Assuming that the pressure required to expand a cavity is affected by the geometry of the tip (Greacen et al., 1968), it can be hypothesized that $F_{Z,M}$ is

proportional to the respective iSF. This would yield a geometry factor for a conical (GF_{cone}) and spheroid root tip ($GF_{spheroid}$) of, respectively:

$$GF_{cone} = iSF_{cone} \frac{l_C}{r_C} = \frac{r_R}{l_R} \frac{l_C}{r_C} \quad (3.11)$$

and

$$GF_{spheroid} = iSF_{spheroid} \frac{l_C}{r_C} = \frac{2r_R}{\pi l_R} \frac{l_C}{r_C} \quad (3.12)$$

3.2.3. Experiment 2: Root anatomy of embryonic and post-embryonic roots

Four individual pre-germinated seeds (25°C, 48 h) of similar size for each treatment combination were selected and grown for 23 days under the conditions described above. After 23 days, roots were washed out from the soil and 20 mm long root samples were taken 3 cm from the root base for anatomical measurements. Root anatomy was investigated in seed-borne roots and nodal roots from the first whorl, which represent embryonic and post-embryonic roots, respectively. The samples were fixed and stored in FAA (10:50:5:35) at 3°C until further analysis. Root cross sections of around 150 μm thickness were cut manually with a razor blade and stained with toluidine blue (0.25% in distilled water) for 1 min. Cross sections were imaged using a 1 megapixel camera (*Olympus XC10, Olympus Corporation, Tokyo, Japan*) connected to a bright field microscope (*Olympus AX70, Olympus Corporation, Tokyo, Japan*). Root cross sectional area, the cross sectional area of the stele and the root cortex, the area in the cortex occupied with root cortex aerenchyma and the number of cortical cell files were manually measured in ImageJ version 1.50b. Using this information, cortical cell file diameter (dm_{CF}) could be calculated as:

$$dm_{CF} = \frac{\sqrt{\frac{A_{root}}{\pi}} - \sqrt{\frac{A_{stele}}{\pi}}}{No_{CF}} \quad (3.13)$$

where A_{root} and A_{stele} is the cross sectional area of the root and the stele, respectively, and No_{CF} is the number of cortical cell files.

3.2.4. Statistics

Statistical analyses were performed in R version 3.1.3 (R Core Team, 2015). Two-way analysis of variance was used to evaluate effects of soil bulk density and genotype on root traits. Treatment means were compared using Tukey's honest significant difference test at $p < 0.05$. Analysis of covariance models based on treatment level means was used to determine whether root diameter or root tip geometry significantly influenced root growth. Non-linear regressions were performed based on treatment level means with the non-linear least square method ("nls") provided by the R package "stats".

3.3. Results

The axial penetration force obtained from cone penetrometer measurements (semi-apex angle: 30°; base radius: 2.5 mm) at -100 hPa matric potential was 6.7 N ($\pm$ 0.8, s.e.m.), 8.7 N ($\pm$ 0.3, s.e.m.) and 20.9 N ($\pm$ 2.1, s.e.m.), for soil bulk densities of 1.3 g cm^{-3}, 1.45 g cm^{-3} and 1.6 g cm^{-3}, respectively (n=4). Thus mechanical impedance calculated for the cone penetrometer was 0.34 MPa ($\pm$ 0.04, s.e.m.), 0.44 MPa ($\pm$ 0.01, s.e.m.) and 1.06 MPa ($\pm$ 0.10, s.e.m.) under low, moderate and high soil bulk density, respectively.

3.3.1. Effects of soil mechanical impedance and genotype on root elongation rate, root tip properties and root diameter

Soil mechanical impedance affected root growth and root morphology in 2-day-old seedlings. Increased mechanical impedance resulted in reduced root length and root volume. Root elongation rate decreased by 40% and 64% under moderate and high soil bulk density, respectively, compared with roots grown in low density soil (Table 3.1). Root volume also decreased significantly, but the decrease was smaller than that in length because root diameter increased with increasing soil mechanical impedance. Root shaft diameter, which was determined as the mean of three random diameter measurements along the root, increased with soil strength. An increase in soil bulk density from 1.3 g cm^{-3} to 1.45 g cm^{-3} and to 1.6 g cm^{-3} resulted in an increase in root diameter of 16% and 44%, respectively (Table 3.1). The geometry of the root tip was determined from high-resolution flatbed scans with a pixel edge length of 0.1 mm using an automated image processing tool (Figure 3.1).

These scans showed that the radius and the length of the root tip significantly increased under high soil strength compared to low and moderate soil strength (Table 3.1). The shape of the root tip was quantified as the inverse of the shape factor for a cone (Eq 3.11) or half spheroid (Eq 3.12), respectively. Despite the effects of soil strength on the size of the root tip, the geometry of the root tip was not significantly affected by increasing soil mechanical impedance (Table 3.1).

Table 3.1: Effects of genotype (GT), soil bulk density (BD) and their interaction on root tip geometry and root morphology after 48 hours of growth, analysed with analysis of variance (ANOVA). * and ** denote significant effects at $p < 0.05$ and $p < 0.01$, respectively, n.s. denotes non-significant effects (n = 6). Different letters indicate significant differences between different soil bulk densities using Tukey's honest significant difference (HSD) test at $p < 0.05$.

	ANOVA			Bulk density average		
Trait	GT	BD	GT:BD	1.3 g cm^{-3}	1.45 g cm^{-3}	1.6 g cm^{-3}
Tip radius [mm]	P=0.06	**	n.s.	0.255^a	0.264^a	0.300^b
Tip length [mm]	*	**	n.s.	1.13^a	1.16^a	1.31^b
iSF$_{cone}$ [mm mm^{-1}]	**	n.s.	n.s.	0.230	0.232	0.233
Tip semi-opening angle [°]	**	n.s.	n.s.	13.1	13.0	13.2
iSF$_{spheroid}$ [mm mm^{-1}]	**	n.s.	n.s.	0.148	0.147	0.148
Root tip base area [mm^2]	P=0.08	**	n.s.	0.206^a	0.221^a	0.290^b
Root length [mm]	**	**	n.s.	45.45^a	27.45^b	16.35^c
Root elongation rate [mm d^{-1}]	**	**	n.s.	22.73^a	13.72^b	8.17^c
Root diameter [mm]	**	**	*	0.524^a	0.609^b	0.754^c
Root volume [mm^3]	**	**	n.s.	10.01^a	8.05^b	7.35^b

Abbreviations: iSF = inverse of cone ($r_{root\ tip}/l_{root\ tip}$) and spheroid shape factor ($2r_{root\ tip}/\pi l_{root\ tip}$); $r_{root\ tip}$ = radius at base of root tip, $l_{root\ tip}$ = length of root tip.

Apart from the radius and the area at the base of the root tip, root properties determined in 2-day-old seedlings were significantly influenced by genotype. Genotypic differences were observed for root elongation rate and root volume, as well as root tip length and root shaft diameter (Table 3.1). Furthermore, significant genotypic diversity was observed for root tip geometry (Supporting Information Figure S3.1), which was particularly pronounced under high soil bulk density (1.6 g cm^{-3}).

Analysis of covariance models applied on treatment level mean values showed that root tip geometry significantly affected root elongation rate, whereas for root diameter this was not observed (Table 3.2).

Table 3.2: Summary statistics from analysis of covariance model of root length as influenced by root tip geometry or root diameter, soil bulk density (1.3 g cm^{-3}, 1.45 g cm^{-3}, 1.6 g cm^{-3}) and their interaction, based on mean values (n = 6) of genotype-bulk density combinations. Numbers indicate F-values. * and ** denote significant effects at $p < 0.05$ and $p < 0.01$, respectively, n.s. denotes non-significant effects.

Assumed root tip shape	Effect	Root elongation rate [mm d^{-1}]
Cone	Bulk density	121.1**
	iSF$_{cone}$	5.2*
	Bulk density:iSF$_{cone}$	0.5 n.s.
	R^2	0.87
Spheroid	Bulk density	121.1**
	iSF$_{spheroid}$	5.2*
	Bulk density:iSF$_{spheroid}$	0.5 n.s.
	R^2	0.87
	Bulk density	107.3**
	dm$_{root}$	0.1 n.s.
	Bulk density:dm$_{root}$	18.8 n.s.
	R^2	0.86

Abbreviations: iSF = inverse of cone ($r_{root\ tip}/l_{root\ tip}$) and spheroid shape factor ($2r_{root\ tip}/\pi l_{root\ tip}$); $r_{root\ tip}$ = radius at base of root tip, $l_{root\ tip}$ = length of root tip, dm$_{root}$ = root diameter.
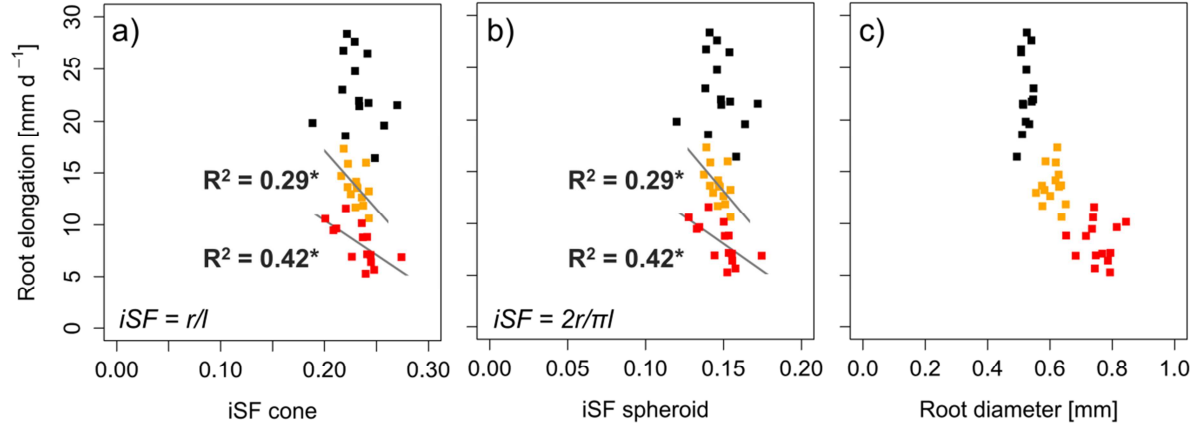

3.3.2. Influence of root tip geometry and root diameter on root elongation rate

As indicated by the results obtained from analysis of covariance (Table 3.2), root tip geometry was related to root elongation rate. The genotypic diversity of root tip geometry resulted in different root elongation rates, an effect which was particularly pronounced under high soil bulk density (Figure 3.2). Root tip radius to length ratio, which was used to calculate the inverted shape factor of the conical and spheroid tip geometry (Eq 3.11 and Eq 3.12), was negatively correlated to root elongation rate ($R^2 = 0.42$, $p < 0.05$) in the soil with bulk density 1.6 g cm^{-3}. A similar relationship was observed

under moderately increased soil bulk density (1.45 g cm^{-3}), whereas under low soil bulk density (1.3 g cm^{-3}) root tip geometry was not related to root elongation rate (Figure 3.3). Despite the significant responses of root diameter to increased mechanical impedance, no correlation between root diameter and root elongation was observed under any of the soil bulk densities tested (Figure 3.3). Similarly to root elongation rate, root volume was negatively correlated ($R^2 = 0.44$ p < 0.01) with root tip radius to length ratio under high soil bulk density (Supporting Information Figure S3.2). These results strongly suggest that the shape of the root tip is a better predictor than root diameter for genotypic root elongation rate under increased soil strength.
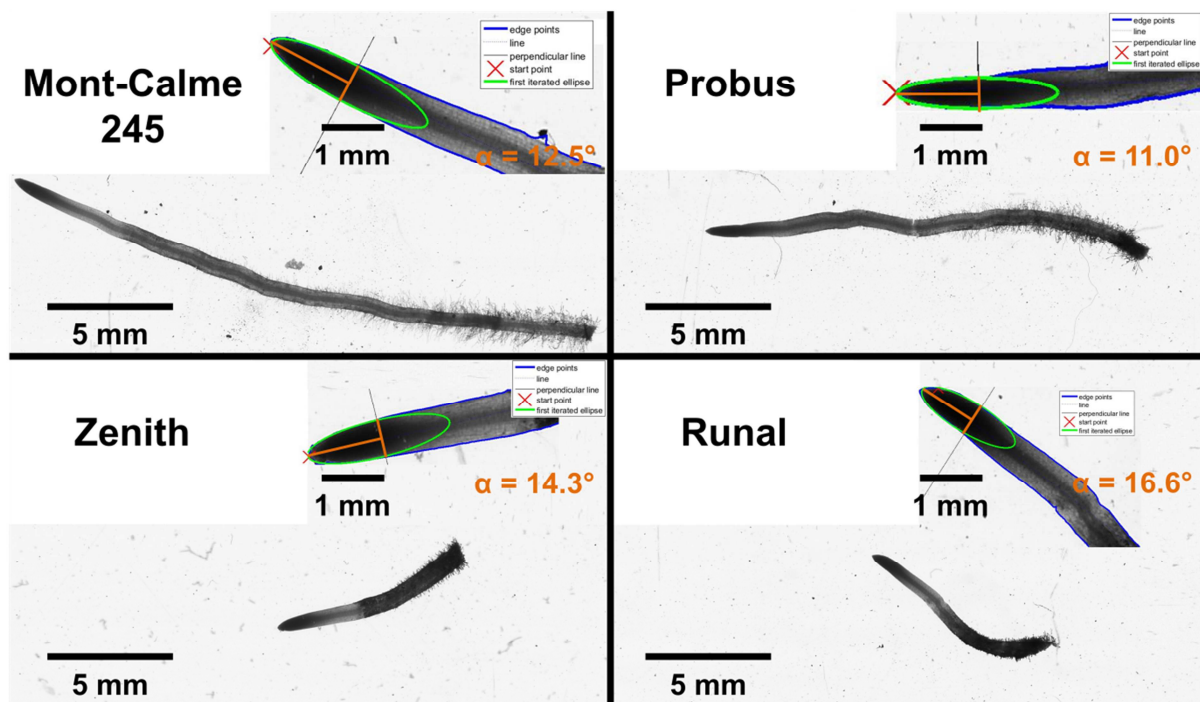
Figure 3.2: Illustration of genetic diversity of root tip geometry and root length after 48 hours of growth into soil with 1.6 g cm^{-3} bulk density: 'Mont-Calme 245' and 'Probus' represent genotypes with acute root tip opening angles whereas 'Zenith' and 'Runal' are characterized by blunt root tip opening angles. α is the value of the semi-root apex angle.
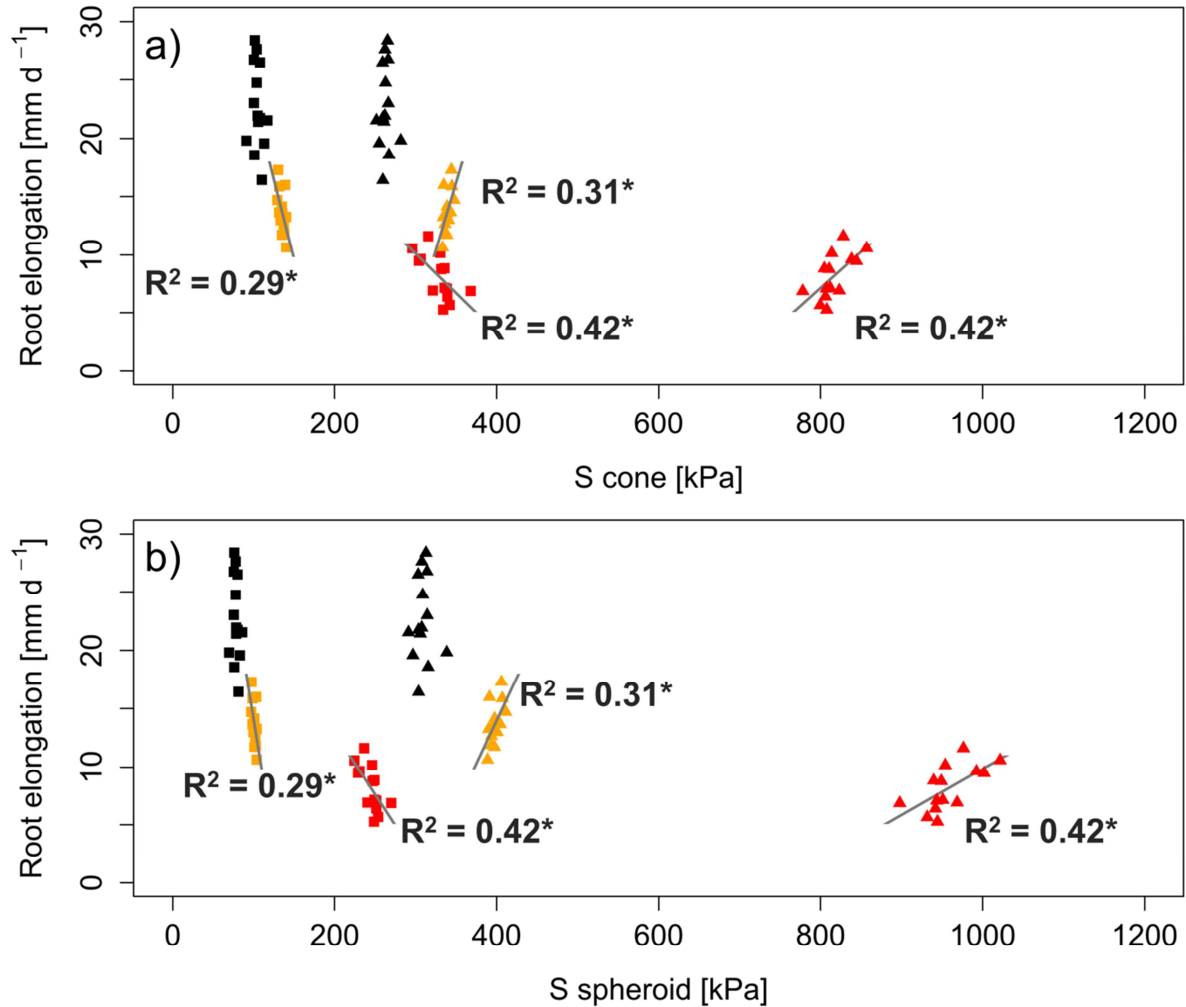
Figure 3.3: Influence of root tip geometry and root diameter on root elongation rate determined in 14 wheat genotypes (n = 6). Linear regressions between root elongation rate and inverse shape factor (iSF; calculated using root tip radius (r) and length (l)) of a) a cone and b) a spheroid geometry and c) root diameter. Black, orange and red symbols represent soil bulk density of 1.3 g cm^{-3}, 1.45 g cm^{-3} and 1.6 g cm^{-3}, respectively. R^2 represents multiple r-squared, * denotes significant regression at p < 0.05.

3.3.3. Relating root penetration force and stress to root elongation rate and root diameter

Combining cone penetrometer measurements with information about the geometry of the cone and the root tips permitted calculation of penetration forces (Eq 3.6 and Eq 3.8) and stresses (Eq 3.9 and Eq 3.10) occurring at the root tip during root elongation. A geometry factor (*GF*, Eq 3.11 and Eq 3.12) was introduced to account for the differences in tip geometry between the steel cone and the roots and between the roots of different genotypes (Table 3.1 and Supporting Information Figure S3.1). The values for *GF* ranged from 0.33 to 0.48 if root tips were assumed to have a conical shape and from 0.21 to 0.30 if root tips were assumed to have a spheroid shape (Supporting Information Table S3.2). Calculated penetration forces ranged between 19 mN and 143 mN under the assumption of a conically shaped root tip and from 14 mN to 105 mN for a spheroid tip shape. The resulting root tip penetration stresses were between 91 kPa and 368 kPa and between 69 kPa and 270 kPa for conical and spheroid tip geometry, respectively (Supporting Information Table S3.3). Calculated genotype mean penetration stresses were significantly related to root elongation rate under high (R^2 = 0.42, p < 0.05) and moderate soil strength (R^2 = 0.29, p < 0.05). Lower root tip penetration stress resulted in increased root elongation rate under high and moderate soil strength, whereas under low soil bulk density no such correlation was observed (Figure 3.4). It is worth mentioning that these relationships

64

changed when the differences in tip geometry and hence the form of cavity were not taken into account. The exclusion of *GF* in the calculations of penetration stresses resulted in positive correlations between root tip penetration stress and root elongation rate (Figure 3.4). Furthermore, root tip and root shaft diameter was not significantly related to root tip penetration stress under any of the assessed levels of soil strength (Supporting Information Figure S3.3).

Figure 3.4: Linear regressions between root tip penetration stress (S) and root elongation rate determined in 14 wheat genotypes (n = 6) for a) conical and b) spheroid root tip geometry. Penetration stresses were calculated excluding (triangles) or including (square) geometry factors (Eq 3.11 and Eq 3.12). Black, orange and red symbols represent soil bulk density of 1.3 g cm^{-3}, 1.45 g cm^{-3} and 1.6 g cm^{-3}, respectively. R^2 represents multiple r-squared, * denotes significant regression at $p < 0.05$.

Figure 3.5 presents root elongation rate and root shaft diameter, respectively, as a function of calculated penetration forces exerted by roots while elongating in soil. Axial root tip penetration force

was related to root elongation rate following a negative power law function (R^2 = 0.75) for both

conical (Eq 3.6 and Eq 3.10) and spheroid tip shape (Eq 3.8 and Eq 3.11). An exponential function,

which asymptotically approached an upper limit, was used to relate root shaft diameter and root tip

penetration force (R^2 = 0.90). For both tip geometries assumed, this upper limit was at a root diameter

of 0.78 mm (Figure 3.5), suggesting that adjustment to increased soil strength in the form of root

thickening is limited. The same relationships between root elongation and root elongation rate and root

diameter, respectively, were obtained when *GF* was excluded from the calculations (Supporting

Information Figure S3.4).
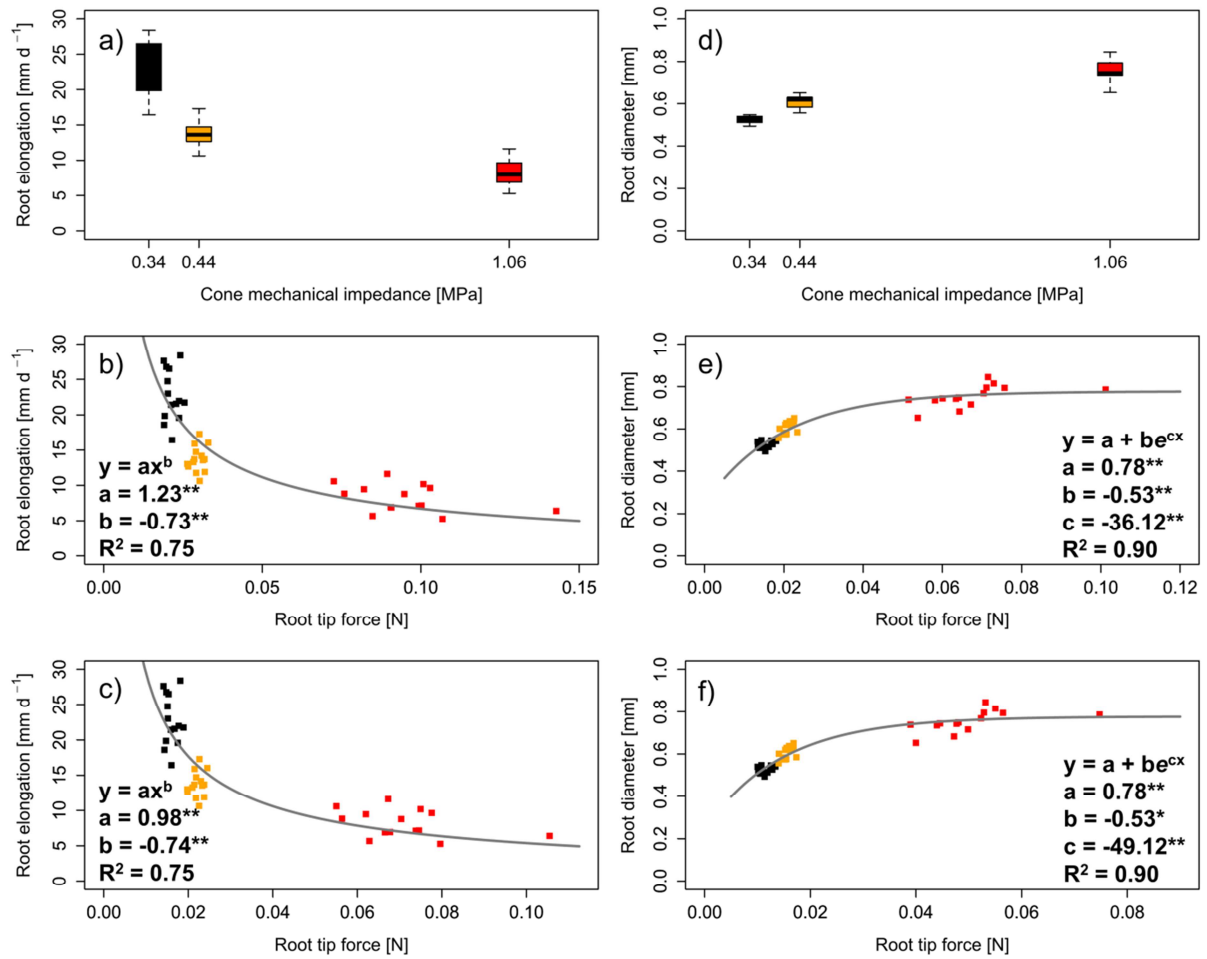
Figure 3.5: Root a), b), c) elongation rate and d), e), f) diameter of 14 wheat genotypes (n = 6) grown at a soil bulk densities of 1.3 g cm^{-3} (black), 1.45 g cm^{-3} (orange) and 1.6 g cm^{-3} (red). a) and d) Cone mechanical impedance was obtained from penetrometer measurements, root tip radial force for b) and e) conical and c) and f) spheroid geometry calculated according to Eq 3.11 and Eq 3.12. R^2 represents multiple r-squared, * and ** denotes significant regression coefficients at $p < 0.05$ and $p < 0.01$, respectively.

3.3.4. Effects of soil mechanical impedance and genotype on root anatomy

In embryonic and post-embryonic roots of 23-day-old plants, root cross sectional area, the area of the stele and the root cortex as well as the cortical cell file number were significantly affected by genotype (Table 3.3). Remarkably, the observed root anatomical responses to increased soil strength were not always consistent between embryonic and post-embryonic roots.

Table 3.3: Effects of genotype (GT), soil bulk density (BD) and their interaction on root anatomical traits in embryonic and post-embryonic roots after 23 days of growth, analysed with analysis of variance (ANOVA). * and ** denote significant effects at $p < 0.05$ and $p < 0.01$ respectively, n.s. denotes non-significant effects (n = 4). Different letters indicate significant differences between levels of soil strength using Tukey's honest significant difference (HSD) test at $p < 0.05$.

| Root class	Trait	ANOVA			Bulk density average		
		GT	BD	GT:BD	1.3 g cm^{-3}	1.45 g cm^{-3}	1.6 g cm^{-3}
Embryonic	Cross section area [mm^2]	**	**	n.s.	0.123^a	0.186^b	0.469^c
	Stele area [mm^2]	**	**	*	0.049^a	0.059^b	0.059^b
	Cortical area [mm^2]	*	**	n.s.	0.074^a	0.128^b	0.410^c
	RCA [mm^2]	n.s.	**	n.s.	0.002^a	0.011^a	0.088^b
	RCA [%]	n.s.	**	n.s.	1.6^a	7.6^b	21.8^c
	Cortical cell file number [#]	**	**	*	2.3^a	3.0^b	4.9^c
	Cortical cell file diameter [mm]	n.s.	**	n.s.	0.032^a	0.036^b	0.051^c
Post-embryonic	Cross section area [mm^2]	**	**	n.s.	0.359^a	0.413^b	0.430^b
	Stele area [mm^2]	**	**	n.s.	0.079^a	0.080^a	0.065^b
	Cortical area [mm^2]	**	**	n.s.	0.281^a	0.333^b	0.365^b
	RCA [mm^2]	**	**	n.s.	0.084^a	0.102^b	0.111^b
	RCA [%]	n.s.	n.s.	n.s.	29.9	30.5	30.3
	Cortical cell file number [#]	**	n.s.	**	6.3	6.5	6.2
	Cortical cell file diameter [mm]	P= 0.06	**	*	0.029^a	0.031^a	0.037^b

Abbreviation: RCA = Root cortex aerenchyma

In embryonic roots, the cross sectional area increased from 0.12 mm^2 under low soil bulk density to 0.19 mm^2 under moderate and 0.47 mm^2 and high soil bulk density. In post-embryonic roots this response was much less pronounced and no significant difference was observed between roots grown under moderate and high bulk density (Figure 3.6). The average root cross sectional area under high soil bulk density corresponded to calculated root diameters of 0.77 mm and 0.74 mm in embryonic and post-embryonic roots, respectively (Table 3.3). These values coincided well with the upper limit of 0.78 mm, to which root diameters of 2-day-old seedlings asymptotically converged with increasing penetration force (Figure 3.5). Similar results were obtained for root cortical area and cortical cell file number, both of which increased in embryonic roots with increasing soil mechanical impedance. In post-embryonic roots, however, cortical area was less affected and cell file number remained unaffected by soil bulk density (Table 3.3). The stele cross sectional area of embryonic roots increased due to soil compaction, whereas in post-embryonic roots stele area decreased in response to compaction (Table 3.3).

Consistent responses to increased soil strength between both root classes were observed for root cortex aerenchyma and cortical cell diameter. In embryonic roots, the percentage of the root cortex occupied with aerenchyma was several orders of magnitude higher under moderate and high soil bulk density when compared to roots from the low bulk density treatment. No difference in the proportion of aerenchyma within the cortex of post-embryonic roots was observed between different levels of soil bulk density. The area of root cortex aerenchyma increased significantly in response to increased soil strength in both root classes (Table 3.3). Cortical cell file diameter increased in response to increased soil bulk density (Figure 3.6) and coincided, particularly under high bulk density, with increasing root cross sectional area (Figure 3.7). Under high soil bulk density (1.6 g cm^{-3}) genotypic root cross sectional area in both root classes was positively correlated to cortical cell file diameter ($R^2 = 0.42$, $p < 0.05$, Figure 3.6). Linear regressions between root cross sectional area and cortical cell file diameter showed that root thickening in response to increased soil strength was related to increased cortical cell file diameter in both embryonic ($R^2 = 0.84$, $p < 0.01$) and post-embryonic roots ($R^2 = 0.33$, $p < 0.01$) (Figure 3.6). Despite the differences between different root classes, these results showed that root

morphological adjustments to soil compaction in the form of root thickening coincided with increased cortical cell file diameter and accelerated formation of cortical aerenchyma.
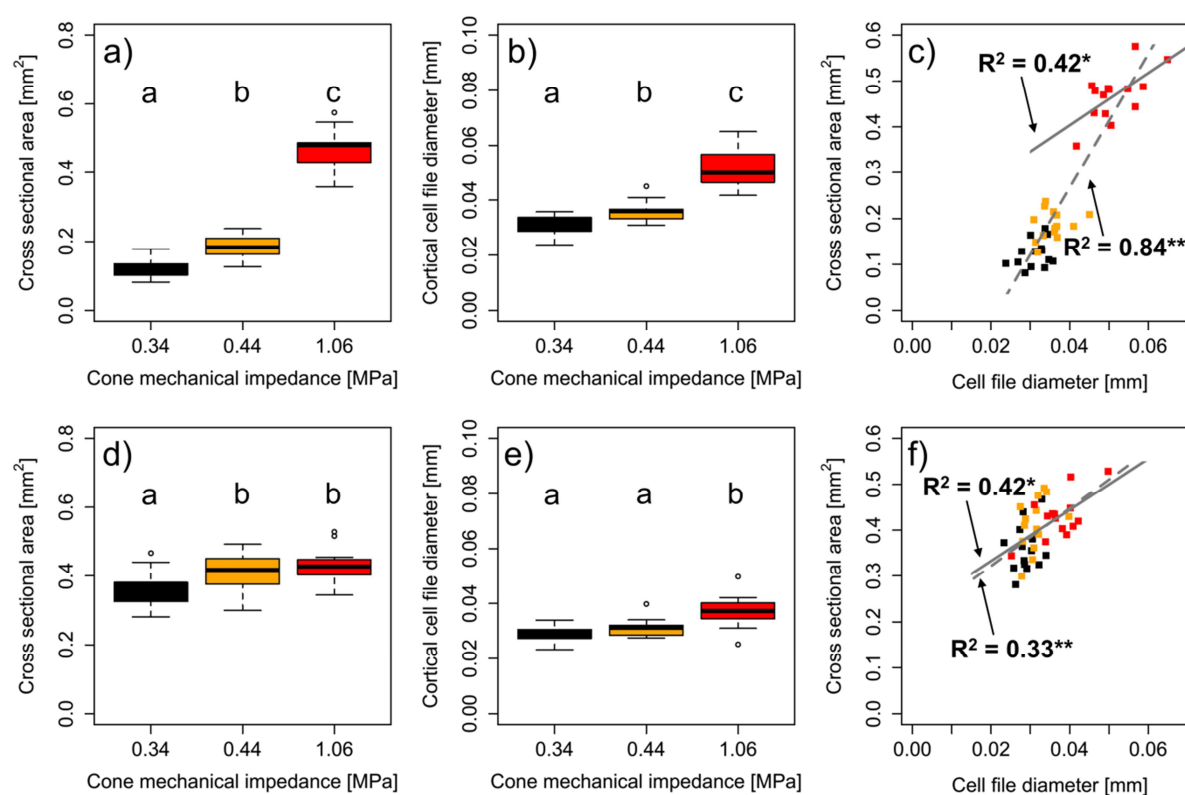
Figure 3.6: Root anatomy in a), b), c) embryonic and d), e), f) post-embryonic roots of 14 wheat genotypes 23 days after planting: a) and d) Total root cross-sectional area, b) and, e) cortical cell file diameter and c) and f) linear correlations between cross-sectional area and cell file diameter, based on treatment means (n = 4). Colours indicate soil bulk density (black: 1.3 g cm^{-3}, orange: 1.45 g cm^{-3}, red 1.6 g cm^{-3}), dashed and continuous regression lines denote regressions including all bulk densities and highest soil bulk density, respectively. Different letters indicate significant differences using Tukey's honest significant difference (HSD) test at p < 0.05, R^2 represents multiple r-squared, * and ** denote significant regression at p < 0.05 and p < 0.01, respectively.
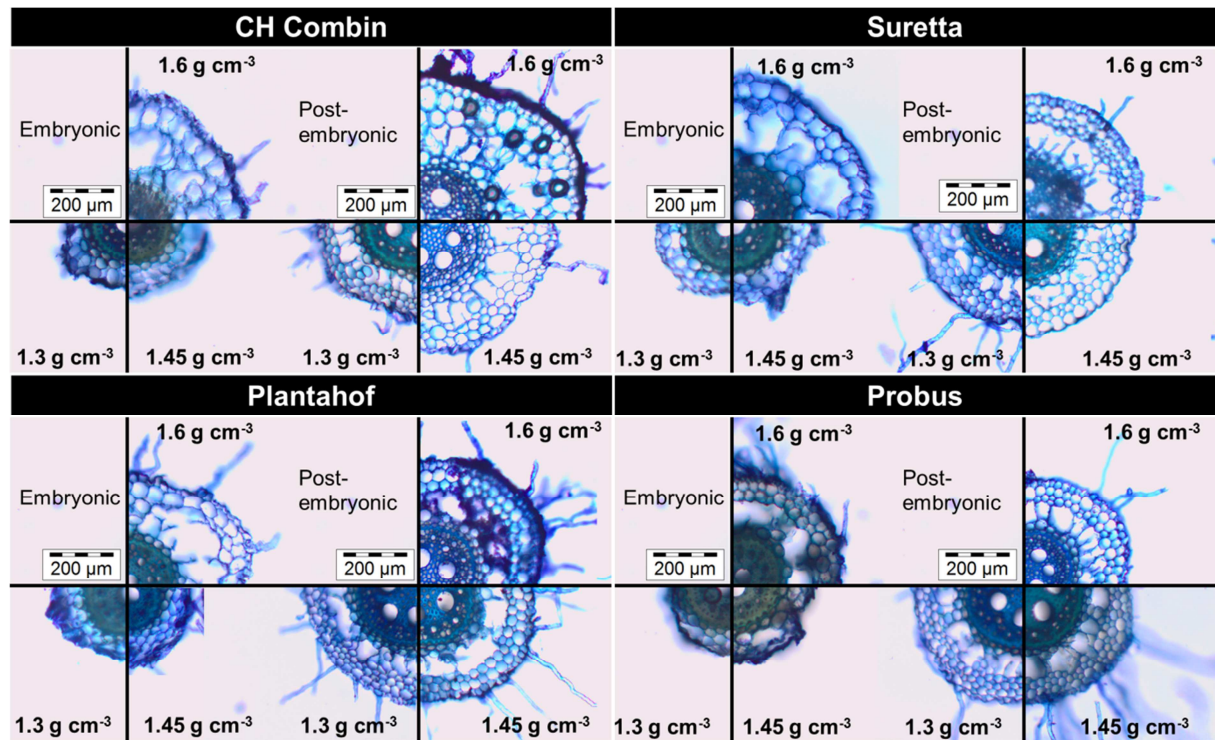
Figure 3.7: Illustration of genotypic diversity in root anatomy sampled 23 days after planting 3 cm from the root base of embryonic and post-embryonic roots under soil bulk densities of 1.3 g cm^{-3}, 1.45 g cm^{-3} and 1.6 g cm^{-3}.

3.4. Discussion

Quantification of root traits in 14 wheat genotypes allowed identification of functional root traits that determine genotypic root elongation rates under increased soil strength. Furthermore, it proved possible to show how and to what extent roots may adjust to increased mechanical impedance with respect to root tip properties, root morphology and anatomy. Combining this phenotypic information with calculated penetration forces and stresses revealed mechanical and physiological implications of genotypic differences and root phenotypic adjustments to increased soil strength.

Root elongation rate decreased with increasing soil bulk density (Table 3.1), which is in agreement with previous findings (Atwell, 1990b; Bengough and Mullins, 1991; Young et al., 1997; Jin et al., 2013; Colombi and Walter, 2016). However, while root elongation rate decreased with increasing soil strength in all genotypes assessed, the magnitude of this response differed significantly between genotypes (Table 3.1). Apart from root elongation rate, significant genotypic differences were observed for root diameter and for the shape and size of the root tip (Table 3.1). Under high soil bulk density (1.6 g cm^{-3}) in particular, but also under moderate soil bulk density (1.45 g cm^{-3}), it was

observed that genotypic root elongation rate correlated with root tip shape. Roots of genotypes with an acute root opening angle, represented by small root tip radius to length ratio, elongated faster in soil with high and moderate soil bulk density compared with roots of genotypes with a rather blunt tip (Figure 3.3). Similar results have been reported for root cap removal, which results in blunted root tips, on root elongation in maize (Iijima et al., 2003b; Vollsnes et al., 2010). This effect of root tip geometry on root elongation rates could be attributed to the distribution of local soil compaction around the root tip induced by the growing root. The lack of an intact root cap resulted in increased penetration stress (Iijima et al., 2003b) due to increased soil compaction at the tip forefront rather than around the tip as observed for roots with intact caps (Vollsnes et al., 2010). Theoretical considerations showed that more acute root tip opening angles cause a shift in the form of cavity expansion from a more spherical to a rather cylindrical deformation field (Greacen et al., 1968; Ruiz et al., 2016). Moreover, Ruiz et al. (2016) found that differences between measured and modeled penetration stress in cone penetrometer experiments are influenced by the cone opening angle.

Based on this, a geometry factor (Eq 3.11 and Eq 3.12) was introduced in this study to account for the influence of genotypic root tip geometry on the form of cavity expansion. It was shown that decreased penetration stress caused by more acute root opening angle (Eq 3.11 and Eq 3.12) resulted in increased elongation rate under high and moderate soil bulk density (Figure 3.4). Inclusion of the geometry factor resulted in penetration forces and stresses that were between 25% and 44% of the values calculated without the geometry factor (Supporting Information Table S3.3). These reductions are almost identical to values presented by Greacen et al. (1968). Penetration force was highly correlated ($R^2 = 0.75$) with root elongation rate, following a negative power law function (Figure 3.5). We are aware, that the reported penetration forces and stresses may differ from the actually occurring values. In the present study, the radial stress of cavity expansion (σ_r) was treated as an inherent soil property and therefore σ_r was assumed to be the same for the steel cone and root tip despite their differing diameter. Furthermore, the different penetration rates of roots (0.004 to 0.02 mm min^{-1}) and the cone penetrometer (4 mm min^{-1}) might further influence penetration forces and stresses (Bengough et al., 1997). However, the penetration forces and stresses as calculated in the present study (Eq 3.1 to

71

Eq 3.12) are within the range of previously reported results for different plant species (Misra et al., 1986; Bengough and McKenzie, 1997; Iijima et al., 2003b; Azam et al., 2013; Bizet et al., 2016).

It has been argued that root diameter is a crucial trait for root growth in compacted soil, since thick roots may reduce penetration stress and prevent buckling of roots (Materechera et al., 1992; Chimungu et al., 2015). In the present study genotypic differences in root diameters (Table 3.1) were not related to root elongation rate (Figure 3.3) or penetration stress (Supporting Information Figure S3.3) and root buckling was not observed. As observed for different small grain cereals in previous studies (Barraclough and Weir, 1988; Materechera et al., 1992; Grzesiak et al., 2013; Hernandez-Ramirez et al., 2014; Colombi and Walter, 2016), root diameters of 2-day-old seedlings increased with increasing soil bulk density (Table 3.1). However, the data obtained from our study strongly suggest that this acclimation of root morphology to increased soil strength was limited by a maximum root diameter. This limitation was observed when comparing root thickening in response to increased bulk density between embryonic and post-embryonic roots, which was determined in 23-day-old plants (Figure 3.6). In embryonic roots, average root cross sectional area increased clearly with increasing soil bulk density (Table 3.3). In post-embryonic roots, which are inherently thicker than embryonic roots, this response was much less pronounced and root cross sectional area was similar under moderate and high soil bulk density (Table 3.3). The same conclusions were reached on examining the regression between root tip penetration force and root diameter (Figure 3.5). This relationship closely followed an exponential function that asymptotically converged to an upper limit ($R^2 = 0.90$), which may be interpreted as a maximum root diameter. It is worth noting that this upper limit, which was 0.78 mm, corresponded to the diameter calculated from the observed average cross sectional area of embryonic and post-embryonic roots under high bulk density (Table 3.3). To our knowledge, such saturation of phenotypic or physiological adjustment in response to soil physical stress has not been reported previously. Saturation of phenotypic or physiological adjustment has been observed for root exudation in response to increasing aluminum toxicity (Pellet et al., 1995; Li et al., 2000) and for the activity of antioxidative enzymes with increasing shoot manganese concentrations (de la Luz Mora et al., 2009). The limitation of root thickening as observed in the present study can be most likely explained by root surface to volume ratio, which is critical for nutrient and water uptake (Varney and Canny, 1993;

Casper and Jackson, 1997). A further increase in root diameter would probably have resulted in root surface to volume ratios being too low for an adequate supply of water and nutrients. The finding that there was no significant adjustment of root tip shape in response to increased bulk density (Table 3.1) is a further indication of the limited potential of roots to adjust to increased soil strength.

The energy requirement for root growth and hence soil exploration increases with increasing soil strength due to greater penetration force and stress (Ruiz et al., 2015). Results from previous studies suggest that the metabolic costs of root elongation increases with increasing soil strength due to lower root length to volume ratios (Atwell, 1990a) and due to increased root meristem activity and cell detachment rate at the root cap (Iijima et al., 2003a). The results from the current study support these findings, since penetration forces and stresses (Figure 3.4 and Figure 3.5) as well as root diameter and root tip size (Table 3.1) were increased in response to increased soil strength. Furthermore, root anatomical properties indicated that plants seek to counterbalance these increased energy demand by altering the anatomy of the root cortex. As shown in previous studies (Atwell, 1990b; Colombi and Walter, 2016), high soil strength led to increased abundance of root cortical aerenchyma and larger cortical cell diameters (Table 3.3). It was shown previously that a high abundance of aerenchyma and large cortical cells decreases the metabolic costs of soil exploration (Chimungu et al., 2014; Saengwilai et al., 2014). In these and the current study, root anatomy was determined near to the root base, whereas mechanical stress is perceived primarily at the root tip (Kirby and Bengough, 2002). Therefore, these root anatomical properties cannot be directly related to the energy that is required for root penetration but rather to the energy that is consumed in the already grown root. However, root tip geometry governed root elongation rate (Figure 3.3), root penetration stress (Figure 3.4) and thus most likely the energy needed to penetrate soils of increasing strength. Therefore, acute root tip opening angels are a promising target trait that can be integrated into plant breeding programmes aiming to develop crop cultivars that can better explore soils of increased strength at low metabolic costs.

3.5. Conclusions

In this study it could be shown that the shape of the root tip in wheat is a pivotal trait determining genotypic root elongation rate in soil of increased strength. Combining information about the

geometry of the root tip with cone penetrometer measurements and cavity expansion theory enabled to relate root elongation rate with root tip opening angle. Acute root tip opening angles resulted in lower penetration forces and stresses due to a more cylindrical form of cavity expansion. Roots could only partially adjust to increased mechanical impedance, since root tips of a certain genotype did not become more acute with increasing soil strength and root thickening was limited. Apart from governing root elongation rate, the observed relationship between root tip geometry and penetration stress indicated that an acute root tip opening angle reduced the energy and hence the metabolic costs needed to penetrate soil of increased strength. Hence, the geometry of the root tip and the resulting penetration forces and stresses must be taken into account when selecting for crop varieties that tolerate high soils strength.

Acknowledgements

Chapter 4: Genetic diversity under soil compaction in wheat: root number as a promising trait for early plant vigour

Tino Colombi[1*] and Achim Walter[1]

[1]ETH Zurich, Institute of Agricultural Sciences (IAS), Zurich, Switzerland

[*]Corresponding author, tino.colombi@usys.ethz.ch

Abstract

Soil compaction of arable land, caused by heavy machinery constitutes a major threat to agricultural soils in industrialized countries. The degradation of soil structure due to compaction leads to decreased (macro-)porosity resulting in increased mechanical impedance, which adversely affects root growth and crop productivity. New crop cultivars, with root systems that are adapted to conditions of increased soil strength, are needed to overcome the limiting effects of soil compaction on plant growth. This study aimed i) to quantify the genetic diversity of early root system development in wheat and to relate this to shoot development under different soil bulk densities and ii) to test whether root numbers are suitable traits to assess the genotypic tolerance to soil compaction. Fourteen wheat genotypes were grown for three weeks in a growth chamber under low (1.3 g cm^{-3}), moderate (1.45 g cm^{-3}) and high soil bulk density (1.6 g cm^{-3}). Using X-ray computed tomography root system development was quantified in weekly intervals, which was complemented by weekly measurements of plant height. The development of the root system, quantified via the number of axial and lateral roots was strongly correlated ($0.78 < r < 0.88$, $p < 0.01$) to the development of plant height. Furthermore, significant effects ($p < 0.01$) of the genotype on root system development and plant vigour traits were observed. Under moderate soil strength final axial and lateral root numbers were significantly correlated ($0.57 < r < 0.84$, $p < 0.05$) to shoot dry weight. Furthermore, broad-sense heritability of axial and lateral root number was higher than 50% and comparable to values calculated for shoot traits. Our results showed that there is genetic diversity in wheat with respect to root system responses to increased soil strength and that root numbers are suitable indicators to explain the responses and the tolerance to such conditions. Since root numbers are heritable and can be assessed at high throughput rates under laboratory and field conditions, root number is considered a promising trait for screening towards compaction tolerant varieties.

4.1. Introduction

It is estimated that an area of 68 million hectares of arable land is degraded by soil compaction (Hamza and Anderson, 2005; Batey, 2009), which is caused by the increasing use of heavy agricultural machinery in modern agriculture (Tracy et al., 2011). In comparison to undisturbed soils, compacted soils are characterized by lower (macro-)porosity and decreased pore connectivity (Bottinelli et al., 2014; Chen et al., 2014a; Kuncoro et al., 2014a). This soil structural degradation adversely affects soil physical functions, which limit root growth and therefore decrease agricultural productivity (Barraclough and Weir, 1988; Botta et al., 2010; Arvidsson et al., 2014). Decreased void space in compacted soils leads to higher mechanical impedance and hence results in reduced root growth rates and resource uptake (Bengough and Mullins, 1991; Young et al., 1997; Jin et al., 2013). Furthermore, crop growth in compacted soils may be limited due to low levels of plant available water (Lipiec and Hatano, 2003) and decreased fluid transport rates (Kuncoro et al., 2014b; Colombi et al., 2017). Together these adverse changes of soil physical functions lead to decreased physical soil fertility caused by soil compaction (Abbott and Murphy, 2007). High soil strength may also occur in dry soils, which are also characterized by increased mechanical impedance (Masle and Passioura, 1987; Bengough et al., 2011). Since high soil strength reduces primarily root system vigour, varieties with adapted root system traits are needed in order to overcome adverse effects of soil compaction on crop productivity. The integration of root traits into breeding programmes is suggested to increase the tolerance of crops to soil derived abiotic stress and therefore to contribute to crop productivity under limited soil fertility (York et al., 2013).

In recent years, the concept of adapting the root system architecture of crops in a way that allows improving crop productivity under poor soil fertility received growing attention (Bishopp and Lynch, 2015). Root system architecture describes the spatial configuration of coarse structures of the root system based on the quantification of root numbers, lateral branching density and root angles in soil (Lynch, 1995). Among other root architectural properties, root numbers were shown to be related in different crops to the genotypic tolerance to low soil fertility. In maize for example, low axial and lateral root number were observed to enhance plant performance under conditions of low soil nitrogen

(Saengwilai et al., 2014b; Zhan and Lynch, 2015) and under low soil moisture (Zhan et al., 2015; Gao and Lynch, 2016). In common bean instead, a high number of basal roots in the topsoil improved phosphorus uptake and plant vigour in low phosphorus soils (Miguel et al., 2013). A major advantage of root system architectural traits and root numbers in particular is that they can be assessed in large diversity panels under field conditions at high throughput rates (Trachsel et al., 2011; Colombi et al., 2015; Burridge et al., 2016). The quantification of root dry weight or length instead is much more laborious and not feasible under field conditions. The heritability of root numbers was reported to be relatively high in a wide range of crop species (Wilcox and Farmer, 1968; Bucksch et al., 2014; Colombi et al., 2015; Li et al., 2015; Richard et al., 2015; Burridge et al., 2016). Besides increasing awareness about the importance of roots for crop production, it has been suggested that holistic phenotyping approaches are needed to understand plant responses to abiotic stress. This may include simultaneous assessments of above- and belowground traits and continuous measurements of plant traits instead of measurements taken at one single point in time (Walter et al., 2015).

Like other abiotic stresses such as water or nutrient scarcity, soil compaction causes alterations of the root system phenotype. These phenotypic responses are consistent between different crop species including major mono- and dicotyledonous crops such as small grain cereals, maize or soybean (Tracy et al., 2012a; Grzesiak et al., 2014; Pfeifer et al., 2014a; Chen et al., 2014b; Colombi and Walter, 2016). Apart from shallower root growth and increased root diameters, crop root systems show decreased axial and lateral root numbers in response to soil compaction. In most of these studies such alterations of the root phenotype resulted in decreased shoot biomass both under laboratory (Grzesiak et al., 2014; Pfeifer et al., 2014a) and field conditions (Chen et al., 2014b; Colombi and Walter, 2016). It has been shown that these root architectural responses to soil compaction obtained from mature plants in the field can be reproduced in pots with young plants (Colombi and Walter, 2016). In the same study it was also observed that lateral root initiation in wheat, triticale and soybean seedlings is delayed due to increased soil strength. However, in this study only one variety per crop species was assessed and thus no conclusive statement could be made about genetic diversity of plant responses to soil compaction within one species. Leaf and root growth rates of wheat, barley, maize and pea were reported to decrease within minutes to hours when soil strength increased (Masle and Passioura, 1987;

Bengough and Mullins, 1991; Beemster et al., 1996; Young et al., 1997). The susceptibility to increased soil strength varies considerably between different species. It has been shown that legumes are more sensitive to soil compaction than grasses (Arvidsson and Håkansson, 2014) and that small grain cereals show a higher tolerance to increased mechanical impedance than maize (Grzesiak et al., 2014).

Despite the information about phenotypic responses of crops to soil compaction and the differences between species, information about differences within a single species is scarce, but would be highly desired for plant breeding purposes. A detailed understanding of the genotypic diversity is needed to identify root traits, which determine the tolerance to increased soil strength (Hamza and Anderson, 2005). This includes the understanding of root-shoot relationships in compacted soils as well as quantitative information about root traits, which determine growth responses and the tolerance to increased soil strength. Genotypic differences of axial and lateral root number and shoot vigour were shown in young triticale, maize and soybean plants. Depending on the genotype, moderate soil compaction in particular led to decreased, constant or even increased root numbers (Bushamuka and Zobel, 1998; Grzesiak et al., 2014). However, in these studies only two to four genotypes were evaluated, which did not allow for quantitative statements about the influence of root traits on the tolerance to soil compaction. In other studies soil compaction was simulated with paraffin-vaseline discs and the capability to penetrate these discs was compared between seedlings of 24 and 81 wheat genotypes (Kubo et al., 2004; Kubo et al., 2006). These studies reported a positive relationship between the number of roots penetrating through the paraffin-vaseline layer and shoot dry weight. Similar results were reported for eight varieties of narrow-leafed lupin grown in the field, where the number of lateral roots was positively correlated to the agronomic performance of the different cultivars (Chen et al., 2014b). These studies indicated the use of certain root system architectural traits in order to increase the tolerance to soil compaction. However, due to the destructive measurements, root-shoot relationships could not be quantified dynamically in any of these studies. X-ray computed tomography (CT) or magnetic resonance imaging are promising approaches to study root system development in soil over time. Using X-ray micro computed tomography temporal dynamics of root

system architecture in response to soil compaction were quantified in tomato, wheat and soybean seedlings (Tracy et al., 2012a; Tracy et al., 2013; Colombi and Walter, 2016).

In this study we test the hypothesis whether root number is a suitable trait that could be used in crop breeding programmes aiming to improve the tolerance to compacted soils by: i) investigating how root system development is related to shoot development under increasing soil strength, ii) quantifying the genetic diversity of root and shoot responses to increased soil strength and iii) testing whether root numbers may be used to assess the tolerance of different wheat varieties to increased soil strength. Fourteen wheat varieties were grown under three different levels of soil bulk density for three weeks, during which root system development and shoot growth were quantified in weekly intervals.

4.2. Material and Methods

4.2.1. Plant material and soil physical conditions

The fourteen winter wheat (*Triticum aestivum* L.) varieties used in this study, originate from Swiss public breeding programmes and were released to the market between 1910 and 2010 (Table 4.1). Plants were grown in PVC columns of 4.9 cm inner diameter and 15 cm height, which were filled with field soil (Pseudogleyed Cambisol) excavated at Agroscope Zurich (8°31'E, 47°27'N, 443 m above sea level). For the experiments, soil was taken from the uppermost 15 cm, dried to approximately 22% gravimetric water content and homogenized before being sieved through a 2 mm sieve. Soil pH (CaCl$_2$) in the top 20 cm was 6.9 with an organic carbon content of 1.7% and textural composition of 25% clay, 50% silt and 25% sand. The soil was stored at 3° C until further use. Different levels of soil strength were achieved by compressing the soil to three different soil bulk densities. Soil was packed into the columns to low (1.3 g cm^{-3}), moderate (1.45 g cm^{-3}) and high (1.6 g cm^{-3}) bulk density in six layers of 2 cm height. In order to ensure homogenous packaging surfaces of each layer were slightly abraded. To ensure proper soil aeration, the columns were closed at the bottom with sheep wool. Each variety-bulk density combination was replicated four times.

Four individual soil cores of 5.1 cm diameter and 5 cm height per bulk density were packed with the same sieved soil as used for plant growth studies in 1 cm layers to low (1.3 g cm^{-3}), moderate (1.45 g cm^{-3}) and high (1.6 g cm^{-3}) soil bulk density. These samples were saturated slowly from below and

equilibrated on a ceramic plate to a matric potential of -100 hPa in order to determine gravimetric water content at field capacity (Schjonning and Rasmussen, 2000). Mechanical impedance at -100 hPa was determined by two penetrometer insertions into the center of the bottom side of the soil cores as described by Colombi and Walter, (2016). Measured penetration resistance was 0.34 ($\pm$ 0.04, s.e.m.) MPa, 0.44 ($\pm$ 0.01, s.e.m.) MPa and 1.06 ($\pm$ 0.10, s.e.m.) MPa for low, moderate and high bulk density, respectively.

Table 4.1: Winter wheat varieties used in the study ordered according to the year of market release.

Variety name	Year of release
Plantahof	1910
Mont-Calme 245	1926
Mont-Calme 268	1926
Probus	1948
Zenith	1969
Arina	1981
Runal	1995
Titlis	1996
Zinal	2003
CH-Claro	2007
Forel	2007
CH-Combin	2008
Suretta	2009
Simano	2010

4.2.2. Growth conditions

Pre-germinated seeds (25° C, 48 h) were selected according to similar radicle length and seed size. The emerged radicle (length $\approx$ 2 mm) was placed into a hole of 1 mm diameter and 5 mm length, which was inserted into the centre of the soil columns. Seeds were covered with 1 cm of loose soil (1.0 g cm^{-3}). Plants were allocated in a randomized complete block design with four blocks and grown for

23 days in a growth chamber at a day/night cycle of 14/10 h. Incident light was 510 ($\pm$ 33, SD) μmol s^{-1} m^{-2} and recorded average temperature and relative air humidity were 21.4° C and 63%, respectively. Soil moisture content was kept at field capacity (-100 hPa) by daily weighing and watering.

4.2.3. Root and shoot growth dynamics

Both root and shoot development was recorded four times during growth. This was done in weekly intervals, starting at leaf emergence, which occurred in all plants two days after planting. Similar to previous studies (Tracy et al., 2012a; Tracy et al., 2013; Colombi and Walter, 2016) root system development was quantified using an X-ray micro computed tomography scanner (Phoenix v|tome|x s 240; GE Sensing and Inspection Technologies GmbH, Wunstorf, Germany). The top 6 cm of the pot were scanned at 120kV and 450 µA with 0.1 mm Cu filter. To reduce noise in the scans and scanning time binning of 2 by 2 voxels was applied. The used settings (Supporting Information Table S4.1) resulted in a scan time of 7 min and a voxel edge length of 0.068 mm. The number of axial and lateral roots was manually counted in each scan using Visual Studio Max 2.2 (Volume Graphics GmbH, Heidelberg, Germany) in a segment of 4 cm height, starting 1 cm below the seed base. Axial roots were only counted if they penetrated deeper than 1 cm below the seed base and lateral roots were counted if they emerged from axial roots at depths between 1 and 5 cm below the seed base (Figure 4.1). Visual detection limits for structures in CT scans are commonly seen to be at diameters that exceed twice the voxel edge length (Jähne, 2002). Hence, the chosen resolution of 0.068 mm voxel edge length enabled to quantify first order lateral roots. The first time point two days after sowing was only used to confirm that roots successfully penetrated the soil and was excluded from further analysis. At the same days at which CT scans were performed, shoot development was determined. These measurements included the number of fully developed leaves, the number of tillers and plant height. To quantify plant height, the coleoptile was marked and plant height was measured from this mark to the tip of the longest leaf.
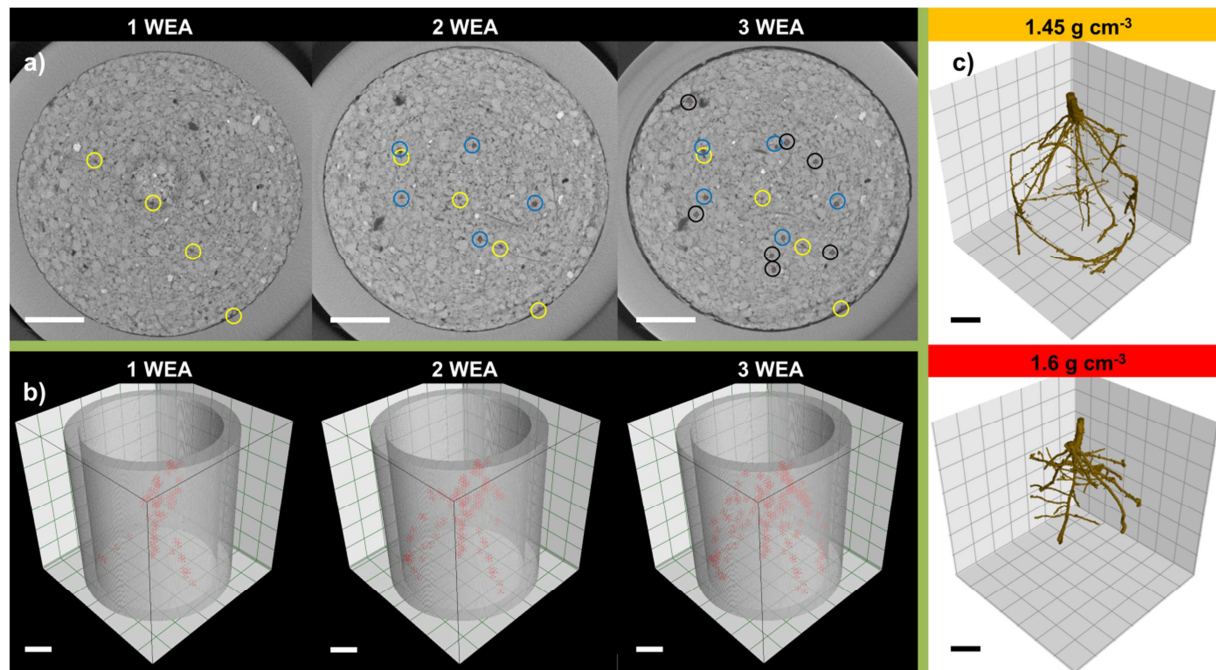
Figure 4.1: Illustration of root system quantification by means of X-ray computed tomography: a) cross sections taken 1 cm below seed base one, two and three weeks after shoot emergence (WAE) with axial roots marked (circles). b) Three dimensional arrangement of lateral branching points (red markers) within the top 6 cm of the soil column one, two and three WAE. c) Segmentation of root system two WAE under moderate (1.45 g cm^{-3}) and high soil bulk density (1.6 g cm^{-3}). Scale bar = 1 cm.

4.2.4. Diversity of root and shoot traits three weeks after emergence

In addition to axial and lateral root number determined from the µCT scans three weeks after emergence, final root branching density was determined by dividing lateral by axial root number. After the final CT scan, roots were gently washed out from the soil and dried at 60° C for at least 72 hours before determining root dry weight. Shoot dry weight and root-shoot ratio were further plant vigour traits that were measured at the end of the experiment three weeks after emergence. As for roots, shoots were dried for 72 hours before weighing. Four additional replications per bulk density of the variety "Arina" were grown under the exactly same conditions but were never scanned in order to check whether X-ray irradiation adversely affected plant development (Flavel et al., 2012). Comparing their root and shoot dry weights with plants from the same variety, which were regularly scanned, allowed excluding effects of X-ray on plant development (Supporting Information Table S4.2). Final plant height, leaf and tiller number as well as root-shoot ratio were used as additional plant vigour indicators.

4.2.5. Data analysis and statistics

Data analysis and statistics were performed in R version 3.1.3 (R Core Team, 2015). In order to account for effects of repeated measurements, root system and shoot development were evaluated in the ASReml package (Guilmour et al., 2009) for R with the following linear mixed effect model:

$$Y_{ijkl} = \mu + \alpha_i + \beta_j + \alpha\beta_{ij} + w_l + \alpha\beta w_{ijl} + \beta w_{jl} + p_k + \varepsilon_{ijkl} \qquad (4.1)$$

where Y represents the measured trait of the ith variety ($i = 1,2,…,13, 14$) and of the jth bulk density ($j = 1.3$ g cm^{-3}, 1.45 g cm^{-3}, 1.6 cm^{-3}), within the lth week after emergence ($l = 1, 2, 3$) and the kth pot ($k = 1, 2,…, 167, 168$); α is the variety effect, β is the effect of the soil bulk density, $\alpha\beta$ is the interaction between the variety and the bulk density, w is the effect of the week after emergence, $\alpha\beta w$ is the interaction between the variety, the bulk density and the week after emergence, βw is the interaction between the bulk density and the week after emergence, p is the effect of the pot and ε is the residual error. Variety, bulk density, variety-bulk density interaction and the week after emergence were treated as fixed factors whereas the remaining factors were set as random. The numbers of axial and lateral root were converted by square root transformation to better meet the model (Eq 4.1) assumptions (Supporting Information Figure S4.1). Based on the model predictors for all variety-bulk density combinations, plant height and back-transformed root numbers were related using the following square root function:

$$h = a * r^{0.5} + b \qquad (4.2)$$

where h is the plant height at one, two or three weeks after emergence, r is the axial or lateral root number at one, two or three weeks after emergence, a is the scaling factor and b the intercept. Performing analysis of covariance (ANCOVA) based on model predictors (Eq 4.1) allowed determining whether bulk density significantly affected root-shoot relationships. To do so, soil bulk density and transformed (square root) root numbers were used as factorial and continuous variable, respectively and plant height was treated as response variable.

The set of root and shoot traits obtained three weeks after emergence was evaluated with a two-factorial analysis of variance (ANOVA), in which the effects of the variety, the soil bulk density and their interaction were treated as fixed effects. Again, the number of roots was converted by square root

transformation (Supporting Information Figure S4.2). To compare the relative genotypic variability of root numbers and root and shoot dry weight between different levels of soil strength, coefficients of variation (CV) were calculated for each treatment level (n = 4). Using one factorial ANOVA, the relative genotypic variability of root and shoot traits could be compared across the three studied levels of soil strength. Means between soil bulk density levels and genotypes were compared using least significant difference (LSD) and Tukey's honest significant difference (HSD) tests, respectively at significance level of $p < 0.05$. The tolerance of varieties to increased soil bulk density was assessed based on the proportion between variety mean trait values under high (1.6 g cm^{-3}) or moderate (1.45 g cm^{-3}) soil bulk density and low bulk density (1.3 g cm^{-3}), respectively. In doing so, values were standardized in order to account for the effects of the breeding background (pre- and post-green revolution).

Furthermore, broad-sense heritability was calculated for root and shoot traits, which were quantified three weeks after emergence. To check for the stability of the inheritance under increased soil strength, heritability was calculated separately for each bulk density level. Genotypic variance was obtained by setting the replication and the variety as a fixed and random factor, respectively. Mean based heritability was estimated as proposed by Falconer and Mackay (1996):

$$H^2 = \frac{\sigma_g{}^2}{\sigma_g{}^2 + \frac{\sigma_e{}^2}{r}} \qquad (4.3)$$

where $\sigma_g{}^2$ and $\sigma_e{}^2$ represents the genotype and residual error variance, respectively and r is the number of replications.

4.3. Results

4.3.1. Root system and shoot development in response to increased soil bulk density

Soil bulk density significantly ($p < 0.01$) affected all root system and shoot traits, which were assessed in weekly intervals during plant growth (Table 4.2). Increased soil strength caused delayed plant development and resulted in decreased plant height, lower tiller and leaf number as well as decreased axial and lateral root number. Compared to low and moderate soil bulk density, plant height and leaf number under high soil bulk density were decreased already one week after leaf emergence by

25-44%. Two and three weeks after emergence leaf number and plant height under high soil bulk density were around 35% lower compared to the plants grown under low and moderate bulk density (Table 4.3). Moderate soil compaction also led to a slight reduction in leaf number and plant height of around 7% compared to the low bulk density treatment. The strongest effects of increased soil strength on shoot development were observed for the number of tillers. Under low bulk density plants developed 2.7 and 4.0 tillers two and three weeks after emergence, respectively. These numbers decreased under moderate soil compaction to 2.0 and 3.0 tillers per plant two and three weeks after emergence, respectively, whereas under high soil bulk density almost no tillers were developed (Table 4.3). In terms of root number, the responses to increased soil bulk density were in a similar order of magnitude as for shoot traits. Under high soil strength, lateral root number decreased by around 70% compared to the plants grown at low bulk density at all three measurement points. A reduction of axial roots due to high soil bulk density could be observed two and three weeks after emergence (Table 4.3). Under moderate soil compaction axial root number decreased only slightly compared to the low bulk density treatment, whereas two and three weeks after emergence lateral root number was decreased by 11% and 19%, respectively (Table 4.3).

Table 4.2: Effects of variety (V), soil bulk density (BD), their interaction and week after emergence (WAE) on axial and lateral root number (NoAx and NoLat, respectively), plant height, number of fully developed leaves and number of tillers. Significance of effects was determined using linear mixed model (Eq 4.1) and Wald-tests. * and ** denote significant effects at $p < 0.05$ and < 0.01, respectively, n.s. denotes non-significant effects (n = 4).

Trait	Transformation	V	BD	V:BD	WAE
NoAx [#]	sqrt	**	*	n.s.	**
NoLat [#]	sqrt	**	**	**	**
Plant height [mm]		**	**	*	**
Leaf number [#]		**	**	n.s.	**
Tiller number [#]		**	**	*	*

Table 4.3: Bulk density mean values of predictors obtained from linear mixed model (Eq 4.1) for axial and lateral root numbers (NoAx and NoLat, respectively), plant height, leaf and tiller number under low (1.3 g cm^{-3}), moderate (1.45 g cm^{-3}) and high (1.6 g cm^{-3}) soil bulk density one, two and three weeks after emergence (WAE). Values are based on 4 replications of 14 varieties and root numbers represent back-transformed values.

	1 WAE			2 WAE			3 WAE		
Bulk density [g cm^{-3}]	**1.3**	**1.45**	**1.6**	**1.3**	**1.45**	**1.6**	**1.3**	**1.45**	**1.6**
NoAx [#]	4.6	4.9	4.5	10.2	10.1	7.2	16.7	16.0	9.1
NoLat [#]	50.5	48.1	15.3	77.1	68.9	25.4	116.5	94.1	34.9
Plant height [mm]	187.1	176.5	132.4	282.0	261.4	168.4	320.1	292.9	181.4
Leaf number [#]	1.94	1.88	1.05	3.28	3.00	2.05	4.39	4.18	2.94
Tiller number [#]	0.36	0.34	0.00	2.70	2.05	0.02	4.03	3.07	0.06

Using a square root function (Eq 4.2) the development of lateral and axial root numbers was observed to be significantly ($p < 0.01$) correlated with the development of plant height. Pearson correlation coefficients were between 0.78 and 0.88 indicating a reasonably strong non-linear relationship between root number and plant height over time (Figure 4.2). Analysis of covariance with bulk density as a fixed factor allowed determining the influence of increased soil strength on root-shoot relationships. The relationship between the number of axial roots and plant height was affected significantly ($p < 0.01$) by bulk density but not by the interaction of bulk density and root number. Bulk density explained 16% of the total variance, whereas the interaction between bulk density and root number only explained 0.1% of the total variance (Table 4.4). In contrast to that, the relationship between the development of lateral root number and plant height remained unaffected by increased soil bulk density (Table 4.4). Hence, it can be concluded that more axial roots are needed to maintain shoot growth under increased soil strength compared to conditions of loose soil (Figure 4.2).
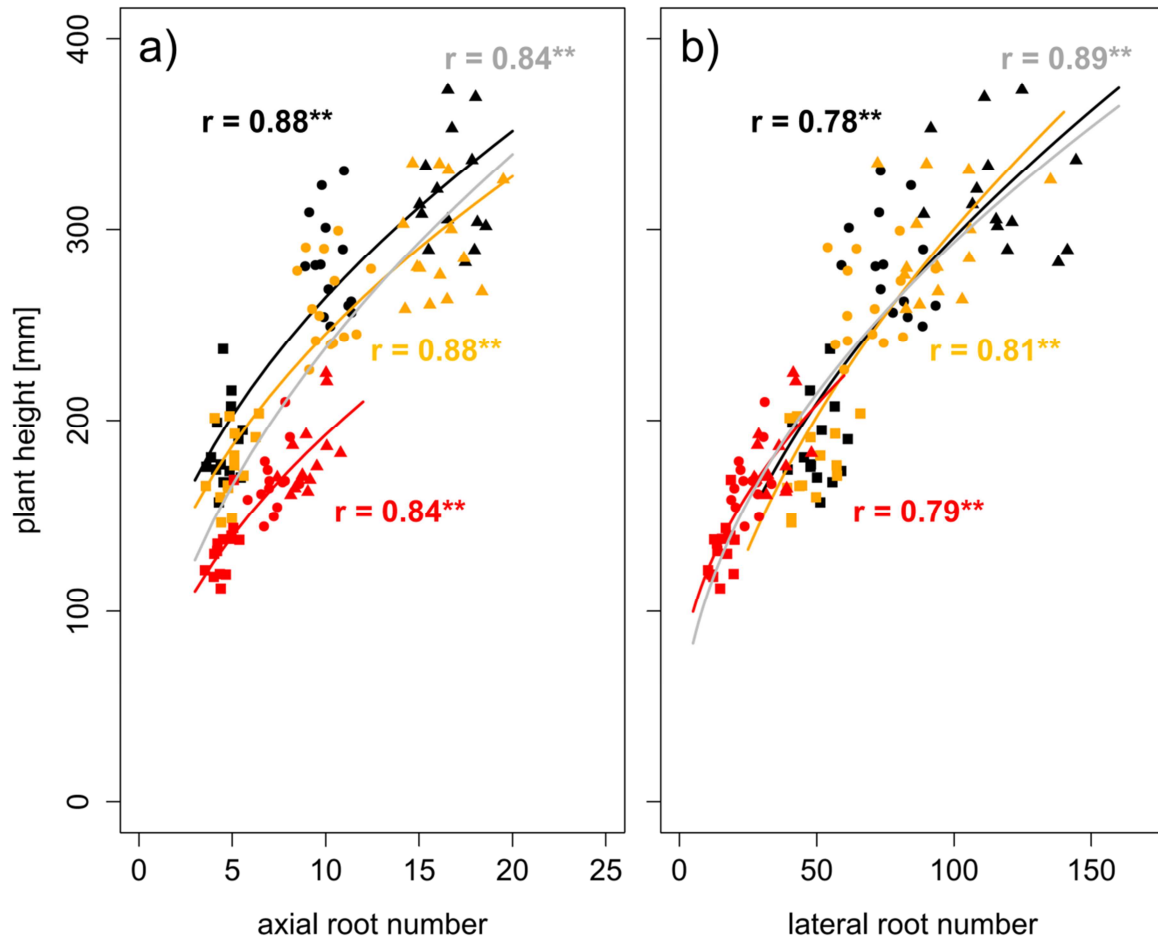
Figure 4.2: Non-linear regressions and Pearson correlation coefficients between a) axial and b) lateral root number and plant height under bulk densities of 1.3 g cm^{-3} (black), 1.45 g cm^{-3} (orange) and 1.6 g cm^{-3} (red), grey represents regression over all three bulk densities; Square, circle and triangle symbol shapes represents values obtained one, two and three weeks after leaf emergence, respectively; ** denotes significant correlation at p < 0.01 (n = 4).

Table 4.4: Effects of soil bulk density, axial and lateral root numbers (NoAx and NoLat, respectively) based on linear mixed model predictors (Eq 4.1) and their interaction on plant height using analysis of covariance model: bulk density (1.3 g cm^{-3}, 1.45 g cm^{-3} and 1.6 g cm^{-3}) was treated as a factor and transformed root number (square root) was treated as continuous variable; numbers indicate proportion of variance (SS$_{xx}$/SS$_{tot}$) in percentage explained by each effect; ** denotes significant effects at $p < 0.01$, n.s. denotes non-significant effects and R^2 represents multiple r-squared.

Effect	SS$_{xx}$/SS$_{tot}$
Bulk density	16.3 **
NoAx$^{0.5}$	70.6 **
Bulk density : NoAx$^{0.5}$	0.1 n.s.
R^2	0.87
Bulk density	0.5 n.s.
NoLat$^{0.5}$	78.4 **
Bulk density : NoLat$^{0.5}$	0.5 n.s.
R^2	0.79

4.3.2. Genotypic diversity of root and shoot traits under different levels of soil compaction

Besides increased soil strength, root system and shoot development were also influenced by the variety. Axial and lateral root number, plant height as well as leaf and tiller number were significantly ($p < 0.01$) different between the fourteen investigated varieties (Table 4.2). As observed for the development of root systems and shoots, genetic diversity of root and shoot properties were also observed three weeks after emergence at the end of the experiment. Lateral and axial root number as well as the lateral-axial root number ratio was significantly different ($p < 0.01$) between the different varieties. The same responses were observed for shoot traits such as plant height, leaf and tiller number, root and shoot dry weight as well as root-shoot ratio (Table 4.5).

Table 4.5: Effects of variety (V), soil bulk density (BD) and their interaction on axial and lateral root number (NoAx and NoLat, respectively) and plant vigour parameters three weeks after emergence analyzed with analysis of variance (ANOVA). Minimum (Min), average (Mean) and maximum (Max) values and Tukey honest significant difference (HSD) at $p < 0.05$, values in brackets for NoAx, NoLat and NoLat/NoAx represent back-transformed values. * and ** denote significant effects at $p < 0.05$ and < 0.01 respectively, n.s. denotes non-significant effects (n = 4).

Trait	Transformation	V	BD	V:BD	Min	Mean	Max	HSD
NoAx [#]	sqrt	**	**	n.s.	2.69 (7.25)	3.70 (13.70)	4.49 (20.16)	0.68
NoLat [#]	sqrt	**	**	**	5.27 (27.82)	8.80 (77.47)	12.29 (151.04)	1.57
NoLat/NoAx [#]	sqrt	**	**	**	1.76 (3.10)	2.34 (5.48)	2.92 (8.54)	0.42
Root dry weight [g]		**	**	n.s	0.059	0.386	0.733	0.217
Shoot dry weight [g]		**	**	*	0.097	0.454	0.767	0.148
Root-Shoot-Ratio [-]		**	**	n.s.	0.58	0.80	1.07	0.365
Plant height [mm]		**	**	**	160.3	264.8	373.3	42.3
Leaf number [#]		**	**	*	2.25	3.83	5.00	0.93
Tiller number [#]		**	**	**	0.00	2.39	5.5	2.04

Furthermore, the obtained data showed that the genotypic variability of root numbers and root and shoot dry weight increased with increasing soil strength. The relative genotypic difference of axial and lateral root number and root and shoot biomass to the respective bulk density mean value increased significantly with increasing bulk density (Figure 4.3). This effect of increasing genotypic variability with increasing soil strength was pronounced especially for axial root number and root and shoot dry weight and less for lateral root number. Coefficients of variation for axial root number, which were calculated for each soil bulk density treatment were 9.3% under low soil strength and increased to 12.0% and 14.3% under moderate and high soil strength, respectively. Also for root and shoot dry weight, a significant increase of CV with increased soil compaction could be observed. Under low soil bulk density CV for root and shoot dry weight was 15.2% and 7.5% respectively. These values increased to 17.3% and 21% for root dry weight and 11.3% and 14.1% for shoot dry weight due to a

moderate and severe increase in soil bulk density, respectively. For lateral root number bulk density mean CVs of 10.1%, 11.1% and 16.4% were obtained under low, moderate and high soil strength, respectively also indicating a slight increase of genotypic variability with increasing soil bulk density (Figure 4.3).
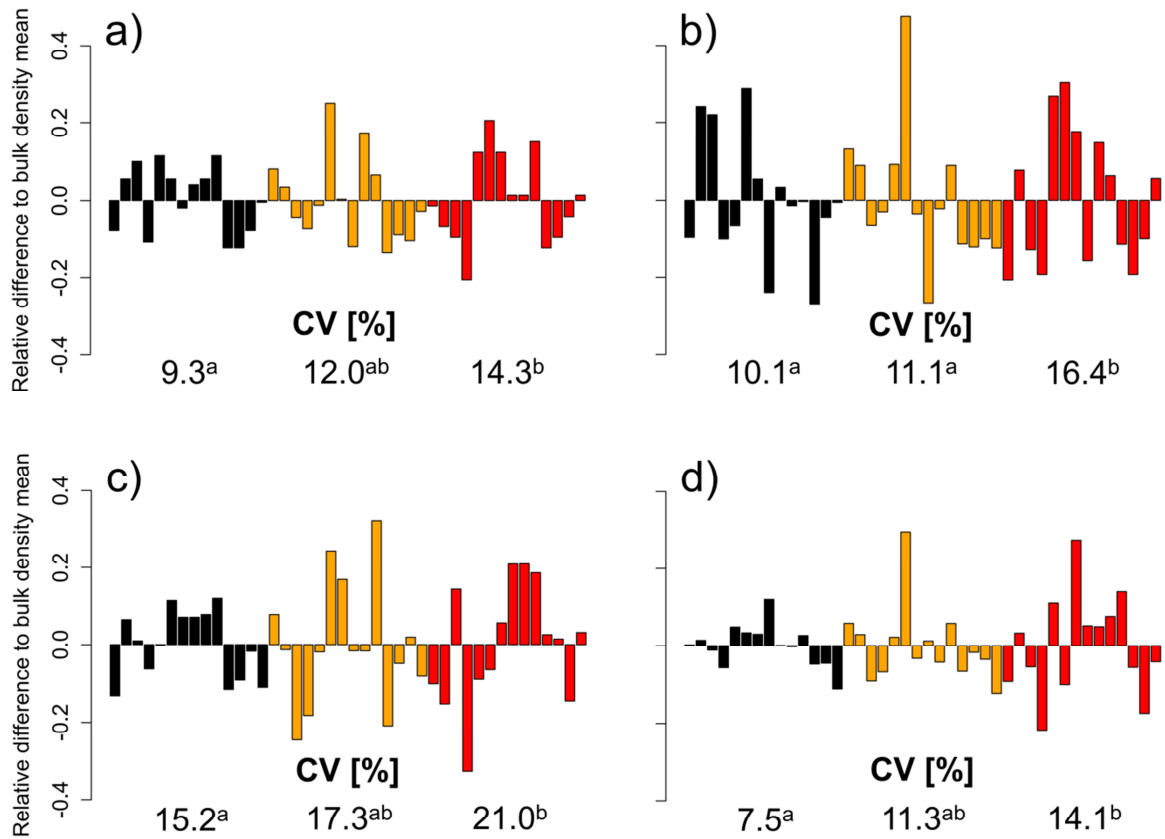
Figure 4.3: Relative difference to the bulk density mean (black = 1.3 g cm^{-3} , orange = 1.45 g cm^{-3}, red = 1.6 g cm^{-3}) of fourteen genotypes for a) axial and b) lateral root number, c) root and d) shoot dry weight based on genotype mean values (n = 4), represented by individual bars. Coefficients of variation (CV) between different levels of soil bulk density were compared using least significant difference (LSD) tests at p < 0.05. Significant differences are indicated with different letters.

Estimations of broad-sense heritability (Eq 4.3) showed that the degree of inheritance is comparable between shoot and root traits. Furthermore, it was observed that the heritability of most traits decreased only slightly in response to increased soil strength. Lateral root number and plant height showed heritabilities of more than 75% under all three soil compaction levels. For axial root number and the number of leaves, broad-sense heritability ranged from 58% to 75% and was also only

slightly lower under high and moderate soil bulk density compared to low soil strength. The lowest heritability estimations were observed shoot dry weight under low soil bulk density (Table 4.6). Most likely this relatively low value of 48% was caused by the relatively low genotypic variance of shoot dry weight under low soil strength (Figure 4.3).

Table 4.6: Estimated broad sense heritability (Eq 4.3) of axial and lateral root number (NoAx and NoLat, respectively) and plant vigour traits using variance components three weeks after shoot emergence. Heritability based on means (n = 4) of fourteen varieties was calculated separately for low (1.3 g cm^{-3}), moderate (1.45 g cm^{-3}) and high soil bulk density (1.6 g cm^{-3}).

		Heritability		
Trait	**Transformation**	**1.3 g cm^{-3}**	**1.45 g cm^{-3}**	**1.6 g cm^{-3}**
NoAx [#]	sqrt	0.67	0.66	0.56
NoLat [#]	sqrt	0.92	0.89	0.75
NoLat/NoAx [#]	sqrt	0.86	0.66	0.50
Root dry weight [g]		0.54	0.70	0.56
Shoot dry weight [g]		0.48	0.65	0.64
Plant height [mm]		0.95	0.91	0.93
Leaf number [#]		0.74	0.67	0.65

4.3.3. Tolerance to increased soil strength among varieties

Besides significant genotypic responses to different levels of soil bulk density, root and shoot traits that were assessed three weeks after emergence were significantly affected by increased soil bulk density (Table 4.5). Furthermore, as illustrated in Figure 4.4, the magnitude of the responses in root numbers to soil compaction differed among the assessed varieties. Generally, increased soil strength resulted in decreased plant vigour and root numbers. Average shoot dry weight decreased by 19% and 82% under moderate and high soil strength, respectively when compared to plants grown under low bulk density. In comparison to plants from the low bulk density treatment, root dry weight was 36% and 87% lower due to moderate and high soil compaction, respectively (Supporting Information Table S4.3). Therefore, root-shoot ratios decreased from 0.96 under low soil strength to 0.75 and 0.70 under moderate and high soil bulk density, respectively. Furthermore, lateral and axial root number as well

as lateral-axial root number ratio decreased due to moderate and high soil compaction by 4% to 19% and 45% to 70%, respectively.
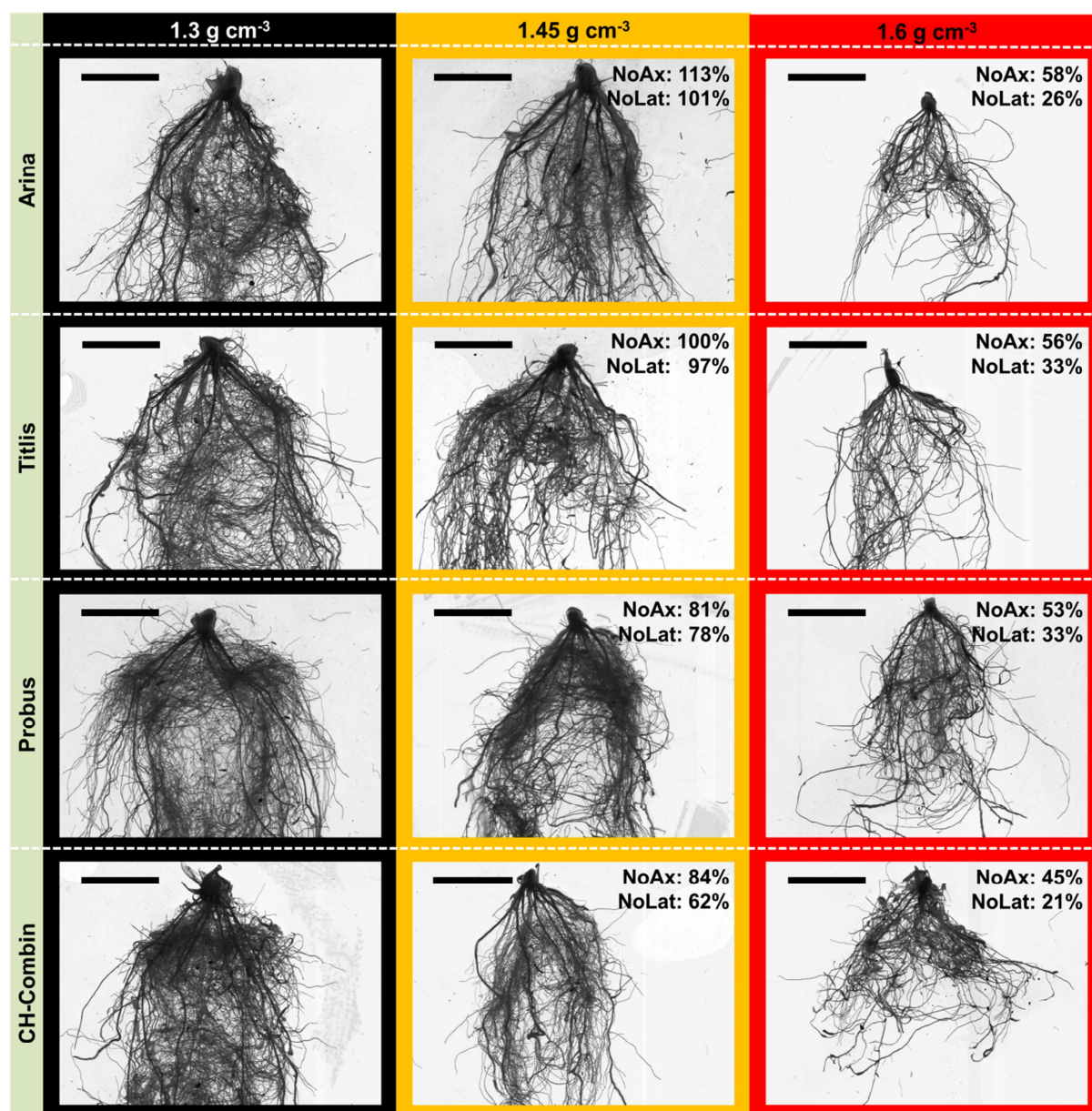
Figure 4.4: Genetic diversity of root system phenotype among four selected genotypes under low (1.3 g cm^{-3}), moderate (1.45 g cm^{-3}) and high soil bulk density (1.6 g cm^{-3}) three weeks after shoot emergence. "Arina" and "Titlis" represent cultivars, which are relatively tolerant to moderate soil compaction indicated by showing no or only small decrease in root numbers, "Probus" and "CH-Combin" represent cultivars, which are sensitive to moderate soil compaction. Percentage values indicate the relative number of axial (NoAx) and lateral roots (NoLat) when comparing genotype mean values under moderate and high soil bulk density to low soil bulk density. Scale bar = 3 cm.

Despite these general responses of root numbers and root and shoot dry weight to increased levels of soil compaction, the magnitude of these responses differed particularly under moderate soil compaction. The strongest responses to moderate soil compaction were observed in root dry weight, followed by lateral root number and shoot dry weight. The number of axial roots were least affected by the increase of soil bulk density from 1.3 to 1.45 g cm^{-3} (Figure 4.5). Furthermore, the effect of moderate soil compaction on axial and lateral root number varied considerably between different varieties. In certain varieties (Arina, Mont-Calme 268, Titlis) axial root number was not affected or even increased in response to moderately increased soil bulk density, whereas in other varieties (CH-Combin, Mont-Calme 245, Probus) the number of axial roots decreased by almost 20% (Figure 4.5). Similar responses were observed for the number of lateral roots, which decreased by more than 25% in some varieties (CH-Combin, Probus, Plantahof), whereas in other varieties (Arina, Mont-Calme 268, Titlis) the number of lateral roots remained constant under moderately increased soil strength (Figure 4.5). This genetic diversity in the responses to moderate soil compaction was also observed for shoot dry weight. The reduction of shoot dry weight due to moderately increased soil strength in the most sensitive varieties was more than 25%. In other varieties instead, moderately increased soil bulk density did not affect shoot dry weight (Figure 4.5). In contrast to root numbers and shoot dry weight, root dry weight was reduced in all varieties under moderate soil bulk density compared to the plants grown under low soil strength. However, also for responses of root dry weight to moderately increased bulk density considerable genetic diversity was observed (Figure 4.5). Under high soil strength root numbers and root and shoot dry weight decreased in all varieties compared to low and moderate soil compaction. As observed for plants grown under moderate soil strength, the responses of axial and lateral root number to high soil compaction among the investigated varieties covered a wider range than those of root and shoot dry weight (Figure 4.5).
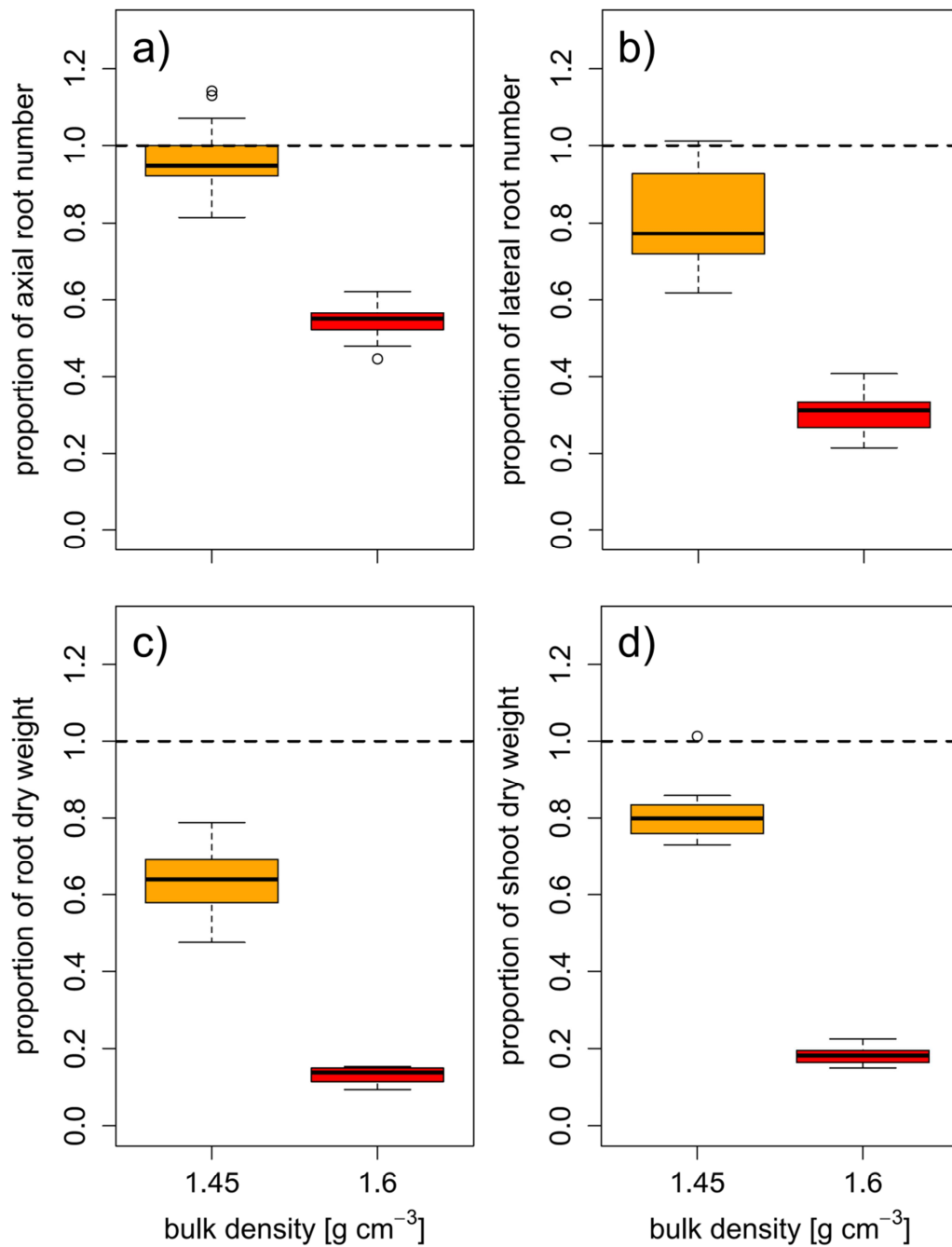
Figure 4.5: Boxplots of relative a) axial and b) lateral root numbers, c) root and d) shoot dry weight based on mean values (n = 4) of 14 genotypes under moderate (1.45 g cm^{-3}, orange) and high bulk density (1.6 g cm^{-3}, red), expressed as the ratio between genotype mean values under increased and low (1.3 g cm^{-3}) bulk density; Dashed line represents low bulk density.

To assess the tolerance of the different varieties to soil compaction, correlations between root traits and shoot dry weight were performed based on proportions of the respective traits. This was achieved by dividing the variety mean value obtained under moderate or high soil bulk density by the variety mean value under low soil bulk density. In doing so, values could be standardized and corrected for

the influence of the different breeding background. These analyses showed significant ($p < 0.05$) positive correlations between the root system traits and shoot dry weight under moderate soil bulk density. Proportions of shoot dry weight, were positively correlated ($0.57 < r < 0.65$) with proportions of axial and lateral root number as well as with proportions of root dry weight (Figure 4.6). Shoot dry weight of varieties, which maintained or increased their axial root number under moderate soil compaction, decreased only slightly even though the respective root dry weight decreased by more than 20%. The same but less pronounced findings were obtained for the relationship between relative lateral root number and relative shoot dry weight under moderately increased soil bulk density. Under high soil strength, no significant correlation between proportions of shoot dry weight and root numbers were found (Figure 4.6). The same results were achieved, when correlating actual root numbers and root dry weight to actual shoot dry weight. Under moderate soil compaction increased numbers of roots as well as root dry weight were related to increased shoot dry weight ($0.68 < r < 0.84$). Yet under high and low soil bulk density no significant relationship between below- and aboveground traits was (Figure 4.7). These results showed that the tolerance to soil compaction differs significantly among wheat varieties and that root numbers are suitable to explain this genetic diversity.
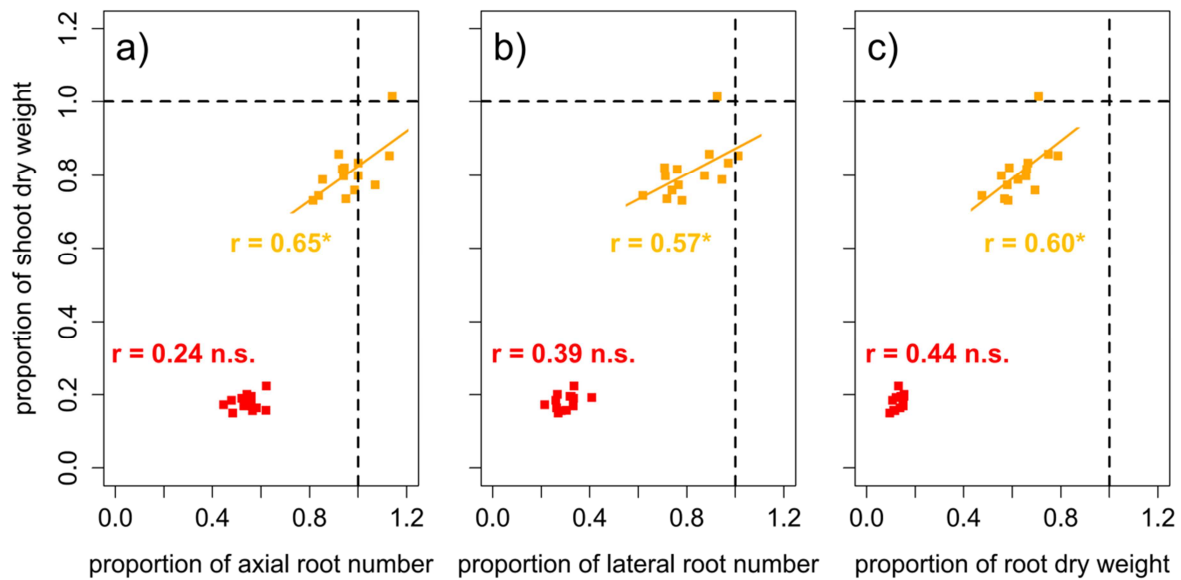
Figure 4.6: Linear regressions and Pearson correlation coefficients between relative shoot dry weight and relative a) axial and b) lateral root number and c) relative root dry weight, expressed as the ratio between genotype mean values under increased (1.45 g cm^{-3}, orange; 1.6 g cm^{-3}, red) and low (1.3 g cm^{-3}) bulk density. Dashed lines represent low bulk density. * denotes significant correlation at $p < 0.05$, n.s. denotes non-significant correlations ($n = 4$).
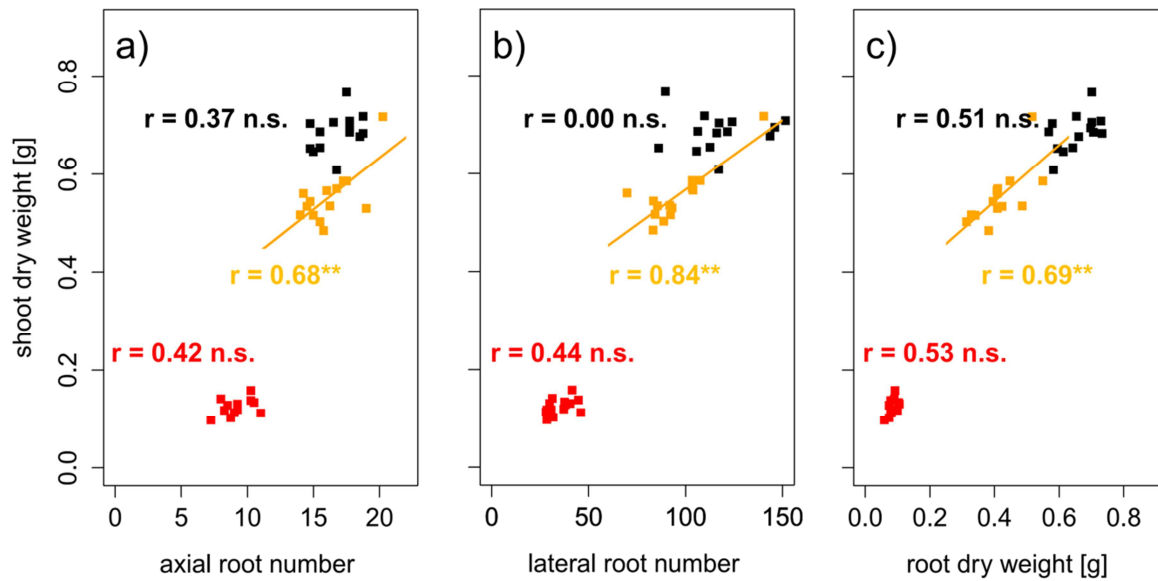
Figure 4.7: Linear regressions and Pearson correlation coefficients between shoot dry weight and a) axial and c) lateral root number and c) root dry weight; black, orange and red symbols represent soil bulk density of 1.3 g cm^{-3}, 1.45 g cm^{-3} and 1.6 g cm^{-3}, respectively. * and ** denotes significant correlation at $p < 0.05$ and < 0.01 respectively, n.s. denotes non-significant correlations ($n = 4$).

4.4. Discussion

The main aim of the current study was to evaluate the suitability of root number as a target trait for improving the tolerance to soil compaction. Quantifying root system and shoot development across fourteen wheat varieties grown under three levels of soil bulk density revealed how root-shoot relationships are affected by increasing soil strength. Furthermore, it was possible to show that root numbers are heritable and may explain the genotypic tolerance to compacted soils.

4.4.1. Axial root number determines shoot growth dynamics under increased soil bulk density

To better understand how increased soil strength affects whole plant growth and root-shoot relationships, lateral and axial root number as well as plant height, leaf and tiller number were quantified in weekly intervals. Compared to the columns packed to 1.3 g cm^{-3}, mechanical impedance increased by around 30% and 200% under moderate and high soil bulk density, respectively. This increase of soil strength due to higher soil bulk density is comparable to previous studies (Grzesiak et al., 2014; Nosalewicz and Lipiec, 2014; Colombi and Walter, 2016) and significantly affected root

system and shoot development (Table 4.2). Shoot development was delayed due to increased soil strength (Table 4.3), which corresponds to previous studies in wheat, barley and maize (Masle and Passioura, 1987; Beemster et al., 1996; Young et al., 1997). Similar to shoot growth, root system development was delayed due to increased soil bulk density. As observed previously in different small grain cereals (Colombi and Walter, 2016), the initiation of axial and lateral roots was deferred in response to increased soil strength at early stages of plant development (Table 4.3).

The simultaneous quantification of plant height and root numbers in response to increased soil bulk density over time enabled to relate above- and belowground growth. These results showed that under all levels of soil strength, axial and lateral root numbers were highly correlated ($0.78 < r < 0.88$) with plant height following a square root function (Figure 4.2). Similar results were obtained in broccoli seedlings, where it has been shown that root length explained responses of leaf area to soil compaction (Montagu et al., 2001). In this and other studies (Grzesiak et al., 2014; Nosalewicz and Lipiec, 2014) root traits were not assessed continuously during growth, which does not allow investigating how soil strength affects the dynamics of root-shoot relationship. If soil bulk density increased, more axial roots were needed to maintain shoot growth (Figure 4.2), whereas no such effect could be observed for the relationship between lateral root number and plant height (Table 4.4). This finding demonstrated that early plant development under increased soil strength was mainly driven by axial and only partially by lateral roots. Most probably this was caused by the fact that thick roots are less prone to buckling compared to thin roots (Materechera et al., 1992; Lipiec et al., 2012; Chimungu et al., 2015a). Hence, the obtained results indicate that axial roots, which are inherently thicker than lateral roots, were of increasing importance for early plant vigour when soil strength increases.

4.4.2. Root numbers are suited to assess tolerance to increased soil bulk density

Root system and shoot development (Table 4.2) as well as root and shoot traits obtained three weeks after emergence (Table 4.5) were significantly different among the fourteen investigated varieties. Genotypic differences in response to increased soil strength were observed in maize, wheat and triticale (Bushamuka and Zobel, 1998; Kubo et al., 2004; Kubo et al., 2006; Grzesiak et al., 2014), whereas other studies did not report significant differences between genotypes (Tracy et al., 2012a).

Certain studies investigated only two to four genotypes (Bushamuka and Zobel, 1998; Tracy et al., 2012a; Grzesiak et al., 2014), which did not allow relating root traits to genotypic plant performance or compaction was simulated using paraffin-vaseline disks instead of using actually compacted soil (Kubo et al., 2004; Kubo et al., 2006). The results obtained in the current study revealed a genetic diversity of root and shoot traits in wheat in response to soil compaction. Besides this genetic diversity of root and shoot traits (Table 4.5), increasing variability of traits among varieties were observed due to increased soil bulk density, which corresponds to previous studies (Bushamuka and Zobel, 1998; Grzesiak et al., 2014). Compared to loosely packed soil, the genetic variability of axial and lateral root number three weeks after emergence increased under moderate and high soil bulk density, which is indicated by the increase of coefficients of variation with increasing soil strength (Figure 4.3). Also genotypic diversity of root and shoot dry weight at the end of the experiment was higher under moderate and high soil strength compared to plants grown under low soil bulk density (Figure 4.3).

Below- and aboveground responses to compacted soil were observed to differ between varieties, as illustrated in Figure 4.4, and the magnitude of these responses was different for root numbers and shoot dry weight when compared to root dry weight (Figure 4.5). Under moderate soil compaction some varieties increased their root numbers and shoot dry weight remained unaffected. In other varieties instead, already a moderate increase of soil strength led to a reduction of root numbers and shoot dry weight of 18% to more than 30% (Figure 4.5). Decreasing, constant or even increasing plant vigour in response to moderate soil compaction was observed in wheat, barley and maize (Bushamuka and Zobel, 1998; Bingham and Bengough, 2003; Grzesiak et al., 2014; Nosalewicz and Lipiec, 2014). Relative root dry weight instead was reduced in all varieties due to moderately increased soil compaction (Figure 4.5), resulting in reduced root-shoot ratio under moderate compared to low soil bulk density. The discrepancy between root numbers and root dry weight in response to moderate soil compaction can be most likely explained by decreased root length, which was observed in response to compaction in a wide range of monocotyledonous crop species (Bingham and Bengough, 2003; Tracy et al., 2012a; Grzesiak et al., 2014). Under high soil bulk density similar but more severe responses were observed. Compared to low and moderate soil bulk density, root and shoot biomass as well as

root numbers decreased in all genotypes and the strongest response was observed for root dry weight followed by shoot biomass and root numbers (Figure 4.5).

Previous studies observed that root numbers influence crop performance under abiotic stress including low water availability (Zhan et al., 2015; Gao and Lynch, 2016) or low levels of plant available soil nitrogen (Saengwilai et al., 2014b; Zhan and Lynch, 2015) and phosphorus (Miguel et al., 2013). Furthermore, the assessment of root numbers is possible under field conditions at high throughputs in a wide range of mono- and dicotyledonous crops (Trachsel et al., 2011; Colombi et al., 2015; Burridge et al., 2016; Colombi and Walter, 2016). Measurements of root biomass or root length in the field instead are challenging and laborious. Results from the current study showed that axial and lateral root numbers not only respond to soil compaction but also determine early shoot vigour under moderately increased soil strength. Similar to results reported for narrow-leafed lupins (Chen et al., 2014b), variety mean values of relative axial and lateral root number were significantly related ($0.57 < r < 0.65$, $p < 0.05$) to relative shoot dry weight (Figure 4.6). Varieties, which maintained their root numbers under moderate soil compaction compared to conditions of loose soil showed less decreasing shoot dry weight than varieties, in which moderate compaction led to a decrease of root numbers. Remarkably, this relationship could be shown even though root dry weight decreased in all assessed varieties due to moderate soil compaction (Figure 4.6). Also absolute root numbers were positively correlated to shoot dry weight ($0.68 < r < 0.84$, $p < 0.01$) under moderately increased soil strength (Figure 4.7). Under severe soil compaction no significant relationship between shoot dry weight and root numbers or root dry weight could be observed (Figure 4.6 and Figure 4.7). Mechanical impedance in the severely compacted columns was most likely above the limit at which genotypic differences affect shoot performance (Kubo et al., 2004). Furthermore, calculations of broad-sense heritability showed that root numbers are supposed to be relatively highly heritable. Even under high soil strength, estimations of 56% and 75% heritability were obtained for axial and lateral root number, which was in a similar range than the values observed for plant height, leaf number or shoot dry weight (Table 4.6). These results are comparable to other studies, in which heritability estimations for shoot and root traits were evaluated in mono- and dicotyledonous crops (Wilcox and Farmer, 1968; Bucksch et al., 2014; Colombi et al., 2015; Li et al., 2015; Richard et al., 2015; Burridge et al., 2016). Taking into account

these heritability estimations and the significant influence of root number on shoot biomass, the number of roots is suggested to be a suitable indicator to assess the genotypic tolerance to soil compaction.

4.5. Conclusions

With the current study we demonstrated that early shoot development of wheat on compacted soil is closely related to the number of axial roots. Thereby, significant genetic variability between fourteen different wheat varieties could be shown with respect to their tolerance to increased soil bulk density. In particular under moderate soil compaction, the genotypic capacity to maintain the number of axial and lateral roots resulted in higher shoot biomass production. Furthermore, root numbers showed relatively high heritabilities and can be assessed at high throughput rates even under field conditions. Therefore, it can be stated that root number is a promising target trait for crop breeding programmes aiming to improve the tolerance of crops to compacted soil. For future studies, it would be desirable to evaluate whether the presented findings are transferable to other species and to quantify root-soil interactions underlying crop productivity on compacted soils.

Chapter 5: Artificial macropores attract crop roots and enhance plant productivity on compacted soils

Tino Colombi[1*], Serge Braun[1], Thomas Keller[2,3], and Achim Walter[1]

[1]ETH Zurich, Institute of Agricultural Sciences (IAS), Zurich, Switzerland

[2]Agroscope, Department of Natural Resources and Agriculture, Zurich, Switzerland

[3]Swedish University of Agricultural Sciences, Department of Soil and Environment, Uppsala, Sweden

[*]Corresponding author, tino.colombi@usys.ethz.ch

Abstract

The structure of compacted soils is characterized by decreased (macro-)porosity, which leads to increased mechanical impedance and decreased fluid transport rates, resulting in reduced root growth and crop productivity. Particularly in soils with high mechanical impedance, macropores can be used by roots as pathways of least resistance. This study investigated how different soil physical states relate to whole plant growth and whether roots grow towards spots with favourable soil physical conditions. Experiments were conducted under controlled and field conditions. Soybean (*Glycine max* L.), wheat (*Triticum aestivum* L.) and maize (*Zea mays* L.) were grown on uncompacted soil, compacted soil and compacted soil with artificial macropores. The interactions between roots and artificial macropores were quantified using X-ray computed tomography. Active growth of roots towards artificial macropores was observed for all three species. Roots grew either into macropores (predominantly in maize) or crossed them (predominantly in wheat). The presence of artificial macropores in compacted soil enabled all three species to compensate for decreased early vigour at later developmental stages. These results show that roots sense their physical environment, enabling them to grow towards spots with favourable soil conditions. The different kinds of root-macropore interaction indicated that macropores serve as a path of least resistance and a source of oxygen, both resulting in increased crop productivity on compacted soils.

Graphical abstract
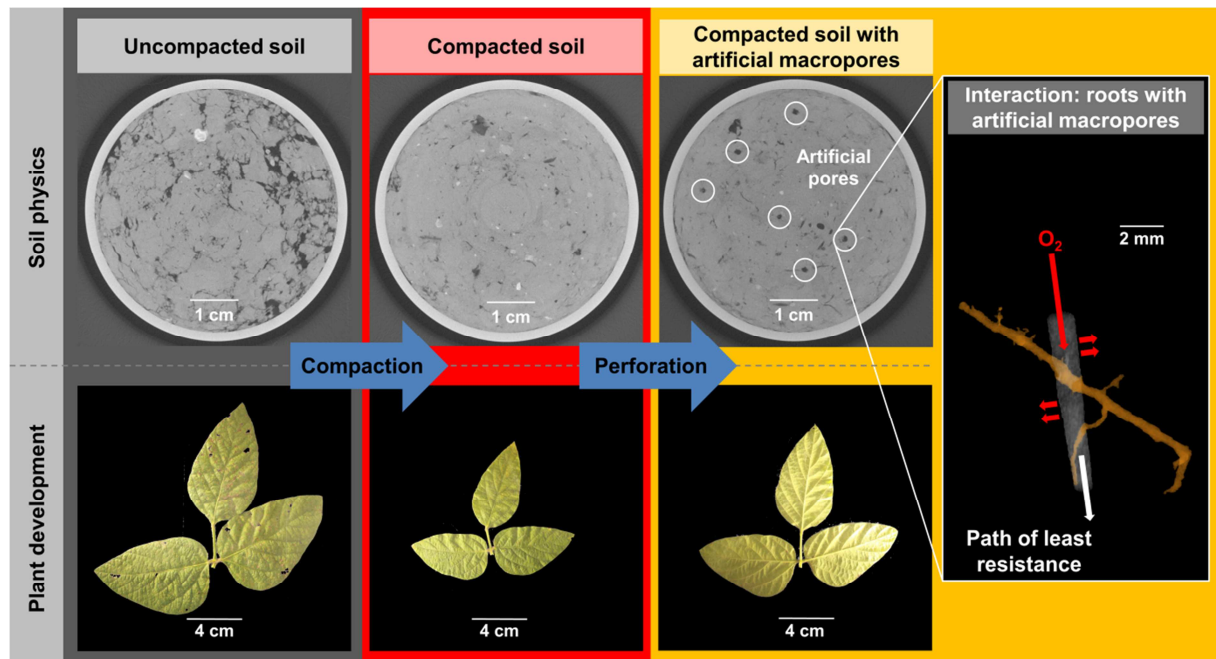
5.1. Introduction

An estimated 33 million hectares of arable land in Europe and 68 million hectares worldwide are degraded due to soil compaction (Van den Akker and Canarache, 2001; Hamza and Anderson, 2005; Batey, 2009). This soil compaction, which is mainly caused by heavy agricultural machinery (Tracy et al., 2011), results in increased soil bulk density and decreased pore connectivity. In particular, macropore volume is reduced in compacted soils (Bottinelli et al., 2014; Chen et al., 2014a). Bulk density and porosity are relatively simple measurements to quantify soil compaction, but do not describe actual soil functions. It has been proposed that soil physical functions such as mechanical impedance, gas diffusivity, air permeability and hydraulic conductivity are more suitable to relate soil compaction and plant productivity (Stirzaker et al., 1996; Colombi and Walter, 2016).

Due to their decreased void space, which is needed for displacement of soil particles, compacted soils exert higher mechanical impedance than uncompacted soils (Valentine et al., 2012; Suzuki et al., 2013; Hernandez-Ramirez et al., 2014). Furthermore, decreased macroporosity and pore connectivity cause decreased water infiltration rates and hydraulic conductivity (Lipiec and Hatano, 2003; Chen et al., 2014a; Kuncoro et al., 2014b) as well as lower gas diffusivity and air permeability (Stirzaker et al., 1996; Scholl et al., 2014; Kuncoro et al., 2014b). This increases the risk of anaerobic conditions in compacted soils compared with uncompacted soils (Tracy et al., 2011). Due to less plant available water in compacted soils (Lipiec and Hatano, 2003), evapotranspiration dries out compacted soils more likely than uncompacted soils, which further increases penetration resistance. Increased mechanical impedance and decreased fluid transport rates decrease root growth and can both be summarized as loss of soil physical fertility (Abbott and Murphy, 2007) caused by compaction. Decreased root growth leads to restricted access to belowground resources and therefore decreased plant productivity (Hamza and Anderson, 2005; Batey, 2009; McKenzie et al., 2009; Walter et al., 2009; Tracy et al., 2011; Downie et al., 2012).

Besides decreased root growth, soil compaction causes tremendous alterations to the root phenotype. Decreasing numbers of axial and lateral roots in response to soil compaction have been observed for several crops, including small grain cereals, maize and soybean (Coelho Filho et al.,

2013; Grzesiak et al., 2013; Grzesiak et al., 2014; Pfeifer et al., 2014a; Colombi and Walter, 2016).

Furthermore, roots from compacted soils have been reported to show greater root diameter, larger root cortical area and increased abundance of root cortex aerenchyma compared with roots grown in uncompacted soil (Iijima and Kato, 2007; Alameda and Villar, 2012; Lipiec et al., 2012; Siczek et al., 2013; Colombi and Walter, 2016). In most of those studies, such changes in root phenotype were related to decreasing plant vigour (Grzesiak et al., 2013; Siczek et al., 2013; Grzesiak et al., 2014; Pfeifer et al., 2014a; Colombi and Walter, 2016). Furthermore, it has been shown that legumes are more sensitive to soil compaction than grasses (Arvidsson and Håkansson, 2014) and that the tolerance to mechanical impedance differs between species (Bushamuka and Zobel, 1998; Busscher et al., 2000a; Grzesiak et al., 2014).

Despite this knowledge on the responses of plants to compacted soils, relatively little is known about how roots interact with spots within the soil that provide more favourable or more hostile conditions for growth. Detailed information about the relationships between soil physical properties and whole plant development is needed to identify ecophysiological processes limiting plant growth under compaction. Such information can help in developing mitigation strategies for compacted soils (Hamza and Anderson, 2005), since plant roots are among the major drivers for the recovery of soil functions after compaction. Roots contribute to this structural recovery by creating new macropores due to bioturbation and acceleration of localized soil drying which can result in crack formation (Dexter, 1991; Bottinelli et al., 2014; Scholl et al., 2014).

It has been proposed that roots sense their surrounding environment not only by direct contact with the soil matrix or soil solution (Passioura, 2002). The term "trematotropism" was introduced by Dexter (1986) to describe the ability of roots to sense holes from a certain distance and grow towards them to exploit them as paths of least resistance. Porterfield and Musgrave (1998) used the term "oxytropism" to describe growth of pea roots towards higher concentrations of oxygen. Trematotropism and oxytropism can both be interpreted as an ability of roots to adjust to soil heterogeneity and avoid unfavourable soil conditions. For example, it has been shown that roots of different wild grass species avoid obstructions in the form of large pieces of gravel (Semchenko et al., 2008). A number of studies investigating the interaction between roots and macropores under laboratory and field conditions have

107

concluded that roots use either naturally occurring macropores (Stirzaker et al., 1996; de Freitas et al., 1999; White and Kirkegaard, 2010; Athmann et al., 2013; Kautz et al., 2013; Han et al., 2015) or artificial macropores that were experimentally inserted into the soil with steel rods (Stirzaker et al., 1996; Nakamoto, 1997) as pathways to reach deeper soil layers. This behaviour of roots in following the path of least resistance is more pronounced if the impedance of the surrounding bulk soil is increased (de Freitas et al., 1999; White and Kirkegaard, 2010; Kautz et al., 2013). Some studies have concluded that such root-pore interaction must result from active growth of the roots towards the pores, rather than from random growth (Stirzaker et al., 1996; White and Kirkegaard, 2010).

However, the methodologies used in these studies have their limitations. For example, endoscopy only allows rather large pores (> 5 mm) to be investigated, while measurements along a profile wall or of slices of soil only permit quantification in two dimensions. Non-destructive imaging approaches such as X-ray computed tomography (CT) or magnetic resonance imaging are promising tools to overcome these limitations. Using these techniques, root traits have been quantified at sub-millimetre resolution in pots (Metzner et al., 2015) and in undisturbed samples excavated from the field (Pfeifer et al., 2015). In such a pot study it was observed that barley roots predominantly cross artificial macropores, rather than growing into them (Pfeifer et al., 2014b).

Another methodological limitation is that studies investigating the response of plants to compaction and macroporosity are often performed with young plants (Stirzaker et al., 1996; Nakamoto, 1997; Pfeifer et al., 2014b). This allows only immediate effects of soil physical functions on plant performance to be observed and not effects arising later during plant development. Combined assessment of soil physical functions, root-soil structure relationships and sophisticated shoot phenotyping is necessary to identify soil physical phenomena controlling plant development and drivers for soil recovery after compaction.

The aim of the present study was to determine how soil compaction and the presence of vertical macropores in compacted soil affect whole plant development. This was done by: i) quantifying the effects of soil compaction and the presence of artificial macropores in compacted soil on crop development and performance and ii) investigating whether and how crop roots interact with artificial

macropores in compacted soil. Experiments were conducted with soybean, winter wheat and maize in a growth chamber (young plants) and in the field (mature plants), representing a controlled and natural field environment, respectively. Plant-pore interactions were quantified using X-ray micro CT and a set of soil physical properties and plant vigour traits were determined.

5.2. Material and Methods

5.2.1. Plant material and root system properties

The crop species used in the study were: soybean (*Glycine max* L., variety Merlin), winter wheat (*Triticum aestivum* L., variety Arina) and maize (*Zea mays* L., variety LG 30.222). Beside their importance for global agriculture, these crops were chosen due to their differing root systems. Soybean is characterized by a taproot system, whereas wheat and maize have a fibrous root system with roots of rather small and large diameter, respectively.

5.2.2. Experimental set-up and growth conditions

Experiments were conducted under controlled conditions in a growth chamber and in the field. The soil (Pseudogleyed Cambisol) used in the growth chamber experiments was taken from the same site at Agroscope Zurich, Switzerland (8°31'E, 47°27'N, 443 m above sea level) where the field experiments were conducted. Soil texture consisted of 25% clay, 50% silt and 25% sand with 1.7% organic carbon and pH ($CaCl_2$) of 6.9 in the top 20 cm.

5.2.2.1. Soil columns for growth chamber experiments

Soil was excavated from the top 15 cm of the soil profile, dried to approximately 22% gravimetric water content, homogenized and sieved through a 2 mm sieve. Plants were grown in PVC columns of 4.9 cm inner diameter and 15 cm height. The bottom of the columns was closed off with filter paper and a 1 cm quartz-sand layer (particle size 0.2-1.7 mm) was added. On top of the sand layer, soil was packed in six layers of 2 cm height to a bulk density of 1.3 and 1.6 g cm^{-3}, representing loose (Ctrl) and compacted (Com) soil, respectively. The surface of each packed layer was slightly abraded to ensure homogeneous packing. In a third soil treatment, densely packed soil (1.6 g cm^{-3}) was vertically

perforated five times with a stainless steel wire of 1.25 mm diameter to create artificial macropores (ComAP). The artificial macropores were allocated in a cross-like pattern (Figure 5.1a).

Seeds were germinated at 25°C for 48 h and selected according to homogeneous length of radicle and seed size. In every column, 1 cm of loose soil (1 g cm^{-3}) was added on top of the packed layers and a 1 mm wide and 5 mm deep hole was made in the centre. The seed with emerged radicle was placed into this hole and covered with 0.5 cm loose soil (0.8 g cm^{-3}). Before planting, soybean seeds were coated with rhizobia inoculum (*Bradyrhizobium japonicum*; HiStick; Becker Underwood, BASF, Little Hampton, United Kingdom). Each soil treatment (Ctrl, Com and ComAP) was replicated four times for each crop species.

All plants were grown for 20 days in a growth chamber with a day/night cycle of 14/10 h at 59% relative air humidity and an average temperature of 20.6°C. Average incident light was 417 ($\pm$ 20, SD) μmol s^{-1} m^{-2}. Columns were weighed and watered daily to keep the soil water content constant at a level corresponding to a matric potential of -100 hPa, which represents a typical value for field capacity (Schjonning and Rasmussen, 2000).

5.2.2.2. Field experiments

Field experiments were conducted on the Soil Structure Observatory (SSO) at Agroscope in Zurich, Switzerland. The SSO was established in spring 2014 as a long-term field experiment with compacted (Com) and uncompacted (Ctrl) plots arranged in three blocks to study recovery of compacted soil. In March 2014, plots were compacted using a heavy agricultural vehicle with four wheels and 80 kN wheel load (for detailed information see Colombi and Walter (2016)). Tillage treatments varied slightly between crops (Supporting Information Table S5.1).

Soybean seeds were inoculated with *B. japonicum* before sowing on 20 May 2014. Until harvest on 24 October, mean day and night temperature was 21.3°C and 11.9°C, respectively, and total precipitation was 528 mm. Winter wheat was sown on 11 November 2014 and harvested on 4 August 2015. Until harvest, average day and night temperature was 13.7°C and 5.2°C, respectively, and 736 mm of precipitation were recorded. Maize was sown on 27 May 2015 and experienced mean day and night temperature of 24.2°C and 13.3°C, respectively, until harvest on 28 September. Cumulative

precipitation from sowing to harvest was 262 mm. Sowing density and fertilisation rate were similar to on-farm conditions (Supporting Information Table S5.1).

In the compacted plots of all crops, artificial macropores (ComAP) were created shortly after germination in five or six 0.25 m^2 squares along a 2 cm by 2 cm grid (Figure 5.1b), using the same stainless steel wire as in the growth chamber experiments. In the context of soil management, soil perforation could be seen as an alternative approach to commonly applied tillage operations in order to create potential pathways for roots and to improve soil drainage and aeration. Perforation depth was around 30 cm for soybean and wheat and, due to relatively dry soil, 20 cm for maize. Roots and shoots were sampled 91 days after sowing (DAS) for soybean, 218 DAS for wheat and 70 DAS for maize. This sampling time corresponded to the stage of major grain filling in soybean and to flowering stage in wheat and maize.

5.2.3. Soil physical properties

Soil physical conditions in the growth chamber experiment were determined from packed soil samples of 100 ml volume and 5 cm height. Four soil cores per treatment (Ctrl, Com and ComAP) were packed in 1 cm layers with sieved soil to a bulk density of 1.3 and 1.6 g cm^{-3}. Five artificial macropores were made in the ComAP samples in the same pattern as described above. The samples were slowly saturated from below for two weeks and then equilibrated on a ceramic plate to a matric potential of -100 hPa. Air permeability (Ka [μm^2]) and relative gas diffusion coefficient (Dp/D0 [-]) were measured and calculated according to Martínez et al. (2016). Mechanical impedance was measured by two penetrometer insertions into the bottom end of the soil samples, as described in Colombi and Walter (2016). During wheat growth, the oxygen concentration in soil air was monitored in four additional soil columns of each soil treatment via 4 cm long gas-permeable tubes connected to gastight access tubes inserted to 6 cm depth in the bulk soil. Oxygen concentration in soil air was measured daily from 3 to 18 DAS with a commercial gas analyser (CheckMate 9900 benchtop headspace O_2/CO_2 gas analyser; PBI Dansensor A/S, Ringsted, Denmark) in the morning immediately after watering.

In the wheat plots, three undisturbed soil samples of 100 ml and 5 cm height per block were taken from 10 and 30 cm depth in each treatment. Gas transport characteristics and mechanical impedance were measured as described above, at a matric potential of -100 hPa. Soil bulk density was determined from the same field samples using the oven-drying method (105°C for four days). Soil bulk density was also measured in the soybean plots (only Com and Ctrl) and the maize plots (all treatments) at 10 and 30 cm depth, with three replicates per block.

5.2.4. Interaction of roots with artificial pores

The interaction of crop roots with inserted macropores was quantified from X-ray micro CT scans (Phoenix v|tome|x s 240; GE Sensing and Inspection Technologies GmbH, Wunstorf, Germany). For plants from the growth chamber, the entire soil column was scanned using the multi-scan option. In the field, two undisturbed samples of 10 cm diameter and 10 cm height were excavated in PVC tubes from 0-10 cm and 13-23 cm depth of each perforated square (Figure 5.1c). The excavated samples were kept moist and stored at 3°C until scanning. The settings used resulted in a 68 μm and 120 μm voxel edge length for soil columns and field samples, respectively (Supporting Information Table S5.2). Visual detection limits for structures in X-ray CT scans are at diameters that exceed twice the voxels edge length (Jähne, 2002). Hence the visual detection limit for roots was at a diameter of around 170 μm and 300 μm for samples from the growth chamber and the field, respectively. This represented 2.5 times the respective voxel edge length.

All quantifications from reconstructed CT scans were performed in Visual Studio Max 2.2 (Volume Graphics GmbH, Heidelberg, Germany). In a first step, artificial pores were counted and the number of hits of each pore by roots was determined. To be considered an actual hit, the root needed to fully enter the artificial macropore and not just touch the outer edge. These hits were then divided into two different classes of interaction: "crossings", defined as when the root stayed in the pore for a distance of less than 5 mm, and "colonisations", defined as when the root grew for a distance of more than 5 mm within the pore (Figure 5.1d and 5.1e). In a second step, all visible roots were counted and classified into roots that hit an artificial macropore and roots that never crossed or colonised an

artificial macropore. In the case of field samples, statistical evaluation was based on average values for the two soil depths.
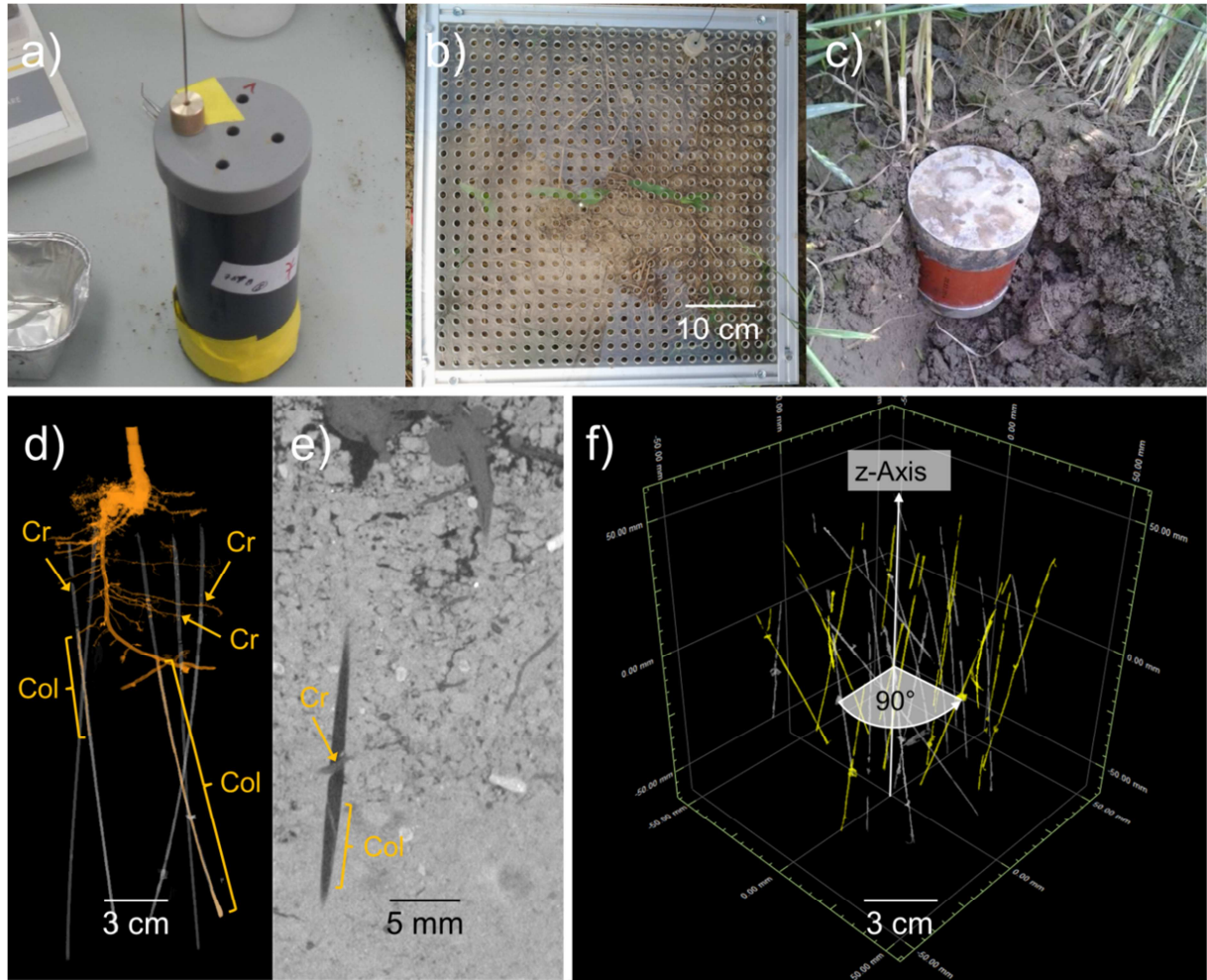
Figure 5.1: Perforation of compacted soil with steel wire along a 2 by 2 cm grid in a) soil columns and b) in the field. c) Root sampling in the field in 0-10 cm depth. d) Crossing (Cr) and colonisation (Col) of artificial macropores by soybean roots grown in soil columns. e) Vertical cross-sections of reconstructed computed tomography scans of crossing and colonising soybean roots grown in soil columns. f) Artificial macropores of a field sample at their actual position (grey) and after rotation around the central z-axis (yellow).

5.2.5. Preferential root growth towards artificial macropores

The observed number of root hits per artificial macropores was compared against the expected number of hits if the roots had grown randomly, which was determined by counting the number of hits per virtually reallocated macropore. For this, artificial pores were segmented using the region-growing algorithm of Visual Studio Max and rotated around the central vertical axis (soil columns 45°, field samples 90°) of the reconstructed scan (Figure 5.1f). As described above, hits were only counted if the

root crossed the virtually reallocated pore and not if it just touched the edge. Expected and observed number of hits were compared in order to determine whether roots grew randomly or grew preferentially towards pores. To further test the hypothesis of preferential root growth, four additional soil columns per crop were prepared. These columns were packed to a bulk density of 1.6 g cm^{-3} and macropores were inserted not in a cross-like pattern, but all in one half of the soil column. To determine the expected number of hits, segmented pores were rotated 180° around the central vertical axis and the observed number of hits was determined as described above.

5.2.6. Plant vigour

In addition to the field samples from ComAP, four field samples of 10 cm diameter and 10 cm height were taken per block from 0-10 cm and 13-23 cm depth in Ctrl and Com. Roots from all field samples and soil columns were washed gently over a 1 mm sieve and dried at 60°C for four days before weighing.

Just after root samples were excavated from the field, aboveground plant traits were determined using the same plants from which the roots were sampled. In soybean and maize, each belowground sample corresponded to a single plant, whereas in wheat each belowground sample corresponded to 5-8 individual plants. Shoots of plants grown under controlled conditions were sampled 20 DAS immediately after the root system was scanned by X-ray CT. To determine leaf area, leaves of different positions on the stem were harvested, placed on a blue background and covered with a transparent plastic sheet. Together with a size reference, images of leaves were captured under constant illumination with an 18 megapixel camera (Canon EOS 600D; Canon, Tokyo, Japan) with a lens (EF-S18-55mm f/3.5-5.6 ISII; Canon, Tokyo, Japan) fixed to a focal length of 35 mm and an aperture value of 9, resulting in pixel edge length of 60-80 μm. In order to relate the effect of soil treatments to plant development stages, images were taken separately for each leaf level of the main shoot. Leaf area was evaluated in ImageJ version 1.49g (National Institute of Health, Bethesda, MD, United States). Afterwards, entire shoots were dried at 60°C for four days prior to weighing.

5.2.7. Statistical evaluation

Chi-square tests were used to compare observed and expected number of root hits per artificial macropores. All other evaluations were based on analysis of variance (ANOVA) and treatment means were compared using ANOVA least significant difference (LSD) tests. For air permeability, the raw data were converted to base 10 logarithm before statistical evaluation. All statistical analyses were performed in R version 3.1.3 (R Development Core Team, Vienna, Austria).

5.3. Results

5.3.1. Soil physical properties

Soil physical responses to soil compaction and to subsequent perforation of compacted soil were highly consistent between packed soil from the growth chamber and undisturbed soil from the field experiments. Mechanical impedance in packed and undisturbed soil samples was increased by 20-200% due to soil compaction and not affected by artificial macropores in compacted soil (Table 5.1). However, the artificial macropores created possible pathways of very low or no mechanical impedance. Air permeability (Ka) and relative gas diffusion coefficient (Dp/D0) decreased as a result of compaction. Creation of artificial macropores in compacted soil significantly increased gas transport rates in undisturbed and packed soil samples. The Dp/D0 and $\log_{10}$(Ka) values obtained were at least 1.5-fold higher in compacted soil with artificial macropores than in compacted soil without artificial macropores (Table 5.1). Furthermore, oxygen concentrations in soil air measured during wheat growth under controlled conditions differed between soil treatments. Measured oxygen concentrations in bulk soil air were highest in uncompacted soil, followed by compacted soil with artificial macropores. The lowest oxygen concentrations were recorded in the air from compacted soil without artificial macropores (Supporting Information Figure S5.1). Soil bulk density in the field was increased by soil compaction, particularly at 10 cm depth. Artificial macropores in compacted soil did not affect soil bulk density compared with that in compacted soil without artificial macropores, except at 10 cm depth in the wheat plots (Table 5.2). The difference in bulk density between ComAP and Com in that case was possibly caused by the long time span of 218 days between soil perforation and sampling.

Table 5.1: Mechanical impedance, air permeability (Ka) and relative gas diffusion coefficients (Dp/D0) of uncompacted (Ctrl), compacted (Com) and compacted soil with artificial macropores (ComAP) measured in packed (soil columns) and undisturbed (field) soil cores at a matric potential of -100 hPa. Different letters indicate significant differences of the means using least significant difference (LSD) test at p < 0.05 (soil columns: n = 4, field n: = 3).

Environment	Parameter	Ctrl	Com	ComAP	LSD
Soil columns	Impedance [MPa]	0.34^a	1.06^b	0.98^b	0.26
	$\log_{10}$(Ka [μm^2])	0.32^a	0.04^a	1.40^b	0.62
	Dp/D0 [-]	0.0008^a	0.0009^a	0.0027^b	0.0017
Field 10 cm depth	Impedance [MPa]	0.81	1.09	0.95	0.42
	$\log_{10}$(Ka [μm^2])	0.60^{ab}	0.38^a	1.11^b	0.53
	Dp/D0 [-]	0.0040	0.0013	0.0089	0.0079
Field 30 cm depth	Impedance [MPa]	0.56^a	0.86^b	1.08^b	0.25
	$\log_{10}$(Ka [μm^2])	0.65^{ab}	0.38^a	1.05^b	0.59
	Dp/D0 [-]	0.0036^{ab}	0.0002^a	0.0064^b	0.0060

Table 5.2: Soil bulk density (ρ_b) in the field in uncompacted (Ctrl), compacted (Com) and compacted soil with artificial macropores (ComAP) for the three crop species tested. Different letters indicate significant differences of the means using least significant difference (LSD) test at p < 0.05 (n = 3).

Year	Crop	Depth [cm]	ρ_b [g cm^{-3}]: Ctrl	ρ_b [g cm^{-3}]: Com	ρ_b [g cm^{-3}]: ComAP	LSD
2014	Soybean	10	1.34^a	1.46^b	NA	0.09
		30	1.50	1.55	NA	0.16
2015	Wheat	10	1.50^{ab}	1.55^a	1.43^b	0.08
		30	1.44	1.49	1.50	0.11
	Maize	10	1.45^a	1.61^b	1.59^b	0.12
		30	1.40	1.46	1.48	0.10

5.3.2. Interaction of roots with artificial pores

For all three crop species studied, between 0.74 and 1.65 root hits per single artificial macropore were counted in the CT scans from the growth chamber and the field. Once reaching an artificial

macropore, the roots of soybean, wheat and maize behaved differently. Under both controlled and field conditions, the interactions of maize roots with artificial pores were predominantly characterized as colonisations, which occurred 54-122% more frequently than crossings (Figure 5.2). In contrast to maize, soybean roots crossed and colonised artificial macropores at an equal extent (Figure 5.2). Due to sample size and the resulting visual detection limit for roots in the reconstructed CT scans, fine roots of soybean could not be quantified in the field samples. This resulted in a lower number of observed hits in field samples compared with samples from the growth chamber (Figure 5.2, Table 5.3). Also due to different voxel resolutions lateral roots of wheat could be seen in scans from the growth chamber, but not in scans from the field. Under controlled conditions, interactions of wheat roots with artificial macropores were predominantly classified as crossings (Figure 5.2). In the field, colonisations of artificial pores by wheat roots occurred slightly more often than crossings (Figure 5.2). However, the number of crossings in the field was probably underestimated, since lateral roots, which grow more horizontally than main roots, were not visible in the scans.

Although root-pore interactions were quantified in all three species, most of the roots in the samples did not interact with the artificial macropores. Between 72 and 91% of the roots visible in the reconstructed CT scans neither crossed nor colonised artificial macropores (Figure 5.3).

Figure 5.2: Interaction of roots with artificial macropores in compacted soil in a) and b) in soil columns and c) and d) the field, expressed as a) and c) mean number of crossing roots and b) and d) mean number of colonising roots per individual artificial macropore. Different letters indicate significant differences of the means using the least significant difference (LSD) test at $p < 0.05$. Error bars represent standard error (soil columns: n = 4, field: n = 3).
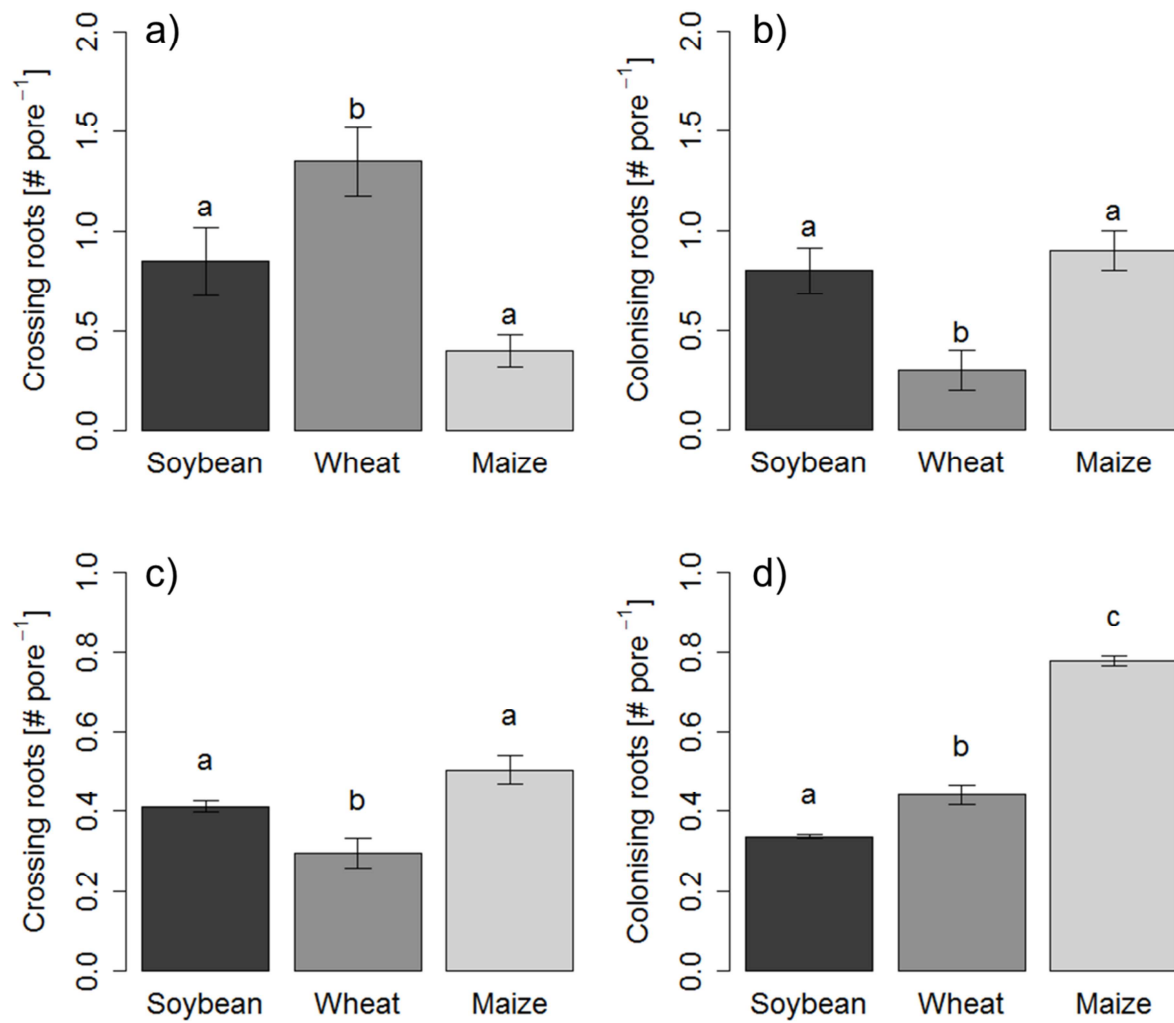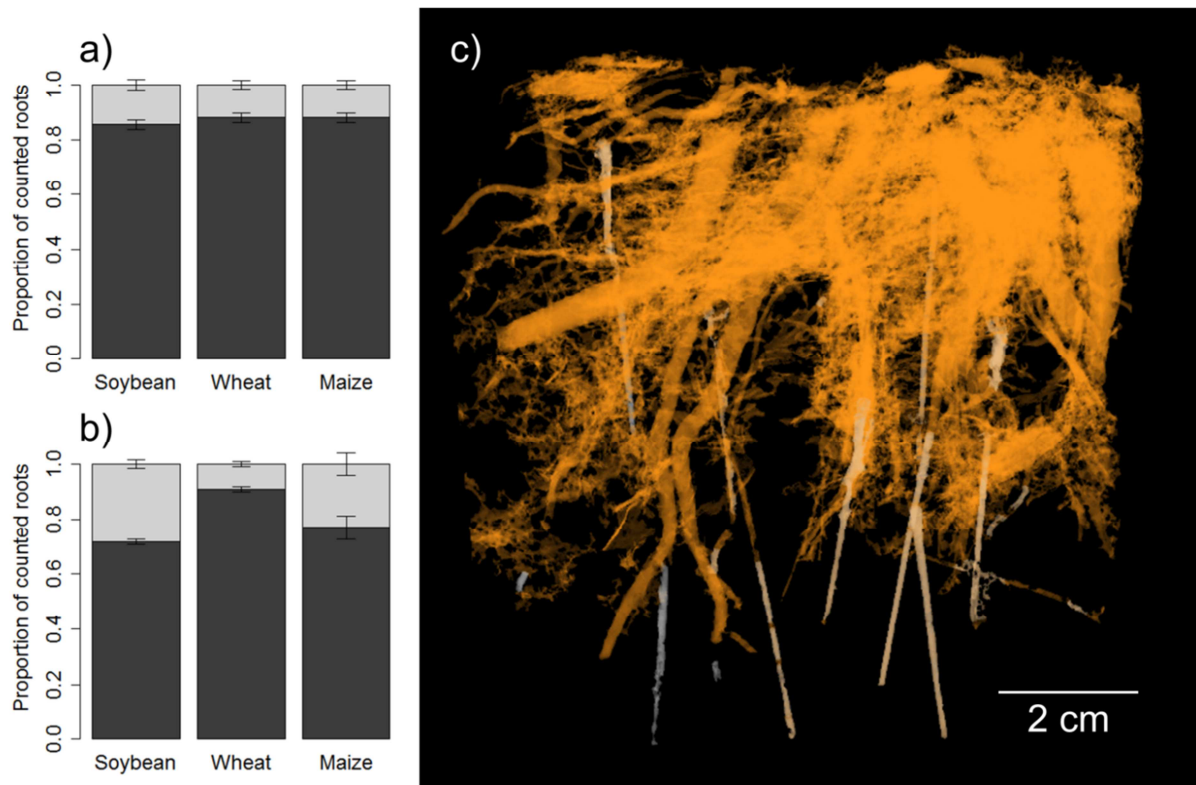
Figure 5.3: Proportion of total number of counted roots either crossing or colonising (grey) artificial pores or neither crossing or colonising (black) artificial pores in a) soil columns and b) the field. c) Typical picture of maize root system (orange) and artificial macropores (grey transparent) from 0 to 10 cm depth in the field. Error bars represent standard error (soil columns: n = 4, field n: = 3).

5.3.3. Preferential root growth towards artificial macropores

Virtually reallocating the artificial macropores within the reconstructed scans (Figure 5.1f) allowed the expected number of hits per pore if roots had grown randomly to be estimated. For all three crops and in both environments, the expected number of hits was between 36% and 64% lower than the observed number when pores were at their actual position. This was particularly obvious in the soil columns where the artificial macropores were limited to one half of the column. Chi-square tests were highly significant for all crop-environment combinations (p-values between 0.025 and < 0.001; Table 5.3). Based on these findings, the quantified interaction of roots with artificial macropores was not a coincidence, but was the result of directed root growth towards the pores. This directed growth was also evident when using a rather qualitative and visual approach, where bending of roots towards a nearby artificial macropore was observed (Figure 5.4a). Furthermore, in the treatment where macropores were inserted into only one half of the soil columns, more roots were

present in the perforated half than in the unperforated half and roots in the perforated half grew deeper (Figure 5.4b and 5.4c).

Table 5.3: Observed root hits per artificial macropores at their actual position and expected hits of reallocated artificial macropores by roots under controlled conditions in soil columns and the field. Artificial pores were inserted into the soil columns either in a cross-like pattern (Cross) or only in one half of the column (Split), (soil columns: n = 4, field: n = 3; chi-square test).

Environment	Pattern	Crop	Observed hits [# pore^{-1}]	Expected hits [# pore^{-1}]	p-value
Soil columns	Cross	Soybean	1.65	1.05	0.025
		Wheat	1.65	0.70	< 0.001
		Maize	1.30	0.75	< 0.001
	Split	Soybean	1.2	0.45	< 0.001
		Wheat	1.65	0.65	< 0.001
		Maize	1.2	0.65	< 0.001
Field		Soybean	0.75	0.39	< 0.001
		Wheat	0.74	0.40	< 0.001
		Maize	1.28	0.46	< 0.001
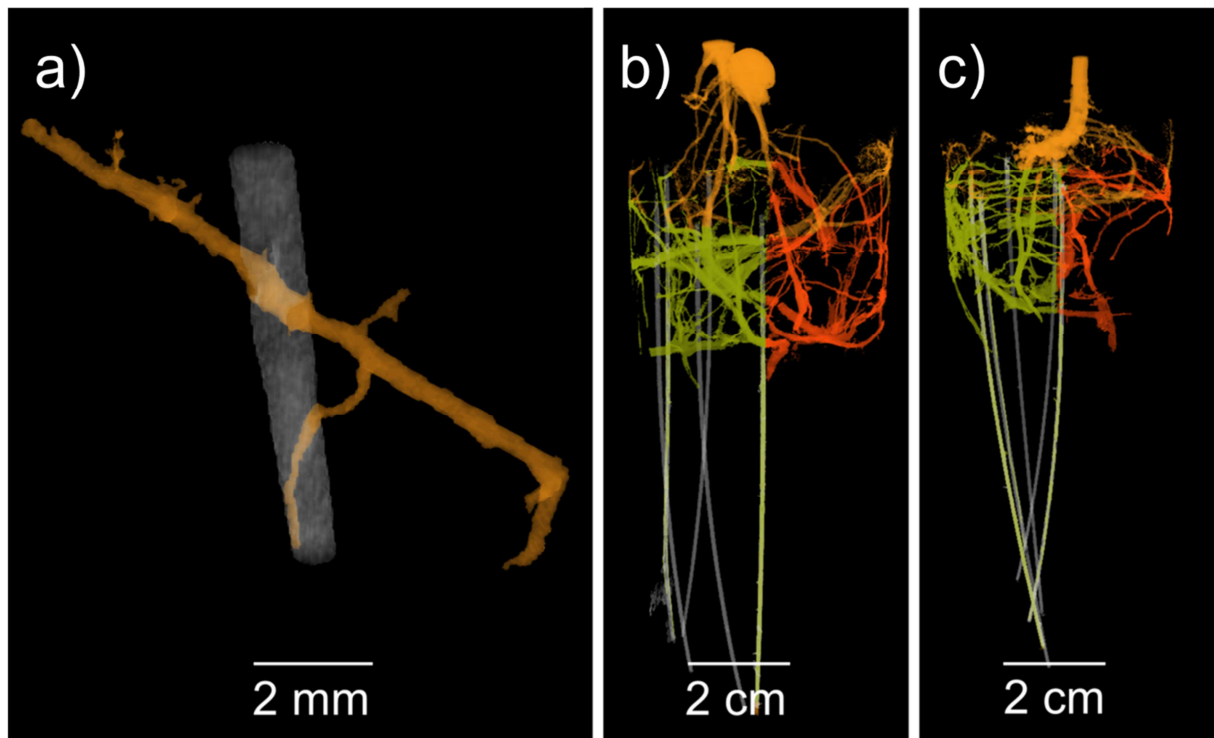
Figure 5.4: Illustration of directed root growth towards artificial macropores (grey transparent): a) Soybean main root crossing artificial macropore and lateral root colonising the same artificial macropore. b) maize and c) soybean seedling grown in soil columns: red colour represents roots in compacted soil, green colour roots in perforated compacted soil.

5.3.4. Plant vigour

Significant differences in vigour traits of 20-day-old seedlings from the growth chamber were observed between densely and loosely packed soil columns. Artificial macropores increased plant vigour compared with plants from compacted columns, but the differences were not significant (Supporting Information Table S5.3). Root dry weight of all crops decreased by 36-72% in Com and ComAP compared with Ctrl. The reduction in shoot dry weight was of a similar order of magnitude for wheat and maize, whereas for soybean the decrease in shoot dry weight was not significant. Total leaf area was reduced by 26-70% in the ComAP and Com treatments compared with loosely packed columns. Root-shoot ratio of all species was not affected by different soil treatments (Supporting Information Table S5.3).

In the field, all three species showed decreased plant vigour due to soil compaction, but also significantly increased vigour due to the presence of artificial macropores in the compacted soil.

Comparison of leaf area for different leaf positions on the stem showed that the beneficial effects of artificial macropores in compacted soil on plant growth occurred later than the adverse effects of compaction. In soybean, leaf area decreased in Com and ComAP compared with Ctrl starting at the 6th leaf. Leaf area from the 7th to the 10th leaf was larger in ComAP than in Com (Figure 5.5). In maize, the observed pattern of leaf area with respect to leaf position was very similar to that in soybean. Adverse effects of soil compaction on plant vigour were visible at the 4th leaf, while from the 8th leaf onwards, leaf area increased under ComAP compared with Com (Figure 5.5). The effects of the different soil treatments on the productivity of winter wheat were slightly different. Leaf area at individual leaf positions reflected the effect of soil compaction, but not of artificial pores in compacted soil, on plant vigour development. However, compared with wheat plants grown on compacted soil, plants from compacted plots with artificial macropores developed significantly more tillers (Figure 5.5). Shoot dry weight also responded significantly to soil compaction and the presence of artificial macropores in compacted soil. On uncompacted and compacted soil with artificial macropores, the mean dry weight of individual soybean plants was around 22 g, compared with 15 g under compaction without artificial macropores. In wheat, the effects of soil treatments on plant dry weight were of a similar order of magnitude: Shoot dry weight dropped from around 6 g per plant in Ctrl and ComAP to 3.6 g per plant in Com (Figure 5.5). Due to strong block effects, significant differences in plant dry weight were only found between Ctrl and Com (Supporting Information Table S5.4). Dry weight of single plants decreased from 131 g in the uncompacted plots to 107 g and 85 g under ComAP and Com, respectively (Figure 5.5).

Root dry weight, expressed as the sum of root dry matter in both sampled depths, was also reduced due to soil compaction. In soybean, wheat and maize, root dry weight was decreased under compaction by roughly 40% compared with the uncompacted plots. Root dry weight in compacted plots with artificial macropores was around 40% higher than in compacted plots for wheat and soybean, whereas in maize just a very small increase in root dry weight was observed due to macropores in compacted soil (Supporting Information Table S5.3).
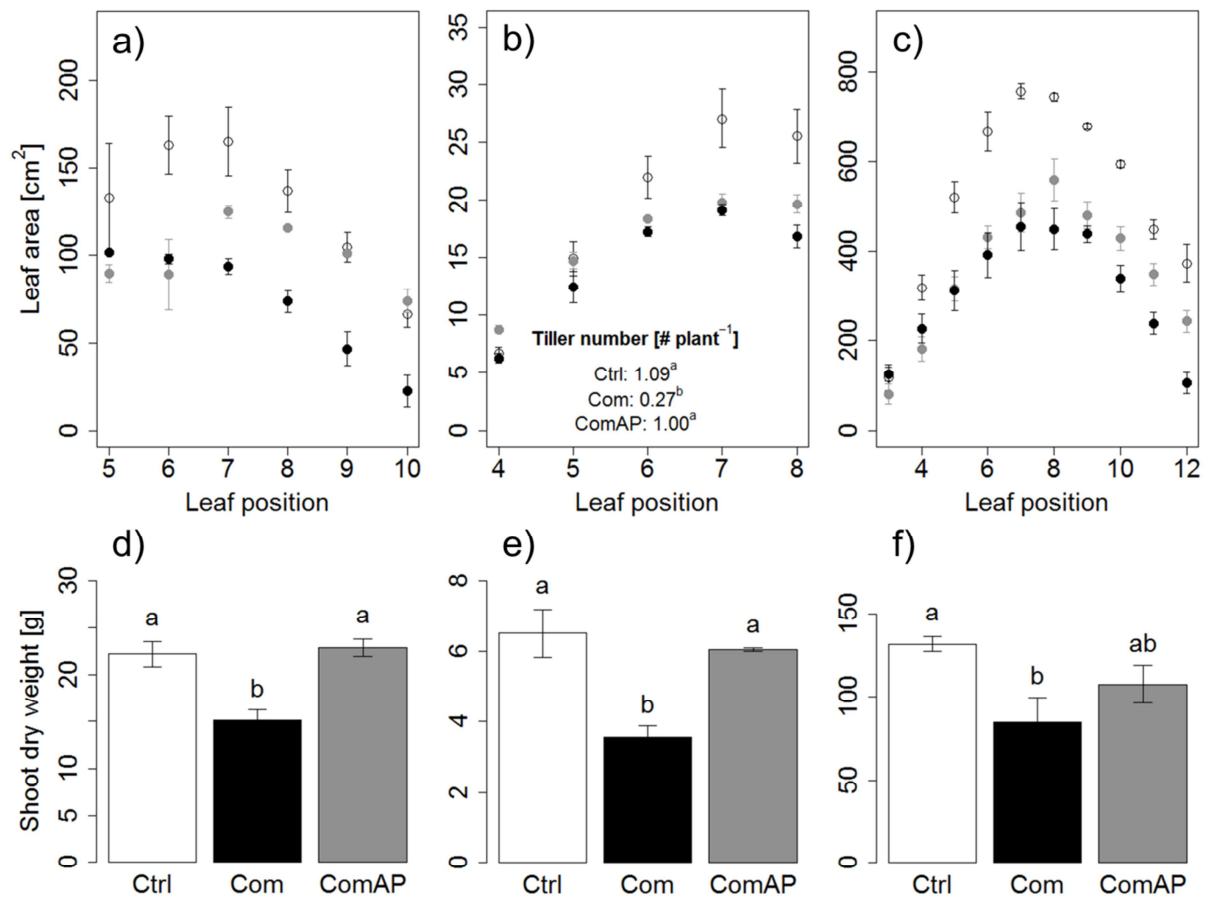
Figure 5.5: Leaf area with respect to different leaf positions for field-grown a) soybean, b) wheat and c) maize plants. Shoot dry weight of field-grown d) soybean, e) wheat and f) maize plants. Shading of all symbols and bars: uncompacted soil (open symbols; Ctrl), compacted soil (closed black symbols; Com) and compacted soil with artificial macropores (closed grey symbols; ComAP). Different letters indicate significant differences of the means using least significant difference (LSD) test at $p < 0.05$. Error bars represent standard error (n = 3).

5.4. Discussion

Quantification of the interactions between roots and artificial macropores in compacted soil revealed that roots of the three crop species studied grew preferentially towards spots with more favourable soil physical conditions. The X-ray micro CT scans showed that roots of different species interacted differently with artificial macropores created in compacted soil. By combining experiments in a growth chamber with field experiments, it was possible to show that these responses were consistent between controlled and field conditions. The data also showed that soil compaction

decreased plant growth at an early developmental stage, whereas artificial pores in compacted soil enabled the plant to compensate for the decreased early vigour at later developmental stages.

5.4.1. Artificial macropores increased gas transport rates in compacted soil

Soil physical properties differed significantly between loose, compacted and compacted soil with artificial macropores. As proposed previously (Stirzaker et al., 1996; Colombi and Walter, 2016), the combination of different soil physical measurements provided an adequate picture of the physical environment of roots. In particular, the measurements of soil physical functions showed the effects of the different soil treatments on soil physical fertility. The highest gas diffusivity and air permeability values were recorded in ComAP, followed by Ctrl and Com (Table 5.1). Furthermore, the oxygen concentration in soil air measured in soil columns was increased in compacted bulk soil due to the presence of nearby artificial macropores (Supporting Information Figure S5.1). Particularly in poorly aerated soil such as compacted soil and under wet conditions, macropores can mediate soil hypoxia. These observations confirm findings in previous studies regarding the effects of macropores on soil physical fertility. Naturally occurring and experimentally constructed macropores increase fluid transport rates and were described as potential pathways for roots to reach water and nutrients (Stirzaker et al., 1996; Valentine et al., 2012; Kuncoro et al., 2014a). Mechanical impedance in the bulk soil was only affected by soil compaction and not by the presence of artificial macropores (Table 5.1). Soil bulk density in the field was generally not different between Com and ComAP, except at 10 cm depth in the wheat plots (Table 5.2). Uplift of soil caused by increased root growth (Supporting Information Table S5.3) or more pronounced wetting-drying cycles due to the presence of artificial macropores may have caused this discrepancy. Nevertheless, these results show that certain soil physical functions that are adversely affected by compaction can be recovered by inserting continuous vertical macropores into compacted soil.

5.4.2. Roots of different species interacted differently with artificial macropores

In the present study roots of soybean, wheat and maize showed differing behaviour towards cylindrical and vertical artificial macropores, which provided a potential path of least resistance and a continuous connection to atmospheric air. In the case of maize, the artificial pores were mainly used as

a path of least resistance, since most interactions were classified as colonisations (Figure 5.2). Such root behaviour in searching for and following a pore, as a path of least resistance, was described as "trematotropism" by Dexter (1986). Trematotropism was also observed to some extent for soybean roots and to a lesser extent for wheat roots. In soybean, less than 50% of the roots that reached a pore remained within it. The remaining soybean roots interacting with artificial pores crossed the pores (Figure 5.2). In contrast to maize, wheat roots predominantly crossed artificial pores rather than remaining within them (Figure 5.2). This behaviour was particularly observed in scans from the growth chamber samples, where lateral roots were clearly visible. Owing to their horizontal growth direction, lateral roots are more likely to re-enter the bulk soil immediately after entering an artificial macropore than vertically growing main roots. Furthermore, it has been shown that lateral roots preferentially grow into less porous areas in the soil (Bao et al., 2014). The number of crossings in field samples may have been underestimated, however, since lateral roots of wheat were not visible due to the lower voxel resolution. Overall, the observed trematotropic behaviour of crop roots is in line with other reports of artificial and natural macropores being used by roots as a path of least resistance to reach deeper soil layers (Dexter, 1986; Stirzaker et al., 1996; Nakamoto, 1997; de Freitas et al., 1999; White and Kirkegaard, 2010; Athmann et al., 2013; Kautz et al., 2013; Han et al., 2015).

The methodologies used in previous studies, such as endoscopy and examinations of profile walls or slices of soil cores, did not allow crossings of macropores by roots as defined in the present study to be observed. Use of X-ray CT in a previous pot study revealed that barley roots also cross, rather than colonise, artificial macropores in compacted soil (Pfeifer et al., 2014b). The observed crossings of artificial macropores by roots indicate that roots used the macropores as a source for oxygen, which is needed to maintain aerobic root respiration. This effect would be particularly pronounced under moist and poorly aerated conditions (Dexter, 1986). Continuous and vertical macropores accelerate soil drainage (Lipiec and Hatano, 2003; Chen et al., 2014a; Kuncoro et al., 2014a; Kuncoro et al., 2014b) and increase oxygen supply to the soil (Supporting Information Figure S5.1). Based on the results of the present study, there are two possible explanations for the differing behaviour of roots of different plant species to macropores. On the one hand, the difference between the species could be explained by their tolerance to increased mechanical impedance. Maize, which predominantly used macropores

as a path of least resistance (Figure 5.2), is known for its relatively low tolerance to increased mechanical impedance compared with small grain cereals (Grzesiak et al., 2014). Wheat, in contrast, predominantly crossed macropores (Figure 5.2) and is known to be less sensitive to increased impedance than maize (Grzesiak et al., 2014). The tolerance of soybean roots to increased mechanical impedance was observed to be higher than that of maize (Bushamuka and Zobel, 1998), but lower than that of wheat (Busscher et al., 2000a). This corresponds to our finding that soybean roots were equally likely to cross or colonise an artificial macropore. Besides the different degree of tolerance to mechanical impedance among the investigated species, soil physical properties are suggested to determine as well whether roots remain in artificial macropores or only cross them. The likelihood that roots would stay in the pores presumably increases when the mechanical impedance of the bulk soil increases due to soil drying. Therefore it is also suggested that roots would rather cross such vertical macropores under moist conditions, when re-entering into the bulk soil is less restricted by mechanical impedance.

A second possible explanation for the distinctly different behaviour between roots of different species with artificial macropores is root-soil contact, which is crucial for uptake of e.g. phosphorus or potassium (Stirzaker et al., 1996; Tracy et al., 2011). It has been observed previously that macropores are often occupied by more than one living or dead root (White and Kirkegaard, 2010), which enables better root-soil contact than with a single root. In the present study, the artificial pores made in compacted soil were 1.25 mm in diameter and the diameter of maize roots is usually larger than 1 mm (Lipiec et al., 2012), enabling good root soil contact within the artificial macropores. Wheat and newly emerging soybean roots have smaller diameter (Lipiec et al., 2012; Tracy et al., 2012a; Colombi and Walter, 2016), which would not allow for sufficient root-soil contact within artificial pores.

5.4.3. Roots grew preferentially towards artificial macropores

Despite the differences in interaction with artificial macropores between roots of wheat, soybean and maize, all three species showed directed root growth towards artificial macropores. The observed number of hits (sum of crossing and colonising roots per artificial pore) of roots on the artificial pores was 57-178% higher than the number, which could be expected if the roots had grown randomly

(Table 5.3, Figure 5.4). Since the roots needed to grow through compacted bulk soil to reach an artificial macropore, trematotropism alone does not serve as an explanation for such directed growth. "Oxytropism", a phenomena describing the movement or growth towards higher oxygen concentration, has been observed for pea roots (Porterfield and Musgrave, 1998). Taking into account the increased gas diffusivity and air permeability due to artificial macropores in the present study (Table 5.1, Supporting Information Figure S5.1), oxytropism seems to be the driving mechanism for roots to sense pores and grow towards them. It has been suggested that roots sense different environmental properties and prefer to grow into more favourable parts of the soil and avoid more hostile parts (Passioura, 2002). In our study, artificial macropores and the bulk soil immediately beside these represented such spots of favourable soil physical conditions. Moreover, they provided roots with an environment in and around which soil physical functions had at least partially recovered from compaction. Oxygen transport to the bulk soil around the artificial pores was accelerated (Supporting Information Figure S5.1) and the artificial macropores served as a continuous connection to atmospheric air and as a path of least resistance. A few other studies have observed similar results, such as increased lateral root initiation into wetter soil (Bao et al., 2014) and avoidance of unfavourable soil structure (Semchenko et al., 2008). Attraction of roots to macropores has been proposed (Stirzaker et al., 1996; White and Kirkegaard, 2010; Pfeifer et al., 2014b), but to the best of our knowledge has not been quantified previously. As reported in other studies (Cornish, 1993; Rasse and Smucker, 1998; Pfeifer et al., 2014b; Han et al., 2015), the vast majority ($> 70\%$) of the roots neither crossed nor colonised artificial macropores (Figure 5.3).

5.4.4. Artificial macropores in compacted soil compensated for decreased early vigour at later developmental stages

Plant vigour of wheat, soybean and maize was significantly altered by the different soil treatments. Compared with the uncompacted treatment, dry shoot biomass of all three crop species was decreased due to compaction, by 24-70% and 31-45% in the columns and the field, respectively (Figure 5.5, Supporting Information Table S5.3). Dry root biomass in the samples excavated from the field and the soil columns decreased in a similar order of magnitude in response to compaction (Supporting Information Table S5.3). Decreasing crop productivity resulting from restricted access to deeper soil

layers (McKenzie et al., 2009) and soil compaction has been shown for various species in the field (Barraclough and Weir, 1988; Botta et al., 2010; Arvidsson and Håkansson, 2014; Colombi and Walter, 2016). Also in young plants, grown under laboratory conditions soil compaction results in reduced plant vigour (Young et al., 1997; Buttery et al., 1998; de Freitas et al., 1999; Bingham and Bengough, 2003; Grzesiak et al., 2013). Such studies with seedlings have shown that the adverse effects of soil compaction on plant growth occur at very early developmental stages, which corresponds to the findings in this study. In response to soil compaction, dry shoot biomass of plants from the growth chamber in the present study was decreased at 20 DAS (Supporting Information Table S5.3). Plants grown in compacted soil in the field showed progressively decreasing leaf area starting between leaf position 4 and 6 compared with plants from uncompacted soil (Figure 5.5). Comparing the experimental data for young and mature plants showed that the beneficial effects of artificial macropores in compacted soil on plant vigour occurred later than the adverse effects of compaction. In the growth chamber, plants were too young to show increased vigour due to artificial macropores in compacted soil (Supporting Information Table S5.3). In the field, leaf area increased from leaf position 7 and 9 onwards in soybean and maize, respectively, in ComAP compared with Com. In wheat, this effect occurred during tillering stage (Figure 5.5). As previously observed in laboratory studies (Stirzaker et al., 1996; de Freitas et al., 1999), dry shoot biomass in the field was 27-67% higher due to the artificial pores in compacted soil (Figure 5.5). Remarkably, this increase in biomass occurred even though less than 30% of the roots crossed or colonised artificial macropores (Figure 5.3). These findings suggest that in an early stage of plant development, the increased mechanical impedance of compacted bulk soil led to decreased early vigour. As plant development progressed, soil functions provided specifically by artificial macropores in compacted soil, allowed the plant to compensate for poor early vigour. Since crossing and colonisation occurred in all three studied species, the artificial macropores in compacted soil fulfilled different purposes for the growing plant. Increased soil aeration due to the artificial macropores helped to maintain aerobic root respiration, whereas roots used artificial macropores as a path of least resistance to reach resources in deeper soil layers. This combination of providing oxygen and a potential path of least resistance for growing roots

was most likely the cause for the beneficial effects of artificial macropores in compacted soil on plant vigour.

5.5. Conclusions

Combining soil physical measurements with observations of root-pore interactions and detailed shoot measurements allowed the influence of different soil physical conditions on belowground and aboveground plant development to be quantified. The results showed that roots sense their physical environment and grow preferentially towards artificial macropores. The benefit of vertical macropores for plant growth is evident when considering the increased soil aeration due to perforation of compacted soil (Table 5.1) and the different interactions of roots with these pores (Figure 5.2). Besides serving as a path of least resistance to reach deeper soil strata, macropores served as a source of oxygen for growing roots. Thus creation of vertical macropores increased soil physical fertility and resulted in increased crop productivity of all three species. For future research it would be desirable to investigate root-macropore interactions and directed root growth towards macropores at a range of soil physical conditions and to look at the underlying mechanisms of preferential growth. Since macropores in naturally structured soil cover a wide range of shapes, geometries and orientations, this should additionally be taken into account in further studies on root-macropore interactions.

Acknowledgements

6. General discussion

The major aim of the presented thesis was to identify possible strategies for the recovery of crop yields after arable soil has been compacted. This was approached i) by testing whether compaction effects occurring in the field can be adequately simulated in soil columns and hence evaluating the suitability of soil columns as a model system, ii) by quantifying the genetic diversity with respect to the penetration ability of roots through soil of increased strength and root-shoot relationships under compaction and iii) by evaluating how roots interact with artificial macropores in compacted soil and how these pores affect soil physical functions and crop development. The obtained results suggest that soil columns may serve as a model system for the field, since phenotypic responses as well as the interactions of roots with artificial macropores occurring in the field were reproducible in soil columns. However, certain soil physical properties of compacted soil such as low soil oxygen contents are –without further manipulation– neglected in small columns. Genetic diversity of root and shoot traits among the investigated fourteen wheat varieties could be shown. The geometry of the root tip and root numbers were observed to be pivotal traits, which determine the capability to penetrate compacted soil and shoot development on compacted soil, respectively. These observations demonstrate that specific root traits might be integrated into plant breeding programmes aiming to develop varieties that are tolerant to compaction. Furthermore, it could be shown that roots actively grow towards spots of higher soil physical fertility represented by artificial macropores in compacted soil. This preferential root growth enabled plants to compensate for decreased early vigour at later plant developmental stages.

Thus, it can be stated that multi-level phenotyping (Supporting Information Table S8.1) is a suitable approach to identify and evaluate strategies, which contribute to yield recovery on compacted soils. Since the evaluated strategies were promoting root growth, they will not only mitigate crop yield but also recover soil physical functions that were adversely changed by soil compaction.

6.1. Soil columns are suitable model systems for compaction experiments

Evaluating whether soil columns can be used as a model system for the field is crucial, since confounding factors occurring in the field can be controlled to a large extent in experiments conducted

under controlled conditions. Furthermore, experiments in pots allow for far higher throughput compared to field studies. Nevertheless, experiments in growth chambers or greenhouses may neglect certain phenomena that are present in the field. Therefore, the reproducibility of results derived from the field under controlled conditions needs be ensured.

6.1.1. High consistency of phenotypic responses to soil compaction between field and controlled conditions

Soil compaction caused tremendous alterations of the root phenotype, including changes of rooting depth, root system architecture and root morphology and anatomy under field conditions. As observed in other studies (Barraclough and Weir, 1988; Botta et al., 2010; Hernandez-Ramirez et al., 2014; Chen et al., 2014b), roots of triticale and soybean grew more shallow in response to soil compaction (Table 2.3). Corresponding to these field derived results, the penetration of roots into compacted soil in soil columns was significantly lower compared to soil columns that were loosely packed. Soil penetration after two days of growth by roots of triticale, soybean and wheat decreased between 56% and 82% due to an increase of soil bulk density from 1.34 g cm^{-3} to 1.6 g cm^{-3}. Furthermore, also a moderate increase of soil bulk density from 1.3 g cm^{-3} to 1.45 g cm^{-3} in soil columns resulted in a reduction of root elongation rates in wheat of 40% (Table 3.1). These observations correspond to previous studies, in which reduced root elongation rates due to increased mechanical impedance were observed in seedlings of various mono- and dicotyledonous species (Goss and Russell, 1980; Atwell, 1990; Bengough and Mullins, 1991; Young et al., 1997; Croser et al., 1999a; Croser et al., 1999b; Iijima and Kato, 2007).

As observed for rooting depth and root elongation rates, root architectural as well as plant vigour responses of crops to soil compaction were similar between soil columns and the field. Decreased lateral and axial root number in response to compaction was observed in soil columns for triticale, soybean (Figure 2.5) and different wheat genotypes (Figure 4.2 and Figure 4.4). The same responses were obtained in field-grown soybean and triticale plants 42 and 91 days after planting (Figure 2.2) and these results correspond to observations in other studies (Barraclough and Weir, 1988; Tracy et al., 2012b; Grzesiak et al., 2014; Hernandez-Ramirez et al., 2014; Chen et al., 2014b). These root

architectural responses to soil compaction may also be interpreted as a delay or reduction in the development of the root system. This reduction in the development of the root system resulted in reduced shoot development in triticale and soybean in the field (Table 2.5) and under controlled conditions in wheat (Figure 4.2). Consequently, plant biomass of young and mature plants as well as actual crop yields decreased due to soil compaction in triticale, soybean, maize and wheat (Table 2.5, Figure 4.5, Figure 5.5, Supporting Information Table S5.3 and Supporting Information Table S6.1), which is in agreement with results from other studies (Barraclough and Weir, 1988; Buttery et al., 1998; Bingham and Bengough, 2003; Czyż, 2004; Botta et al., 2010; Siczek and Lipiec, 2011; Grzesiak et al., 2013; Arvidsson and Håkansson, 2014; Grzesiak et al., 2014; Pfeifer et al., 2014a).

Furthermore, root morphological and anatomical adjustments to increased soil bulk density, which occurred in the field could be reproduced in plants that were grown in soil columns. Root thickening in response to soil compaction was observed in soybean, triticale (Figure 2.5) and wheat (Table 3.1, Figure 3.6 and Supporting Information Figure S2.1) under controlled conditions and in field-grown triticale (Figure 2.2). Due to secondary radial root growth in soybean, increased root diameters in the field in response to compacted soil could only be observed in newly emerged roots (Figure 2.2). Particularly in wheat and triticale and to a smaller extent also in soybean, increased root diameters coincided under field and laboratory conditions with increased cortical area and increased abundance of cortical aerenchyma (Figure 2.3, Figure 2.4, Table, 3.3 and Figure 3.7). These findings about root morphological and anatomical acclimations to soil compaction correspond to results from other studies, in which root thickening and an increase of the cortical share within root cross sections were observed in response to soil compaction (Materechera et al., 1992; Iijima and Kato, 2007; Ramos et al., 2010; Alameda and Villar, 2012; Lipiec et al., 2012; Tracy et al., 2012b; Grzesiak et al., 2013; Hernandez-Ramirez et al., 2014; Pfeifer et al., 2014a).

Not only responses of plant growth or the root phenotype to soil compaction could be compared between experimental scales, but also the interaction of roots with artificial macropores in compacted soil. As concluded previously (Stirzaker et al., 1996; White and Kirkegaard, 2010), roots were actively growing towards these artificial macropores under field and controlled conditions (Table 5.3). In spite of this common behaviour of wheat, soybean and maize, the species interacted differently with these

macropores. Irrespective of the experimental scale, wheat roots predominantly crossed the artificial macropores, whereas maize roots predominantly grew inside the pore and in soybean both types of interactions occurred to an equal extent (Figure 5.2).

6.1.2. Controlled conditions may not entirely address field conditions

Despite the high consistency between field and laboratory conditions, certain results observed under field conditions could not be reproduced in soil columns. It is known that soil structural degradation caused by soil compaction increases the risk of hypoxia and it was discussed that this may affect root growth (Iijima and Kato, 2007; Tracy et al., 2011; Hernandez-Ramirez et al., 2014). Fluid transport rates like air permeability or gas diffusivity, which can be used to quantify compaction induced degradation of soil structure, were comparable between undisturbed und packed soil cores (Table 5.1). However, measurements of oxygen contents in the soil air from soil columns did not show signs of hypoxia in compacted soil (Supporting Information Figure S5.1). This implies that it would be necessary to manipulate soil air to simulate soil hypoxia of compacted soils, which was shown to be possible in a similar set up as the ones used in the presented thesis (Masle and Passioura, 1987).

A further limitation of experiments at the pot or soil column scale is that plants can only be grown for a few weeks. This limited growth period does not allow quantifying processes, which happen beyond the initial plant developmental stages. As observed previously in tomato, soybean and pea (Iijima and Kato, 2007; Ramos et al., 2010; Tracy et al., 2012b), the diameter of young soybean roots increased in response to soil compaction (Figure 2.2 and Figure 2.5). However, due to slower secondary root thickening under compaction, soybean root diameter was smaller in compacted soil compared to loose soil at later developmental stages (Figure 2.2 and Figure 2.3). Furthermore, also the effects of artificial macropores on plant performance were not observed in plants grown for 20 days in soil columns (Supporting Information Table S5.3). Looking at leaf sizes of field-grown plants, which were taken from different positions at the plant, revealed that the beneficial effects of artificial macropores in compacted soil are temporally shifted compared to the adverse effects of compaction. As observed in 20-day-old plants grown in soil columns (Supporting Information Table S5.3), the size of early developed leaves was reduced due to compaction and was not affected by soil perforation. The

beneficial effects of artificial macropores in compacted soil on plant development instead occurred at later developmental stages. This resulted in increased final dry biomass compared to plants from compacted but not perforated soil (Figure 5.5), which corresponds to results from similar studies (Stirzaker et al., 1996; de Freitas et al., 1999).

6.2. Focal root traits may be used to overcome adverse effects of soil compaction

The integration of functional root traits into breeding programmes is suggested to be a promising approach to enhance crop productivity under limited soil fertility or low input conditions (White et al., 2013; York et al., 2013). Genetic diversity within a single species was successfully used to identify functional root traits, which enable to sustain crop productivity under low soil fertility. Most of the work that has been done so far focused on water or nutrient scarcity and not on soil physical stresses. It has been shown that low numbers of axial and lateral roots enhance water uptake under low soil moisture in maize resulting in higher biomass production (Zhan et al., 2015; Gao and Lynch, 2016). Steep root growth angles and low root numbers were observed to improve nitrogen uptake and plant growth in maize under low soil nitrogen (Saengwilai et al., 2014b; Zhan and Lynch, 2015). Increased root porosity was shown to be related to the tolerance to flooding in barley (Broughton et al., 2015), whereas increased topsoil rooting contribute to higher phosphorus uptake in common bean (Miguel et al., 2013). Furthermore, other results suggested that a high abundance of root cortical aerenchyma and large cortical cells contribute to higher plant productivity under drought and low soil nitrogen in maize (Chimungu et al., 2014a; Saengwilai et al., 2014a; Chimungu et al., 2015b).

6.2.1. Root tip shape governs root elongation under increased soil strength

To ensure enough root soil contact, which is required in particular for the uptake of immobile nutrients like phosphorus or potassium, roots need to grow through bulk soil (Stirzaker et al., 1996; Tracy et al., 2011). Hence, root traits that increase root elongation rates in soil of increased mechanical impedance need to be identified in order to select for compaction tolerant varieties. There is evidence that the shape of the root tip is related to root elongation in compacted soil and that this might be explained by the penetration stresses occurring during cavity expansion. Local soil compaction, which is induced by growing roots, was shown to be concentrated at the forefront of the root tip when the tip

opening angle is rather blunt. For a root with an acute tip shape, these zones of local compaction were located not at the front of the tip but were distributed around the root tip (Vollsnes et al., 2010). Comparing simulated stress fields around cones with blunt and acute opening angles, respectively resulted in the same observation (Ruiz et al., 2016). Furthermore, decapped root tips exerted higher penetration forces and stresses than roots with an intact root tip when penetrating into compacted soil (Iijima et al., 2003b).

Both, soil compaction at the forefront of the root tip and increased penetration stress due to a blunt tip opening angle, resulted in decreased root elongation rates (Iijima et al., 2003b; Vollsnes et al., 2010), which corresponds to the results presented in the current thesis. Under high soil bulk density (1.6 g cm^{-3}) genotypic root elongation rates were correlated to low root tip radius to length ratio (Figure 3.3). If the shape of the root tips was taken into account when calculating penetration forces and stresses (Eq 3.11 and Eq 3.12), it could be shown that roots with a rather acute opening angle exerted less penetration stress resulting in higher root elongation rates (Figure 3.4). It was proposed that the penetration forces and stresses required for a cylindrical cavity expansion are only 25% to 40% of the forces and stresses needed for a spherical cavity expansion (Greacen et al., 1968). These considerations correspond to the experimental data presented in the current thesis. Forces and stresses, which were calculated without the suggested geometry factors (Eq 3.11 and Eq 3.12), were around 2.5 to 4 times higher than the respective values when calculated including these geometry factors (Supporting Information Table S3.3). Irrespective whether calculations of penetration forces and stresses included the geometrical conversion factors or not, the resulting values were in the range of previous studies (Misra et al., 1986; Iijima et al., 2003b; Azam et al., 2013; Bizet et al., 2016). These results strongly suggest that acute tip opening angles contribute significantly to the penetrability of compacted soil since they reduced penetration stresses at the root tip.

6.2.2. Genetic differences in root diameter do not affect root elongation

Root thickening as an acclimation to increased soil strength was observed in field-grown triticale and soybean (Figure 2.2). Under controlled conditions the same responses were observed in soybean, triticale (Figure 2.5) and wheat (Table 3.1, Table 3.3 and Supporting Information Figure S2.1). Since

increased root diameters reduce penetration stress and the risk of buckling (Materechera et al., 1992; Chimungu et al., 2015a), it has been proposed that thicker roots promote root growth in soil of increased strength (Materechera et al., 1992; Kirby and Bengough, 2002). Furhtermore, root and stele diameter were observed to determine root bending and tensile strength, which was related to the genotypic penetrability of roots through wax layers (Chimungu et al., 2015a). Root diameter and root cross sectional area were significantly different among the assessed fourteen wheat genotypes (Table 3.1 and Table 3.3). However, the obtained results did not show any significant relationship between root diameter and root elongation rates (Table 3.2 and Figure 3.3). Similar to results reported by Vollsnes et al., (2010) and Iijima et al., (2003b), root elongation rate was determined by the shape of the root tip and not by the root diameter when comparing different genotypes under the same soil bulk density. Furthermore, root thickening as a morphological adjustment of roots to increased soil mechanical impedance seemed to be limited. In embryonic roots, root diameter (Table 3.1) and root cross sectional area (Table 3.3 and Figure 3.6) increased clearly due to higher soil bulk density. However, in post-embryonic roots, which are inherently thicker, the response of root diameter to increased bulk density was much less pronounced (Table 3.3 and Figure 3.6). This limitation of root thickening was also observed when comparing root diameter and calculated penetration force. The two parameters were related following an exponential function that asymptotically converged to an upper limit of 0.78 mm diameter (Figure 3.5 and Supporting Information Figure S3.4). Hence, even though more penetration force was required for growth, no increase in diameter occurred. Most likely this limitation of root morphological adjustment and mechanical optimization occurred due to too high root volume to surface ratio. A further increase in root diameter would cause the volume to surface ratio to be too high to sustain the required uptake of water and nutrients (Varney and Canny, 1993; Casper and Jackson, 1997).

6.2.3. Shoot growth responses to soil compaction are related to root numbers

Root numbers were shown to be related to the genotypic tolerance to soil compaction in wheat and narrow leafed lupin (Kubo et al., 2004; Kubo et al., 2006; Chen et al., 2014b). It was possible in the current thesis to study root system development over time by means of X-ray computed tomography (Figure 2.5, Figure 4.2 and Supporting Figure S2.1). Combining weekly counts of roots with weekly

measurements of plant height in fourteen wheat varieties under three different levels of soil bulk density (1.3 cm^{-3}, 1.45 cm^{-3} and 1.6 g cm^{-3}) showed that there are significant differences between genotypes regarding their root and shoot development (Table 4.2). This approach further enabled to show that the development of the root system –expressed as the number of axial and lateral roots at each scanning time point– was correlated to the development of plant height (Figure 4.2). Root numbers were also suited to describe the genotypic tolerance to increased soil strength. Varieties, which show a high number of axial and lateral roots or which maintained their root number were relatively tolerant to moderate soil compaction. Under moderate soil bulk density (1.45 g cm^{-3}) relative or absolute root numbers counted three weeks after germination were significantly correlated with shoot dry biomass (Figure 4.6 and Figure 4.7). It is worth noting that these relationships occurred even though root dry weight decreased in all assessed genotypes by at least 25% due to an increase in bulk density from 1.3 g cm^{-3} to 1.45 g cm^{-3} (Figure 4.5). Under low (1.3 g cm^{-3}) and high soil bulk density (1.6 g cm^{-3}) instead, no such relationship could be observed (Figure 4.6 and Figure 4.7).

Root numbers are suggested to be a promising trait, when screening for compaction tolerant varieties, not only due to these root-shoot relationships. It has been demonstrated that root numbers can be assessed at high throughput rates even under field conditions (Trachsel et al., 2011; Colombi et al., 2015; Burridge et al., 2016). The possibility to phenotype a large number of plants in a relatively short time is crucial for breeders (Passioura, 2012), since in such programmes hundreds of genotypes need to be evaluated at multiple sites. A further crucial aspect, when discussing about the potential of a certain plant trait to be integrated into breeding programmes, is its heritability. As reported in previous studies (Wilcox and Farmer, 1968; Bucksch et al., 2014; Colombi et al., 2015; Li et al., 2015; Richard et al., 2015; Burridge et al., 2016), root numbers showed even under compaction heritabilities above 50% and were comparable to heritabilities estimated for shoot traits such as plant height or leaf number (Table 4.6).

6.2.4. Beneficial effects need to be validated under field conditions

The presented data showed that several root traits are involved determining the genotypic tolerance to soil compaction. Root tip geometry was more related to the potential of certain varieties to elongate

in soil of increased mechanical impedance, whereas the number of roots was related to early plant vigour under increased soil bulk density. Since both parameters can be assessed at relatively high throughput rates, they seem promising target traits for breeding programmes aiming to develop compaction tolerant varieties. However, the data presented and discussed here is only based on experiments, which were performed with seedlings under controlled conditions. It will be crucial to evaluate, whether acute root tip opening angles or high numbers of roots are related to the genotypic tolerance to soil compaction in the field. There is evidence that this might be the case. It has been shown that root traits, which determine the tolerance to low soil moisture or nitrogen were the same in pot experiments and in the field (Chimungu et al., 2014a; Saengwilai et al., 2014a; Chimungu et al., 2014b; Saengwilai et al., 2014b; Zhan and Lynch, 2015; Gao and Lynch, 2016). Such laboratory to field correlations were even found when comparing rapeseed genotypes that were grown on filter paper with the same genotypes grown in the field (Thomas et al., 2016). Furthermore, the comparability between results obtained from soil columns and the field as discussed in chapter 6.1. suggests that root number and root tip shape are also of importance in the field. It is important to note that soil mechanical impedance was most likely the only limiting factor for root growth in the experiments presented in the third and fourth chapter. Due to regular watering and the resulting matric potential of -100 hPa, water was unlikely to be limiting and the measured oxygen contents of the soil air were far from hypoxia (Supporting Information Figure S5.1). Since soil hypoxia and low plant available water content result from soil structural degradation in compacted soils, both phenomena are likely to affect plant growth in compacted soil. Hence, traits that help the plant to acquire and use water more efficiently or traits that enable to maintain aerobic root respiration need to be taken into account, when screening for compaction tolerant varieties.

6.3. Soil perforation as an alternative to tillage

Crop yields in the field were significantly increased due to tillage of initially compacted soil. In the two first field seasons after compaction in March 2014, grain and silage yield of triticale and maize, respectively, were increased due to tillage in initially compacted plots when compared to yields from compacted but unploughed plots (Supporting Information Table S6.1). This positive effect of tillage

after soil compaction on crop productivity could be expected and has been observed previously (Botta et al., 2006; Botta et al., 2010; Wang et al., 2015). However, intensive tillage over long periods of time may lead to subsoil compaction in the form of plough layers, which show the same adverse soil physical properties like compacted soil (Krzic et al., 2000; Martínez et al., 2016a; Martínez et al., 2016b). Deep tillage or deep ripping, which is used sometimes to alleviate soil compaction, may also cause severe recompaction and might be too expensive (Hamza and Anderson, 2005). Therefore, alternative soil management approaches, which sustainably contribute to the recovery of soil physical functions and crop yields on compacted soils, are needed.

A possible approach might be the perforation of soil in order to create artificial cylindrical macropores. Such macropores, particularly when oriented vertically, are relatively stable to uniaxial compression that may result from tractor passing (Schäffer et al., 2008a; Schäffer et al., 2008b). Besides providing a path of least resistance for roots in compacted soil, natural or artificial macropores are known to increase fluid transport rates in soil (Stirzaker et al., 1996; Valentine et al., 2012; Kuncoro et al., 2014b). This recovery of soil physical functions, which were adversely changed due to compaction, was observed in the current thesis in undisturbed and repacked soil samples (Table 5.1). Furthermore, the perforation of compacted soil led to increased oxygen diffusion into the bulk soil in comparison to compacted soil without artificial macropores (Supporting Figure S5.1). The interaction of roots with artificial macropores (Figure 5.2), which was quantified for maize, wheat and soybean in the field and repacked soil columns, resulted from directed root growth (Table 5.3). As proposed by others (Stirzaker et al., 1996; White and Kirkegaard, 2010), roots were growing actively towards the artificially created macropores. This preferential root growth might be explained by a phenomenon called "oxytropism". It describes the movement or growth of organisms towards higher oxygen concentrations and has been shown to occur in roots of pea seedlings (Porterfield and Musgrave, 1998).

Once reaching such a pore, distinctly different behaviour was observed for the different species. Maize roots predominantly stayed in artificial macropores and used them as pathways of least resistance (Figure 5.2). This strategy of a root to search for a pore and exploit it as a path of least resistance is known as "trematotropism" (Dexter, 1986). In wheat instead, roots were predominantly

crossing the artificial pores and in soybean crossing and colonisation of pores by roots occurred to an equal extent (Figure 5.2). These differences in the interaction of roots with artificial macropores, could have been caused by the different degree of susceptibility to increased mechanical impedance between the three species investigated (Bushamuka and Zobel, 1998; Busscher et al., 2000b; Grzesiak et al., 2014). However, for a final conclusion about this additional studies are required, in which macropores are inserted into soils of different bulk density and mechanical impedance.

In all three species, the presence of artificial macropores showed similar effects on shoot growth. Like tillage, the perforation of compacted soil resulted in increased shoot growth compared to plants grown in compacted soil, which was not perforated (Figure 5.5). This finding corresponds to other studies, in which plants were grown on compacted and perforated soil (Stirzaker et al., 1996; de Freitas et al., 1999). Considering the fact that less than 30% of all roots interacted with these pores (Figure 5.3) and that wheat roots predominantly crossed the artificial pores suggests that these pores did not only serve as a path of least resistance. The increase in plant vigour due to artificial macropores was at least partially caused by other soil physical functions than mechanical impedance, which were affected by compaction and subsequent perforation. As shown in the current thesis (Table 5.1) and in a previous study (Stirzaker et al., 1996), fluid transport rates were increased in compacted and perforated soil compared to compacted soil without artificial macropores. Therefore, it is suggested that increased oxygen availability in combination with the possibility to use artificial pores as a path of least resistance caused the increase in plant vigour.

These results demonstrate that root growth and crop productivity on compacted soils are not only restricted by increased mechanical impedance but also due to decreased fluid transport rates. Hence, soil management approaches aiming to alleviate adverse effects of soil compaction in the long-term need to holistically address soil structural degradation, which was caused by soil compaction. Soil perforation seems to fulfil these requirements, since it opens pathways of least or no resistance to growing roots while increasing at the same time soil drainage and aeration. However, substantial development especially on the technical side is needed until such an approach can be applied at the hectare scale.

6.4. General conclusion: multi-level phenotyping enabled strategies for yield recovery after soil compaction to be identified

Combining different phenotyping methodologies to quantify plant properties from the tissue to the canopy level enabled to gain a broad understanding about soil-plant relationships under soil compaction. It was possible to show that compaction affects root properties such as root elongation rates and root system development or root morphology and anatomy. Particularly for root tip geometry and root system development genetic variability among different wheat cultivars could be shown. Since these properties were positively correlated to root elongation rate and shoot development under increased soil strength, they seem to be promising target traits for the integration into breeding programmes aiming to develop compaction tolerant varieties. Furthermore, plant responses to compacted soil were to a large extent comparable between the field and controlled conditions. This shows that pot experiments can be used as model systems that allow soil structural and physical properties of compacted field soil to be simulated. Hence, investigations at the soil column scale may be used to screen large diversity panels or to identify functional root traits prior to more laborious field experiments. Beside the identification of root traits that are of use in compacted soils, multi-level phenotyping also enabled to relate soil structural and physical properties to root growth and plant performance. It could be demonstrated that roots of different species grow actively towards spots of more favourable soil physical conditions in compacted soil, which were represented by artificial macropores. Even though only a small proportion of all roots interacted with these pores, plants showed increased shoot growth compared to plants grown on compacted soil without artificial pores.

Therefore, multi-level phenotyping is suggested to be a promising approach to identify strategies to overcome limitations of compacted soils on root and shoot growth. Since the presented approaches increased root growth, they will not only contribute to yield recovery but also to the recovery of soil physical functions that were changed due to soil compaction. For future research it would be desirable to expand the presented approaches to other soil physical stresses such as soil hypoxia or fluctuations of soil moisture. The integration of more diverse plant material –either species or genotypes– in such studies would further advance the understanding about soil-plant interactions.

7. References

Abbott LK, Murphy D V (2007) Soil Biological Fertility. A key to sustainable Land Use in Agriculture. Springer Netherlands

Van den Akker JJH, Canarache A (2001) Two European concerted actions on subsoil compaction. L Use Dev **42**: 15–22

Alameda D, Villar R (2012) Linking root traits to plant physiology and growth in Fraxinus angustifolia Vahl. seedlings under soil compaction conditions. Environ Exp Bot **79**: 49–57

Angers DA, Caron J (1998) Plant-induces changes in soil structure: Processes and feedbacks. Biogeochemistry **42**: 55–72

Arvidsson J, Etana A, Rydberg T (2014) Crop yield in Swedish experiments with shallow tillage and no-tillage 1983–2012. Eur J Agron **52**: 307–315

Arvidsson J, Håkansson I (2014) Response of different crops to soil compaction—Short-term effects in Swedish field experiments. Soil Tillage Res **138**: 56–63

Athmann M, Kautz T, Pude R, Köpke U (2013) Root growth in biopores—evaluation with in situ endoscopy. Plant Soil **371**: 179–190

Atwell BJ (1990a) The effect of soil compaction on wheat during early tillering. I. Growth, development and root structure. New Phytol **115**: 43–49

Atwell BJ (1990b) The effect of soil compaction on wheat during early tillering. III. Fate of carbon transported to the roots. New Phytol **115**: 43–49

Atwell BJ (1993) Response of roots to mechanical impedance. Environ Exp Bot **33**: 27–40

Azam G, Grant CD, Misra RK, Murray RS, Nuberg IK (2013) Growth of tree roots in hostile soil: A comparison of root growth pressures of tree seedlings with peas. Plant Soil **368**: 569–580

Bao Y, Aggarwal P, Robbins NE, Sturrock CJ, Thompson MC, Tan HQ, Tham C, Duan L, Rodriguez PL, Vernoux T, et al (2014) Plant roots use a patterning mechanism to position lateral root branches toward available water. Proc Natl Acad Sci U S A **111**: 9319–24

Barraclough PB, Weir AH (1988) Effects of a compacted subsoil layer on root and shoot growth, water use and nutrient uptake of winter wheat. J Agric Sci **110**: 207–216

Batey T (2009) Soil compaction and soil management - a review. Soil Use Manag **25**: 335–345

Beemster GTS, Masle J, Williamson RE, Farquhar GD (1996) Effects of soil resistance to root penetration on leaf expansion in wheat (Triticum aestivum L): kinematic analysis of leaf elongation. J Exp Bot **47**: 1663–1678

Bengough AG, Bransby MF, Hans J, McKenna SJ, Roberts TJ, Valentine T a (2006) Root responses to soil physical conditions; growth dynamics from field to cell. J Exp Bot **57**: 437–47

Bengough AG, Kirby JM (1999) Tribology of the root cap in maize (Zea mays) and peas (Pisum sativum). New Phytol **142**: 421–425

Bengough AG, McKenzie BM (1997) Sloughing of root cap cells decreases the frictional resistance to maize (Zea mays L.) root growth. J Exp Bot **48**: 885

Bengough AG, McKenzie BM, Hallett PD, Valentine TA (2011) Root elongation, water stress, and mechanical impedance: a review of limiting stresses and beneficial root tip traits. J Exp Bot **62**: 59–68

Bengough AG, Mullins CE (1991) Penetrometer resistance, root penetration resistance and root elongation rate in two sandy loam soils. Plant Soil **131**: 59–66

Bengough AG, Mullins CE (1990) The resistance experienced by roots growing in a pressurised cell. A reappraisal. Plant Soil **123**: 73–82

Bengough AG, Mullins CE, Wilson G (1997) Estimating soil frictional resistance to metal probes and its relevance to the penetration of soil by roots. Eur J Soil Sci **48**: 603–612

Bengough GA, Loades K, McKenzie BM (2016) Root hairs aid soil penetration by anchoring the root surface to pore walls. J Exp Bot **67**: 1071–1078

Besson A, Séger M, Giot G, Cousin I (2013) Identifying the characteristic scales of soil structural recovery after compaction from three in-field methods of monitoring. Geoderma **204**–**205**: 130–139

Bingham IJ, Bengough AG (2003) Morphological plasticity of wheat and barley roots in response to spatial variation in soil strength. Plant Soil **250**: 273–282

Bishopp A, Lynch JP (2015) The hidden half of crop yields. Nat Plants **1**: 15117

Bizet F, Bengough AG, Hummel I, Bogeat-Triboulot M-B, Dupuy LX (2016) 3D deformation field in growing plant roots reveals both mechanical and biological responses to axial mechanical forces. J Exp Bot erw320

Blackwell PS, Wells EA (1983) Limiting oxygen flux densities for oat root extension. Plant Soil **73**: 129–139

Blake A, Isard M (1998) Active Contours. Bmvc. doi: 10.1007/978-1-4471-1555-7

Boone FR, Vermeulen GD, Kroesbergen B (1994) The effect of mechanical impedance and soil aeration as affected by surface loading on the growth of peas. Soil Tillage Res **32**: 237–251

Botta GF, Jorajuria D, Balbuena R, Ressia M, Ferrero C, Rosatto H, Tourn M (2006) Deep tillage and traffic effects on subsoil compaction and sunflower (Helianthus annus L.) yields. Soil Tillage Res **91**: 164–172

Botta GF, Tolon-Becerra a., Lastra-Bravo X, Tourn M (2010) Tillage and traffic effects (planters and tractors) on soil compaction and soybean (Glycine max L.) yields in Argentinean pampas. Soil Tillage Res **110**: 167–174

Bottinelli N, Hallaire V, Goutal N, Bonnaud P, Ranger J (2014) Impact of heavy traffic on soil macroporosity of two silty forest soils: Initial effect and short-term recovery. Geoderma **217**–**218**: 10–17

Broughton S, Zhou G, Teakle NL, Matsuda R, Zhou M, O'Leary R a., Colmer TD, Li C (2015) Waterlogging tolerance is associated with root porosity in barley (Hordeum vulgare L.). Mol Breed **35**: 27–27

Bucksch A, Burridge J, York LM, Das A, Nord E, Weitz JS, Lynch JP (2014) Image-based high-throughput field phenotyping of crop roots. Plant Physiol **166**: 470–486

Burridge J, Jochua CN, Bucksch A, Lynch JP (2016) Legume shovelomics: High-Throughput phenotyping of common bean (Phaseolus vulgaris L.) and cowpea (Vigna unguiculata subsp, unguiculata) root architecture in the field. F Crop Res **192**: 21–32

Burton AL, Williams M, Lynch JP, Brown KM (2012) RootScan: Software for high-throughput analysis of root anatomical traits. Plant Soil **357**: 189–203

Bushamuka VN, Zobel RW (1998) Differential genotypic and root type penetration of compacted soil layers. Crop Sci **38**: 776–781

Busscher WJ, Frederick JR, Bauer PJ (2000a) Timing effects of deep tillage on penetration resistance and wheat and soybean yield. Soil Sci Soc Am J **64**: 999–1003

Busscher WJ, Lipiec J, Bauer PJ, Carter T E J (2000b) Improved root penetration of soil hard layers by a selected genotype. Commun Soil Sci Plant Anal **31**: 3089–3101

Buttery BR, Tan CS, Drury CF, Park SJ, Armstrong RJ, Park KY (1998) The effects of soil compaction , soil moisture and soil type on growth and nodulation of soybean and common bean. Can J Plant Sci 571–576

Casper BB, Jackson RB (1997) Plant Competition Underground. Annu Rev Ecol Syst **28**: 545–570

Chen G, Weil RR, Hill RL (2014a) Effects of compaction and cover crops on soil least limiting water range and air permeability. Soil Tillage Res **136**: 61–69

Chen YL, Palta J, Clements J, Buirchell B, Siddique KHM, Rengel Z (2014b) Root architecture alteration of narrow-leafed lupin and wheat in response to soil compaction. F Crop Res **165**: 61–70

Chimungu JG, Brown KM, Lynch JP (2014a) Large root cortical cell size improves drought tolerance in maize (Zea mays L.). Plant Physiol **166**: 2166–2178

Chimungu JG, Brown KM, Lynch JP (2014b) Reduced Root Cortical Cell File Number Improves Drought Tolerance in Maize. Plant Physiol **166**: 1943–1955

Chimungu JG, Loades KW, Lynch JP (2015a) Root anatomical phenes predict root penetration ability and biomechanical properties in maize (Zea Mays). J Exp Bot **66**: 3151–3162

Chimungu JG, Maliro MF a., Nalivata PC, Kanyama-Phiri G, Brown KM, Lynch JP (2015b) Utility of root cortical aerenchyma under water limited conditions in tropical maize (Zea mays L.). F Crop Res **171**: 86–98

Coelho Filho M a., Colebrook EH, Lloyd DP a., Webster CP, Mooney SJ, Phillips AL, Hedden P, Whalley WR (2013) The involvement of gibberellin signalling in the effect of soil resistance to root penetration on leaf elongation and tiller number in wheat. Plant Soil **371**: 81–94

Colombi T, Braun S, Keller T, Walter A (2016) Artificial macropores attract crop roots and enhance plant productivity on compacted soils. Sci Total Environ. doi: 10.1016/j.scitotenv.2016.07.194

Colombi T, Kirchgessner N, Le Marié CA, York LM, Lynch JP, Hund A (2015) Next generation shovelomics: set up a tent and REST. Plant Soil **388**: 1–20

Colombi T, Walter A (2016) Root responses of triticale and soybean to soil compaction in the field are reproducible under controlled conditions. Funct Plant Biol **43**: 114–128

Cornish PS (1993) Soil macrostructure and root growth of establishing seedlings. Plant Soil **151**: 119–126

Croser C, Bengough AG, Pritchard J (1999a) The effect of mechanical impedance on root growth in pea (Pisum sativum). II. Cell expansion and wall rheology during recovery. Physiol Plant **107**: 277–286

Croser C, Bengough AG, Pritchard J (1999b) The effect of mechanical impedance on root growth in pea (Pisum sativum). I. Rates of cell flux, mitosis, and strain during recovery. Physiol Plant **107**: 277–286

Czyż EA (2004) Effects of traffic on soil aeration, bulk density and growth of spring barley. Soil Tillage Res **79**: 153–166

Dexter AR (1986) Model experiments on the behaviour of roots at the interface between a tilled seed-bed and a compacted sub-soil III. Entry of pea and wheat roots into cylindrical biopores. Plant Soil **95**: 149–161

Dexter AR (1991) Amelioration of soil by natural processes. Soil Tillage Res **20**: 87–100

Downie H, Holden N, Otten W, Spiers AJ, Valentine T a, Dupuy LX (2012) Transparent soil for imaging the rhizosphere. PLoS One **7**: e44276

Dresbøll DB, Thorup-Kristensen K, McKenzie BM, Dupuy LX, Bengough a. G (2013) Timelapse scanning reveals spatial variation in tomato (Solanum lycopersicum L.) root elongation rates during partial waterlogging. Plant Soil **369**: 467–477

Falconer DS, Mackay TF (1996) Introduction to quantitative genetics, 4th ed. Longman, Harlow

Flavel R, Guppy C, Tighe M (2012) Non-destructive quantification of cereal roots in soil using high-resolution X-ray tomography. J Exp Bot **63**: 2503–2511

de Freitas PL, Zobel RW, Snyder VA (1999) Corn Root Growth in Soil Columns with Artificially Constructed Aggregates. Crop Sci **39**: 725–730

Galmés J, Ochogavía JM, Gago J, Roldán EJ, Cifre J, Conesa MÀ (2013) Leaf responses to drought stress in Mediterranean accessions of Solanum lycopersicum: Anatomical adaptations in relation to gas exchange parameters. Plant, Cell Environ **36**: 920–935

Gao Y, Lynch JP (2016) Reduced crown root number improves water acquisition under water deficit stress in maize (Zea mays L.). J Exp Bot **67**: 4545–4557

Goss RJ, Russell RS (1980) Effects of Mechanical Impedance on Root Growth in Barley (Hordeum vulgare L .). J Exp Bot **31**: 577–588

Greacen EL, Farrell DA, Cockroft B (1968) Soil resistance to metal probes and plant roots. ransactions 9th Congr Int Soc Soil Sci 769–779.

Grieder C, Trachsel S, Hund A (2014) Early vertical distribution of roots and its association with drought tolerance in tropical maize. Plant Soil **377**: 295–308

Grift TE, Novais J, Bohn M (2011) High-throughput phenotyping technology for maize roots.
Biosyst Eng **110**: 40–48

Grzesiak MT, Ostrowska A, Hura K, Rut G, Janowiak F, Rzepka A, Hura T, Grzesiak S (2014)
Interspecific differences in root architecture among maize and triticale genotypes grown under
drought, waterlogging and soil compaction. Acta Physiol Plant **36**: 3249–3261

Grzesiak S, Grzesiak MT, Hura T, Marcińska I, Rzepka A (2013) Changes in root system
structure, leaf water potential and gas exchange of maize and triticale seedlings affected by soil
compaction. Environ Exp Bot **88**: 2–10

Guilmour AR, Gogel BJ, Cullis BR, Thompson R (2009) ASReml User Guide Release 3.0. VSN
Int. Ltd, Hemel Hempstead, HP1 1ES, UK

Hakansson I, Reeder RC (1994) Subsoil compaction by vehicles with high axle load extent ,
persistence and crop response. Soil &Tillage Res **29**: 277–304

Hamza M a., Anderson WK (2005) Soil compaction in cropping systems. Soil Tillage Res **82**: 121–
145

Han E, Kautz T, Perkons U, Uteau D (2015) Root growth dynamics inside and outside of soil
biopores as affected by crop sequence determined with the profile wall method. Biol Fertil … **51**:
847–856

Hargreaves C, Gregory P, Bengough A (2009) Measuring root traits in barley (Hordeum vulgare
ssp. vulgare and ssp. spontaneum) seedlings using gel chambers, soil sacs and X-ray
microtomography. Plant Soil **316**: 285–297

**Hernandez-Ramirez G, Lawrence-Smith EJ, Sinton SM, Tabley F, Schwen A, Beare MH, Brown
HE** (2014) Root Responses to Alterations in Macroporosity and Penetrability in a Silt Loam Soil.
Soil Sci Soc Am J **78**: 1392–1403

Hutchings LM (1992) Triblology. Edward Arnold, London UK

Iijima M, Barlow PW, Bengough AG (2003a) Root cap structure and cell production rates of maize
(Zea mays) roots in compacted sand. New Phytol **160**: 127–134

Iijima M, Higuchi T, Barlow PW, Bengough AG (2003b) Root cap removal increases root penetration resistance in maize (Zea mays L.). J Exp Bot **54**: 2105–2109

Iijima M, Kato J (2007) Combined Soil Physical Stress of Soil Drying , Anaerobiosis and Mechanical Impedance to Seedling Root Growth of Four Crop Species. Plant Prod Sci **10**: 451–459

Iyer-Pascuzzi AS, Symonova O, Mileyko Y, Hao Y, Belcher H, Harer J, Weitz JS, Benfey PN (2010) Imaging and analysis platform for automatic phenotyping and trait ranking of plant root systems. Plant Physiol **152**: 1148–1157

Jabro JD, Iversen WM, Evans RG, Allen BL, Stevens WB (2014) Repeated Freeze-Thaw Cycle Effects on Soil Compaction in a Clay Loam in Northeastern Montana. Soil Sci Soc Am J **78**: 737

Jähne B (2002) Digital Image Processing 5th revised and extended edition, 5th ed. doi: 10.1007/3-540-27563-0

Jin K, Shen J, Ashton RW, Dodd IC, Parry M a J, Whalley WR (2013) How do roots elongate in a structured soil? J Exp Bot **64**: 4761–77

Kaiser J (2004) Wounding Earth's Fragile Skin. Science (80-) **304**: 1616–1618

Kautz T, Amelung W, Ewert F, Gaiser T, Horn R, Jahn R, Javaux M, Kemna A, Kuzyakov Y, Munch J, et al (2013a) Nutrient acquisition from arable subsoils in temperate climates : A review. Soil Biol Biochem **57**: 1003–1022

Kautz T, Perkons U, Athmann M, Pude R, Köpke U (2013b) Barley roots are not constrained to large-sized biopores in the subsoil of a deep Haplic Luvisol. Biol Fertil Soils **49**: 959–963

Kirby JM, Bengough AG (2002) Influence of soil strength on root growth: Experiments and analysis using a critical-state model. Eur J Soil Sci **53**: 119–127

Krzic M, Fortin M-C, Bomke AA (2000) Short-term responses of soil physical properties to corn tillage-planting systems in a humid maritime climate. Soil Tillage Res **54**: 171–178

Kubo K, Iwama K, Yanagisawa A, Watanabe Y, Terauchi T, Jitsuyama Y, Mikuma T (2006) Genotypic variation of the ability of root to penetrate hard soil layers among Japanese wheat cultivars. Plant Prod Sci **9**: 47–55

Kubo K, Jitsuyama Y, Iwama K, Hasegawa T, Watanabe N (2004) Genotypic difference in root penetration ability by durum wheat (Triticum turgidum L. var. durum) evaluated by a pot with paraffin-Vaseline discs. Plant Soil **262**: 169–177

Kuncoro PH, Koga K, Satta N, Muto Y (2014a) A study on the effect of compaction on transport properties of soil gas and water. II: Soil pore structure indices. Soil Tillage Res **143**: 180–187

Kuncoro PH, Koga K, Satta N, Muto Y (2014b) A study on the effect of compaction on transport properties of soil gas and water I: Relative gas diffusivity, air permeability, and saturated hydraulic conductivity. Soil Tillage Res **143**: 172–179

Kutscherea L, Lichtenegger E (1960) Wurzelatlas mitteleuropäischer Ackerunkräuter und Kulturpflanzen. DLG-Verlag, Frankfurt am Main

de la Luz Mora M, Rosas A, Ribera A, Rengel Z (2009) Differential tolerance to Mn toxicity in perennial ryegrass genotypes: Involvement of antioxidative enzymes and root exudation of carboxylates. Plant Soil **320**: 79–89

Lemming C, Oberson A, Hund A, Jensen LS, Magid J (2016) Opportunity costs for maize associated with localised application of sewage sludge derived fertilisers, as indicated by early root and phosphorus uptake responses. Plant Soil **406**: 201–217

Lesturgez G, Poss R, Hartmann C, Bourdon E, Noble A, Development L (2004) Roots of Stylosanthes hamata create macropores in the compact layer of a sandy soil. Plant Soil **260**: 101–109

Li R, Zeng Y, Xu J, Wang Q, Wu F, Cao M, Lan H, Liu Y, Lu Y (2015) Genetic variation for maize root architecture in response to drought stress at the seedling stage. Breed Sci **65**: 298–307

Li XF, Ma JF, Matsumoto H (2000) Pattern of aluminum-induced secretion of organic acids differs between rye and wheat. Plant Physiol **123**: 1537–1544

Lipiec J, Hatano R (2003) Quantification of compaction effects on soil physical properties and crop growth. Geoderma **116**: 107–136

Lipiec J, Horn R, Pietrusiewicz J, Siczek A (2012) Effects of soil compaction on root elongation and anatomy of different cereal plant species. Soil Tillage Res **121**: 74–81

Lynch JP (2013) Steep, cheap and deep: an ideotype to optimize water and N acquisition by maize root systems. Ann Bot **112**: 347–357

Lynch JP (1995) Root architecture and plant productivity. Plant Physiol **109**: 7–13

Lynch JP (2015) Root phenes that reduce the metabolic costs of soil exploration: Opportunities for 21st century agriculture. Plant, Cell Environ **38**: 1775–1784

Mairhofer S, Sturrock CJ, Bennett MJ, Mooney SJ, Pridmore TP (2015) Extracting Multiple Interacting Root Systems using X-ray Micro Computed Tomography. Plant J n/a-n/a

Mairhofer S, Zappala S, Tracy S (2013) Recovering complete plant root system architectures from soil via X-ray μ-Computed Tomography. Plant Methods **9**: 1–7

Mairhofer S, Zappala S, Tracy S (2012) RooTrak: Automated recovery of three-dimensional plant root architecture in soil from x-ray microcomputed tomography images using visual tracking. Plant Physiol **158**: 561–569

Marashi SK, Mojaddam M (2014) Adventitious root and aerenchyma development in wheat (Triticum aestivum L .) subjected to waterlogging. Int J Biosci **6655**: 168–173

Le Marié C, Kirchgessner N, Flütsch P, Pfeifer J, Walter A, Hund A, Hund A, Ruta N, Liedgens M, Watt M, et al (2016) RADIX: rhizoslide platform allowing high throughput digital image analysis of root system expansion. Plant Methods **12**: 40

Le Marié C, Kirchgessner N, Marschall D, Walter A, Hund A (2014) Rhizoslides: paper-based growth system for non-destructive, high throughput phenotyping of root development by means of image analysis. Plant Methods **10**: 13

Martínez I, Chervet A, Weisskopf P, Sturny WG, Etana A, Stettler M, Forkman J, Keller T (2016a) Two decades of no-till in the Oberacker long-term fi eld experiment : Part I . Crop yield , soil organic carbon and nutrient distribution in the soil profile. Soil Tillage Res **163**: 141–151

Martínez I, Chervet A, Weisskopf P, Sturny WG, Rek J, Keller T (2016b) Two decades of no-till in the Oberacker long-term field experiment: Part II. Soil porosity and gas transport parameters. Soil Tillage Res **163**: 130–140

Masle J, Passioura J (1987) The effect of soil strength on the growth of young wheat plants. Aust J Plant Physiol 643–656

Masuka B, Araus JL, Das B, Sonder K, Cairns JE (2012) Phenotyping for abiotic stress tolerance in maize. J Integr Plant Biol **54**: 238–49

Materechera SA, Alston AM, Kirby JM, Dexter AR (1992) Influence of root diameter on the penetration of seminal roots into a compacted subsoil. Plant Soil **144**: 297–303

McKenzie BM, Bengough AG, Hallett PD, Thomas WTB, Forster B, McNicol JW (2009) Deep rooting and drought screening of cereal crops: A novel field-based method and its application. F Crop Res **112**: 165–171

McKenzie BM, Mullins CE, Tisdall JM, Bengough AG (2013) Root-soil friction: Quantification provides evidence for measurable benefits for manipulation of root-tip traits. Plant, Cell Environ **36**: 1085–1092

McNeill JR (2004) Breaking the Sod: Humankind, History, and Soil. Science (80-) **304**: 1627–1629

Metzner R, van Dusschoten D, Bühler J, Schurr U, Jahnke S (2014) Belowground plant development measured with magnetic resonance imaging (MRI): exploiting the potential for non-invasive trait quantification using sugar beet as a proxy. Front Plant Sci. doi: 10.3389/fpls.2014.00469

Metzner R, Eggert A, van Dusschoten D, Pflugfelder D, Gerth S, Schurr U, Uhlmann N, Jahnke S (2015) Direct comparison of MRI and X-ray CT technologies for 3D imaging of root systems in soil: potential and challenges for root trait quantification. Plant Methods **11**: 17

Miguel MA, Widrig A, Vieira RF, Brown KM, Lynch JP (2013) Basal root whorl number: A modulator of phosphorus acquisition in common bean (Phaseolus vulgaris). Ann Bot **112**: 973–982

Misra RK, Dexter AR, Alston AM (1986) Maximum axial and radial growth pressures of plant roots. Plant Soil **326**: 315–326

Mitchell T (2008) Contour Dynamics Simulation of Kirchhoff Elliptical Vortex. https://ch.mathworks.com/matlabcentral/fileexchange/19306-kirchhoff-vortex-contour-dynamics- simulation

Montagu KD, Conroy JP, Atwell BJ (2001) The position of localized soil compaction determines root and subsequent shoot growth responses. J Exp Bot **52**: 2127–33

Nagel KA, Bonnett D, Furbank R, Walter A, Schurr U, Watt M (2015) Simultaneous effects of leaf irradiance and soil moisture on growth and root system architecture of novel wheat genotypes: Implications for phenotyping. J Exp Bot **66**: 5441–5452

Nagel KA, Putz A, Gilmer F, Heinz K, Fischbach A, Pfeifer J, Faget M, Blossfeld S, Ernst M, Dimaki C, et al (2012) GROWSCREEN-Rhizo is a novel phenotyping robot enabling simultaneous measurements of root and shoot growth for plants grown in soil-filled rhizotrons. Funct Plant Biol **39**: 891–904

Nakamoto T (1997) The Distribution of Maize Roots as Influenced by Artificial Vertical Macropores. Japanese J Crop Sci **66**: 331–332

Nosalewicz A, Lipiec J (2014) The effect of compacted soil layers on vertical root distribution and water uptake by wheat. Plant Soil **375**: 229–240

Otsu N (1979) A threshold selection method from gray-level histogrmas. IEEE Trans Syst Man Cybern **9**: 62–6

Ozcoban MS, Cetinkaya N, Celik SO, Demirkol GT, Cansiz V, Tufekci N (2013) Hydraulic conductivity and removal rate of compacted clays permeated with landfill leachate. Desalin Water Treat **51**: 6148–6157

Passioura JB (2002) Soil conditions and plant growth. Plant, Cell Environ **25**: 311–318

Passioura JB (2012) Phenotyping for drought tolerance in grain crops: when is it useful to breeders? Funct Plant Biol **39**: 851–859

Passot S, Gnacko F, Moukouanga D, Lucas M, Guyomarc'h S, Ortega BM, Atkinson JA, Belko MN, Bennett MJ, Gantet P, et al (2016) Characterization of Pearl Millet Root Architecture and Anatomy Reveals Three Types of Lateral Roots. Front Plant Sci. doi: 10.3389/fpls.2016.00829

Pellet DM, Grunes DL, Kochian L V. (1995) Organic acid exudation as an aluminum-tolerance mechanism in maize (Zea mays L.). Planta An Int J Plant Biol **196**: 788–795

Perkons U, Kautz T, Uteau D, Peth S, Geier V, Thomas K, Holz KL, Athmann M, Pude R, Kopke U (2014) Root-length densities of various annual crops following crops with contrasting root systems. Soil Tillage Res **137**: 50–57

Pfeifer J, Faget M, Walter A, Blossfeld S, Fiorani F, Schurr U, Nagel K a. (2014a) Spring barley shows dynamic compensatory root and shoot growth responses when exposed to localised soil compaction and fertilisation. Funct Plant Biol **41**: 581–597

Pfeifer J, Kirchgessner N, Colombi T, Walter A (2015) Rapid phenotyping of crop root systems in undisturbed field soils using X-ray computed tomography. Plant Methods **11**: 41

Pfeifer J, Kirchgessner N, Walter A (2014b) Artificial pores attract barley roots and can reduce artifacts of pot experiments. J Plant Nutr Soil Sci **177**: 903–913

Porterfield DM, Musgrave ME (1998) The tropic response of plant roots to oxygen: Oxytropism in Pisum sativum L. Planta **206**: 1–6

R Core Team (2015) R: A Language and Environment for Statistical Computing.

Rahaman MM, Chen D, Gillani Z, Klukas C, Chen M (2015) Advanced phenotyping and phenotype data analysis for the study of plant growth and development. Front Plant Sci **6**: 619

Ramos JC, Del S, Imhoff C, Pilatti MÁ, Carlos A (2010) Morphological characteristics of soybean root apexes as indicators of soil compaction. Sci Agric **67**: 707–712

Rasse DP, Smucker AJM (1998) Root recolonization of previous root channels in corn and alfalfa rotations. Plant Soil **204**: 203–212

Richard CA, Hickey LT, Fletcher S, Jennings R, Chenu K, Christopher JT (2015) High-throughput phenotyping of seminal root traits in wheat. Plant Methods **11**: 13

Ruiz S, Or D, Schymanski SJ (2015) Soil Penetration by Earthworms and Plant Roots-Mechanical Energetics of Bioturbation of Compacted Soils. PLoS One **10**: e0128914

Ruiz S, Straub I, Schymanski SJ, Or D (2016) Experimental Evaluation of Earthworm and Plant Root Soil Penetration–Cavity Expansion Models Using Cone Penetrometer Analogs. Vadose Zo J. doi: 10.2136/vzj2015.09.0126

Saengwilai P, Nord E a, Chimungu JG, Brown KM, Lynch JP (2014a) Root cortical aerenchyma enhances nitrogen acquisition from low-nitrogen soils in maize. Plant Physiol **166**: 726–35

Saengwilai P, Tian X, Lynch JP (2014b) Low Crown Root Number Enhances Nitrogen Acquisition from Low-Nitrogen Soils in Maize. Plant Physiol **166**: 581–589

Saglio P, Raymond P, Pradet A (1983) Oxygen Transport and Root Respiration of Maize Seedlings. Plant Physiol **72**: 1035–1039

Schäffer B, Mueller TL, Stauber M, Müller R, Keller M, Schulin R (2008a) Soil and macro-pores under uniaxial compression. II. Morphometric analysis of macro-pore stability in undisturbed and repacked soil. Geoderma **146**: 175–182

Schäffer B, Stauber M, Mueller TL, Müller R, Schulin R (2008b) Soil and macro-pores under uniaxial compression. I. Mechanical stability of repacked soil and deformation of different types of macro-pores. Geoderma **146**: 183–191

Schjonning P, Rasmussen KJ (2000) Soil strength and soil pore characteristics for direct drilled and ploughed soils. Soil Tillage Res **57**: 69–82

Scholl P, Leitner D, Kammerer G, Loiskandl W, Kaul H-P, Bodner G (2014) Root induced changes of effective 1D hydraulic properties in a soil column. Plant Soil **381**: 193–213

Semchenko M, Zobel K, Heinemeyer A, Hutchings MJ (2008) Foraging for space and avoidance of physical obstructions by plant roots: A comparative study of grasses from contrasting habitats. New Phytol **179**: 1162–1170

Shimamura S, Mochizuki T, Nada Y, Fukuyama M (2003) Formation and function of secondary aerenchyma in hypocotyl , roots and nodules of soybean (Glycine max) under flooded conditions. Plant Soil **251**: 351–359

Siczek A, Lipiec J (2011) Soybean nodulation and nitrogen fixation in response to soil compaction and surface straw mulching. Soil Tillage Res **114**: 50–56

Siczek A, Lipiec J, Wielbo J, Szarlip P, Kidaj D (2013) Pea growth and symbiotic activity response to Nod factors (lipo-chitooligosaccharides) and soil compaction. Appl Soil Ecol **72**: 181–186

Simojoki A, Fazekas-becker O, Horn R (2008) Macro- and microscale gaseous diffusion in a Stagnic Luvisol as affected by compaction and reduced tillage. Agric Food Sci **17**: 252–264

Stirzaker RJ, Passioura JB, Wilms Y (1996) Soil structure and plant growth: Impact of bulk density and biopores. Plant Soil **185**: 151–162

Striker GG, Insausti P, Grimoldi AA, Vega AS (2007) Trade-off between root porosity and mechanical strength in species with different types of aerenchyma. Plant Cell Environ **30**: 580–589

Suzuki LEAS, Reichert JM, Reinert DJ (2013) Degree of compactness, soil physical properties and yield of soybean in six soils under no-tillage. Soil Res **51**: 311–321

Takahashi H, Yamauchi T, Colmer TD (2014) Low-Oxygen Stress in Plants. *In* JT van Dongen, F Licausi, eds, Low-Oxygen Stress Plants. Springer Vienna, Vienna, pp 247–265

Thomas A, Guerreiro SMC, Sodek L (2005) Aerenchyma formation and recovery from hypoxia of the flooded root system of nodulated soybean. Ann Bot **96**: 1191–8

Thomas CL, Graham NS, Hayden R, Meacham MC, Neugebauer K, Nightingale M (2016) High-throughput phenotyping (HTP) identifies seedling root traits linked to variation in seed yield and nutrient capture in field-grown oilseed rape (Brassica napus L .). Ann Bot **118**: 2–11

Thomson CJ, Colmer TD, Watkin ELJ, Greenway H (1992) Tolerance of wheat (Triticum aestivum cvs . Gamenya and Kite) and triticale (Triticosecale cv . Muir) to waterlogging. New Phytol **120**: 335–344

Trachsel S, Kaeppler SM, Brown KM, Lynch JP (2013) Maize root growth angles become steeper under low N conditions. F Crop Res **140**: 18–31

Trachsel S, Kaeppler SM, Brown KM, Lynch JP (2011) Shovelomics: high throughput phenotyping of maize (Zea mays L.) root architecture in the field. Plant Soil **341**: 75–87

Tracy SR, Black CR, Roberts J a., McNeill A, Davidson R, Tester M, Samec M, Korošak D, Sturrock C, Mooney SJ (2012a) Quantifying the effect of soil compaction on three varieties of wheat (Triticum aestivum L.) using X-ray Micro Computed Tomography (CT). Plant Soil **353**: 195–208

Tracy SR, Black CR, Roberts J a, Sturrock C, Mairhofer S, Craigon J, Mooney SJ (2012b) Quantifying the impact of soil compaction on root system architecture in tomato (Solanum lycopersicum) by X-ray micro-computed tomography. Ann Bot **110**: 511–9

Tracy SR, Black CR, Roberts JA, Mooney SJ (2013) Exploring the interacting effect of soil texture and bulk density on root system development in tomato (Solanum lycopersicum L.). Environ Exp Bot **91**: 38–47

Tracy SR, Black CR, Roberts JA, Mooney SJ (2011) Soil compaction: a review of past and present techniques for investigating effects on root growth. J Sci Food Agric **91**: 1528–37

Tubeileh A, Groleau-Renaud V, Plantureux S, Guckert A (2003) Effect of soil compaction on photosynthesis and carbon partitioning within a maize–soil system. Soil Tillage Res **71**: 151–161

Valentine TA, Hallett PD, Binnie K, Young MW, Squire GR, Hawes C, Bengough GA (2012) Soil strength and macropore volume limit root elongation rates in many UK agricultural soils. Ann Bot **110**: 259–70

Varney GT, Canny MJ (1993) Rates of water uptake into the mature root system of maize plants. New Phytol **123**: 775–786

Vollsnes A V., Futsaether CM, Bengough AG (2010) Quantifying rhizosphere particle movement around mutant maize roots using time-lapse imaging and particle image velocimetry. Eur J Soil Sci **61**: 926–939

Wall DH, Six J (2015) Give soils their due. Science (80-) **347**: 695

Walter A, Liebisch F, Hund A (2015) Plant phenotyping: from bean weighing to image analysis. Plant Methods **11**: 14

Walter A, Silk WK, Schurr U (2009) Environmental effects on spatial and temporal patterns of leaf and root growth. Annu Rev Plant Biol **60**: 279–304

Walter A, Studer B, Kölliker R (2012) Advanced phenotyping offers opportunities for improved breeding of forage and turf species. Ann Bot **110**: 1271–1279

Wang X, Zhou B, Sun X, Yue Y, Ma W, Zhao M (2015) Soil Tillage Management Affects Maize Grain Yield by Regulating Spatial Distribution Coordination of Roots, Soil Moisture and Nitrogen Status. PLoS One **10**: 1–19

Watkin EL, Thomson CJ, Greenway H (1998) Root Development and Aerenchyma Formation in Two Wheat Cultivars and One Triticale Cultivar Grown in Stagnant Agar and Aerated Nutrient Solution. Ann Bot **81**: 349–354

Weaver JE (1925) Investigations on The Root Habits of Plants. Am J Bot **12**: 502–509

Weaver J.E., Kramer J, Reed M (1924) Development of Root and Shoot of Winter Wheat Under Field Environment. Ecology **5**: 26–50

White PJ, George TS, Gregory PJ, Bengough a G, Hallett PD, McKenzie BM (2013) Matching roots to their environment. Ann Bot **112**: 207–22

White RG, Kirkegaard JA (2010) The distribution and abundance of wheat roots in a dense, structured subsoil – implications for water uptake. Plant Cell Environ **33**: 133–148

Wilcox JR, Farmer RE (1968) Heritability and C effects in early root growth of eastern cottonwood cuttings. Heredity (Edinb) **23**: 239–245

Wu J, Pagès L, Wu Q, Yang B, Guo Y (2014) Three-dimensional architecture of axile roots of field-grown maize. Plant Soil **387**: 363–377

Xu QT, Yang L, Zhou ZQ, Mei FZ, Qu LH, Zhou GS (2013) Process of aerenchyma formation and reactive oxygen species induced by waterlogging in wheat seminal roots. Planta **238**: 969–82

Yamauchi T, Abe F, Kawaguchi K, Oyanagi A, Nakazono M (2014) Adventitious roots of wheat seedlings that emerge in oxygen-deficient conditions have increased root diameters with highly developed lysigenous aerenchyma. Plant Signal Behav **9**: e28506

Yamauchi T, Shimamura S, Nakazono M, Mochizuki T (2013) Aerenchyma formation in crop species: A review. F Crop Res **152**: 8–16

York LM, Galindo-Castaneda T, Schussler JR, Lynch JP (2015) Evolution of US maize (Zea mays L.) root architectural and anatomical phenes over the past 100 years corresponds to increased tolerance of nitrogen stress. J Exp Bot **66**: 2347–2358

York LM, Nord E a, Lynch JP (2013) Integration of root phenes for soil resource acquisition. Front Plant Sci **4**: 1–15

Young IM, Montagu K, Conroy J, Bengough AG (1997) Mechanical impedance of root growth directly reduces leaf elongation rates of cereals. New Phytol **135**: 613–619

in 't Zandt D, Le Marie C, Kirchgessner N, Visser EJW, Hund a. (2015) High-resolution quantification of root dynamics in split-nutrient rhizoslides reveals rapid and strong proliferation of maize roots in response to local high nitrogen. J Exp Bot. doi: 10.1093/jxb/erv307

Zhan A, Lynch JP (2015) Reduced frequency of lateral root branching improves N capture from low-N soils in maize. J Exp Bot **66**: 2055–2065

Zhan A, Schneider H, Lynch JP (2015) Reduced Lateral Root Branching Density Improves Drought Tolerance in Maize. Plant Physiol **168**: 1603–1615

Zhong D, Novais J, Grift TE, Bohn M, Han J (2009) Maize root complexity analysis using a Support Vector Machine method. Comput Electron Agric **69**: 46–50

Zhu J, Ingram P a, Benfey PN, Elich T (2011) From lab to field, new approaches to phenotyping

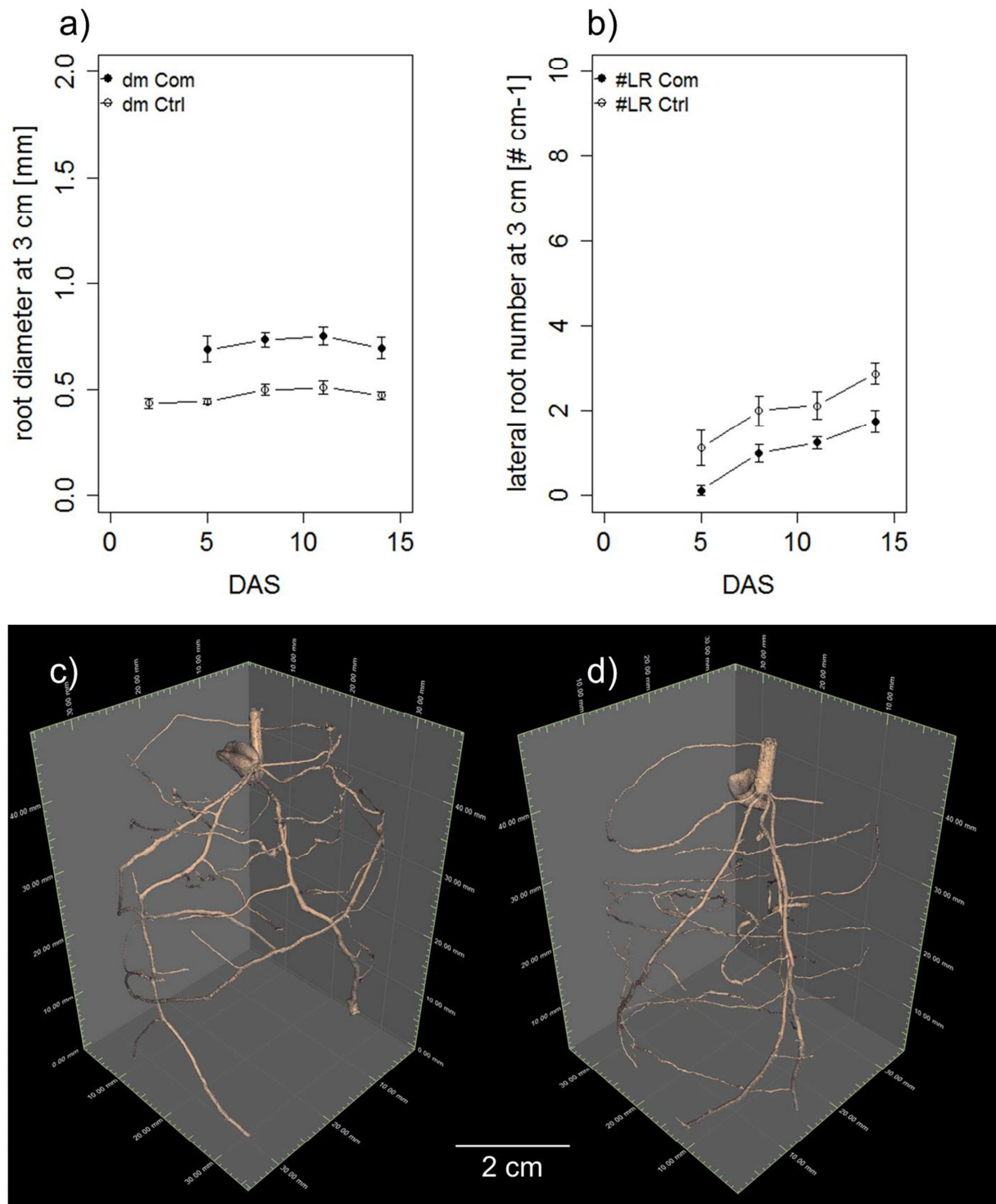root system architecture. Curr Opin Plant Biol **14**: 310–317

8. Supporting Information

8.1. Supporting Information: General introduction

Supporting Information Table S1.1: Chapter overview with experimental scales, used plant material, plant phenotypic and physical quantifications.

Chapter	Experimental scale	Plant material	Root phenotyping	Shoot phenotyping	Soil physical quantifications
2	Field Soil columns	Triticale (× *Triticosecale*) Soybean (*Glycine max* L.) Winter wheat (*Triticum aestivum* L.)	Root system architecture Root system development Root morphology Rooting depth Root anatomy Root dry biomass	Shoot dry biomass Leaf area index Leaf greenness (SPAD)	Soil bulk density Soil mechanical impedance
3	Soil columns	14 varieties of winter wheat (*Triticum aestivum* L.)	Root tip geometry Root morphology Root growth Root anatomy		Soil bulk density Soil mechanical impedance Root tip axial forces Root tip penetration stress
4	Soil columns	14 varieties of winter wheat (*Triticum aestivum* L.)	Root system architecture Root system development Root dry biomass	Shoot development Shoot dry biomass	Soil bulk density Soil mechanical impedance
5	Field Soil columns	Soybean (*Glycine max* L.) Winter wheat (*Triticum aestivum* L.) Maize (*Zea mays* L.)	Root soil interactions Root dry biomass Preferential root growth	Leaf area per leaf level Shoot dry biomass	Soil bulk density Soil mechanical impedance Air permeability Gas diffusivity

8.2. Supporting information: Chapter 2

Supporting Information Figure S2.1: a) Root diameters (dm) of wheat seminal roots and b) lateral root number (#LR) at wheat seminal roots grown under compacted (Com) and loosely (Ctrl) packed soil and measured 2, 5, 8, 11 and 14 days after sowing (DAS). Error bars represent standard errors (n = 4). Typical pictures of triticale roots from c) Com and d) Ctrl.

Supporting Information Table S2.1: Treatment means of root architectural traits 42 and 91 DAS from field-grown triticale under topsoil compaction (TSCom), subsoil compaction (SSCom) and without compaction (Ctrl) and field-grown soybean on compacted soil with shallow tillage (Com) and without compaction (Ctrl); different letters indicate significant differences of the means based on ANOVA with least significant test at $p < 0.05$ (n = 3).

|			Triticale						Soybean		
DAS	**Trait**	**Root**	**Distance from root base [cm]**	**TSCom**	**SSCom**	**Ctrl**	**Trait**	**Root**	**Distance from root base [cm]**	**Com**	**Ctrl**
42	Diameter [mm]	NR_{No1}	10	NA	NA	NA	Diameter [mm]	TR	10	0.720^a	1.478^b
								AR	10	0.613	0.531
	Number of LR [# cm^{-1}]	NR_{No1}	9-11	NA	NA	NA	Number of LR [# cm^{-1}]	TR	9-11	3.667	5.333
								AR	9-11	4.583	3.583
91	Diameter [mm]	NR_{No1}	10	0.715^a	0.631^a	0.517^b	Diameter [mm]	TR	10	0.935^a	2.225^b
		NR_{No3}	5	NA	0.873^a	0.612^b		AR	10	0.906	0.966
			10	NA	0.555	0.485					
	Number of LR [# cm^{-1}]	NR_{No1}	9-11	2.069^a	2.583^a	4.069^b	Number of LR [# cm^{-1}]	TR	9-11	3.444^a	6.167^b
								AR	9-11	5.167	4.625

Abbreviations: NR_{No1} = nodal root from the first whorl, NR_{No3} = nodal root from the third whorl, TR = taproot, AR = adventitious root, LR = lateral root

Supporting Information Table S2.2: Treatment means of root architectural and anatomical traits and plant vigour traits 14 days after sowing of winter wheat grown under controlled conditions in compacted (Com) and loose soil (Ctrl). Different letters indicate significant differences of the means based on ANOVA with least significant test at $p < 0.05$ (n = 4). Abbreviations cf. Table 2.1.

Trait	Root	Distance from root base [cm]	Com	Ctrl
Number of NR	NR		0.5	0
Diameter [mm]	PR	3	0.68	0.478
Diameter [mm]	SR	3	0.698[a]	0.472[b]
Number of LR [# cm-1]	PR	4-6	1.00	2.75
Number of LR [# cm-1]	SR	4-6	1.750[a]	2.875[b]
ArV [mm2]	PR	3	0.0421	0.0441
ArC [mm2]	PR	3	0.241	0.168
ArCP [%]	PR	3	84.92	73.59
ArC/ArV	PR	3	5.859	4.059
RCA [%]	PR	3	21.530[a]	6.397[b]
Shoot DW [g]			0.0284[a]	0.0531[b]
Root DW [g]			0.0226	0.0246
Root-shoot ratio			0.873	0.464
SPAD			38.05	43.55

Abbreviations: NR = nodal root, PR = primary root, LR =lateral root, DW = dry weight

8.3. Supporting information: Chapter 3
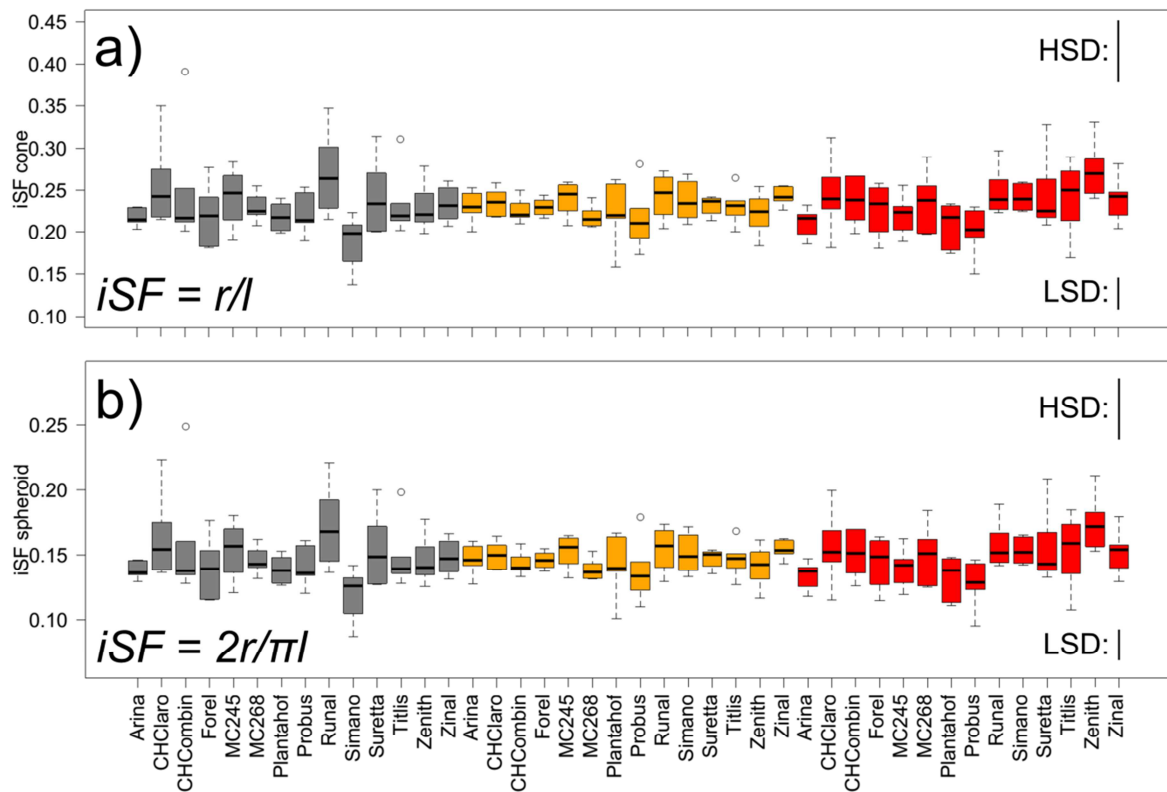
Supporting Information Figure S3.1: Diversity of root tip shape determined in 14 wheat genotypes under low (1.3 g cm^{-3}, grey), moderate (1.45 g cm^{-3}, orange) and high (1.6 g cm^{-3}, red) soil bulk density (n = 6). Root tip shape is expressed as the inverse of shape factor (iSF) of a) a cone and b) a spheroid, using root tip radius (r) and length (l). Vertical bars represent least and honest significant difference (LSD and HSD, respectively) at p < 0.05.
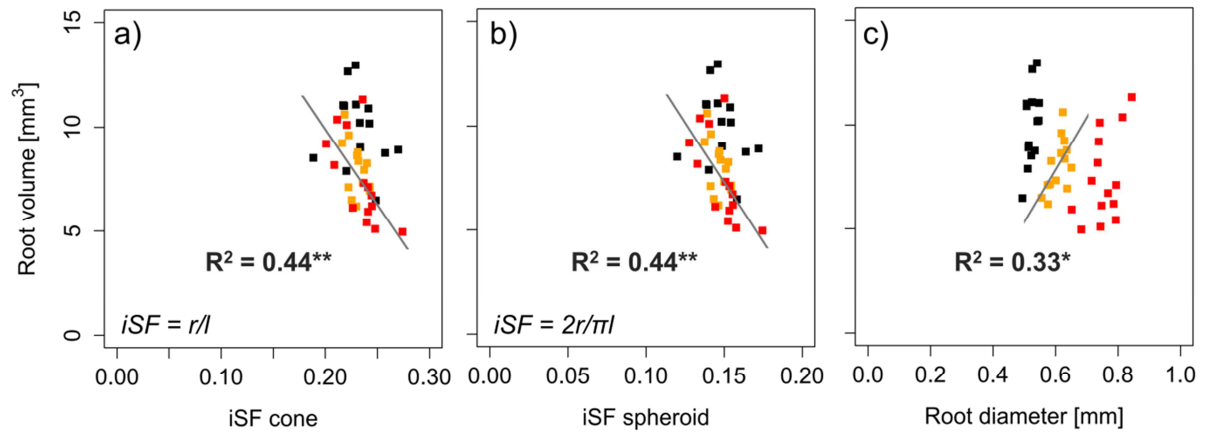
Supporting Information Figure S3.2: Influence of root tip geometry and root diameter on root volume after 48 h of growth determined in 14 wheat genotypes (n = 6). Linear regressions between root volume and inverse shape factor (iSF; calculated using root tip radius (r) and length (l)) of a) a cone and b) a spheroid geometry and c) root diameter. Black, orange and red represent soil bulk density of 1.3 g cm^{-3}, 1.45 g cm^{-3} and 1.6 g cm^{-3}, respectively. R^2 represents multiple r-squared, * and **denotes significant regression at $p < 0.05$ and $p < 0.01$, respectively.
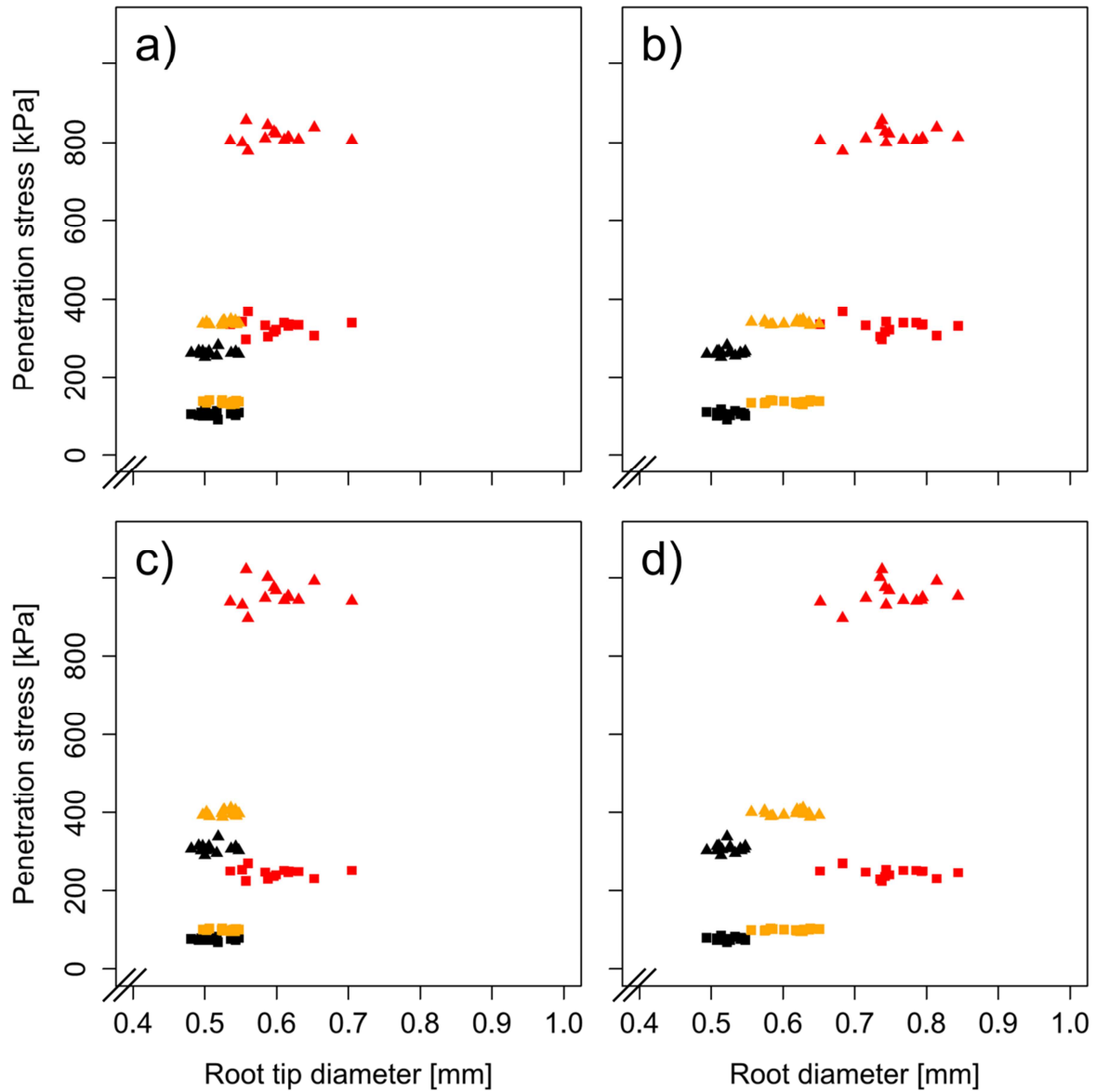
Supporting Information Figure S3.3: Relationship between estimated root tip penetration stresses and a) and c) root tip diameter and b) and d) average root diameter measured at three positions along the root in fourteen wheat varieties (n = 6); Penetration stresses were calculated excluding (triangles) or including (square Eq 3.11 and Eq 3.12) geometrical conversion factors assuming a) and b) cone and c) and d) spheroid tip shape. Colours denote soil bulk densities of 1.3 g cm^{-3} (black), 1.45 g cm^{-3} (orange) and 1.6 g cm^{-3}.
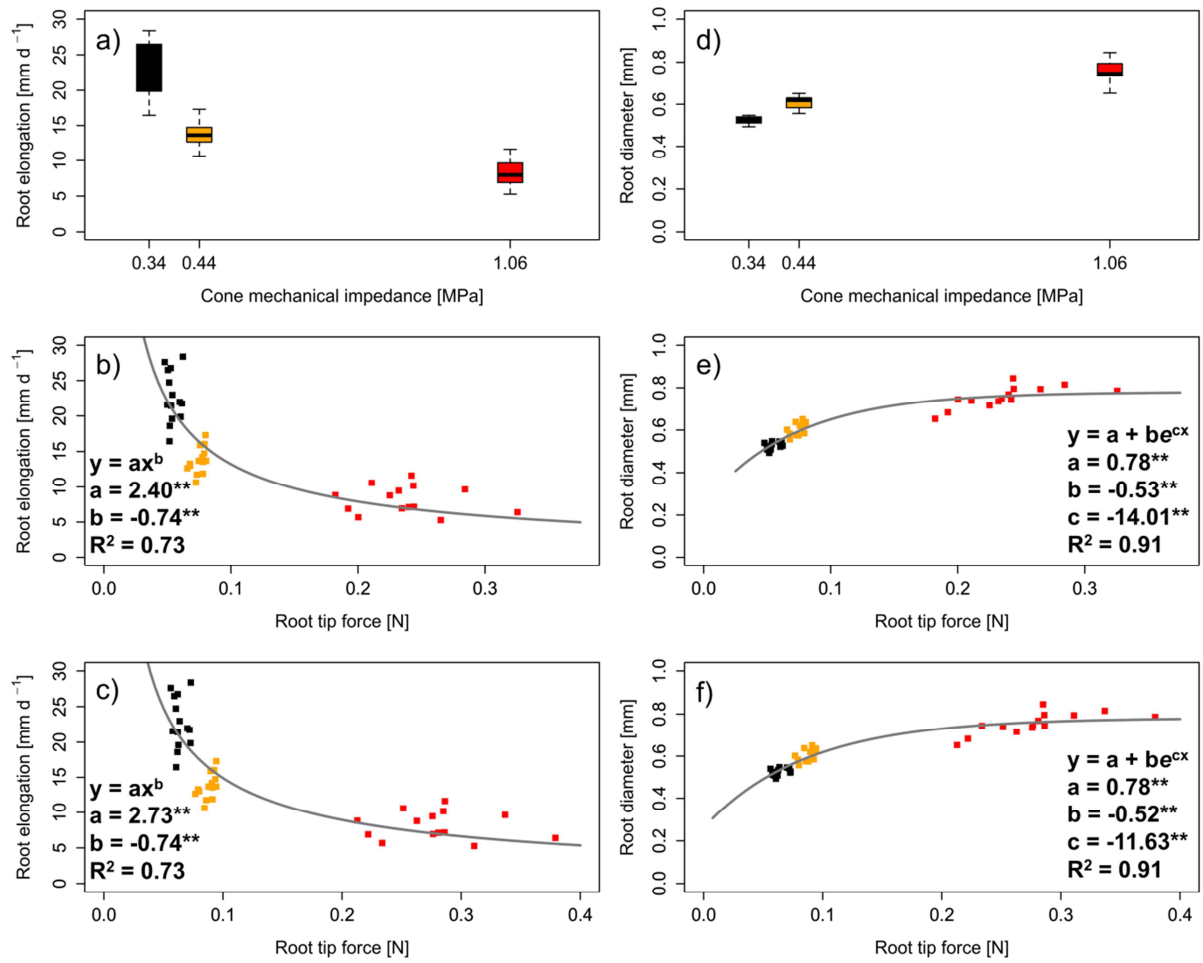
Supporting Information Figure S3.4: Root a), b), c) elongation rate and d), e), f) diameter of 14 wheat genotypes (n = 6) grown at a soil bulk densities of 1.3 g cm^{-3} (black), 1.45 g cm^{-3} (orange) and 1.6 g cm^{-3} (red). a) and d) Cone mechanical impedance was obtained from penetrometer measurements, root tip radial force for b) and e) conical and c) and f) spheroid geometry calculated according to Eq 3.6 and Eq 3.8, respectively. R^2 represents multiple r-squared, ** denotes significant regression coefficients at $p < 0.01$.

Supporting Information Table S3.1: Winter wheat varieties of Swiss origin used in the study ordered according to the year of market release.

Variety name	Year of release
Plantahof	1910
Mont-Calme 245	1926
Mont-Calme 268	1926
Probus	1948
Zenith	1969
Arina	1981
Runal	1995
Titlis	1996
Zinal	2003
CH-Claro	2007
Forel	2007
CH-Combin	2008
Suretta	2009
Simano	2010

Supporting Information Table S3.2: Inverse shape factors for root tip shape (iSF) and resulting geometry factors (GF) used to account for different geometries of cone penetrometer and roots (Eq 3.11 and Eq 3.12 for cone and spheroid root tip shape, respectively). Values represent genotype mean values (n = 6) under bulk densities of 1.3 g cm^{-3}, 1.45 g cm^{-3} and 1.6 g cm^{-3}.

	iSF_{cone}			GF_{cone}			$iSF_{spheroid}$			$GF_{spheroid}$		
Variety	**1.3**	**1.45**	**1.6**	**1.3**	**1.45**	**1.6**	**1.3**	**1.45**	**1.6**	**1.3**	**1.45**	**1.6**
Arina	0.217	0.230	0.211	0.376	0.399	0.366	0.138	0.147	0.135	0.240	0.254	0.233
CHClaro	0.257	0.236	0.244	0.446	0.408	0.423	0.164	0.150	0.156	0.284	0.260	0.269
CHCombin	0.248	0.225	0.237	0.430	0.390	0.411	0.158	0.143	0.151	0.274	0.249	0.261
Forel	0.220	0.230	0.226	0.381	0.398	0.392	0.140	0.146	0.144	0.243	0.253	0.250
MC245	0.241	0.240	0.221	0.418	0.416	0.382	0.154	0.153	0.140	0.266	0.265	0.243
MC268	0.229	0.218	0.236	0.397	0.378	0.409	0.146	0.139	0.150	0.253	0.241	0.260
Plantahof	0.218	0.222	0.209	0.378	0.385	0.361	0.139	0.142	0.133	0.241	0.245	0.230
Probus	0.221	0.216	0.201	0.384	0.374	0.348	0.141	0.138	0.128	0.244	0.238	0.221
Runal	0.270	0.243	0.248	0.468	0.420	0.429	0.172	0.155	0.158	0.298	0.268	0.273
Simano	0.188	0.237	0.241	0.326	0.411	0.417	0.120	0.151	0.153	0.208	0.262	0.266
Suretta	0.242	0.232	0.245	0.419	0.402	0.424	0.154	0.148	0.156	0.267	0.256	0.270
Titlis	0.233	0.231	0.241	0.404	0.400	0.417	0.148	0.147	0.153	0.257	0.255	0.266
Zenith	0.229	0.222	0.274	0.397	0.385	0.475	0.146	0.141	0.175	0.253	0.245	0.302
Average	0.232	0.230	0.234	0.402	0.399	0.405	0.148	0.147	0.149	0.256	0.254	0.258

Abbreviations: iSF = inversion of cone ($r_{root\ tip}/l_{root\ tip}$) and spheroid shape factor ($2r_{root\ tip}/\pi l_{root\ tip}$); $r_{root\ tip}$ = radius at base of root tip, $l_{root\ tip}$ = length of root tip

Supporting Information Table S3.3: Influence of geometry factor (GF) on axial force (F) and penetration stress (S) exerted by root tips during soil penetration. GF was used to account for geometry of cone penetrometer and cone (Eq 3.11) and spheroid root tip shape (Eq 3.12), respectively. Presented minimum (Min), average (Mean) and maximum (Max) values are based on average of six individual roots in 14 genotypes and three soil bulk densities.

Shape	GF	F [N]			S [kPa]		
		Min	Mean	Max	Min	Mean	Max
Cone	No	0.047	0.122	0.323	251.5	472.7	856.7
	Yes	0.019	0.049	0.143	91.0	189.4	368.1
Half spheroid	No	0.056	0.143	0.379	291.1	397.3	1022.0
	Yes	0.014	0.036	0.105	69.42	141.3	270.1

8.4. Supporting information: Chapter 4
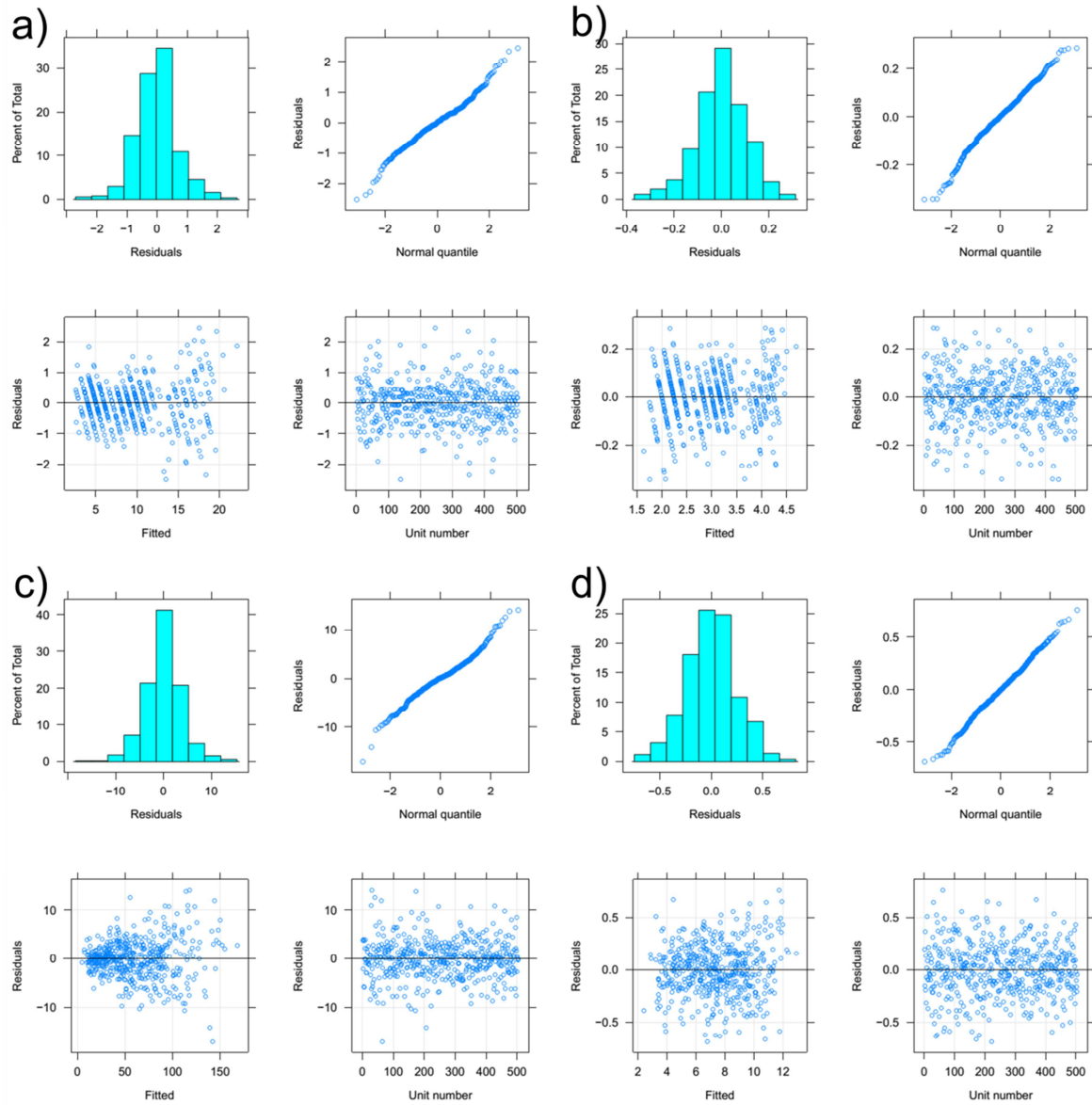
Supporting Information Figure S4.1: Residual plots from linear mixed models (Eq 4.1) using ASReml for R for a) and b) axial root number and c) and d) lateral root number a) and c) before square root transformation and b) and d) after square root transformation (n = 4).
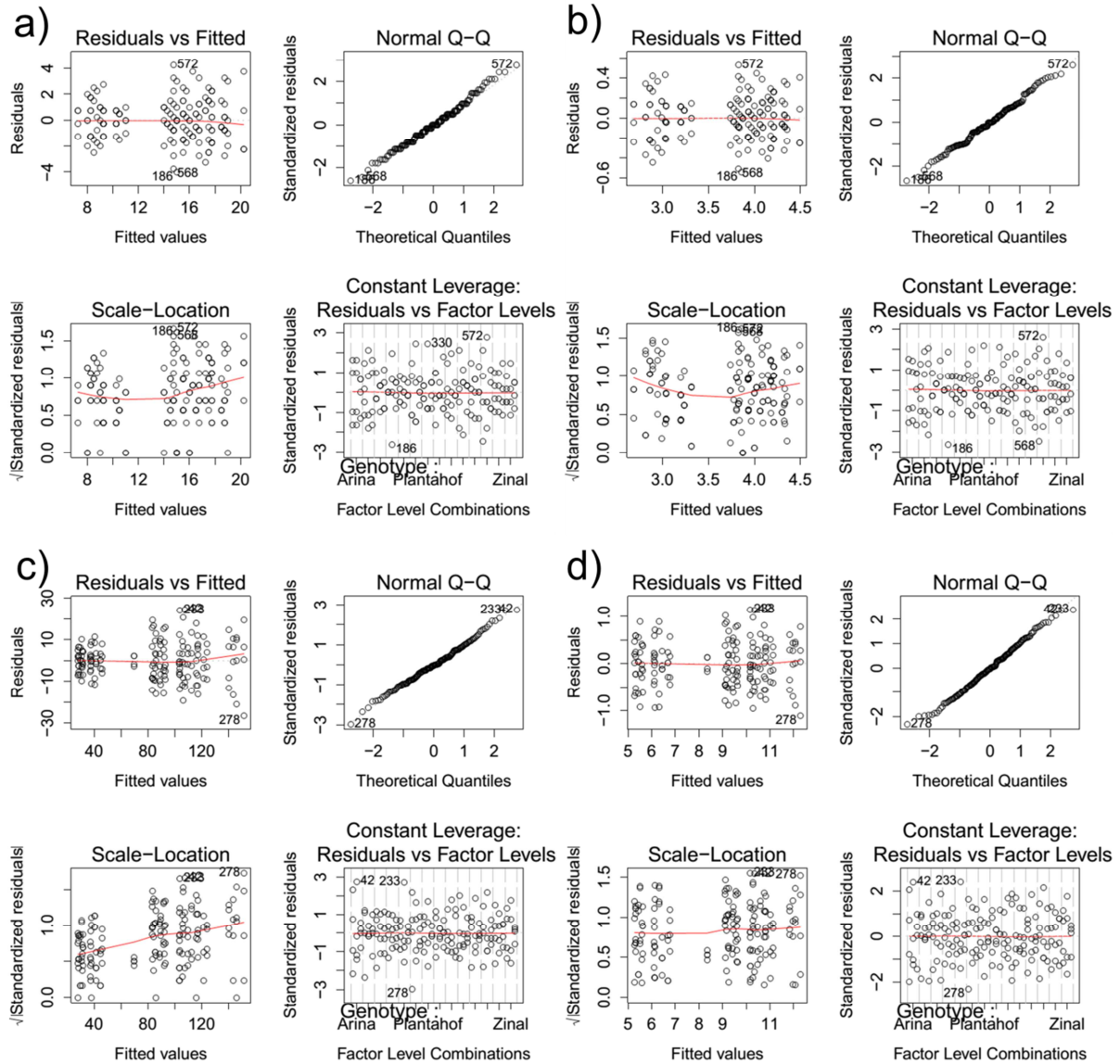
Supporting Information Figure S4.2: Residual plots from two factorial analysis of variance model for a) and b) axial root number and c) and d) lateral root number a) and c) before square root transformation and b) and d) after square root transformation (n = 4).

Supporting Information Table S4.1: Settings of X-ray computed tomography scanner and reconstruction details.

Parameter	Setting
Images scan [#]	1600
Averaged images [#]	1
Skipped images [#]	0
Current [μA]	450
Voltage [kV]	120
Illumination time per image [ms]	131
Filter	0.1 mm copper
Binning 2 by 2 voxel	yes
Scanning time [min]	7
Voxel edge length [μm]	68
Beam hardening corrections	3.6

Supporting Information Table S4.2: Effects of radiation exposure (X-ray), soil bulk density (BD) and their interaction in the variety "Arina" on root and shoot dry weight; ** denotes significant differences at $p < 0.01$, n.s. denotes non-significant responses ($n = 4$).

Trait	X-ray	BD	X-ray:BD
Root dry weight [g]	n.s.	**	n.s.
Shoot dry weight [g]	n.s.	**	n.s.

Supporting Information Table S4.3 Summary of variety mean values (n = 4) of axial and lateral root numbers (NoAx and NoLat, respectively), root and shoot dry weight (RootDW and ShootDW, respectively) under low (1.3 g cm^{-3}), moderate (1.45 g cm^{-3}) and high (1.6 g cm^{-3}) soil bulk density three weeks after emergence and bulk density mean values (Average).

	NoAx [#]			NoLat [#]			RootDW [g]			ShootDW [g]		
Variety	**1.3**	**1.45**	**1.6**	**1.3**	**1.45**	**1.6**	**1.3**	**1.45**	**1.6**	**1.3**	**1.45**	**1.6**
Arina	15.5	17.5	9.0	106.3	107.5	28.0	0.568	0.448	0.078	0.686	0.586	0.113
CHClaro	17.8	16.8	8.5	146.0	103.5	38.0	0.697	0.410	0.074	0.695	0.570	0.128
CHCombin	18.5	15.5	8.3	143.5	88.8	30.8	0.661	0.314	0.100	0.677	0.504	0.117
Forel	15.0	15.0	7.3	105.8	92.3	28.5	0.613	0.340	0.059	0.646	0.516	0.097
Mont-Calme 245	18.8	16.0	10.3	109.8	103.8	44.8	0.653	0.407	0.079	0.718	0.566	0.138
Mont-Calme 268	17.8	20.3	11.0	151.5	140.3	46.0	0.729	0.517	0.081	0.708	0.717	0.112
Plantahof	16.5	16.3	10.3	124.0	91.8	41.5	0.701	0.486	0.092	0.705	0.535	0.158
Probus	17.5	14.3	9.3	89.5	69.8	29.8	0.701	0.409	0.105	0.767	0.561	0.131
Runal	17.8	19.0	9.3	121.5	93.0	40.5	0.706	0.409	0.105	0.685	0.530	0.130
Simano	18.8	17.3	10.5	116.0	103.5	37.5	0.733	0.549	0.103	0.683	0.586	0.134
Suretta	14.8	14.0	8.0	117.3	84.3	31.3	0.579	0.329	0.089	0.703	0.517	0.141
Titlis	14.8	14.8	8.3	86.0	83.5	28.5	0.595	0.395	0.088	0.652	0.544	0.117
Zenith	15.5	14.5	8.8	112.5	85.5	31.8	0.643	0.424	0.074	0.654	0.534	0.103
Zinal	16.8	15.8	9.3	117.0	83.3	37.3	0.582	0.382	0.090	0.609	0.486	0.119
Average	16.9	16.2	9.2	117.6	95.1	35.3	0.654	0.416	0.087	0.685	0.554	0.124

8.5. Supporting information: Chapter 5
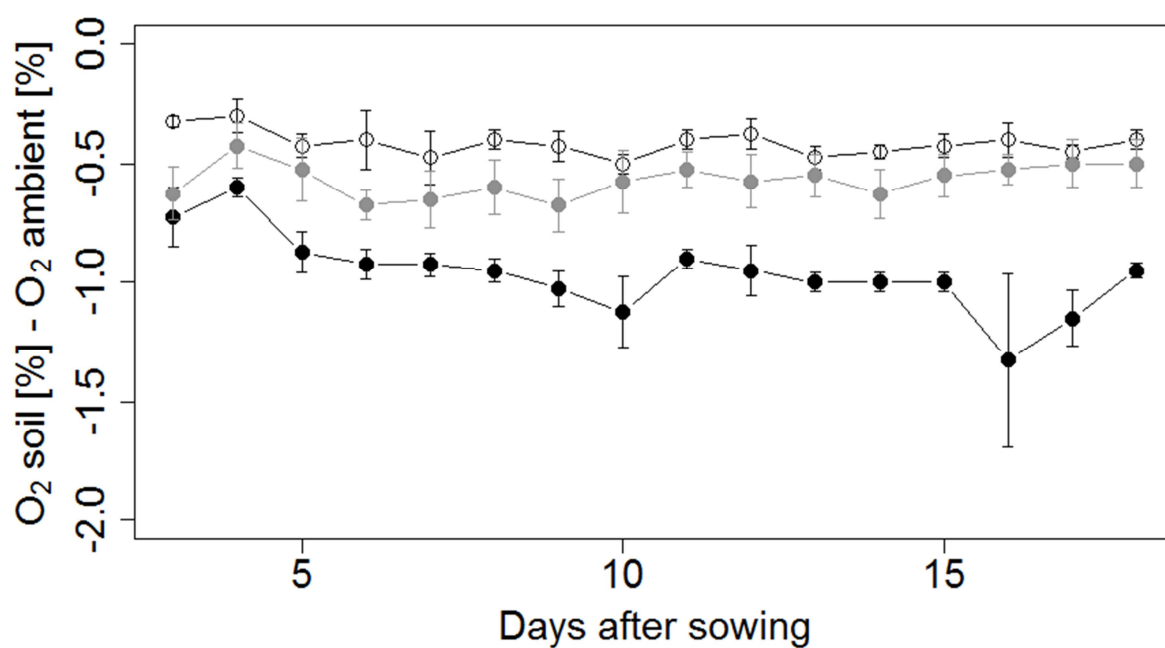
Supporting Information Figure S5.1: Difference in O2 concentration between ambient air in the growth chamber and soil air measured in soil columns during wheat growth from 3 to 18 days after sowing in uncompacted soil (open symbols), compacted soil (closed black symbols) and compacted soil with artificial macropores (closed grey symbols). Error bars represent standard error (n = 4).

Supporting Information Table S5.1: Agronomic information on the field experiments at the Soil Structure Observatory (SSO), Agroscope, Switzerland. Tillage treatments in uncompacted (Ctrl), compacted (Com) and compacted plots with artificial macropores (ComAP), sowing density and fertilisation rates.

Year	Crop	Previous crop	Tillage Ctrl	Tillage Com & ComAP	Sowing density [# seeds m^{-2}]	Fertilisation [kg ha^{-1}]	Remarks
2014	Soybean	Perennial grass-legume mixture	Mouldboard plough; 22 cm deep	Chisel plough; 5 cm deep	60	K: 50.0; Mg: 4.3	
2014	Summer triticale	Perennial grass-legume mixture	Mouldboard plough; 22 cm deep	No tillage	280	N: 93.2; K: 105; Mg: 8.5	Not part of this study
2014/15	Winter wheat	Soybean	Chisel plough; 5 cm deep	Chisel plough; 5 cm deep	280	N: 131.0; P: 7.8 K: 30.7; Mg: 2.9	
2015	Maize	Summer triticale	Mouldboard plough; 22 cm deep	No tillage	9	N: 113.4; P: 20.1 K: 124.5; Mg: 4.6	

Supporting Information Table S5.2: Sample dimensions and X-ray computed tomography settings of soil columns and field samples.

Parameter	Soil columns	Field
Sample diameter [mm]	49	100
Sample height [mm]	150	100
Subscans per sample [#]	4	1
Images per subscan [#]	1600	1600
Averaged images [#]	1	1
Skipped images [#]	0	0
Current [µA]	450	450
Voltage [kV]	150	120
Illumination time per image [ms]	131	1000
Filter	0.1 mm copper	0.4 mm copper
Binning 2 by 2 voxel	yes	yes
Total scan time [min]	28	27
Voxel edge length [µm]	68	120

Supporting Information Table S5.3: Plant vigour parameters obtained from soil columns of uncompacted (Ctrl), compacted (Com) compacted soil with artificial macropores (ComAP) and root dry weight of field samples (sum of two samples from 0-10 cm and 13-23 cm depth) under Ctrl, Com and ComAP. Different letters indicate significant differences of the means using least significant difference (LSD) test at $p < 0.05$, (soil columns n = 4, field n = 3).

Environment	Crop	Trait	Ctrl	Com	ComAP	LSD
Soil columns	Soybean	Root dry weight [g]	0.25[a]	0.14[b]	0.16[ab]	0.086
		Shoot dry weight [g]	0.55	0.42	0.43	0.14
		Root/Shoot ratio [g g^{-1}]	0.44	0.33	0.36	0.11
		Leaf area [cm^2]	57.5[a]	38.1[b]	39.4[b]	11.3
	Wheat	Root dry weight [g]	0.33[a]	0.091[b]	0.11[b]	0.060
		Shoot dry weight [g]	0.28[a]	0.083[b]	0.098[b]	0.031
		Root/Shoot ratio [g g^{-1}]	1.16	1.15	1.13	0.62
		Leaf area [cm^2]	34.2[a]	10.2[b]	13.0[b]	7.8
	Maize	Root dry weight [g]	0.58[a]	0.23[b]	0.28[b]	0.15
		Shoot dry weight [g]	0.59[a]	0.22[b]	0.25[b]	0.13
		Root/Shoot ratio [g g^{-1}]	1.00	1.06	1.13	0.41
		Leaf area [cm^2]	68.4[a]	45.3[b]	50.8[ab]	19.7
Field	Soybean	Root dry weight [g]	1.65[a]	0.91[b]	1.33[ab]	0.43
	Wheat	Root dry weight [g]	2.92[a]	1.87[b]	2.53[ab]	0.90
	Maize	Root dry weight [g]	10.45	6.54	6.79	4.27

Supporting Information Table S5.4: Effect of soil treatment (Trt) and block on shoot dry weight in the field and average shoot dry weight on uncompacted (Ctrl), compacted (Com) and compacted soil with artificial macropores (ComAP). * and ** indicate significant effects at $p < 0.05$ and $p < 0.01$, respectively. Different letters indicate significant differences ($p < 0.05$) of the means using least significant difference (LSD) test at $p < 0.05$ ($n = 3$).

Factor			Shoot dry weight [g]			
Crop	Trt	Block	Ctrl	Com	ComAP	LSD
Soybean	*	0.723	22.1[a]	15.2[b]	22.7[a]	5.0
Wheat	*	0.313	6.5[a]	3.6[b]	6.0[a]	1.6
Maize	**	*	131.7[a]	84.8[c]	107.5[b]	20.7

8.6. Supporting information: General discussion

Supporting Information Table S6.1: Crop yields from crop rotation treatments in the soil structure observatory after compaction in 2013. Triticale yield refers to dry grain yield, maize yield refers to dry silage yield.

Year	Crop	Compaction	Tillage	Yield [t ha^{-1}]
2014	Triticale	No	Yes	3.5
		Yes	Yes	2.8
		Yes	No	0.3
2015	Maize	No	Yes	17.1
		Yes	Yes	15.2
		Yes	No	5.9

9. Acknowledgements

At this point, I would like to express my sincere gratitude to all people who directly or indirectly worked with me during the last years.

Achim and Thomas, what shall I say except of "it was a very nice time". Thanks a lot to you both for all the support and trust you gave me during the last years. I owe you my sincere gratitude for giving me the opportunity to be part of such an exciting project and to give me the freedom I received during the last years.

It was a pleasure for me having a Ph.D. fellow like you, Siul. Thanks for all the fruitful discussions we had and for introducing me to the jungle of mechanics and mathematics. Apart from this, you being such a cool dude was as important to me as the scientific input I received from you.

Andi, you cannot be missed in this list, since without meeting you, I would probably never have started to work in science. Also to Frank, Kang, Sebastian and Norbert I would like to say thank you for all the off-work time we spent together during the last years.

This thesis would not have been possible with all the help I received from the bachelor and master students working with me. Serge, Vanathy, Patrick and Laurin, I hope you enjoyed working with me as much as I did enjoyed the work with you.

I would like to express my gratitude to the group of crop science at ETH Zurich and the group for soil fertility and soil protection at Agroscope Zurich Reckenholz for offering me such a nice work environment. In particular, Marlies, Peter and Jan are thanked for all the technical assistance and Steven for the help with statistics. Furthermore, Fritz and his field team and Patrick and Michi from the LFW workshop are thanked.

Dani and Stan, meetings with you were always an enormous inspiration for me. Thanks a lot for this. Further gratitude is expressed to Dani and Hans from the soil and terrestrial environmental physics group at ETH Zurich for all the help during the duration of my Ph.D.

Such a list would be incomplete if people from my private environment would not be addressed. Hence, big up to all my friends from suburbia, with whom I am connected through sincere friendship

since years. Mama, Papa and Alina, without you I would never be at the point I am now. Thanks for all the support, inspiration and patience I received from you during the last years. Last but not least, Jasmin, I would like to thank you to be such a wonderful and lovely person and simply just for sharing your life with me.

10. Curriculum vitae

Tino Colombi, MSc. ETH in Agricultural Sciences

Date of birth: 31st of May 1988

Main research interests

Plant phenotyping: Development and application of new tools to quantify plant trait diversity and plant responses to the environment under controlled and field conditions

Plant eco-physiology: Understanding plant responses to changes in environmental conditions, including soil degradation, climate change and agricultural management

Soil physics: Using soil physical and mechanical properties to understand and predict plant development and root-soil interactions in agro-ecosystems

Sustainable agriculture: Identification of soil management approaches and plant traits that improve crop productivity with minimum environmental impacts

---

Education

09/2013 to 12/2016: Ph.D. studies in environmental system science at ETH Zurich, Switzerland (Prof. Achim Walter) in collaboration with Agroscope Zurich, Switzerland (Prof. Thomas Keller)
Thesis title: Strategies for yield recovery after soil compaction assessed by multi-level phenotyping

03/2012 to 09/2013: MSc studies in agricultural sciences at ETH Zurich with major in crop science; Master thesis in collaboration with Pennsylvania State University, United States (Prof. Jonathan Lynch)
Thesis title: Responses of root system architecture to low nitrogen: phenotyping the EURoot core set of maize using "shovelomics"

09/2008 to 03/2012: BSc studies in agricultural sciences at ETH Zurich

08/2001 to 09/2007: High School ("Kantonsschule") with major in mathematics and physics in Dübendorf, Switzerland

---

Teaching experience

Regular courses:	Teaching assistant (supervision and correction of exercises) in MSc course "experimental design and applied statistics in agro-ecosystems" at ETH Zurich, main lecturers: Prof. Werner Eugster and PD Dr. Andreas Hund
Thesis supervision:	One MSc thesis and three BSc theses supervised and graded

Language skills

German:	Native
English:	Fluent in spoken and written
French:	Good in spoken, intermediate in written

Publications

Colombi, T., Kirchgessner, N., Walter, A., Keller T., (*in press*). Root tip shape governs root elongation rates under increased soil strength in wheat. Plant Physiol.

Colombi, T., Walter, A., 2017. Genetic diversity under soil compaction in wheat: root number as a promising trait for early plant vigour. Front Plant Sci. 8. doi: 10.3389/fpls.2017.00420.

Keller T., **Colombi T.**, Ruiz S., Manalili M. P., Rek J., Stadelmann V., Wunderli H., Breitenstein D., Reiser R., Oberholzer H., Schymanski S., Romero-Ruiz A., Linde N., Weisskopf P., Walter A., Or D. 2017. Long-term Soil Structure Observatory for Monitoring Post-compaction Evolution of Soil Structure. Vadose Zone Journal 16. doi: 10.2136/vzj2016.11.0118.

Colombi, T., Braun, S., Keller, T., Walter, A., 2017. Artificial macropores attract crop roots and enhance plant productivity on compacted soils. Sci. Total Environ. 574, 1283-1293. doi: 10.1016/j.scitotenv.2016.07.194.

Colombi, T., Walter, A., 2016. Root responses of triticale and soybean to soil compaction in the field are reproducible under controlled conditions. Funct. Plant Biol. 43, 114-128. doi: 10.1071/FP15194.

Pfeifer, J., Kirchgessner, N., **Colombi, T.**, Walter, A., 2015. Rapid phenotyping of crop root systems in undisturbed field soils using X-ray computed tomography. Plant Methods 11. doi: 10.1186/s13007-015-0084-4.

Colombi, T., Kirchgessner, N., Le Marié, C.A., York, L.M., Lynch, J.P., Hund, A., 2015. Next generation shovelomics: set up a tent and REST. Plant Soil 388, 1-20. doi: 10.1007/s11104-015-2379-7

Zurich, June 2017